

Monoaminergic Regulation of MeCP2 Phosphorylation in Mouse Models of Psychiatric Disease

Ashley N. Hutchinson

Department of Pharmacology
Duke University

Date _____

Approved:

Anne West, Supervisor

Marc Caron

Cynthia Kuhn

Donald McDonnell

Theodore Slotkin

William Wetsel

Dissertation submitted in partial fulfillment of the requirements
of the degree of Doctor of Philosophy in the Department of Pharmacology and Cancer Biology
in the Graduate School of Duke University

2011

ABSTRACT

Monoaminergic Regulation of MeCP2 Phosphorylation in Mouse Models of Psychiatric Disease

Ashley N. Hutchinson

Department of Pharmacology
Duke University

Date _____

Approved:

Anne West, Supervisor

Marc Caron

Cynthia Kuhn

Donald McDonnell

Theodore Slotkin

William Wetsel

An abstract of a dissertation submitted in partial fulfillment of the requirements
of the degree of Doctor of Philosophy in the Department of Pharmacology and Cancer Biology
in the Graduate School of Duke University

2011

Copyright by
Ashley Hutchinson
2011

ABSTRACT

Activation of monoaminergic receptors is essential to the mechanism by which psychostimulants and antidepressants induce changes in behavior. Although these drugs rapidly increase monoaminergic transmission, they need to be administered for several weeks or months in order to produce long-lasting alterations in behavior. This observation suggests that it is likely that molecular mechanisms downstream of receptor activation contribute to the effects of psychostimulants and antidepressants on behavior.

Recently, we and others have demonstrated that the methyl-CpG-binding protein 2 (MeCP2) contributes to both neural and behavioral adaptations induced by repeated psychostimulant exposure (Deng *et al*, 2010, Im *et al*, 2010). Psychostimulants induce rapid and robust phosphorylation of MeCP2 at Ser421 (pMeCP2), a site that is thought to modulate MeCP2-dependent chromatin regulation (Cohen *et al*, 2011), and this phosphorylation event is selectively induced in the GABAergic interneurons of the nucleus accumbens (NAc). In order to understand the signaling pathways that contribute to the pattern of pMeCP2 we observe, I characterized the monoaminergic signaling pathways that regulate pMeCP2. I found that activation of dopamine (DA) and serotonin (5-HT) transmission is sufficient to induce pMeCP2. The novel finding that drugs that activate serotonergic signaling induce pMeCP2 suggests that pMeCP2 may be involved in serotonergic mediated behaviors.

To determine the requirement of pMeCP2 in serotonergic mediated behaviors, I utilized mice that bear a knockin (KI) mutation that converts serine to alanine at 421 (S421A) (Cohen *et al*, 2011). After characterizing the behavioral phenotype of these mice, I conducted tests to assess anxiety- and depression-like behavior. I found that the

KI mice do not display heightened anxiety in several assays. However, the KI mice exhibit depression-like behavior in the forced swim and tail suspension but show no differences compared to wild-type (WT) littermates in the sucrose preference test, suggesting that pMeCP2 may be implicated in the behavioral response to stressful stimuli.

Because we are interested in examining the role of pMeCP2 in the behavioral adaptations to chronic monoaminergic signaling, I then put the KI mice and their WT littermates through chronic social defeat stress, a behavioral paradigm in which repeated exposure to aggressive mice causes social avoidance that is reversed by chronic but not acute antidepressant treatment. Although the WT mice show an increase in social interaction following chronic imipramine treatment, the KI mice fail to show a behavioral response to chronic treatment. These data suggest that pMeCP2 may be implicated in the antidepressant action of chronic imipramine. Finally, investigation of the brain regions in which pMeCP2 may be contributing to the behavioral response to chronic imipramine treatment revealed that chronic but not acute imipramine treatment induces pMeCP2 in the lateral habenula (LHb), a brain region involved in the behavioral response to stress and reward. Together, these data implicate a novel role for pMeCP2 in depression-like behavior and the behavioral response to chronic antidepressant treatment.

CONTENTS

Abstract.....	iv
List of Tables.....	xiii
List of Figures.....	xiv
Abbreviations and acronyms.....	xxii
Acknowledgements.....	xxiv
1. Introduction.....	1
1.1 Behavioral adaptations to chronic monoaminergic signaling.....	1
1.1.1 The behavioral responses to repeated psychostimulant and antidepressant exposure.....	1
1.1.2 Epigenetic mechanisms of gene regulation.....	3
1.1.3 The role of epigenetic mechanisms in the behavioral adaptations to repeated psychostimulant exposure.....	5
1.1.4 Epigenetic mechanisms and the behavioral responses to repeated antidepressant treatment.....	9
1.2 MeCP2: A transcriptional regulator linking DNA methylation and chromatin modifications.....	12
1.2.1 MeCP2 is a methyl-DNA binding protein.....	12
1.2.2 Examination of the mechanisms by which MeCP2 regulates transcription.....	13
1.3 Studies from mouse lines bearing mutations in MeCP2.....	15
1.3.1 Mutations in MeCP2 cause the neurodevelopmental disorder Rett syndrome.....	15
1.3.2 Mouse models of RTT.....	16
1.3.3 Brain region- and cell-type-specific MeCP2 mutant mice.....	18
1.3.4 Utilizing mouse models of RTT to investigate the function of MeCP2.....	19

1.4 MeCP2 plays a role in the behavioral adaptations to repeated psychostimulant exposure	21
1.4.1 MeCP2 expression in NAc contributes to neural and behavioral responses to psychostimulants	22
1.4.2 MeCP2 in the dorsal striatum mediates compulsive drug-taking behavior.....	24
1.5 Psychostimulant exposure regulates MeCP2 phosphorylation.	26
1.5.1 Neuronal activity induces MeCP2 phosphorylation at Ser421.	26
1.5.2 Functional consequences of pMeCP2 <i>in vitro</i>	28
1.5.3. The role of activity-dependent MeCP2 phosphorylation <i>in vivo</i> ...	29
1.5.4 pMeCP2 as a target of regulation by psychostimulants and DA signaling.....	33
1.5.5 pMeCP2 levels correlate with degree of behavioral sensitization to repeated AMPH.....	34
1.6 Research objectives.....	35
2. Differential regulation of MeCP2 phosphorylation in the CNS by dopamine and serotonin.....	37
2.1 Summary.	37
2.2 Introduction.....	38
2.3 Materials and Methods.....	40
2.3.1 Animals	40
2.3.2 Immunofluorescent staining of brain sections	41
2.3.3 Image Analyses.	42
2.3.4 Bilateral guide cannula surgery.....	43
2.3.5 Intra-striatal infusions.	44

2.3.6 Striatal cultures	44
2.3.7 Locomotor activity in the open field.....	45
2.3.8 Behavioral sensitization	46
2.3.9 Statistical analyses	46
2.4 Results.....	47
2.4.1 Selective blockade of the DAT or SERT is sufficient to induce pMeCP2	47
2.4.2 Dopamine and serotonin receptor agonists differentially induce pMeCP2.	52
2.4.3 AMPH-induced pMeCP2 is reduced in SERT-KO mice.....	60
2.4.4 pMECP2 in the NAc following repeated AMPH does not predict behavioral sensitization.....	64
2.5 Discussion	68
3. Examination of the behaviors that require MeCP2 phosphorylation at S421.....	75
3.1 Summary	75
3.2 Introduction.....	75
3.3 Materials and methods.....	77
3.3.1 Animals.....	77
3.3.2 Neurophysiological screen.....	78
3.3.3 Assessment of spontaneous motor activity.....	78
3.3.4 Rotarod assay	78
3.3.5 Light-dark box	78
3.3.6 Elevated zero maze.....	79
3.3.7 Assay of sociability and preference for social novelty	79
3.3.8 Novel object recognition test	81

3.3.9 Morris water maze	81
3.3.10 Context-dependent fear conditioning.....	82
3.3.11 Forced swim	83
3.3.12 Statistical analyses.	83
3.4 Results.....	84
3.4.1 S421A mutant mice do not display abnormalities in motor activity.....	84
3.4.2 pMeCP2 at Ser421 is not required for learning and memory in the Morris water maze or context-dependent fear conditioning	86
3.4.3 MeCP2 S421A mutation results in abnormal behavioral responses to novelty	89
3.4.4 S421A knockin mice do not exhibit heightened anxiety.....	92
3.4.5 S421A knockin mice display depression-like behavior	94
3.5 Discussion	94
4. Role of pMeCP2 in depression-like behavior and the behavioral response to chronic antidepressant treatment.....	97
4.1 Summary.	97
4.2 Introduction.....	97
4.3 Materials and methods.	100
4.3.1 Animals.	100
4.3.2 Immunofluorescent staining of brain sections	100
4.3.3 Image analyses	101
4.3.4 Forced swim.....	102
4.3.5 Tail suspension.....	103
4.3.6 Sucrose preference test.....	103

4.3.7 Chronic social defeat stress.....	104
4.3.8 Statistical analyses	105
4.4 Results.....	105
4.4.1 Imipramine is sufficient to induce pMeCP2 in the NAc.....	105
4.4.2 S421A mice show depression-like phenotype and respond to acute imipramine.....	107
4.4.3 S421A mice fail to respond to chronic imipramine in social defeat stress.....	110
4.4.4 Acute and chronic imipramine treatment differentially regulate pMeCP2 following social defeat stress.....	114
4.5 Discussion.....	117
5. Discussion.....	123
5.1 The role of pMeCP2 in depression-like behavior	123
5.2 pMeCP2 as a mechanism of antidepressant action	126
5.3 Understanding the mechanism by which pMeCP2 mediates behavioral responses to antidepressant treatment.....	129
5.4 pMeCP2, RTT, and depression	131
Appendix A: Reduced cortical BDNF expression and aberrant memory in <i>Carf</i> knock-out mice.....	133
A.1 Summary	133
A.2 Introduction.....	134
A.3 Materials and methods	135
A.3.1 Generation of <i>Carf</i> knockout mice and genotyping.....	135
A.3.2 Luciferase assays.....	137
A.3.3 Preparation of recombinant mouse CaRF and antibody purification.....	137

A.3.4 Nuclear extracts	138
A.3.5 Western blotting.....	138
A.3.6 Electrophoretic mobility shift assay	139
A.3.7 Mouse embryonic fibroblasts	139
A.3.8 RNA harvesting and RT-PCR.....	140
A.3.9 Neuronal and glial cell cultures.....	140
A.3.10 BDNF protein measurements	141
A.3.11 Synapse immunohistochemistry	141
A.3.12 SHIPRA phenotypic screen	143
A.3.13 Morris water maze.....	143
A.3.14 Fear conditioning.....	145
A.3.15 Novel object recognition	146
A.3.16 Statistical analyses.....	147
A.4 Results	148
A.4.1 Generation of <i>Carf</i> knockout mice and validation of a CaRF-specific antibody	148
A.4.2 CaRF expression in the CNS.....	154
A.4.3 Brain-region selective role for CaRF in regulation of <i>Bdnf</i> <i>expression</i>	155
A.4.4 Altered GABAergic synaptic protein expression in <i>Carf</i> KO mice.....	158
A.4.5 Behavioral analyses of <i>Carf</i> KO mice.....	160
A.5 Discussion	171
A.6 References	176

Appendix B: Transcriptional regulators that mediate neural and behavioral adaptations to psychostimulants	180
B.1 Summary	180
B.2 Introduction	180
B.3 Sequence-specific DNA-binding transcription factors	182
B.3.1 Cyclic-AMP response element binding protein (CREB)	182
B.3.2 Fos, FosB and Δ FosB	190
B.3.3 Myocyte enhancer factor (MEF2)	194
B.3.4 Nuclear factor κ B (NF- κ B)	197
B.3.5 Nuclear factor of activated T cells (NFAT)	200
B.3.6 Nucleus accumbens 1 (NAC1)	202
B.3.7 Summary	205
B.4 Chromatin regulation	206
B.4.1 CREB binding protein (CBP)	208
B.4.2 Histone deacetylases (HDACs)	210
B.4.3 Histone methyltransferases (HMTs)	214
B.4.4 DNA methylation	216
B.4.5 Summary	219
B.5 Conclusions	219
B.6 References	220
References	232
Biography	242

LIST OF TALBES

Table 1: Mice bearing mutations in the methyl-CpG-binding protein 2 (MeCP2).

These mouse models have been used to understand how the loss of MeCP2 contributes to RTT as well as to assess the function of MeCP2.16

Table 2: Changes in locomotor activity following acute DAT, SERT, or NET

blockade. (a-c) The effects of 10 or 15 mg/kg GBR12909, 5 or 10 mg/kg citalopram, and 3 or 5 mg/kg reboxetine on locomotor activity in C57BL/6 mice 1 hr post-injection.

All values of locomotor activity were normalized to Veh control for each drug. n=6-8

mice/group. * $p < 0.05$ compared to Veh. Error bars indicate S.E.M.50

LIST OF FIGURES

Figure 1: Map of MeCP2 protein. MeCP2 contains a methyl DNA-binding domain (MBD) and a transcriptional repressor domain (TRD) that recruits histone modifying enzymes. S80, S421, and S424 are sites of phosphorylation.13

Figure 2: Working hypothesis addressed in research objectives. Our previous work suggests that pMeCP2 may be involved in the behavioral response to repeated activation of monoaminergic signaling. Based on these findings and the evidence that drugs that activate 5-HT induce pMeCP2, I hypothesized that the phosphorylation of MeCP2 at Ser421 is involved in the behavioral response to chronic antidepressant treatment.36

Figure 3: Selective DAT and SERT blockade differentially induce pMeCP2 in the NAc. (a) pMeCP2 and total MeCP2 induction following vehicle or 3 mg/kg AMPH. Solid gray box indicates representative section of NAc used to quantify pMeCP2 immunofluorescence. Dashed white box was used as the inset image to examine total MeCP2 and Hoechst (nuclear marker) overlay. ac, anterior commissure. (b) pMeCP2 immunostaining in the NAc (left column) and c-Fos immunostaining (right column) 2 hrs after treatment with Veh, 10 mg/kg GBR12909, 10 mg/kg citalopram, or 3 mg/kg reboxetine. (c, e, g) number of cells in which pMeCP2 was induced following treatment of GBR12909, citalopram, or reboxetine. (d, f, h) pMeCP2 integrated intensity in the NAc following treatment with GBR12909, citalopram, or reboxetine. All values of quantitated immunofluorescence intensity were normalized to Veh control for each drug. n=5-8 mice/group. *p<0.05 compared to Veh. Error bars indicate S.E.M. Scale bars = 10µm.48

Figure 4: DAT and SERT blockers differentially regulate the cell-type specificity of MeCP2 phosphorylation in the NAc. pMeCP2 (red), GAD67 (green), Hoechst nuclear dye (blue), and overlay immunostaining in the NAc 2hrs after treatment with Veh, 3 mg/kg AMPH, 10 mg/kg GBR12909, or 10 mg/kg citalopram. White arrows indicate neurons coimmunolabeled with antibodies for pMeCP2 and GAD67, and blue arrows indicate pMeCP2 induction in neurons that are not GAD67-positive GABAergic interneurons. Scale bar = 20µm.51

Figure 5: Selective DAT blockade induces pMeCP2 in the PLC. (a-c) pMeCP2 integrated intensity in the PLC following treatment with GBR12909, citalopram, or reboxetine. All values of quantified immunofluorescence intensity were normalized to Veh control for each drug. (d) pMeCP2 (red), GAD67 (green), and overlay immunostaining in the PLC 2 hrs after treatment with Veh, 10 mg/kg GBR12909, 10 mg/kg citalopram, or 3 mg/kg reboxetine. White arrows indicate neurons coimmunolabeled with antibodies for pMeCP2 and GAD67, and blue arrows indicate pMeCP2 induction in neurons that are not GAD67-positive GABAergic interneurons. n=5-7 mice/group. *p<0.05 compared to Veh. Error bars indicate S.E.M. Scale bars = 20µm.53

Figure 6: Stimulation of D₁- and D₂-class DA receptors induces different patterns of pMeCP2. (a) pMeCP2 immunostaining in the NAc 2 hrs after treatment with Veh, 7.5 mg/kg SKF81297, 0.4 mg/kg quinpirole, or co-injection of SKF81297 and quinpirole. (b) Quantitation of pMeCP2 immunostaining from panel a (c) pMeCP2 induction in the hippocampus 2 hrs after treatment with Veh, 5 or 7.5 mg/kg SKF81297, or co-injection of 7.5 mg/kg SKF81297 and quinpirole. Enlargement images show the dotted inset regions. (d) pMeCP2 (red), GAD67 (green), and overlay immunostaining in the NAc 2hrs after treatment with 7.5 mg/kg SKF81297, 0.4 mg/kg quinpirole, or co-injection of SKF81297 and quinpirole. White arrows indicate neurons coimmunolabeled with antibodies for pMeCP2 and GAD67, and blue arrows indicate pMeCP2 induction in neurons that are not GAD67-positive GABAergic interneurons. n=4-7 mice/group. *p<0.05 compared to Veh, #p<0.05 SKF compared to SKF+quinpirole. Error bars indicate S.E.M. Scale bar = 20µm.54

Figure 7: Activation of 5-HT receptors by quipazine induces pMeCP2 in the NAc. (a) Quantitation of pMeCP2 integrated intensity in the NAc 2 hrs after treatment with Veh or 3 or 4.5 mg/kg quipazine. (b) pMeCP2 (red), GAD67 (green), and overlay immunostaining in the NAc 2hrs after treatment with Veh or 3 mg/kg quipazine. White arrows indicate neurons coimmunolabeled with antibodies for pMeCP2 and GAD67. Values of quantitated immunofluorescence were normalized to Veh control. n=4-6 mice/group. *p<0.05 compared to Veh. Error bars indicated S.E.M. Scale bar = 20µm.56

Figure 8: Forskolin is sufficient to induce pMeCP2 in the medium spiny neurons *in vivo* but not *in vitro*. (a) Anatomical location of microinjection sites in the striatum. (b) pMeCP2 and Fos immunostaining in the striatum 90 min after treatment with Veh or forskolin. (c,d) Quantitation of Fos and pMeCP2 integrated intensity in the striatum 90 min after treatment with Veh or forskolin. Values of quantitated immunofluorescence were normalized to Veh control. n=9 mice/group. *p<0.05 compared to Veh. Error bars indicated S.E.M. (e) Colocalization of pMeCP2 immunoreactivity with cell type markers in the region at the tip of the cannula in sections from forskolin-treated mice. pMeCP2 (red), the MSN marker DARPP-32 (green, top), the astrocyte marker GFAP (green, bottom). Scale bar= 20µm. (f,g) Cultured embryonic rat striatal neurons (5 days *in vitro*) were treated for 60 min with various pharmacological reagents, the cells were lysed directly in boiling SDS and separated by SDS-PAGE, western blotting was performed using the antibodies indicated, and the blots were visualized with chemiluminescence on film. (f) Cultures were left either untreated (none), or treated with 55mM KCl in an isotonic solution, 10 µM forskolin (Forsk.) to elevate intracellular cAMP, or 50µM of the D₁-class DA receptor agonist SKF38393 (SKF). Western blots were probed for pMeCP2 and total MeCP2, or pCREB (Ser133) and total CREB as a control for the activation of cAMP signaling pathways. No protein was loaded in lane 2. (g) Cultures were left either untreated, or treated with 55mM KCl or 50µM NMDA as indicated. In the lanes indicated the L-type voltage gated calcium channel inhibitor Nimodipine (Nim.) or the NMDA-receptor antagonist APV were added 2 min before stimulation.59

Figure 9: AMPH-induced pMeCP2 is reduced in the NAc of SERT-KO mice. (a,c,e) The effects of Veh or AMPH treatment on locomotor activity in DAT, SERT, and NET mice 1 hr post-injection. **(b,d,f)** pMeCP2 induction in the NAc following Veh or AMPH treatment in DAT, SERT and NET mice. All values of locomotor activity and quantitated immunofluorescence were normalized to the WT Veh control for each strain of mice. Veh treatment is indicated with a white bar, and AMPH treatment (3 mg/kg) is indicated with a dark gray bar. n=6-8 mice/group. * $p < 0.05$ AMPH compared to Veh within the same genotype, + $p < 0.05$ WT Veh compared to mutant Veh, # $p < 0.05$ WT AMPH compared to mutant AMPH. **(g)** pMeCP2 (red) and GAD67 (green overlay) immunostaining in the NAc 2hrs after treatment with 3 mg/kg AMPH in the DAT, SERT, and NET knockout mice. White arrows indicate neurons coimmunolabeled with antibodies for pMeCP2 and GAD67. Error bars indicate S.E.M. Scale bar = 20 μ m.62

Figure 10: pMeCP2 in the NAc of NET-KO mice correlates with locomotor activity but not behavioral sensitization after repeated AMPH treatment. (a, b) The effects of acute (VEH:AMPH) or repeated (AMPH:AMPH) AMPH administration on locomotor activity in NET-WT and NET-KO mice 1 hr post-injection on the challenge day. **(c)** pMeCP2 integrated intensity in the NAc following AMPH treatment on the challenge day in NET-WT and NET-KO mice. **(d-g)** Pearson product correlations of pMeCP2 immunofluorescence intensity in the NAc and cumulative locomotor activity (1 hr following the challenge injection) from individual mice. **(h, i)** Comparison of locomotor activity 1 hr post-injection on Day 1 and the challenge day (Day 12) in NET-WT and NET-KO mice under the AMPH:AMPH condition. **(j, k)** Pearson product correlations of pMeCP2 immunofluorescence intensity in the NAc and the change in locomotor activity from Day 1 to Day 12 from individual mice in the NET-WT and NET-KO AMPH:AMPH groups. * $p < 0.05$ compared to VEH:AMPH. Error bars indicate S.E.M.66

Figure 11: Loss of MeCP2 phosphorylation does not affect motor activity or coordination (a) WT and KI mice were allowed free access to a running wheel for two weeks, and the average number of revolutions per day was measured. **(b)** WT and KI mice were placed on a stationary rod, which was then gradually accelerated from 0 to 45 revolutions per minute (RPM) over a period of 5 minutes. The speed at which each mouse fell off the rod was recorded and averaged over 5 trials. **(c)** WT and KI mice were placed on a stationary rod, which was then accelerated to 24 RPM. The duration each mouse was able to remain on the rod for each of the 5 trials was recorded and averaged. n= 17-19 mice/group. Error bars indicate S.E.M.85

Figure 12: No abnormalities in spatial learning and memory in the MeCP2 S421A KI mice. (a) Mean swim time in order to locate a hidden platform during acquisition training and during the reversal task in the Morris water maze. **(b)** The amount of time WT and KI mice spent swimming during probe tests was measured in order to determine if the mice remembered the location of the hidden platform during training trials. **(c)** WT and KI mice were shocked in a novel context, and 24 h later, context-cued retention of the fear memory was assessed by returning the mice to the same context and measuring the percentage of time spent freezing. n=10 mice/group. Error bars indicate S.E.M.88

Figure 13: Defects in behavioral response to novel experience in MeCP2 S421A KI mice. (a) Behavior of WT and KI mice in a three-chamber apparatus with a single novel mouse placed in a small wire cage on one of the side chambers. Data shown are time spent in each chamber over the 10 minute trial period. (b) Behavior of WT and KI mice in a three-chamber apparatus with a familiar mouse placed in one of the side chambers and a novel mouse placed in the opposite side chamber. Time spent in each chamber over the 10 minute trial period is shown. (c) WT and KI mice were placed in an arena with a familiar inanimate object and a novel inanimate object placed at opposite ends. In the short-term assay (i), the familiar object was first introduced 30 minutes prior to the trial. In the long-term assay (ii), the familiar object was first introduced 24 hours prior to the trial. Total time spent exploring each object over a 10 minute trial period is shown for each assay. n= 21-24 mice/group for (a,b) and 9 mice/group for (c). In all cases, * $p < 0.05$. Error bars indicate S.E.M.90

Figure 14: No evidence of abnormalities in anxious behavior in MeCP2 S421A mutant mice. (a,b) The percentage of time WT and KI mice spent in the open arm of the elevated zero maze (a), and the latency to enter the open arm (b). (c,d) The amount of time WT and KI mice spent in the lit chamber in the light-dark box assay (c), and the latency to enter the dark chamber (d). n=10 mice/group. Error bars indicate S.E.M.93

Figure 15: MeCP2 S421A mutant mice exhibit depression like behavior in forced swim. (a) The time spent treading and immobile in the forced swim assay over the six minutes of testing. n=18-20 mice/group. * $p < 0.008$ compared to WT. Error bars indicate S.E.M.94

Figure 16: Imipramine induces pMeCP2 in the GABAergic interneurons of the NAc. (a) C57BL/6 mice were injected with imipramine (20 mg/kg i.p.) in the home cage and then perfused at 0, 0.5, 2, 4, and 24 h post-injection. pMeCP2 immunoreactivity in the NAc was quantified and averaged across mice at each time point. (b) pMeCP2 induction following vehicle or 20 mg/kg imipramine (2 h post-injection). Dashed white box was used as the inset image to examine pMeCP2 and GAD67 overlay in (c). ac, anterior commissure. (c) pMeCP2 (red), GAD67 (green), and overlay immunostaining in the NAc 2 h after treatment with 20 mg/kg imipramine. White arrows indicate neurons coimmunolabeled with antibodies for pMeCP2 and GAD67. Scale bar= 20 μ m. n= 4-5 mice/group. For (a), * $p < 0.05$. Error bars indicate S.E.M.104

Figure 17: S421A KI mice exhibit a depression-like phenotype in assays involving stress. (a) KI mice and their WT littermates were injected with Veh or imipramine (10 or 20 mg/kg) 30 min prior to the forced swim. Total time immobile and treading over the six minute test was recorded. (b) KI mice and their WT littermates were injected with Veh 30 minutes prior to the tail suspension test, and the amount of time immobile each minute of the six minute test was recorded. (c) KI mice and WT littermates were tested for their preference for increasing concentrations of sucrose in a two-bottle choice test. n=4-10 mice/group for (a), n=6-7 mice/group for (b), and n=7-10 mice/group. For (a),

* $p < 0.05$ compared to Veh within each genotype and # $p < 0.05$ WT Veh compared to KI Veh. For (b), * $p < 0.05$ compared to WT at each time point.

Error bars indicate S.E.M. 109

Figure 18: S421A mutant mice fail to show behavioral response to chronic imipramine treatment in social defeat stress. (a) Schematic representation of the chamber used for the social interaction test. The interaction zone is defined as the region directly surrounding the chamber that is either empty (first 2.5 min of test) or contains a CD1 mouse (last 2.5 min of test). (b,c) After 10 consecutive days of social defeat, KI and WT mice were tested for social interaction. The total time spent in the interaction zone (b) and the total time spent in the corners (c) in the presence of a CD1 aggressor. (d,e) Following 10 days of social defeat, KI and WT mice were treated acutely or chronically with imipramine for 28 days. On the day following the last injection, the mice were tested once again for social interaction. The total time in the interaction zone (d) and the total time in the corners (e) in the presence of a CD1 aggressor. $n = 6-19$ mice/group for (b,c), and $n = 6-13$ mice/group for (d,e). For (b,c), * $p < 0.001$ compared to control within each genotype. For (d,e), * $p < 0.001$ compared to control within each genotype and # $p < 0.001$ WT chronic compared to KI chronic. Error bars indicate S.E.M. 112

Figure 19: pMeCP2 in the lateral habenula is differentially induced by acute and chronic imipramine treatment following social defeat stress. (a) C57BL/6 mice were injected with Veh (28 d), acute imipramine (27 d of Veh injections followed by imipramine injection on day 28), or chronic imipramine (28 d) following 10 consecutive days of social defeat stress. pMeCP2 immunoreactivity was examined in the NAc, PLC, cingulate cortex, hippocampus, and LHb. (b) Inset image of the dashed white box in (a) of pMeCP2 immunoreactivity in the LHb. (c) pMeCP2 immunoreactivity in the LHb following Veh or acute or chronic imipramine treatment. $n = 8-9$ mice/group. For (c), $p < 0.05$ compared to Veh. Error bars indicate S.E.M. Scale bars = 10 μ m. 116

Figure 20: Generation of a *Carf* exon 8 KO mouse. (a) Genomic organization of the *Mus musculus Carf* gene which spans 53kB on chromosome 1. Boxes represent exons. E: *EcoRV*, M: *MscI*, X: *XbaI*. Ovals show *FRT* sites, triangles show *loxP* sites. The box under *Neo/Zeo* represents the position of the *neomycin* resistance gene in the targeting vector. The numbers and arrows indicate the size of genomic fragments generated on Southern blotting by cleavage with the indicated enzymes. (b) Southern blot analysis of ES cell line 112. Positions of the 5' and 3' probes are indicated in part A. WT, wild-type, 112, ES clone 112 with targeted mutation of *Carf* gene. Arrowhead indicates WT allele, asterisk shows targeted allele. (c-e) PCR analysis of targeted clone 112. (c) Primers across the 3' *loxP* site show the 40bp insertion. Position of primers is indicated by the light gray arrows (d) Recombination of the Neomycin resistance cassette. Position of primers is indicated by the black arrows. (e) Deletion of exon 8 with primers that cross the deletion. Position of primers is indicated by the medium gray arrows. (f-g) PCR analysis of cDNA made from neurons of nonrecombined (WT) or *Cre* recombined (d8) targeted mice. (f) Primers spanning from exons 7-9 (black arrows). (g) Primers spanning the full coding region (gray arrows) show a single band approximately 190bp shorter than full length *Carf*. (h) *Bdnf* promoter IV enhanced luciferase reporter gene expression in transfected

293T cells with cotransfected CaRF deletion constructs. d8: deletion of exon 8; d8-12: deletion of exons 8-12. Bars represent the mean and error bars show S.E.M. All data are the result of at least three independent replicates. * $p < 0.05$149

Figure 21: *Carf* exon 8 KO mice lack nuclear CaRF protein and CaRF-dependent transcription. (a) Western blot of nuclear extracts from brains of *Carf* WT and *Carf* KO mice. 10 μ g nuclear extract was separated by SDS-PAGE and transferred to PVDF membrane for probing with antibodies against CaRF and the neuronal transcription factor MEF2D. Four immunoreactive bands spanning from 85-100kD are seen in the WT lanes and absent in the KO lanes. MEF2D is shown as a loading control. (b-c) EMSA with nuclear extracts from neurons of *Carf* WT and KO mice. 1 μ g nuclear extract was incubated with 50fmol ³²P labeled DNA probes containing either (b) a high-affinity consensus CaRF-binding element (cCaRE) or (c) a USF1/2 binding element from the *Bdnf* gene (CaRE2) (Chen et al., 2003). The specificity of slowly migrating bands was determined by competition of the complex with a 100-fold molar excess of unlabeled probe (Ct). Specific retarded bands are marked with an arrow. (d) Western blot of CaRF expression in cultured embryonic fibroblasts from *Carf* WT, HET, and KO mice. 10 μ g nuclear extract was separated by SDS-PAGE and transferred to PVDF for probing with antibodies against CaRF. Histone H3 is shown as a loading control.151

Figure 22: Distribution and developmental regulation of CaRF in the CNS. (a) Western blot of CaRF expression in nuclear extracts from adult brain regions. 10 μ g nuclear extract was loaded for each region. Ctx, cortex; H, hippocampus; Str, striatum; BS, brainstem; Cb, cerebellum. CREB is shown as a control for comparison. (b) Double immunostaining of cortical neuron cultures for CaRF and the neuronal marker MAP2. P0+10DIV *Carf* WT or KO neurons on PDL-coated coverslips were incubated with antibodies against CaRF (red) and MAP2 (green). Nuclei were labeled with Hoeschst in blue. Bright CaRF immunoreactivity is visible in the nuclei of MAP2 positive cells (example marked with white asterisks) in WT cultures, but is not present in KO cultures. (c) *Carf* mRNA expression from brain at different developmental ages. E10, E15, E17, embryonic days; P1, P8, P21, postnatal days; Ad, adult. Expression was normalized to the housekeeping gene *Gapdh* and is depicted as fold change relative to expression at E10. (d) Western blot of CaRF protein expression in whole brain nuclear extracts harvested at different developmental ages. 10 μ g nuclear extract was loaded into each lane. MEF2D is shown for comparison.153

Figure 23: Expression of *Bdnf* exon IV and BDNF protein is reduced in *Carf* KO cortex. (a) *Bdnf* exon IV mRNA expression in cortex dissected from *Carf* WT and KO mice during the first 2 weeks of postnatal life or from P0 cortex cultures that were made from individual WT or KO siblings of HET x HET crosses. Cultured neurons were treated with 1 μ M TTX overnight before mRNA harvesting. Gene expression is normalized to *Gapdh* to control for sample handling and results are scaled to the average value of the WT sample (WT average = 1). Postnatal cortex, $n=7$ WT and 6KO, P0 cortex culture $n=3$ WT and 4KO. (b) KCl-dependent induction of *Bdnf* exon IV expression in *Carf* WT and KO neurons cultured as in (a). Membrane depolarization was induced by

addition of 55mM extracellular KCl for 1, 3, or 6 hours prior to mRNA harvesting. $n=2$ WT and 3KO at each time point. **c)** Expression of *Bdnf* exon I, II, IV, or VI-containing mRNA transcripts in cerebral cortex dissected from adult *Carf* WT and KO mice 2-6 months of age. $n=8$ WT and 10KO. **D)** BDNF protein expression in frontal cortex, hippocampus, or striatum dissected from adult *Carf* WT or KO mice. Results are scaled relative to the average WT level in each tissue (WT average = 100%). Frontal cortex, $n=8$ WT and 9KO; hippocampus $n=3$ WT and 3KO; striatum $n=7$ WT and 8KO. Bars show the mean and error bars show SEM. $*p<0.05$157

Figure 24: Increased expression of GABAergic synaptic proteins in the striatum of *Carf* KO mice. **(a)** Striata were freshly dissociated from coronal sections of 3 *Carf* WT (left three lanes) and 3 KO (right three lanes) adult mouse brains, then the samples were weighed and homogenized in Laemli SDS sample buffer. 20 μ g total lysate was used for immunoblotting with the indicated antibodies and immunoreactivities were visualized with ECL. **(b)** Quantification of the data shown in (a). WT samples are shown in black, KO in gray. Multiple film exposures were taken for each immunoblot and scanned, then band density in each lane was quantified using ImageJ. Expression was normalized to actin for each sample. **(c)** Representative images of GAD-65 immunostaining in coronal sections through the NAc of *Carf* WT or KO brains. Images were chosen that had integrated intensity values closest to the mean for each genotype. The bar shows 10 μ m. **(d)** Representative images of synaptophysin staining in coronal sections as in (c). Bars show the mean and error bars show SEM. $*p<0.05$ compared with WT.161

Figure 25: *Carf* KO mice show normal acquisition of hippocampal-dependent spatial learning and memory, and enhanced performance on a reversal learning task. **(a)** Mean latency to escape to a hidden platform is shown for *Carf* WT, HET, or KO mice over the first 4 consecutive training days. **(b)** Mean latency to escape to a hidden platform on day 5 of training is shown for *Carf* WT, HET and KO mice when spatial cues are visible (cues present) or when curtain has been pulled around the pool (cues removed). **(c)** Percent of total swimming time (60 seconds) spent in each quadrant of the pool when the platform was removed and mice were tested immediately after training. TQ, target quadrant (black); AL, adjacent right quadrant (dark gray); OP, opposite quadrant (light gray); AR, adjacent right quadrant (white). **(d)** Percent of total swimming time (60 seconds) spent in each quadrant of the pool when the platform was removed and mice were tested after a 24 hr retention interval. **(e)** Latency to escape to hidden platform during 4 daily trials of reversal learning over 4 days. **(f)** Percent time spent swimming in each quadrant of the pool on the first day of reversal learning with a new hidden platform location. Quadrants are labeled with respect to the position of the previous target quadrant (previous TQ, black). **(g)** Latency to escape to a visible platform over 4 days of training following reversal learning.163

Figure 26: Impaired extinction of contextual fear conditioning in *Carf* KO mice. On day 0, 11 KO and 7 WT mice were shocked in a novel context (Cond.), and 24 hrs later context-cued retention of the fear memory was measured by returning the animals to the same context (Test). Extinction of fear conditioning was run over 13 consecutive days. The average percent of total time spent freezing over the 5 min test period is graphed for

each day. Points indicate mean, and errors show S.E.M. * $p < 0.05$ for KO compared with WT on a given test day.167

Figure 27: Impaired remote memory for novel object recognition in *Carf* KO mice.

a) Preference for novel object when returned to the test arena 20 min after initial object exposure. **b)** Preference for novel object when returned to the test arena 24 hrs after initial object exposure. **c)** Preference for novel object when returned to the test arena 10 days after initial object exposure. Times of interaction and number of interactions are shown in **Suppl. Tables S3-S4**. Bars indicate mean, and errors show S.E.M. $n = 11$ KO and 7 WT mice. * $p < 0.05$ compared with WT at 0-3 min # $p < 0.05$ compared with WT at 6-9 min.170

Figure 28: Modulation of transcriptional regulatory pathways by psychostimulant-induced intracellular signaling cascades.

Psychostimulants block and/or reverse the dopamine (DA) transporter, leading to an elevation of extracellular DA in the synaptic cleft that activates DA receptors (D1-5). NAc neurons also receive glutamatergic synaptic inputs (Glut) from the prefrontal cortex that activate the AMPA and NMDA-type glutamate receptors. Subsequent membrane depolarization leads the opening of voltage-sensitive calcium channels (L-VSCCs). Calcium (Ca^{2+}) levels may also be elevated by the release of calcium from intracellular stores. The activation of G-protein coupled and calcium-dependent signaling cascades leads to the activation or repression of the kinases and phosphatases shown in yellow. These enzymes regulate phosphorylation of transcription factors or transcription factor associated proteins to modulate the activation of transcriptional pathways. Some transcription factors are regulated by nuclear localization (NF- κ B, NAC1) while others are regulated by posttranslational modifications that alter their association with transcriptional co-regulators (CREB, MEF2). These changes lead to psychostimulant dependent activation (green arrow) or repression (red arrow) of target gene expression.184

Figure 29: Transcriptional regulatory pathways that converge on enhancement of dendritic spine density.

Activation is indicated by green arrows, inhibition by red bars. Dopamine D1 receptor dependent increases in cAMP activate CREB and inactivate MEF2. CREB drives transcription of Δ FosB, which represses transcription of the histone methyltransferase G9a. Because G9a represses NF- κ B, the net outcome is to increase NF- κ B transcription. Δ FosB also activates transcription of Cdk5, which further inhibits MEF2. The net result of simultaneous activating CREB, Δ FosB, NF- κ B and Cdk5 while inactivating MEF2 and G9a is to drive an increase in MSN dendritic spine density.197

Figure 30: Summary of transcriptional regulatory pathways that contribute to the behavioral response to psychostimulants.

Red indicates repressors and repression of gene expression, green indicates transcriptional activators and activation of transcription.220

ABBREVIATIONS AND ACRONYMS

AMPH	amphetamine
BLA	basolateral amygdale
BDNF	brain-derived neurotrophic factor
cAMP	cyclic adenosine monophosphate
CPP	conditioned place preference
DA	dopamine
DAT	dopamine transporter
GAD	glutamic acid decarboxylase
HDAC	histone deacetylase
HPA	hypothalamic-pituitary-adrenal
KI	knockin
KO	knockout
LHb	lateral habenula
MBD	methyl-CpG-binding domain
MeCP2	methyl-CpG-binding protein 2
MSN	medium spiny neuron
NAc	nucleus accumbens
NE	norepinephrine
NET	norepinephrine transporter
PLC	prelimbic region of the frontal cortex
pMeCP2	Ser421 phosphorylation
RTT	Rett syndrome

S421	serine 421
S421A	serine to alanine mutation at 421
SERT	serotonin transporter
VTA	ventral tegmental area
WT	wild-type
5-HT	serotonin

ACKNOWLEDGEMENTS

I am very grateful to my adviser, Anne West, for her guidance and support during my time in the lab. Not only did she help me grow in my ability to conduct research, but she also provided an excellent example of a mentor who deeply cares for those in her lab. Her passion for research and her desire to see the field of activity-dependent transcription advance have motivated me to continue to pursue my career. I would also like to thank the members of my thesis committee, Cynthia Kuhn, Ted Slotkin, Donald McDonnell, William Wetsel, and Marc Caron, for their expertise and encouragement.

I thank William Wetsel, Ramona Rodriguez, and the other members of the Behavioral Core at Duke for helping me conduct behavioral studies in mice. Ramona spent countless hours training me in various behavioral paradigms and teaching me how to perform statistical analyses. I thank Benjamin Sachs for his assistance in conducting chronic social defeat stress. I am also grateful to Herb Covington for helping me interpret my social defeat stress data and advising me in my experimental design.

I am indebted to the members of the West lab for their critical evaluation of my work and assistance in conducting my experiments. Specifically, I would like to thank Jay Deng for challenging me to think critically and assisting me in behavioral analyses. I thank Jay for his encouragement and friendship, and I have truly appreciated working alongside of him for the past 4.5 years.

I thank my husband, Shane, for his loving support during my graduate work. He has encouraged me to pursue excellence and integrity, both in and out of the lab. I would also like to thank my mom, dad, and sister, Courtney, for their continued encouragement and love as I have continued in my career. Finally, I would like to thank the women of

the past 5 senior classes who have participated in Campus Crusade for Christ at Duke.
My involvement as a volunteer staff with Crusade has truly shaped my experience in
graduate school, teaching me to pursue my faith in Christ in everything I do.

1. INTRODUCTION

1.1 BEHAVIORAL ADAPTATIONS TO CHRONIC MONOAMINERGIC SIGNALING

1.1.1 The behavioral responses to repeated psychostimulant and antidepressant exposure

Activation of monoaminergic receptors is essential to the mechanism by which psychostimulants and antidepressants exert long-lasting changes in behavior (Brenes and Fornaguera, 2009; Krishnan and Nestler, 2008; Gainetdinov and Caron, 2003; Missale *et al*, 1998; Xu *et al*, 1998). Psychostimulants bind directly to the dopamine (DAT), serotonin (SERT), and norepinephrine (NET) transporters and increase extracellular levels of these monoamines. The majority of antidepressants increase serotonin (5-HT) and norepinephrine (NE) transmission by blocking the transporters or inhibiting the monoamine oxidase enzymes. Despite the fact that psychostimulants and antidepressants rapidly increase monoaminergic transmission, repeated exposure to these drugs is necessary to produce long-lasting alterations in behavior. Addictive behavior does not appear after one exposure to psychostimulants (Hyman *et al*, 2006), and antidepressants must be administered for several weeks or months in order to alleviate symptoms of depression (Berton and Nestler, 2006). Therefore, it is likely that molecular mechanisms downstream of chronic monoaminergic transmission mediate the observed behavior adaptations.

One mechanism by which chronic activation of monoaminergic signaling mediates behavior adaptations is by altering the function and structure of neural circuits in the brain. For example, psychostimulants drive changes in behavior by inducing structural and functional changes in the mesolimbocortical dopamine (DA) reward

circuit, which is comprised of DA neurons in the ventral tegmental area (VTA) and their synaptic targets in the nucleus accumbens (NAc), prelimbic region of the frontal cortex (PLC), and associated limbic structures (Robinson and Kolb, 1997). Chronic psychostimulant exposure leads to changes in both functional and structural plasticity of synapses in the striatum, and these alterations have been implicated in the expression of behavioral sensitization and conditioned place preference (CPP) (Huang *et al*, 2009; Nestler, 2001; Thomas *et al*, 2001). Given this functional correlation between structural plasticity and behavior, there has been great interest in identifying the molecular pathways that link psychostimulant-induced monoamine receptor activation to changes in synapses. Investigation of the mechanisms underlying changes in synaptic structure and function has shown that this process depends, in part, on the transcription of new gene products that modulate neuronal excitability and synaptic structure or function (Russo *et al*, 2009; Moratalla *et al*, 1996). The program of psychostimulant-regulated gene expression includes genes such as brain-derived neurotrophic factor (*Bdnf*) and cyclin-dependent kinase 5 (*Cdk5*) whose protein products act directly on synapses to modulate their structure and/or function, suggesting a mechanism by which changes in transcription in response to psychostimulant exposure could impact brain function (Pulipparacharuvil *et al*, 2008; Grimm *et al*, 2003; Bibb *et al*, 2001).

Similarly, several brain regions, including the hippocampus, frontal cortex, hypothalamus, NAc, etc., regulate emotion and stress, and dysfunction within these forebrain networks has been implicated in depression (Krishnan and Nestler, 2008). These brain regions are highly innervated by monoamine projections from the VTA (DA), dorsal raphe nuclei (5-HT), and locus coeruleus (NE). The “monoamine

hypothesis” of depression, which was based on the observation that compounds that increase monoaminergic transmission have antidepressant effects, presented the idea that depression is caused by decreased monoamine function in the brain (Berton and Nestler, 2006). However, the long timescale by which antidepressants alleviate symptoms of depression suggests the possibility that these drugs exert their effects by mediating changes in gene expression. For example, chronic social defeat stress, an animal model of depression in which repeated exposure to an aggressor induces social avoidance that is reversed with chronic but not acute antidepressant treatment, causes long-lasting downregulation of *Bdnf* in the hippocampus (Tsankova *et al*, 2006). This downregulation of *Bdnf*, as well as the depression-like phenotype, is reversed with chronic antidepressant treatment. Furthermore, it has been shown that the transcription factor Δ FosB accumulates in the NAc in response to repeated stress exposure and promotes the active coping response to stress (Vialou *et al*, 2010). This increase in Δ FosB induction is required for chronic antidepressants to reverse behavioral symptoms of depression. These results suggest that changes in the expression of genes whose products modulate neurogenesis, synaptic structure and/or function, hypothalamic-pituitary-adrenal (HPA) axis function, and other processes are involved in the behavioral response to antidepressants (Krishnan and Nestler, 2008).

1.1.2 Epigenetic mechanisms of gene regulation

Examination of the molecular processes underlying psychostimulant- and antidepressant-dependent changes in gene expression has revealed a significant role for epigenetic mechanisms of chromatin regulation. Epigenetic mechanisms refer to processes that result in stable changes in gene expression without altering the DNA

sequence itself. Gene transcription does not occur on DNA alone but is carried out in the context of chromatin, which is comprised of genomic DNA and its associated histone proteins. The basic unit of chromatin is the nucleosome, which contains 147 base pairs (bp) of DNA wrapped around a histone octamer containing two copies of each of the core histones (H2A, H2B, H3, and H4) (Tsankova *et al*, 2007). Chromatin exists in two states: an inactivated, closed state that does not allow gene transcription and an activated, open state that is permissive to transcription. The state of the chromatin can be altered via modifications of the N-terminal tail of histones; these epigenetic marks include acetylation, methylation, phosphorylation, and ubiquitination (Jiang *et al*, 2008). Acetylation of lysine residues reduces the electrostatic interactions between histone proteins and DNA, relaxing chromatin and allowing access of transcriptional regulators to the DNA (Borrelli *et al*, 2008). Therefore, high levels of histone acetylation are generally associated with transcriptional activation. Histone acetylation is a dynamic process that is controlled by histone acetyltransferases (HATs), enzymes that add acetyl marks, and histone deacetylases (HDAC), enzymes that remove these marks. Unlike acetylation, histone methylation occurs on lysine or arginine residues in mono-, di-, and tri-methylated states, and methylation of different residues can exert opposite effects on transcription (Renthal and Nestler, 2009). Similar to histone acetylation, histone methylation can also be regulated. Histone methyltransferases (HMTs) add methyl groups and histone demethylases (HDM) remove these marks.

Another well-studied epigenetic mechanism of gene regulation is DNA methylation. DNA methylation occurs by the transfer of a methyl group to cytosine residues at CpG dinucleotides by enzymatic action of a small family of DNA

methyltransferases (DNMT1, DNMT3a, DNMT3b) (Tsankova *et al*, 2007). CpGs are typically heavily methylated throughout the genome. The exception to this trend is CpG islands, which are dense clusters of CpGs that are found at the promoter regions of genes. The amount of DNA methylation at these regions correlates with the extent of gene inactivation. DNA methylation influences gene transcription by two main mechanisms (Kriaucionis and Bird, 2003). First of all, the presence of the bulky methyl group can interfere with the binding of transcription factors to DNA. Secondly, a group of proteins bind methylated DNA (MBDs) and influence transcription through the recruitment of histone modifying enzymes. Therefore, MBDs can serve as a link between DNA methylation and changes in chromatin structure.

1.1.3 The role of epigenetic mechanisms in the behavioral adaptations to repeated psychostimulant exposure

A growing body of evidence suggests that epigenetic mechanisms of gene regulation may contribute to persistent, psychostimulant-dependent changes in gene expression and long-lasting plasticity in the brain. For example, Kumar and colleagues conducted one of the first studies to examine whether chromatin remodeling at specific gene promoters may be a mechanism to account for the persistent changes in gene expression following chronic cocaine exposure (Kumar *et al*, 2005). They found increases in H3 phosphoacetylation and H4 acetylation after acute cocaine on the *cFos* promoter, but saw no changes in histone modifications in mice treated with chronic cocaine compared to saline controls. These data are consistent with the fact that *cFos* is activated by acute cocaine but shows desensitization after chronic exposure. On the other hand, acute cocaine does not induce changes in histone modifications at the *cdk5* and

Bdnf promoters, but chronic cocaine increases H3 acetylation at these promoters, which is coincident with the activation of these genes by chronic cocaine. Together, these results show that cocaine regulates histone modifications at specific gene promoters in a manner that is consistent with the activation status of the underlying genes.

In addition to showing that cocaine can regulate chromatin remodeling, several studies investigated the functional role of histone modifications in the behavioral response to repeated psychostimulant exposure. To examine the functional consequences of changes in histone acetylation, Kumar and colleagues systemically administered trichostatin A (TSA), an HDAC inhibitor and found that this drug enhances the rewarding effects of cocaine in CPP (Kumar *et al*, 2005). Overexpression of HDAC4 in the ventral striatum reduces the amount of time spent in the previously drug-paired chamber in CPP, suggesting that histone acetylation is important for the rewarding effects of cocaine. Further supporting a role for histone acetylation in the behavioral response to repeated cocaine exposure, Renthall and colleagues overexpressed HDAC5 in the NAc and saw that this manipulation decreased the rewarding effects of cocaine as measured by CPP (Renthall *et al*, 2007). These data suggest that the regulation of histone acetylation may be a potential mechanism by which chronic cocaine exposure induces changes in behavior.

Beyond demonstrating a role for HDACs in the behavioral response to psychostimulant exposure, studies have also pointed to the importance of other chromatin regulatory proteins that are targets of modulation by psychostimulant-induced signaling pathways. It is known that recruitment of the transcriptional activator CREB binding protein (CBP) is a major mechanism by which Ser133 phosphorylation induces CREB-

dependent transcription (Mayr and Montminy, 2001). CBP has intrinsic HAT activity (Goodman and Smolik, 2000); therefore, it is possible that CBP mediates changes in histone acetylation in response to cocaine exposure. Levine and colleagues demonstrated that acute cocaine exposure results in an increase in CBP binding to the *Fosb* promoter that is coincident with increased H4 acetylation at this promoter (Levine *et al*, 2005). To determine if CBP directly regulates acetylation of the *Fosb* promoter, the authors utilized CBP haploinsufficient mice. They observed decreased *Fosb* induction following acute cocaine and decreased accumulation of *Fosb* following repeated cocaine exposure in CBP haploinsufficient mice compared to WT littermates. In addition to regulating *Fosb* transcription in response to cocaine exposure, CBP is also involved in the behavioral adaptations to chronic cocaine. CBP haploinsufficient mice show reduced sensitivity to the locomotor stimulating effects of cocaine and reduced sensitization to chronic cocaine compared to wild-type (WT) littermates, supporting the notion that CBP plays a role in mediating behavioral adaptations to cocaine.

Advancing the initial studies that focused on chromatin regulation at specific gene promoters, genome-wide techniques enable one to look at the changes in histone modifications at promoters throughout the genome. In order to study genome-wide chromatin modifications following chronic cocaine, Renthal and colleagues utilized a technique called ChIP-chip (Renthal *et al*, 2009). Chromatin immunoprecipitation (ChIP) is a method used to determine the location of DNA binding sites for a protein of interest. Antibodies are used to immunoprecipitate the protein, and the co-immunoprecipitated DNA is then identified by various methods. The association of the proteins with promoter regions is quantified by hybridizing the co-immunoprecipitated

DNA with genome-wide promoter microarrays. The results of this study showed that histones are modified at select sets of genes and that different kinds of histone modifications are induced by cocaine at different gene promoters. Genome-wide technology in this study also uncovered a novel role for the sirtuins 1 and 2 (SIRT1 and SIRT2), which are class III HDACs, in the behavioral adaptations to chronic cocaine. Administration of sirtinol, a sirtuin inhibitor, decreased the rewarding properties of cocaine in CPP and self-administration, whereas resveratrol, an activator of the sirtuins, had the opposite effect.

The genome-wide study conducted by Renthal and colleagues also revealed a possible role for histone methylation in the response to repeated cocaine exposure (Renthal *et al*, 2009). Their data shows that repeated cocaine induced changes in H3K9 and H3K27 methylation at different gene promoters. In order to see how cocaine mediates changes in histone methylation, Maze and colleagues investigated the regulation of HMTs and HDMs by repeated cocaine exposure and found that repeated cocaine leads to a down-regulation of G9a, a HMT, in the NAc (Maze *et al*, 2010). To examine the consequences of G9a down-regulation on chronic cocaine-induced gene expression, HSV vectors were used to overexpress G9a in the NAc. Overexpression of G9a decreased the expression of 50% of the genes that typically show enhanced expression following repeated cocaine. Finally, in order to determine a functional role for G9a in the behavioral adaptations to repeated cocaine exposure, G9a was overexpressed in the NAc and the behavior of these mice was assessed in CPP. G9a overexpression diminished the rewarding effects of cocaine in CPP, whereas AAV-Cre knockdown of G9a increased the preference for the cocaine-paired chamber. Together, these results suggest a novel role

for histone methylation and HMTs in the adaptations to repeated cocaine exposure.

1.1.4 Epigenetic mechanisms and the behavioral responses to repeated antidepressant treatment

In addition to mediating molecular and behavioral adaptations to chronic psychostimulant exposure, epigenetic mechanisms of gene regulation also play a role in stress, depression, and the behavioral response to chronic antidepressant treatment. Weaver and colleagues demonstrated how events early in life affect patterns of DNA methylation that ultimately influence responses to stress in adulthood (Weaver *et al.*, 2004). They find that the extent to which a mother rat licks and grooms her pups before weaning correlates with reduced expression of anxious behavior when the pups grow to adulthood compared with pups that did not experience high levels of grooming by their mothers. Examination of the molecular mechanisms underlying the differences in behavior between the two sets of pups showed that licking and grooming by the dams alters the pattern of DNA methylation in the promoter region of the glucocorticoid receptor (GR) in the hippocampus of the pups. Pups that were licked and groomed had less DNA methylation at the GR promoter that was coincident with increased expression of GR compared to pups that were not groomed. This study demonstrates how epigenetic modifications can be regulated by environmental stimuli and how these modifications in turn mediate persistent changes in gene expression and behavior.

Furthermore, studies have shown that epigenetic mechanisms also play a role in the response to several treatments for depression. It has been shown that electroconvulsive seizures, one of the most effective treatments of major depression, regulate the expression of several genes in the hippocampus, including *BDNF* and *cFos*

(Nibuya *et al*, 1995; Morgan *et al*, 1987). Tsankova and colleagues examined whether changes in histone modifications following acute and chronic ECS could serve as a possible mechanism by which ECS mediates changes in gene expression (Tsankova *et al*, 2004). In order to ask this question, they utilized ChIP to measure H3 and H4 acetylation as well as H3 phosphoacetylation at the *cfos* and *BDNF* promoters after acute or chronic ECS. Acute ECS resulted in increases in H4 acetylation and H3 phosphoacetylation but no changes in H3 acetylation at the *cFos* promoter. The levels of H4 acetylation and H3 phosphoacetylation were similarly induced in the chronic ECS and acute ESC groups 2 hrs after the last exposure. However, H4 acetylation was significantly decreased 24 hrs after the last exposure in the chronic ESC group compared to the control. These findings support the possibility that decreased H4 acetylation could have a role in the desensitization of *cFos* following chronic ECS. In addition, investigation of histone modifications on the *BDNF* promoter showed that acute ECS increases H4 acetylation, whereas chronic ECS drives increases in H3 acetylation and H3 phosphoacetylation. The increases in H3 acetylation at certain *BDNF* promoters remain elevated 24 hours after the last ECS exposure, and the authors speculate that this increased acetylation may play a role in mediating prolonged *BDNF* transcription in response to chronic ECS.

Similar to ECS, repeated exposure to most medicinal antidepressants is necessary in order to see alleviation from symptoms of depression. Tsankova and colleagues investigated whether chromatin modifications play a role in depression-like symptoms and the behavioral response to antidepressants (Tsankova *et al*, 2006). Their data shows that chronic social defeat stress downregulates *Bdnf* transcripts III and IV coincident with increases in H3-K27dimethylation at their promoters. Although chronic imipramine does

not reverse this dimethylation, it does result in a two-fold increase in H3 hyperacetylation at select *Bdnf* promoters, which drives the de-repression of *Bdnf* III and IV following chronic treatment. To investigate the mechanisms leading to increased histone acetylation following chronic imipramine treatment, Tsankova and colleagues then looked to see if chronic antidepressant treatment regulates the level of specific HDACs. Specifically, *Hdac5* mRNA levels were decreased in defeated mice that had been treated with chronic imipramine. Further supporting a role for HDACs in the molecular response to chronic imipramine, HDAC5 overexpression in the dentate gyrus blocked the ability of chronic imipramine to reverse social avoidance following defeat. Similarly, Covington and colleagues found that inhibitors of class I and II HDACs have antidepressant effects when injected directly into the NAc (Covington *et al*, 2009). These findings implicate a significant role for histone remodeling in the pathophysiology and treatment of depression.

Traditionally, studies have only focused on the role of histone modifications in depression and antidepressant response. Recently, LaPlant and colleagues investigated the role of DNA methylation in the behavioral adaptations to chronic cocaine exposure and chronic social defeat stress (LaPlant *et al*, 2010). Chronic social defeat stress (10 days of defeat) resulted in an increase in *Dnmt3a*, a DNA methyltransferase (Dnmt), in the NAc up to 10 days following the last defeat. In order to determine the functional relevance of this upregulation, *Dnmt3a* was overexpressed in the NAc of mice prior to chronic social defeat stress. *Dnmt3a* overexpression caused mice to show social avoidance after only 1 day of defeat whereas mice expressing control vectors do not exhibit defeat under these parameters, suggesting that *Dnmt3a* has pro-depressive effects

in the NAc. Furthermore, continuous intra-NAc infusion of RG108, a non-nucleoside inhibitor of DNA methylation, 1-10 days after chronic social defeat stress reversed social avoidance in a similar fashion to traditional antidepressants. Therefore, inhibition of Dnmt3a in the NAc has antidepressant-like effects in this paradigm. Like histone modifications, levels of DNA methylation in the NAc play an important role in gating the response to emotional stimuli.

1.2 MECP2: A TRANSCRIPTIONAL REGULATOR LINKING DNA METHYLATION AND CHROMATIN MODIFICATIONS

1.2.1 MeCP2 is a methyl-DNA binding protein

Taken together, these studies suggest that chromatin regulatory proteins downstream of monoaminergic signaling are strong candidates for transducing chronic psychostimulant or antidepressant exposure into persistent changes in brain function and behavior. Another candidate transcription factor that is well-poised to contribute to the behavioral adaptations in response to chronic activation of monoaminergic signaling is the methyl-CpG-binding protein 2 (MeCP2). MeCP2 was purified based on its ability to bind methylated DNA and was shown to colocalize with chromosomal regions that are rich in methyl-CpGs (Lewis *et al*, 1992). Based on the evidence demonstrating a role for methylated DNA in transcriptional repression (Boyes and Bird, 1991; Keshet *et al*, 1985; Stein *et al*, 1982), MeCP2's ability to bind methylated DNA suggested that it may play a role in mediating the effects of methylation on transcription and chromatin structure.

In an effort to understand the role MeCP2 plays in regulating transcription, several studies characterized the function of different domains of the MeCP2 protein

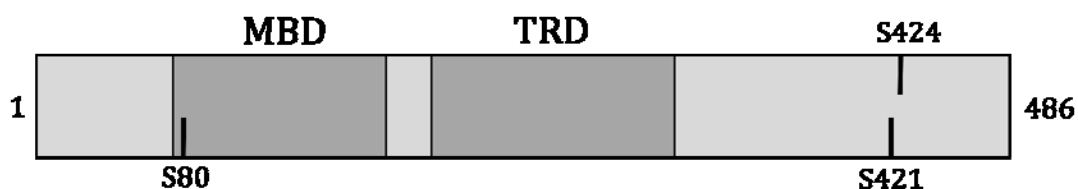


Figure 1: Map of MeCP2 protein. The MeCP2 contains a methyl DNA-binding domain (MBD) and a transcriptional repressor domain (TRD) that recruits histone-modifying enzymes. S80, S421, and S424 are sites of phosphorylation.

(Figure 1). Nan and colleagues isolated the methyl-CpG binding domain (MBD) of MeCP2, which binds to DNA that contains at least one or more symmetrically methylated CpGs and is essential for the chromosomal localization of MeCP2 (Nan *et al*, 1993). The MBD domain is necessary for transcriptional repression, as a mutant version containing a deletion in the MBD failed to repress transcription *in vitro* (Nan *et al*, 1997). However, deletion of the C-terminal half of the protein weakened MeCP2's ability to repress transcription even when the MBD was left intact, suggesting that the C-terminus is required for efficient repression *in vitro*. In addition to the MBD, MeCP2 also contains a transcriptional repressor domain (TRD) by which it recruits a co-repressor complex comprised of HDACs and Sin3a (Nan *et al*, 1998; Jones *et al*, 1998). This co-repressor complex in turn modifies histone proteins and alters the transcriptional potential of nearby genes. *In vivo*, transcriptional repression of MeCP2 is relieved by the HDAC inhibitor Trichostatin A, suggesting that histone acetylation is an important mechanism by which MeCP2 regulates transcription (Nan *et al*, 1998).

1.2.2 Examination of the mechanisms by which MeCP2 regulates transcription

The findings from the initial studies examining the function of MeCP2 support a

model in which MeCP2 binds to methylated DNA at the promoters of genes and represses transcription via the actions of its associated co-repressor complex. Therefore, one would hypothesize that mutations in *Mecp2* would relieve repression and lead to the upregulation of genes that are targets of regulation by MeCP2. Surprisingly, there were only subtle differences in gene expression in brains from *Mecp2*-null mice compared to their WT littermates (Tudor *et al*, 2002). A later study comparing differences in gene expression between *Mecp2*-null mice and their WT littermates found that a small set of genes, which are induced by glucocorticoids, are over-expressed in the absence of MeCP2 (Nuber *et al*, 2005). Furthermore, Chahrour and colleagues examined gene expression patterns in the hypothalamus of mice lacking or overexpressing MeCP2, hypothesizing that changes in gene expression might be occurring in specific brain regions in the absence of MeCP2 (Chahrour *et al*, 2008). Altering MeCP2 levels in the hypothalamus results in subtle changes in the expression of many genes; however, many of the genes appeared to be activated by MeCP2, suggesting the possibility that MeCP2 can also function as an activator of transcription. The lack of robust alterations in gene expression in *Mecp2* mutant mice suggests that MeCP2 may not be acting as a gene-specific transcriptional repressor and may be acting through a more complex mechanism.

In order to investigate alternative mechanisms for MeCP2 function, Skene and colleagues conducted an eloquent study to examine the abundance and distribution of MeCP2 in the mature mouse brain (Skene *et al*, 2010). They found that MeCP2 is highly enriched in neurons but not glia, and the abundance of MeCP2 approaches the levels of the histone octamer. Chromatin immunoprecipitation (ChIP) revealed that MeCP2 binds globally across the genome and its binding tracks the density of methylated DNA in the

genome. Since MeCP2 is so highly expressed, they then wanted to examine changes in chromatin structure in the absence of MeCP2. In *Mecp2*-null mice, the levels of histone H3 acetylation were globally elevated and levels of histone H1, the linker histone, were doubled compared to brains from WT littermates. Finally, the brains from the *Mecp2*-null mice showed elevated transcription of repetitive elements, suggesting that MeCP2 deficiency results in an increase in transcriptional noise. Skene and colleagues propose a model in which MeCP2 binds globally to methylated DNA and dampens transcription genome-wide by recruiting HDACs and acting as a linker histone. These findings go beyond the earlier notion that MeCP2 acts as a transcriptional repressor targeted to a specific set of genes and suggests that MeCP2 may influence chromatin structure genome-wide.

1.3 STUDIES FROM MOUSE LINES BEARING MUTATIONS IN MECP2

1.3.1 Mutations in MeCP2 cause the neurodevelopmental disorder Rett Syndrome

Understanding the mechanism by which MeCP2 regulates transcription is of particular interest in the nervous system because loss-of-function mutations in human *MECP2* cause the neurodevelopmental disorder Rett Syndrome (RTT) (Bienvenu *et al*, 2000; Amir *et al*, 1999). RTT is an X-linked neurodevelopmental disorder that affects 1 in 10,000 live female births and is one of the leading causes of mental retardation in females (Hagberg *et al*, 1983). Individuals with RTT experience normal development up to 6-18 months of age and then enter a period in which they can no longer acquire new skills and experience motor and language skill regression. The features of RTT become more apparent with time and include cognitive and social impairments, autism-like

behavior, stereotypical hand wringing, and irregular breathing. Intriguingly, the onset of RTT occurs around the time period that sensory experience drives synaptic reorganization for properly functioning cortical circuits, which suggests that MeCP2 may be important for neuronal maturation as well as synapse formation.

Table 1: Mice bearing mutations in the methyl-CpG-binding protein 2 (MeCP2). These mouse models have been used to understand how the loss of MeCP2 contributes to RTT as well as to assess the function of MeCP2.

Mutation	Behavioral phenotype	Reference
<i>Mecp2</i> -null	Motor deficits, hindlimb claspings, and irregular breathing by 4-6 weeks of age; die by 6-12 weeks	Chen <i>et al</i> , 2001; Guy <i>et al</i> , 2001
<i>Mecp2</i> ³⁰⁸	Tremors, stereotypic forelimb motions and claspings, motor deficits by 6 weeks of age; display heightened anxiety and deficits in learning and memory	Moretti <i>et al</i> , 2006; Shahbazian <i>et al</i> , 2002
Targeted deletion of <i>Mecp2</i> in the forebrain	Motor deficits, heightened anxiety, deficits in learning and memory, abnormal social interactions; symptoms do not appear until 3 months of age	Gemeli <i>et al</i> , 2005; Chen <i>et al</i> , 2001
Targeted deletion of <i>Mecp2</i> in the GABAergic neurons	Motor deficits, stereotypies, alterations in sensorimotor arousal and gating, deficits in learning and memory, alterations in social interaction	Chao <i>et al</i> , 2010
Targeted deletion of <i>Mecp2</i> from the BLA	Heightened anxiety as seen in open field and elevated plus maze	Adachi <i>et al</i> , 2009
Targeted deletion of <i>Mecp2</i> from <i>Sim1</i> -expressing neurons of hypothalamus	Abnormal stress response, alterations in social interaction, heightened aggression, and hyperphagia	Fyffe <i>et al</i> , 2008
S421A mutation	Abnormal responses to novelty	Cohen <i>et al</i> , 2011
S421A/S424A mutation	Enhanced learning and memory in Morris water maze and context-dependent fear conditioning	Li <i>et al</i> , 2011

1.3.2 Mouse models of RTT

Mice bearing mutations in *Mecp2* recapitulate many of the phenotypic features of RTT and have provided a useful model for studying the function of MeCP2 in the brain

(Table 1). Mice lacking *Mecp2* were generated using Cre-*loxP* technology, and these mice were examined as potential mouse models for RTT (Guy *et al*, 2001; Chen *et al*, 2001). Like RTT patients, they exhibited no initial phenotype at birth but showed motor deficits, hindlimb claspings, and irregular breathing by approximately 4 to 6 weeks of age. Although MeCP2 is expressed in most somatic tissues, it is most highly expressed in the brain, specifically in neurons (Skene *et al*, 2010; Kishi and Macklis, 2004). To test whether the effects of the loss of *Mecp2* are specific to the brain, the *Mecp2*-null mutation was combined with the nestin-Cre transgene to express the mutation selectively in neuronal cells (Chen *et al*, 2001). The phenotype of the mice lacking *Mecp2* in the brain was quite similar to that of the *Mecp2*-null mice, suggesting that the major characteristics of the *Mecp2*-null phenotype are due to the absence of *Mecp2* in the brain.

Although the *Mecp2*-null mice recapitulate several of the symptoms of RTT, they die by approximately 6 to 12 weeks of age. Because these mice appear to represent the more severe cases of the disease, mouse models with less severe mutations in *Mecp2* are required to recapitulate many of the features found in females with RTT. Shahbazian and colleagues generated mice with a truncating mutation in *Mecp2* (*Mecp2*³⁰⁸); the MBD and TRD are still intact in these mice (Shahbazian *et al*, 2002). *Mecp2*³⁰⁸ mice do not display behavioral abnormalities until approximately six weeks of age at which time they have tremors, pronounced stereotypic forelimb motions and claspings, decreased agility, and impairments in motor activity. In addition, *Mecp2*³⁰⁸ mice also spent less time in the center of the open field compared to WT littermates, suggesting that *Mecp2*³⁰⁸ mice may exhibit heightened anxiety. Furthermore, *Mecp2*³⁰⁸ mice have abnormal social interactions, which is another characteristic of RTT. Moretti and colleagues later showed

that *Mecp2*³⁰⁸ mice have deficits in spatial memory in the Morris water maze, context-dependent fear conditioning, and long-term social memory (Moretti *et al*, 2006). The milder phenotype of the *Mecp2*³⁰⁸ mice renders these mice suitable for broader behavioral analyses and to examine the function of MeCP2 in the adult brain.

1.3.3 Brain region- and cell-type-specific MeCP2 mutant mice

In addition to creating *Mecp2* mutant mice with different mutations, several lines have been generated that bear mutations in *Mecp2* in specific cell types and brain regions in order to map the neuroanatomic origins of the behavioral abnormalities of RTT and to better understand the function of MeCP2. Chen and colleagues generated conditional knockout mice by crossing floxed *Mecp2* mice with calcium-calmodulin-dependent protein kinase II (CaMKII)-Cre transgenic mice in order to selectively delete *Mecp2* in the forebrain (Chen *et al*, 2001). The onset of symptoms was delayed in these mice, as changes in weight, ataxic gait, and decreases in nocturnal activity did not appear until 3 months of age. These mice were later utilized to ask whether loss of *Mecp2* in the forebrain during early postnatal development contributes to the behavioral abnormalities of RTT (Gemeli *et al*, 2005). The conditional MeCP2 mutant mice show poor motor coordination, heightened anxiety, deficits in learning and memory, and abnormal social interactions. These data suggest that several of the features of RTT are the result of loss of *Mecp2* function specifically in the forebrain. In addition to investigating the function of MeCP2 in the CaMKII-expressing neurons, Chao and colleagues examined the role of MeCP2 in the GABAergic neurons (Chao *et al*, 2010). They utilized a bacterial artificial chromosome (BAC) containing the *Viaat* (vesicular inhibitory amino acid transporter) promoter to target Cre expression in the GABAergic neurons. Mice lacking *Mecp2* in the

GABAergic neurons displayed stereotypies, motor dysfunction, alterations in sensorimotor arousal and gating, deficits in learning and memory, and increased social interaction, supporting a role for the GABAergic system in many of the behavioral abnormalities of RTT.

Furthermore, several studies have focused on the function of MeCP2 in a single brain region. Adachi and colleagues used a viral-mediated approach to specifically delete *Mecp2* in the basolateral amygdala (BLA) in order to determine if *Mecp2* function in the BLA is required for normal anxiety behavior (Adachi *et al*, 2009). The mice with *Mecp2* deleted in the BLA spent less time in the center of the open field compared to the periphery and less time in the open arm of the elevated plus maze compared to control mice, suggesting that these mice have heightened anxiety. To examine the role of MeCP2 in the hypothalamus, Fyffe and colleagues utilized Cre-*loxP* technology to knockout *Mecp2* from the *Sim1*-expressing neurons in the hypothalamus (Fyffe *et al*, 2008). Loss of *Mecp2* in the *Sim1*-expressing neurons recapitulated the abnormal stress response that is observed when *Mecp2* function is lost in the whole brain, as these mice displayed increased serum levels of corticosterone in response to restraint stress. Deletion of *Mecp2* from the *Sim1*-expressing neurons also resulted in increased social interaction, aggressive behavior, and hyperphagia, uncovering novel roles for MeCP2 in these behaviors. Taken together, these findings demonstrate that the study of mice with conditional deletions of *Mecp2* in different cell types and brain regions enables the identification of the origins of the behavioral features of RTT.

1.3.4 Utilizing mouse models of RTT to investigate the function of MeCP2

In addition to exploring the function of MeCP2 in the behavioral abnormalities of

RTT, mouse models of RTT have also allowed for the study of the role of MeCP2 in the function of neurons. Several developmental synaptic abnormalities have been detected in *Mecp2* mutant mice. Chao and colleagues examined the synaptic properties of mice that lack (*Mecp2*-null) or express twice the normal levels of *Mecp2* (*Mecp2^{Tg1}*) (Chao *et al*, 2007). To determine synaptic output, they examined action-potential evoked excitatory postsynaptic currents (EPSC) in individual hippocampal glutamatergic neurons. They observed a 46% reduction in EPSC amplitude from *Mecp2*-null neurons, whereas neurons from *Mecp2^{Tg1}* mice showed a 116% enhancement in EPSC amplitude compared to their respective WT controls. In order to determine if the differences in EPSC amplitude were due to changes in glutamatergic synapse numbers in the *Mecp2* mutants, the density of glutamatergic synapses was assessed. The loss of MeCP2 results in a reduction in the density of functional glutamatergic synapses; on the other hand, there was an increase in functional synapses in the neurons from *Mecp2^{Tg1}* mice. To confirm that MeCP2 regulates glutamatergic synapse numbers, normal levels of MeCP2 were restored in the *Mecp2*-null mice by using the human transgene *Mecp2^{Null; Tg1}*. Restoring the levels of MeCP2 normalized the amplitude of the EPSC as well as the glutamatergic synapse density. In addition to finding decreases in the number of hippocampal glutamatergic synapses, reduced cortical activity in the pyramidal neurons of the somatosensory cortex has also been observed in *Mecp2*-null mice (Dani *et al*, 2005). Dani and colleagues demonstrated that the reduced activity is due to a shift in the balance between excitatory and inhibitory synaptic transmission that favors inhibition in the *Mecp2*-null mice. Collectively, these results implicate a role for MeCP2 in the development of neurocircuitry and suggest that synaptic abnormalities may contribute to symptoms of

RTT.

MeCP2 levels are low in developing neurons, increase throughout development, and reach peak levels in postmitotic neurons (Balmer *et al*, 2003), suggesting that phenotypes of RTT may arise at least in part from the lack of MeCP2 expression in mature neurons and suggest that MeCP2 may have a role in the function of neurons in the adult brain. *Cre*-mediated recombination of a conditional *Mecp2* allele in cultured hippocampal neurons after neurodevelopment and synaptogenesis induces a decrease in the frequency of mEPSCs, which is indistinguishable from the synaptic phenotype of the *Mecp2*-null mutation (Nelson *et al*, 2006). Therefore, these data suggest a role for MeCP2 in the regulation of synaptic transmission in mature neurons. In order to further determine if MeCP2 has a functional role in mature neurons, Giacometti and colleagues asked whether expression of a *Mecp2* transgene in postmitotic *Mecp2*-null neurons would rescue the null phenotype (Giacometti *et al*, 2007). Postnatal activation of MeCP2 in mice as old as 2-4 weeks of age delayed the onset of disease and prolonged the life span. Similarly, a mouse model of RTT was generated in which the *Mecp2* gene is silenced by insertion of a *lox-Stop* cassette and can later be conditionally activated (Guy *et al*, 2007). Late expression of MeCP2 once clear neurological symptoms were present in these mice reverses RTT-like symptoms and abolishes the hippocampal LTP deficit. Although it is clear that MeCP2 plays a role in synapse development, these findings suggest that MeCP2 also contributes to the function and synaptic properties of mature neurons.

1.4 MECP2 PLAYS A ROLE IN THE BEHAVIORAL ADAPTATIONS TO REPEATED PSYCHOSTIMULANT EXPOSURE

1.4.1 MeCP2 expression in NAc contributes to neural and behavioral responses to psychostimulants

Because MeCP2 affects chromatin structure and plays a role in regulating synaptic structure and function, it is a candidate for contributing to behavioral adaptations downstream of chronic monoaminergic signaling. Deng and colleagues investigated the role of MeCP2 in psychostimulant-mediated behavioral adaptations by manipulating the expression of MeCP2 in the NAc of C57BL/6J mice using lentiviruses and assessing changes in locomotor activity following acute or repeated amphetamine (AMPH) exposure (Deng *et al*, 2010). shRNA-mediated knockdown of MeCP2 significantly enhanced locomotor activity following acute AMPH exposure compared to mice expressing control scrambled shRNA (SCR). When MeCP2 SCR- and MeCP2 shRNA-expressing mice were injected with AMPH for five consecutive days, both treatment groups exhibited progressive enhancement in locomotor activity, but the locomotor activity of the shRNA-expressing mice was greater on each day compared to the controls. In addition to examining locomotor activity, the behavioral adaptations to repeated AMPH were also assessed in CPP. SCR- and MeCP2 shRNA-expressing mice both showed a preference for the chamber paired with 3 mg/kg AMPH; however, the MeCP2 shRNA-expressing mice exhibited a preference for the chamber paired with 1 mg/kg AMPH whereas the control mice did not show a preference for the low dose. Moreover, mice in which MeCP2 was overexpressed in the NAc failed to show a preference for the chamber paired with 3 mg/kg AMPH. These data suggest that MeCP2 in the NAc may be a part of a homeostatic process to limit the rewarding properties of AMPH.

In order to further investigate the role of MeCP2 in the response to chronic

psychostimulant exposure, Deng and colleagues examined psychostimulant-induced behaviors in mice with a truncating mutation in *Mecp2* (*Mecp2*³⁰⁸) (Shahbazian *et al*, 2002). As previously mentioned, these mice have less severe neurological phenotypes compared to other mouse models of RTT. Similar to the MeCP2 shRNA-expressing mice, *Mecp2*^{308/y} mice have increased levels of locomotor activity in response to acute AMPH compared to WT littermates. Furthermore, the *Mecp2*^{308/y} mice fail to show behavioral sensitization to repeated AMPH whereas their WT littermates show enhanced locomotor activity in this paradigm. To determine if the rewarding properties of AMPH are altered in the *Mecp2*^{308/y} mice, these mice and their WT littermates were put through CPP. Surprisingly, the *Mecp2*^{308/y} mice did not show a significant preference for the drug-paired chamber, even though their WT littermates demonstrated a preference at the dose tested. The inconsistency between the behavioral phenotype of the *Mecp2*^{308/y} mice and the results from the viral experiments could be due to the fact that the *Mecp2*^{308/y} mice bear a constitutive, global mutation. Therefore, it is possible that MeCP2 may be influencing behavioral adaptations to AMPH both through its actions in the adult brain in specific brain regions as well as its role in the development.

To explore the mechanisms by which MeCP2 is affecting psychostimulant-mediated behavioral adaptations, synaptic development and plasticity were examined in *Mecp2*^{308/y} mice. These studies showed that there is a significant increase in GABAergic synapses in the NAc in *Mecp2*^{308/y} mice compared to WT littermates, whereas the numbers of glutamatergic synapses are not altered by the truncating MeCP2 mutation. In order to assess the structural plasticity of synapses in the *Mecp2*^{308/y} mice, the density of dendritic spines on medium spiny neurons (MSNs) in the NAc was measured. It is

known that repeated treatment of AMPH increases the density of these spines and may contribute to the behavioral adaptations to chronic psychostimulant exposure (Russo *et al*, 2009; Pulipparacharuvil *et al*, 2008). Chronic AMPH causes an enhancement in the density of dendritic spines in WT mice but fails to alter dendritic spine density in the *Mecp2*^{308/y} mice. The increased GABAergic synapses in the NAc as well as the failure to show structural synaptic plasticity to repeated AMPH may contribute to the altered AMPH-induced behavior in the *Mecp2*^{308/y} mice. Alterations in the gene expression programs induced by psychostimulant exposure may also account for the behavioral phenotype of the *Mecp2*^{308/y} mice. Immediate Early Gene (IEG) expression in the NAc of *Mecp2*^{308/y} mice and their WT littermates was quantified following acute and chronic AMPH exposure. Acute AMPH induced cFos to similar levels in the mutant and WT mice; however, FosB levels were lower, and levels of JunB were reduced. In response to repeated AMPH, WT mice showed desensitization of cFos and FosB and an increase in JunB induction compared to WT mice treated with acute AMPH. On the other hand, there was no difference in the levels of IEGs induced in *Mecp2*^{308/y} mice treated with acute and chronic AMPH, demonstrating that *Mecp2*^{308/y} mice fail to show plasticity in IEG induction in response to repeated AMPH exposure. Taken together, these data reveal novel roles for MeCP2 in mesolimbocortical circuit development and suggest that MeCP2 in the NAc may be part of a homeostatic mechanism to limit the rewarding properties of psychostimulants.

1.4.2 MeCP2 in the dorsal striatum mediates compulsive drug-taking behavior

In addition to examining the role of MeCP2 in the behavioral adaptations to repeated psychostimulant exposure, the contribution of MeCP2 to drug-taking behavior

has also been investigated (Im *et al*, 2010). The transition from initial drug use to compulsive drug-taking has been shown to involve a shift in behavioral control from the ventral to dorsal regions of the striatum (Everitt and Robbins, 2005). Therefore, instead of focusing on the ventral striatum, Im and colleagues asked whether MeCP2 in the dorsal striatum influences compulsive drug-taking behavior. In order to address this question, they designed a lentiviral delivery system of a short hairpin interfering RNA to knock down MeCP2 expression (lenti-sh-MeCP2) in the dorsal striatum. Rats that received intra-striatal injections of empty lentiviral vector exhibited an escalation in drug intake across sessions in an extended access paradigm of self-administration, a paradigm that models uncontrolled drug use in humans. On the other hand, lenti-sh-MeCP2 mice failed to show progressive enhancement in cocaine intake across sessions. In addition, the lenti-sh-MeCP2 rats showed a downward shift in the dose-response curve, which reflects a decrease in the motivation to consume cocaine in these rats. Kenny and colleagues investigated the mechanisms by which MeCP2 affects extended access cocaine self-administration and found that MeCP2 influences cocaine intake through homeostatic interactions with microRNA-212 (miR-212). These data suggest that an interaction between MeCP2 and miR-212 plays a role in regulating cocaine intake, specifically in the extended access paradigm of self-administration.

Interestingly, the findings from Deng and colleagues suggest that MeCP2 acts through a compensatory mechanism to limit the rewarding properties of psychostimulants, whereas Im and colleagues propose that MeCP2 plays a facilitatory role in compulsive drug-taking behavior. Although the two results seem initially contradictory, examination of the behavioral paradigms utilized and the brain regions

implicated in these behaviors reconciles the different models of MeCP2 action. First of all, Deng and colleagues used behavioral sensitization and CPP to examine the behavioral adaptations to repeated psychostimulant exposure, whereas Im and colleagues utilize the extended access self-administration paradigm. In the first two paradigms, drugs are administered by the experimenter; on the other hand, mice administer their own drugs in extended access self-administration. Each of these paradigms models distinct aspects of addiction, and MeCP2 may have different roles in each phase of addiction. Secondly, Deng and colleagues examine MeCP2 function in the NAc, and Im and colleagues knockdown MeCP2 in the dorsal striatum. Therefore, it is possible that manipulations of MeCP2 expression in different brain regions have differential effects on behavior. Although these two studies highlight different mechanisms by which MeCP2 influences behavior, both studies demonstrate the involvement of MeCP2 in the behavioral adaptations to psychostimulant exposure.

1.5 PSYCHOSTIMULANT EXPOSURE REGULATES MECP2

PHOSPHORYLATION

1.5.1 Neuronal activity induces MeCP2 phosphorylation at Ser421

As a chromatin regulatory protein, MeCP2 has both maintenance and stimulus-dependent effects on the genome; therefore, studies in which the entire *Mecp2* protein is deleted confound the identification of its functions regulated by monoaminergic signaling. In order to study these functions, it is necessary to identify and manipulate the site or sites by which chronic monoaminergic signaling modulates MeCP2's ability to function as a chromatin-modifying protein, while leaving the basal activity of MeCP2

unaltered. Chen and colleagues examined the activity-dependent regulation of MeCP2 and found that membrane depolarization of cortical neurons leads to the release of MeCP2 from the *BDNF* promoter (Chen *et al*, 2003). Investigation of the mechanism underlying this observation revealed that membrane depolarization leads to a slow-migrating form of MeCP2 on a Western blot. The slow-migrating form of MeCP2 is most likely due to phosphorylation of the protein, as alkaline phosphatase inhibited the production of this form of MeCP2. Further analysis demonstrated that the slow-migrating form of MeCP2 exhibited reduced binding to methylated DNA, and the appearance of this form was coincident with the induction of *Bdnf* transcription. These findings suggest that phosphorylation of MeCP2 may modulate the ability of MeCP2 to regulate transcription.

In light of this possibility, it was then necessary to identify the site of phosphorylation and conduct a more in-depth characterization of the signaling pathways that regulate the phosphorylation event. Zhou and colleagues found that MeCP2 is phosphorylated at serine 421 (S421) in response to membrane depolarization, as a serine to alanine mutation at 421 (S421A) prevented the production of the slow-migrating form of MeCP2 in Western blot analysis (Zhou *et al*, 2006). The authors raised an anti-MeCP2 S421 antibody and conducted time course studies to examine the kinetics of MeCP2 phosphorylation at S421 (pMeCP2). Unlike other phosphorylation events induced by membrane depolarization, pMeCP2 has much slower kinetics, with maximum levels occurring one hour after stimulation. Investigation of the stimuli that induce pMeCP2 revealed that increases in intracellular calcium via glutamate or NMDA stimulation, as well as application of neurotrophins, induce pMeCP2 in cortical neurons

in vitro. In order to identify the kinase that phosphorylates MeCP2 at S421, the authors incubated cortical neurons with one of several kinase inhibitors, depolarized the neurons, and assessed whether pMeCP2 was induced. KN-93, a CaMKII inhibitor, was the only kinase tested that inhibited the phosphorylation of pMeCP2 *in vitro*. In addition to examining the regulation of pMeCP2 *in vitro*, Zhou and colleagues found that several stimuli regulate pMeCP2 *in vivo*; seizure induces pMeCP2 in the cortex and hippocampus, and a light that causes a shift in the circadian rhythm induces phosphorylation in the suprachiasmatic nucleus (SCN) of the hypothalamus. Although MeCP2 is expressed in all mammalian tissues, pMeCP2 occurs selectively in the brain, suggesting that pMeCP2 may have some specific function in the brain in response to neuronal activity.

1.5.2 Functional consequences of pMeCP2 *in vitro*

Zhou and colleagues further investigated the functional consequences of pMeCP2 in activity-regulated processes. The authors assessed the role of pMeCP2 in dendritic patterning and spine morphogenesis and found that expression of the S421A MeCP2 mutation inhibits the ability of MeCP2 to restrict dendritic growth and spine maturation in hippocampal slice cultures. The role of pMeCP2 in the regulation of activity-dependent gene expression was also examined. The authors infected hippocampal neurons with lentiviruses expressing either reconstituted FLAG-tagged WT or S421A mutant MeCP2 and then measured *Bdnf* expression in untreated and membrane depolarized neurons. Although the levels of *Bdnf* exon IV induction were similar in untreated WT and S421A MeCP2 mutant neurons, activity-dependent induction was reduced in the S421A MeCP2 mutant neurons. These data raise the possibility that

pMeCP2 plays a role in modulating MeCP2's function as a transcriptional regulator and could be a link between environmental stimuli and plasticity.

1.5.3 The role of activity-dependent MeCP2 phosphorylation *in vivo*

Recently, the functional consequences of MeCP2 S421 phosphorylation have also been investigated *in vivo*. To address these questions, Cohen and colleagues generated a mutant mouse bearing a knockin mutation at 421 that converts serine to alanine, rendering this site non-phosphorylatable (Cohen *et al*, 2011). The onset of RTT occurs during a postnatal period in which sensory experience is required for the refinement of developing circuits. This observation suggests that MeCP2 may be involved in synaptic development and maturation, and the absence of activity-dependent regulation of MeCP2 in RTT may contribute to the etiology of this disorder. In order to determine if the absence of activity-regulated pMeCP2 contributes to the abnormalities in dendritic development seen in mouse models of RTT, dendritic growth in cortical cultures from S421A mutant mice was examined. Cortical neurons from S421A mutant mice show increased dendritic complexity compared to WT neurons, suggesting that pMeCP2 is required for proper dendritic development. In addition, the role of pMeCP2 in synaptic development was also assessed using whole-cell patch-clamp recordings from layer II/III pyramidal neurons. Whereas there was no difference in the frequency of mIPSCs recorded from S421A mutant mice and their WT littermates, the amplitude of mIPSCs was increased compared to recordings from WT neurons. These findings suggest that there is a shift in the excitation-inhibition balance that favors inhibition in the S421A mutant mice. This shift is similar to that which is seen in *Mecp2*-null mice (Dani *et al*, 2005), supporting the notion that loss of pMeCP2 may contribute to the synaptic defects

observed in mouse models of RTT.

In addition to examining the contribution of the loss of pMeCP2 to the synaptic abnormalities of RTT, the authors also wanted to investigate the mechanism by which pMeCP2 regulates the function of MeCP2. Previous studies have suggested that MeCP2 is bound to the promoters of activity-regulated genes like *Bdnf* and represses activity of these genes (Chen *et al*, 2003; Martinowich *et al*, 2003, Zhou *et al*, 2006). Activity leads to reduced binding of MeCP2 at these promoters and allows transcription to occur. If this model is correct, then one could hypothesize that there would be activity-induced alterations in MeCP2 binding at specific genes. In order to ask this question, the authors examined MeCP2 binding profiles in cortical neurons before and after membrane depolarization using ChIP-sequencing. There was no difference in MeCP2 binding between the two treatment groups. Although these findings suggest that phosphorylation of MeCP2 at Ser421 does not induce changes in the binding of MeCP2 to DNA, it is possible that pMeCP2 modulates MeCP2's ability to regulate transcription via some other mechanism in response to neuronal activity. Cohen and colleagues compared activity-dependent *Bdnf* induction in S421A mutant and WT mice and found no differences between the two genotypes. Furthermore, microarray analysis was used to assess differences in gene expression genome-wide and revealed that there were no significant differences between membrane depolarized S421A mutant and WT cortical neurons. In order to further investigate the mechanism by which pMeCP2 modulates MeCP2's ability to regulate transcription, ChIP-sequencing was used to determine where across the genome pMeCP2 is induced. Intriguingly, pMeCP2 is induced uniformly across the genome instead of showing enrichment at particular sites (promoters, enhancers, etc.).

Taken together, these data suggest that instead of regulating transcription of specific genes, pMeCP2 may play a more global role in mediating changes in chromatin structure in response to neuronal activity.

Although these data do not follow the previous model that Ser421 phosphorylation modulates MeCP2's ability to regulate the transcription of specific genes, they do not completely rule out the possibility that pMeCP2 affects gene expression under conditions that were not examined in this study. For example, Cohen and colleagues compared gene expression profiles from WT and S421A mutant cortical neurons after a single stimulus (depolarization) and found that there were no significant differences in activity-regulated gene expression. However, it is still possible that pMeCP2 is required for changes in gene expression following chronic stimuli. Furthermore, it is also possible that pMeCP2 has different functions in different brain regions and cell-types. Although the findings from Cohen and colleagues suggest that pMeCP2 may have global effects on chromatin structure, pMeCP2 may perform more local functions in regulating gene expression in specific cell populations

In addition to mice bearing a knockin mutation only at Ser421, mice bearing point mutations at S421 and S424 (*Mecp2*^{S421A;S424A/y}), another site that is thought to be phosphorylated in response to neuronal activity (Tao *et al*, 2009), have also been generated to study the function of MeCP2 phosphorylation at these sites *in vivo* (Li *et al*, 2011). Prior to testing the mutant mice in learning and memory assays, the mice were screened for alterations in locomotor activity and anxiety-like behaviors and did not show overt deficits in any of these tests. When the mutant mice were put through context-dependent fear conditioning, they froze more than their WT littermates, which could

suggest enhanced learning in this assay. To further explore the role of S421/S424 in hippocampal-dependent learning, the mutant mice and WT littermates were tested in the Morris water maze. The *Mecp2*^{S421A;S424A/y} mice and their WT littermates performed similarly during the training phase and learned the location of the hidden platform equally well. However, during the probe trials, the *Mecp2*^{S421A;S424A/y} mice spent more time in the target quadrant than their WT littermates, which could suggest heightened learning in this assay. In addition, studies in hippocampal slices revealed that the S421A/S424A mutation results in enhanced LTP and increased synaptogenesis, two synaptic abnormalities that are consistent with the behavioral phenotype. Finally, the authors find that increased *Bdnf* hippocampal transcription may be mediating the alterations in behavior and synaptic structure and function in these mice.

Surprisingly, the phenotype of the *Mecp2*^{S421A;S424A/y} mice is considerably different from the findings of Cohen and colleagues in the S421A mutant mice. Although both mutant strains exhibit deficits in learning and memory, the *Mecp2*^{S421A;S424A/y} mice show impairments in the Morris water maze and context-dependent fear conditioning, whereas the S421A mutant mice have normal behavior in the Morris water maze but abnormal behavioral responses to novel experience. Furthermore, Li and colleagues found enhanced LTP and increased excitatory synaptogenesis in the hippocampus of *Mecp2*^{S421A;S424A/y} mice, and Cohen and colleagues observed increased inhibition in cortical neurons from S421A mutant mice. In addition to differences in behavior and synaptic function, the two studies made different conclusions about the function of MeCP2 phosphorylation. Li and colleagues saw increased MeCP2 binding at the promoters of several target genes and observed altered expression of these genes in the

Mecp2^{S421A;S424!/y} mice. On the other hand, Cohen and colleagues demonstrated that pMeCP2 occurs globally across the genome and found no differences in activity-regulated gene expression in the S421A mutant mice compared to their WT littermates. A plausible explanation for the contradictory findings of these studies is that phosphorylation of MeCP2 at different sites could have differential effects on MeCP2 binding and function. Despite the differences between the *Mecp2*^{S421A;S424!/y} mice and S421A mutant mice, both of these studies suggest a role for MeCP2 phosphorylation at Ser421 in synaptic function and behavior.

1.5.4 pMeCP2 as a target of regulation by psychostimulants and DA signaling

Because it has been implicated in synaptic function and has a potential role in regulating chromatin structure in response to neuronal activity, Deng and colleagues asked if pMeCP2 is a target of modulation by psychostimulant exposure (Deng *et al*, 2010). In order to address this question, C57BL/6 mice were acutely injected with 3 mg/kg AMPH, were then euthanized at several time points after injection, and levels of pMeCP2 were quantified via immunostaining in several brain regions that receive dopaminergic innervation. The authors found that pMeCP2 was robustly induced in the NAc, reaching peak levels at 2 hours and returning to baseline shortly thereafter. There was a small induction in the PLC as well, although there were high basal levels of pMeCP2 in this brain region as well. Because one of the main mechanisms of AMPH is to increase extracellular levels of DA, the regulation of pMeCP2 by DA was also examined. SKF81297, a D₁-class receptor agonist drove induction of pMeCP2, whereas SCH22390, a D₁-class receptor antagonist, reduced AMPH-induced pMeCP2. These results suggest that DA is required for pMeCP2 induction following AMPH exposure.

Examination of the pattern of pMeCP2 in the NAc revealed that the induction occurred in a very small population of neurons following AMPH exposure, and co-labeling with cell-type specific markers was used to determine the cell-type in which pMeCP2 was induced. Intriguingly, there was no overlap between pMeCP2 and medium spiny neurons (MSN), which make up more than 90% of the neurons in the NAc, even though these neurons express high levels of D₁ or D₂ receptors (Shuen *et al*, 2008). However, pMeCP2 colocalized with parvalbumin and glutamic acid decarboxylase (GAD)-67, which are two markers of fast-spiking GABAergic interneurons (Kawaguchi *et al*, 1995). Due to the fact that activation of DA signaling modulates network excitability and because pMeCP2 is regulated by glutamate receptor-coupled intracellular calcium signaling pathways *in vitro*, it is likely that the pattern of pMeCP2 produced by AMPH arises as the result in changes in neuronal firing rather than direct activation downstream of DA receptors (Zhou *et al*, 2006; Nicola *et al*, 2000).

1.5.5 pMeCP2 levels correlate with degree of behavioral sensitization to repeated AMPH

After observing that AMPH induces pMeCP2 in the NAc, the authors then asked whether pMeCP2 plays a role in mediating the behavioral adaptations to repeated AMPH exposure. C57BL/6 mice were given daily injections of vehicle or AMPH for five consecutive days, withdrawn for one week, and then given a challenge injection of AMPH. Locomotor activity was monitored on the challenge day, and the mice were sacrificed 2 hrs after to quantify pMeCP2 levels. There was no difference in pMeCP2 induction between the acute and chronic groups on the challenge day. Intriguingly, there was a significant difference between the two groups when the correlation between

locomotor activity on the challenge day and pMeCP2 immunoreactivity was considered. Whereas there was no correlation between locomotor activity and pMeCP2 levels in individual mice that had received repeated vehicle injections prior to the challenge day, there was a strong correlation between AMPH-induced locomotion and pMeCP2 immunoreactivity in the group that had received repeated injections of AMPH. The correlation between locomotor activity on the challenge day and the levels of pMeCP2 immunoreactivity suggest that pMeCP2 may play a role in the mechanisms underlying behavioral sensitization.

1.6 RESEARCH OBJECTIVES

MeCP2 phosphorylation at Ser421 is regulated by AMPH in the NAc, and the levels of phosphorylation correlate with the degree of behavioral sensitization to repeated AMPH, suggesting that pMeCP2 may be involved in the behavioral adaptations to repeated AMPH. AMPH induces a very specific pattern of pMeCP2, as induction occurs selectively in the GABAergic interneurons of the NAc. Based on our previous studies showing that both AMPH and DA agonists induce pMeCP2, we hypothesized that activation of multiple signaling pathways produces the pattern of pMeCP2 we observe following AMPH exposure. The goal of the work described in Chapter 2 was to examine the ability of DA, 5-HT, and NE to induce pMeCP2 in order to better understand the signaling pathways that regulate pMeCP2 as well as to uncover additional behaviors in which pMeCP2 is required. These studies revealed that drugs that selectively activate serotonergic signaling induce pMeCP2; therefore, we desired to investigate the role of pMeCP2 in serotonergic-mediated behaviors, specifically in depression-like behavior and

the behavioral response to antidepressants (Figure 2). In order to address these questions, we conducted behavioral studies in mice that bear a KI mutation that converts serine to alanine at 421, rendering this site non-phosphorylatable. Prior to utilizing these mice to investigate the contribution of pMeCP2 to depression-like behavior and antidepressant response, we characterized the behavioral phenotype of S421A mutant mice in Chapter 3. Finally, in the work described in Chapter 4, we assessed depression-like behaviors in S421A mutant mice, compared the response to chronic antidepressant treatment in S421A mutant mice and WT littermates in the social defeat stress paradigm, and examined the pattern of pMeCP2 induced by acute and chronic antidepressant treatment.

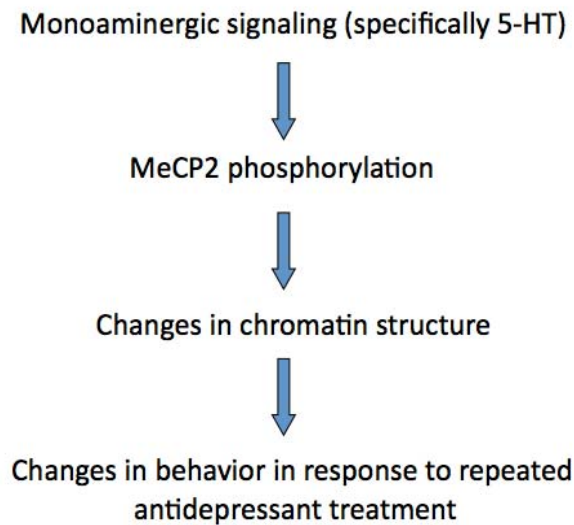


Figure 2: Working hypothesis addressed in research objectives. Our previous work suggests that pMeCP2 may be involved in the behavioral response to repeated activation of monoaminergic signaling. Based on these findings and the evidence that drugs that activate 5-HT induce pMeCP2, I hypothesized that the phosphorylation of MeCP2 at Ser421 is involved in the behavioral response to chronic antidepressant treatment.

2. DIFFERENTIAL REGULATION OF MECP2 PHOSPHORYLATION IN THE CNS BY DOPAMINE AND SEROTONIN

2.1 SUMMARY

Systemic administration of amphetamine (AMPH) induces phosphorylation of MeCP2 at Ser421 (pMeCP2) in select populations of neurons in mesolimbocortical brain regions. Because AMPH simultaneously activates multiple monoamine neurotransmitter systems, here we examined the ability of dopamine (DA), serotonin (5-HT), and norepinephrine (NE) to induce pMeCP2. Selective blockade of the DA transporter (DAT) or the 5-HT transporter (SERT), but not the NE transporter (NET), was sufficient to induce pMeCP2 in the CNS. DAT blockade induced pMeCP2 in the prefrontal cortex and nucleus accumbens (NAc), whereas SERT blockade induced pMeCP2 only in the NAc. Administration of selective DA and 5-HT receptor agonists was also sufficient to induce pMeCP2, however the specific combination of DA and 5-HT receptors activated determined the regional- and cell-type specificity of pMeCP2 induction. The D₁-class DA receptor agonist SKF81297 induced pMeCP2 widely, however co-administration of the D₂-class agonist quinpirole restricted the induction of pMeCP2 to GABAergic interneurons of the NAc. Intra-striatal injection of the adenylate cyclase activator forskolin was sufficient to induce pMeCP2 in medium spiny neurons, suggesting that the combinatorial regulation of cAMP by DA or 5-HT receptors may contribute to the cell-type specificity of pMeCP2 induction. Consistent with the regulation of pMeCP2 by multiple monoamine neurotransmitters, genetic disruption of any single monoamine transporter in DAT-, SERT-, and NET-knockout (KO) mice failed to eliminate AMPH-induced pMeCP2 in the nucleus accumbens (NAc). Together these studies substantially

advance understanding of the neurotransmitters and signaling pathways that regulate pMeCP2 in the CNS.

2.2 INTRODUCTION

Psychostimulant-induced activation of monoamine receptors is essential to the mechanism by which these drugs induce changes in behavior (Gainetdinov and Caron, 2003; Missale *et al*, 1998; Xu *et al*, 1997). Cocaine and AMPH serve as indirect monoamine receptor agonists by inhibiting and/or reversing the function of monoamine transporters. However, despite the fact that these drugs rapidly increase extracellular levels of DA, 5-HT, and NE, repeated exposure is necessary to produce long-lasting alterations in behavior (Hyman *et al*, 2006). This observation suggests that molecular mechanisms downstream of monoamine receptor activation are required to mediate the observed behavioral adaptations.

A substantial body of evidence indicates that psychostimulant-induced changes in gene expression contribute to the long-lasting effects of these drugs on behavior (Nestler, 2008; Kumar *et al*, 2005). Examination of the molecular processes underlying these changes in gene expression has revealed a significant role for epigenetic mechanisms of transcription, which are processes that mediate changes in gene expression by regulating chromatin structure (Maze *et al*, 2010; Renthal *et al*, 2009). Therefore, chromatin regulatory proteins that are targets of modulation by monoaminergic signaling pathways are strong candidates to link psychostimulant exposure to persistent changes in gene expression and behavior. Recently we and others have demonstrated that the methyl-CpG-binding protein-2 (MeCP2) contributes to both neural and behavioral adaptations

induced by repeated psychostimulant exposure (Deng *et al*, 2010; Im *et al*, 2010). We have shown that lentiviral shRNA-mediated knockdown of MeCP2 in the NAc increases sensitivity to AMPH-induced conditioned place-preference (CPP) whereas overexpression of MeCP2 decreases CPP (Deng *et al*, 2010). These data suggest that MeCP2 acts in the NAc to limit the rewarding properties of psychostimulants.

Psychostimulants induce rapid and robust phosphorylation of MeCP2 at Ser421 (pMeCP2), a site that is thought to modulate MeCP2-dependent chromatin regulation (Deng *et al*, 2010; Zhou *et al*, 2006; Chen *et al*, 2003). MeCP2 regulates gene transcription by binding to methylated DNA and recruiting enzymes that modify histones (Nan *et al*, 1998). Although the specific mechanisms by which Ser421 phosphorylation affects MeCP2 function remain poorly understood, overexpression of a Ser421Ala mutant MeCP2 has been shown to inhibit neuronal activity-induced *Bdnf* expression, suggesting that Ser421 phosphorylation could contribute to gene derepression (Zhou *et al*, 2006). Interestingly, systemic administration of AMPH induces a restricted pattern of pMeCP2 induction in select neurons of the NAc and prelimbic cortex (PLC) (Deng *et al*, 2010). D₁-class DA receptor activation is required for AMPH-dependent induction of pMeCP2 in the NAc, and administration of a D₁-class DA receptor agonist is sufficient to induce pMeCP2 (Deng *et al*, 2010). However, AMPH induces pMeCP2 selectively in GAD67- and Parvalbumin-positive GABAergic interneurons of the NAc whereas it fails to induce pMeCP2 in medium spiny neurons (MSNs), despite the fact that these cells express high levels of DA receptors. In addition to its effects on DA neurotransmission, AMPH also impacts 5-HT and NE neurotransmission. Thus, we considered the possibility that the selective pattern of pMeCP2 induced by AMPH might arise as a result

of combinatorial signaling through one or more of these monoaminergic systems.

Here we use both pharmacological and genetic techniques to characterize the differential roles of DA, 5-HT, and NE signaling in the regulation of the regional distribution and cell-type specificity of pMeCP2 induction. We find that selective inhibition of either the DAT or SERT but not the NET is sufficient to induce pMeCP2 in the NAc; however, only DAT inhibition induces pMeCP2 in the PLC. We also find that differential activation of specific classes of DA and 5-HT receptors induces pMeCP2 in distinct cell-types and brain regions, suggesting that combinatorial signaling through these receptors sculpts the specific pattern of pMeCP2 induction *in vivo*. Finally, we discuss potential functional roles for pMeCP2 based on our analyses of AMPH-induced pMeCP2 in DAT-, SERT-, and NET-KO mouse strains, each of which has a distinct profile of behavioral responses to AMPH administration. Taken together, these data significantly enhance understanding of the mechanisms and consequences of monoaminergic regulation of MeCP2 in the CNS.

2.3 MATERIALS AND METHODS

2.3.1 Animals

Adult (8-10 week old) male C57BL/6 mice (Jackson Laboratories, Bar Harbor, ME), DAT, NET, vesicular monoamine transporter 2 (VMAT2) mice (provided by Dr. Marc Caron at Duke University Medical Center, Durham, NC), and SERT mice (provided by Dr. Scott Hall, NIDA, Bethesda, MD) were used in these studies. The wild-type (WT), heterozygous (HET) and KO littermates were generated from HET breedings. Animals were weaned at 21-30 days of age, housed in groups of 3-5, and segregated by sex and

genotype. All animals were given free access to standard laboratory chow and water and were housed in a humidity- and temperature-controlled room on a 14 hr/10 hr light/dark cycle (lights on at 0700 hr). All experiments were conducted with an approved protocol from the Duke University Institutional Animal Care and Use Committee in accordance with guidelines from the National Institutes of Health for the Care and Use of Laboratory Animals.

2.3.2 Immunofluorescent Staining of Brain Sections

Two hrs after vehicle or drug injection, mice were perfused transcardially with 4% paraformaldehyde in 0.1M PBS. Brains were post-fixed in 4% paraformaldehyde/PBS overnight, then sunk into 20% (wt/vol) sucrose/PBS overnight. Coronal sections (40 μ m) were cut on a freezing microtome, and brain regions were identified by anatomical landmarks. One section from each brain region of interest was selected for each mouse, based upon anatomical structures to represent the closest approximation of identical sections between individual mice. To minimize technical variations in immunostaining across genotypes, sections from different individual mice were first photographed for visual identification. The sections were then pooled and incubated with antibodies in a single chamber, and finally they were separated after processing for image analysis (see Deng *et al*, 2010). For immunostaining, tissue sections were permeabilized with either 1% (vol/vol) (for the pMeCP2 antibody) or 0.3% (vol/vol) (all other antibodies) Triton X-100 for 1 hr and then sections were blocked with 3% (wt/vol) BSA (for the DARPP-32 antibody) or 16% (vol/vol) goat serum (all other antibodies) in PBS. Sections were incubated with the following primary antibodies overnight at 4°C: rabbit anti-phospho-

Ser421 MeCP2 1:15,000 (Deng *et al*, 2010), mouse anti-GAD67 1:500 (MAB5406; Chemicon/Millipore, Billerica, MA), rabbit anti-c-Fos 1:15,000 (PC38; Calbiochem, San Diego, CA), goat anti-DARPP-32 1:50 (sc31519; Santa Cruz Biotechnology, Santa Cruz, CA), and mouse anti-GFAP 1:100 (Clone G-A-5, Sigma, St. Louis, MO). Whenever possible, double immunostaining with primary antibodies raised in two different species was used for co-localization on single sections in order to determine the cell-type in which pMeCP2 was induced. After three washes in PBS, sections were incubated with the following species-specific fluorescent-conjugated secondary antibodies for 1 hr at room temperature: goat anti-mouse antibodies conjugated to Cy3 or Cy2 1:500 (Jackson ImmunoResearch, West Grove, PA), Alexa Fluor 488 goat anti-rabbit antibodies at 1:500 (A11034; Molecular Probes/Invitrogen, Carlsbad, CA), Cy3 donkey anti-rabbit antibodies at 1:500 (Jackson ImmunoResearch), or Alexa Fluor 488 donkey anti-goat antibodies (A11055; Molecular Probes/Invitrogen). Sections were washed in PBS, nuclei were labeled with Hoechst dye (Sigma) to facilitate anatomical localization of brain structures, sections were mounted and cover-slipped, and analyzed as described below.

2.3.3 Image Analyses

For quantitative immunofluorescence, images were captured on a Leica DMI4000 inverted fluorescence microscope using a Cascade 512B camera. Digital images were quantified using MetaMorph 7 Image Analysis software (Molecular Devices, Sunnyvale, CA). To minimize variation between samples, images were captured with a uniform exposure time within a single experiment, and immunofluorescence was quantified across a constant-sized region from a single field of each section (as shown in Figure 3a). We

used the Count Nuclei module in MetaMorph 7.0 to first count the total number of cells per section that were positive for pMeCP2 or c-Fos immunoreactivity and then we determined the integrated immunofluorescence intensity of all the pMeCP2 or c-Fos positive nuclei in each image. We defined nuclei as objects of 3-8 μ m in diameter. For each experiment, an investigator blind to genotype and treatment condition chose a random section from which to set a single threshold value of fluorescence intensity above background to score objects of this size as positive for pMeCP2 or c-Fos expression. The threshold value was adjusted until the program's output of detected nuclei most closely matched the distribution of positive nuclei seen by eye. This threshold value was then held constant for every image within the experimental set. The first result of this analysis is a count of the number of cells that are pMeCP2 or c-Fos positive in each image. The Count Nuclei module then creates a mask that covers the area of all of the nuclei identified as positive on each section and quantifies the total immunofluorescence intensity under this area (the "integrated intensity") for each image. Thus our analysis allows us to tell how many cells have induced expression of pMeCP2 or c-Fos in each image as well as to evaluate the magnitude of pMeCP2 or c-Fos induction in these nuclei.

2.3.4 Bilateral guide cannula surgery

Mice were anesthetized with chloral hydrate (400 mg/kg i.p.). A 22 gauge bilateral stainless steel guide cannula assembly with center to center distance of 2.0mm (PlasticsOne, Raanoke, VA) was implanted over the striatum in both hemispheres. Stereotaxic coordinates relative to bregma were A/P +1.42mm, M/L \pm 1.0mm, D/V - 3.6mm.. Guide cannulae were anchored to the skull using carboxylate dental cement

(Durelon®, CMA Microdialysis). A dust cap was placed over the entire cannula assembly. The mice were housed individually after surgery and allowed to recover for 8-9 days. Mice were treated with the antibiotic co-trimoxazole, 3% w/v solution in water, for the first 3 days.

2.3.5 Intra-striatal infusions

All infusions were done in an empty cage that was the same dimension as the home cage and were done in freely moving mice. A 28 gauge stainless steel injector cannula with 3.6mm length was used for all drug infusions. The injector cannula was attached to a 25µL Hamilton syringe (Hamilton Co., Reno, NV). 1µL of drug or saline was simultaneously infused into left and right hemispheres over 6 minutes using a Razel® infusion pump (Razel Scientific Instruments, St. Albans, VT). The mice were infused with 2.5 µg/µL forskolin, 7-deacetyl-7-[0-(N-methylpiperazino)-g-butryl]-, dihydrochloride (Calbiochem, La Jolla, CA) in one hemisphere and vehicle (saline) in the other so that each mouse served as its own control. Side selection was randomized. Injector cannulae were left in place for an additional 2 min to allow drug diffusion and then a dummy cannula was inserted into the guide to prevent backflow. The mice were perfused transcardially with 4% paraformaldehyde 90 minutes after infusion.

2.3.6 Striatal cultures

Whole striatum was dissected from embryonic day 17 CD-1 rats (Charles River Laboratories, Wilmington, MA), dissociated mechanically, and plated on PDL-coated dishes containing DMEM/F12 medium (Invitrogen, Carlsbad, CA) with B27 supplements

(Invitrogen). After 5 days in culture, neurons were stimulated with the following drugs: 55 mM KCl in an isotonic solution (see Tao *et al*, 1998), 50 μ M NMDA (Sigma), 10 μ M forskolin (EMD, Gibbstown, NJ), or 50 μ M SKF38393 (Sigma). In some experiments 5 μ M Nimodipine (Sigma) or 100 μ M APV (Tocris) were added 2 min prior to stimulation with KCl or NMDA. Sixty min after stimulation, cells were lysed in boiling SDS-PAGE sample buffer for analysis of protein phosphorylation by western blotting. In addition to the MeCP2 antibodies described above, the following antibodies were used: rabbit anti-CREB 1:1000 (06-863; Upstate Biotechnology/Millipore), mouse anti-phosphoSer133 CREB 1:1000 (05-667; Upstate Biotechnology/Millipore), goat anti-rabbit-HRP 1:10,000 (Jackson ImmunoResearch), and goat anti-mouse-HRP 1:10,000 (Jackson ImmunoResearch).

2.3.7 Locomotor Activity in the Open Field

Mice were habituated to the open field (Accuscan Instruments, Columbus, OH) for 1 hr to establish baseline activity and then injected with vehicle (Veh) or 3 mg/kg AMPH (Sigma, St. Louis, MO), 5 mg/kg SKF81297 (Tocris Bioscience, Ellisville, MO), 0.25 mg/kg quinpirole (Tocris), 5 or 10 mg/kg citalopram (Tocris), 10 or 15 mg/kg GBR12909 (Tocris), 3 or 5 mg/kg reboxetine (Tocris), or 3 or 4.5 mg/kg quipazine (Tocris). All injections were i.p., and all drugs were dissolved in sterile water, except SKF81297, which was dissolved in DMSO (final concentration 0.5% vol/vol). Following administration of Veh or drug, animals were immediately returned to the open field for 1 hr. Horizontal (distance traveled in cm) was monitored under 340 lux illumination.

2.3.8 Behavioral Sensitization

Two different protocols were used as referenced in the text. In the first protocol, mice were injected with Veh or 3 mg/kg AMPH once a day for 5 consecutive days in the home cage, they were withdrawn from drug for 7 days, then they were challenged with 3 mg/kg AMPH in the open field while horizontal activity (distance traveled in cm) was monitored as described in the “Locomotor Activity in the Open Field” section above. In the second protocol, the first injection of vehicle or AMPH was given in the open field so that locomotor activity could be recorded. The mice were then returned to the home cage where they received daily injections of Veh or 3 mg/kg AMPH for 4 additional consecutive days. The mice were then withdrawn from drug for 7 days, then they were challenged with 3 mg/kg AMPH in the open field while horizontal activity (distance traveled in cm) was monitored.

2.3.9 Statistical Analyses

Statistical analyses were performed using SPSS v11.0 statistical software (SPSS, Chicago, IL). The data are depicted as means and standard errors of the mean (S.E.M.). The pMeCP2 immunoreactivities and locomotor activities of the transporter knockout mice given Veh or AMPH were analyzed using two-way ANOVA for genotype and treatment. Activities of the mice were aggregated over the 1 hr post-injection period. For C57BL/6J mice injected with Veh, GBR12909, citalopram, reboxetine, SKF81297, quinpirole, SKF81297 + quinpirole, quinpirole alone, or quipazine, pMeCP2 immunoreactivities in the NAc were analyzed using univariate ANOVA for treatment condition. Bonferroni corrected pair-wise comparisons were used as the *post-hoc* tests.

We assessed the correlation between pMeCP2 immunoreactivity and locomotor activity with Pearson correlation coefficients. In all cases, $p < 0.05$ was considered statistically significant.

2.4 RESULTS

2.4.1 Selective blockade of the DAT or SERT is sufficient to induce pMeCP2

Pharmacological targets of AMPH in the CNS include the DAT, SERT, and NET plasma membrane transporters, as well as the VMAT2 vesicular transporter (Fleckenstein *et al*, 2007; Han and Gu, 2006; Sulzer *et al*, 2005). Through its interactions with these target proteins, AMPH simultaneously raises extracellular levels of multiple monoamine neurotransmitters. To address the contributions of single monoaminergic neurotransmitter systems to the regulation of MeCP2 phosphorylation, we evaluated the ability of selective monoamine transporter inhibitors to induce pMeCP2 in the NAc (Figure 3). C57BL/6 mice were administered either Veh, a DAT inhibitor (GBR12909, 10 mg/kg or 15 mg/kg), a SERT inhibitor (citalopram, 10 mg/kg or 15 mg/kg), or a NET inhibitor (reboxetine, 3 mg/kg or 5 mg/kg). Open field locomotor activity was monitored for 1 hr then the mice were perfused 2 hrs post-injection to assess pMeCP2 immunoreactivity. For GBR12909, an ANOVA for locomotor activity revealed a significant effect of treatment [$F_{2,15}=13.313$, $p < 0.001$]. Both doses of GBR12909 significantly increased locomotor activity compared to mice treated with Veh ($ps < 0.004$) (Table 2). For pMeCP2 immunoreactivity in mice treated with GBR12909, an ANOVA indicated a significant effect of treatment [$F_{2,14}=12.083$, $p < 0.001$], and Bonferroni comparisons showed that pMeCP2 intensities in both the 10 mg/kg and 15 mg/kg groups were

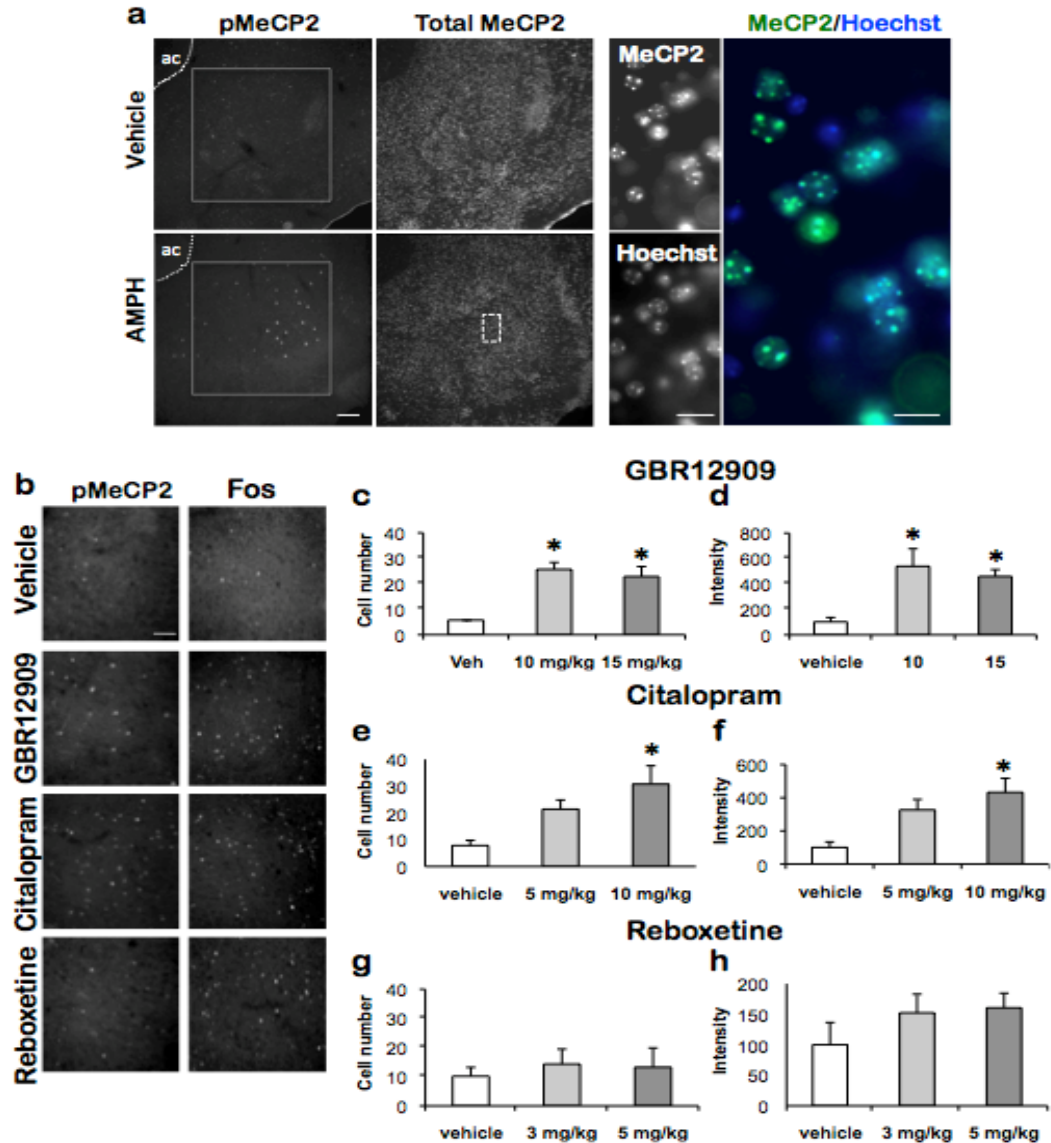


Figure 3: Selective DAT and SERT blockade differentially induce pMeCP2 in the NAc. (a) pMeCP2 and total MeCP2 induction following vehicle or 3 mg/kg AMPH. Solid gray box indicates representative section of NAc used to quantify pMeCP2 immunofluorescence. Dashed white box was used as the inset image to examine total MeCP2 and Hoechst (nuclear marker) overlay. ac, anterior commissure. (b) pMeCP2 immunostaining in the NAc (left column) and c-Fos immunostaining (right column) 2 hrs after treatment with Veh, 10 mg/kg GBR12909, 10 mg/kg citalopram, or 3 mg/kg reboxetine. (c, e, g) number of cells in which pMeCP2 was induced following treatment of GBR12909, citalopram, or reboxetine. (d, f, h) pMeCP2 integrated intensity in the NAc following treatment with GBR12909, citalopram, or reboxetine. All values of quantitated immunofluorescence intensity were normalized to Veh control for each drug. n=5-8 mice/group. *p<0.05 compared to Veh. Error bars indicate S.E.M. Scale bars = 10µm.

significantly higher than the Veh group ($p < 0.05$) (Figure 3b-d). These data demonstrate that selective blockade of the DAT is sufficient to induce pMeCP2 in the NAc.

ANOVA for locomotor activity in citalopram-treated mice revealed a significant effect of treatment [$F_{2,16}=13.02$, $p < 0.001$]. Unlike GBR12909, citalopram treatment led to a reduction in locomotor activity, although 10 mg/kg was the only dose to significantly lower activity ($p < 0.001$) (Table 2). When changes in pMeCP2 induction were considered for citalopram-treated mice, the ANOVA detected a significant effect of treatment [$F_{2,16}=4.236$, $p < 0.04$], *post-hoc* analyses found that the pMeCP2 intensity was significantly higher than the Veh group only for the 10mg/kg dose ($p < 0.05$) (Figure 3b,e,f). These data demonstrate that selective blockade of the SERT is also sufficient to induce pMeCP2 in the NAc. Intriguingly, we note that while GBR12909 and citalopram have opposite effects on locomotor activity, both drugs lead to the induction of pMeCP2 in the NAc. We discuss the relationship between pMeCP2 phosphorylation and locomotor activity further in the Discussion section.

Finally, inspection of the ANOVA for locomotor activity of mice treated with reboxetine revealed a significant effect of treatment [$F_{2,16}=4.317$, $p < 0.041$]. Like citalopram, reboxetine treatment led to a dose-dependent reduction in locomotor activity; only 5 mg/kg reboxetine significantly reduced locomotor activity compared to Veh-treated controls ($p < 0.048$) (Table 2). In contrast to the effects of GBR12909 and citalopram, pMeCP2 immunoreactivity in reboxetine-treated mice did not show an overall effect of treatment [$F_{2,16}=0.806$, $p < 0.463$] suggesting that activation of NE signaling is not sufficient to induce pMeCP2 in this context (Figure 3b,g,h). In order to ensure that the failure to induce pMeCP2 was not due to improper selection of doses, we

Table 2: Changes in locomotor activity following acute DAT, SERT, or NET blockade. (a-c) The effects of 10 or 15 mg/kg GBR12909, 5 or 10 mg/kg citalopram, and 3 or 5 mg/kg reboxetine on locomotor activity in C57BL/6 mice 1 hr post-injection. All values of locomotor activity were normalized to Veh control for each drug. n=6-8 mice/group. * $p < 0.05$ compared to Veh. Error bars indicate S.E.M.

Drug	Distance (cm) Veh	Distance (cm) Dose 1	Distance (cm) Dose 2
GBR12909	3390.3 ± 66.2	13,645.6 ± 1627.6 *	12,482.4 ± 2153.6 *
Citalopram	3946.6 ± 690.1	2,514.2 ± 407.9	729.0 ± 241.9 *
Reboxetine	1727.5 ± 96.1	1036.2 ± 277.8	747.8 ± 118.8 *

also examined the ability of each of these drugs to induce c-Fos expression. 5 mg/kg reboxetine induced expression of c-Fos in the NAc to a similar extent as that seen following administration of 3 mg/kg AMPH, 10 mg/kg GBR12909, and 10 mg/kg citalopram. Hence, the doses of reboxetine used in this study are able to induce a transcriptional response in neurons of the NAc (Figure 3b) (Miyata *et al*, 2005). Together, these data show that selective activation of either DA or 5-HT but not NE signaling is sufficient to drive induction of pMeCP2 in the NAc.

Although most neurons within the NAc express MeCP2, we have shown that AMPH selectively induces pMeCP2 in a specific population of GABAergic interneurons that express the GABA synthesizing enzyme GAD67 and the calcium binding protein Parvalbumin (Deng *et al*, 2010). To determine whether selective monoamine transporter blockade can recapitulate this cell-type specificity of AMPH-induced pMeCP2, we co-labeled NAc sections from mice treated with the selective transporter blockers with antibodies against both pMeCP2 and GAD67. Like AMPH, GBR12909 induced pMeCP2 only in GAD67-positive GABAergic interneurons of the NAc (Figure 4).

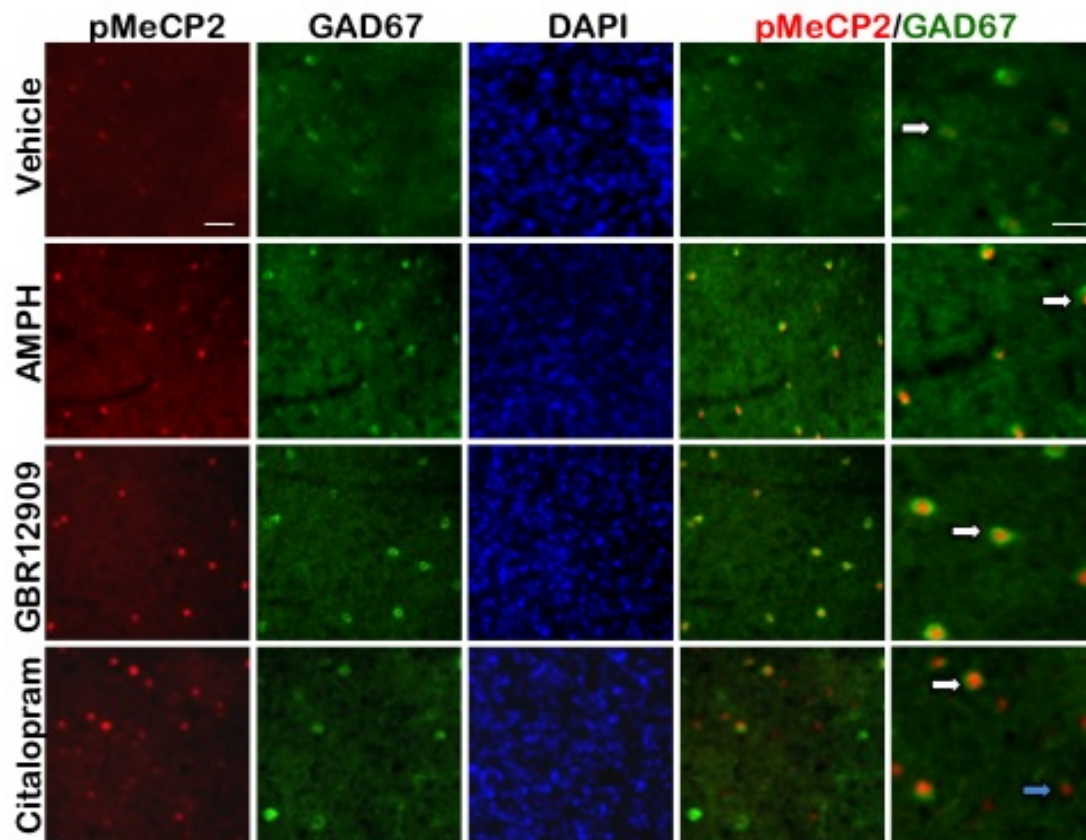


Figure 4: DAT and SERT blockers differentially regulate the cell-type specificity of MeCP2 phosphorylation in the NAc. pMeCP2 (red), GAD67 (green), Hoechst nuclear dye (blue), and overlay immunostaining in the NAc 2hrs after treatment with Veh, 3 mg/kg AMPH, 10 mg/kg GBR12909, or 10 mg/kg citalopram. White arrows indicate neurons coimmunolabeled with antibodies for pMeCP2 and GAD67, and blue arrows indicate pMeCP2 induction in neurons that are not GAD67-positive GABAergic interneurons. Scale bar = 20 μ m.

However, examination of double-immunolabeled sections following citalopram administration revealed that the induced pMeCP2 is not restricted to this cell population.

AMPH-induced phosphorylation of MeCP2 is most robust in the NAc, however AMPH drives a small, but statistically significant increase in pMeCP2 in the PLC (Deng *et al*, 2010). To determine which monoamine neurotransmitters are sufficient to induce

pMeCP2 in this brain region, we asked whether GBR12909, citalopram, or reboxetine induced pMeCP2 in the PLC (Figure 5). ANOVA revealed a significant effect of treatment with GBR12909 [$F_{2,14}=5.667$, $p<0.02$]; 10 mg/kg led to increased pMeCP2 induction compared to Veh controls ($p<0.02$) (Figure 5a). Unlike GBR12909, citalopram or reboxetine failed to induce pMeCP2 in the PLC, despite the fact that citalopram induced pMeCP2 in the NAc of the same animals (Figure 5b, 5c, and 3f, respectively). These data suggest there is a selective role for DA in pMeCP2 induction in the PLC. Examination of PLC sections double-immunolabeled for pMeCP2 and GAD67 revealed that the GBR12909-induced pMeCP2 in the PLC was not restricted to GAD67-positive GABAergic interneurons (Figure 5d). Taken together, these data suggest that DA and 5-HT play selective roles in the induction of pMeCP2 in different brain regions and cell types.

2.4.2 Dopamine and serotonin receptor agonists differentially induce pMeCP2

Because selective inhibition of the DAT and SERT transporters is sufficient to drive pMeCP2, we next asked which DA and 5-HT receptor subtypes mediate this response. DA acts through both D₁- (D₁ and D₅) and D₂-class (D₂, D₃, and D₄) receptors (Missale *et al*, 1998). Previously, we showed that SKF81297, a D₁-class receptor agonist, is sufficient to drive robust phosphorylation of MeCP2 in the NAc (Deng *et al*, 2010). To determine the magnitude and regional distribution of pMeCP2 following D₁-class receptor activation, C57BL/6J mice were treated with 5 mg/kg or 7.5 mg/kg SKF81297. To examine pMeCP2 induction following activation of D₂-class receptors, pMeCP2 levels were quantified following treatment with quinpirole (0.4 mg/kg), a D₂-

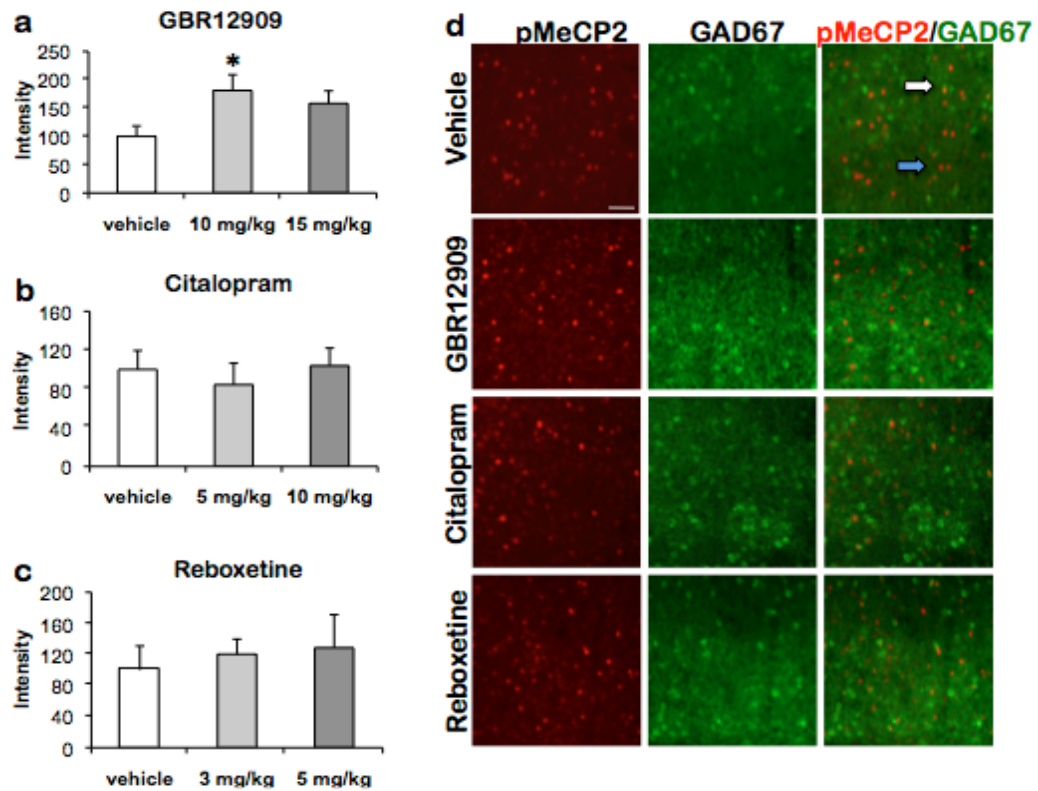


Figure 5: Selective DAT blockade induces pMeCP2 in the PLC. (a-c) pMeCP2 integrated intensity in the PLC following treatment with GBR12909, citalopram, or reboxetine. All values of quantified immunofluorescence intensity were normalized to Veh control for each drug. (d) pMeCP2 (red), GAD67 (green), and overlay immunostaining in the PLC 2 hrs after treatment with Veh, 10 mg/kg GBR12909, 10 mg/kg citalopram, or 3 mg/kg reboxetine. White arrows indicate neurons coimmunolabeled with antibodies for pMeCP2 and GAD67, and blue arrows indicate pMeCP2 induction in neurons that are not GAD67-positive GABAergic interneurons. n=5-7 mice/group. * $p < 0.05$ compared to Veh. Error bars indicate S.E.M. Scale bars = 20 μ m.

class receptor agonist. Finally, because AMPH activates both D₁- and D₂-class receptors simultaneously, we examined how combinatorial DA receptor activation influenced the level and distribution of pMeCP2 induction by co-injecting SKF81297 (7.5 mg/kg) and quinpirole (0.4 mg/kg).

When an ANOVA was applied to pMeCP2 immunoreactivity in the NAc following administration of Veh, SKF81297 (7.5 mg/kg), quinpirole, or co-injection of

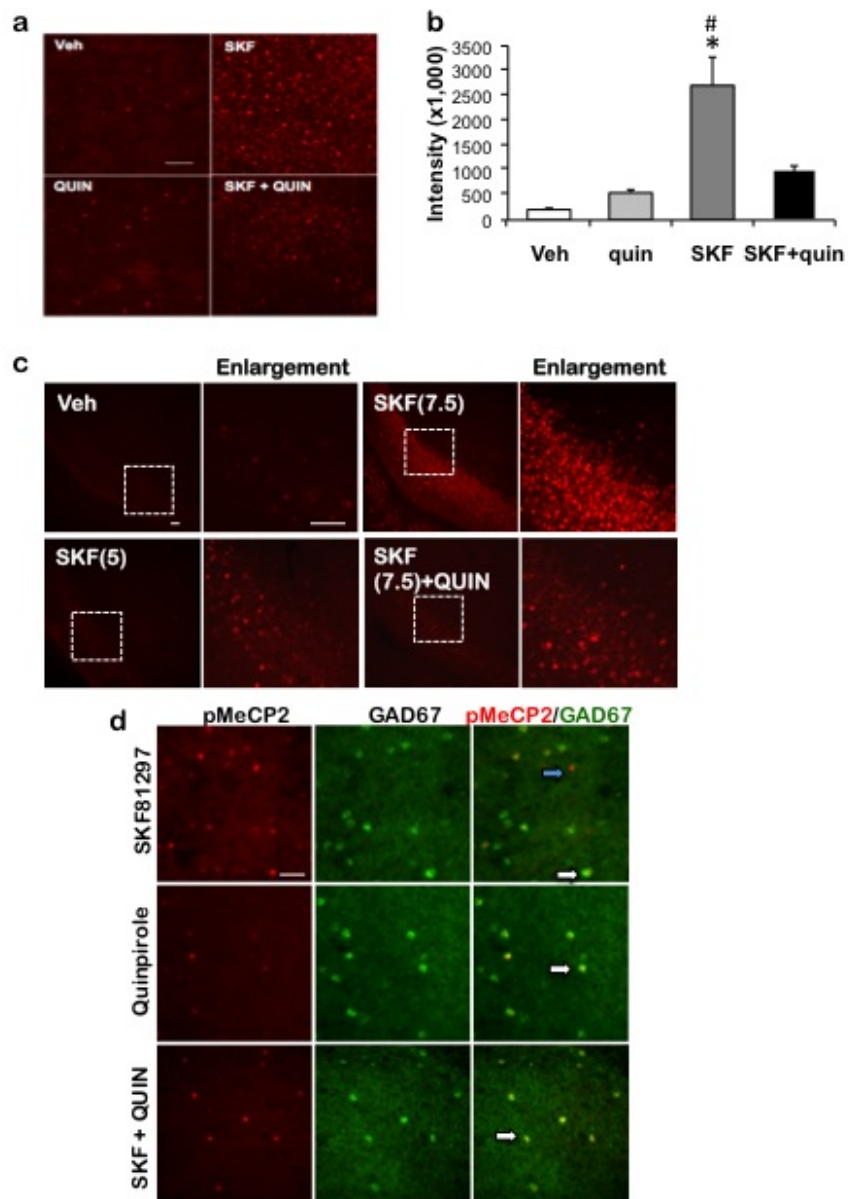


Figure 6: Stimulation of D₁- and D₂-class DA receptors induces different patterns of pMeCP2. (a) pMeCP2 immunostaining in the NAc 2 hrs after treatment with Veh, 7.5 mg/kg SKF81297, 0.4 mg/kg quinpirole, or co-injection of SKF81297 and quinpirole. (b) Quantitation of pMeCP2 immunostaining from panel a (c) pMeCP2 induction in the hippocampus 2 hrs after treatment with Veh, 5 or 7.5 mg/kg SKF81297, or co-injection of 7.5 mg/kg SKF81297 and quinpirole. Enlargement images show the dotted inset regions. (d) pMeCP2 (red), GAD67 (green), and overlay immunostaining in the NAc 2hrs after treatment with 7.5 mg/kg SKF81297, 0.4 mg/kg quinpirole, or co-injection of SKF81297 and quinpirole. White arrows indicate neurons coimmunolabeled with antibodies for pMeCP2 and GAD67, and blue arrows indicate pMeCP2 induction in neurons that are not GAD67-positive GABAergic interneurons. n=4-7 mice/group. *p<0.05 compared to Veh, #p<0.05 SKF compared to SKF+quinpirole. Error bars indicate S.E.M. Scale bar = 20µm.

SKF81297 + quinpirole, an overall effect of treatment was observed [$F_{3,16}=22.3$, $p<0.001$]. SKF81297 led to higher levels of pMeCP2 induction compared to Veh controls ($p<0.001$). Parenthetically, activation of D₁-class receptors alone led to more widespread induction of pMeCP2 than we observe following AMPH, both in the NAc, PLC, and most notably in the hippocampus, where we have not observed any AMPH-induced pMeCP2 (Figure 6a-c). Furthermore, upon examining the cell-types in which pMeCP2 is induced within the NAc following injection of 7.5 mg/kg SKF81297, we find that unlike AMPH, the D₁-class receptor agonist induces pMeCP2 both in GAD67-positive interneurons and additional cell types (Figure 6d). These data suggest that additional AMPH-activated receptor systems may antagonize the effects of D₁-class signaling on the regional and cell-type specific induction of pMeCP2. One candidate for inhibition is D₂-class receptors, which can be activated by the agonist quinpirole. Treatment of mice with 0.4 mg/kg quinpirole alone leads to a small induction of pMeCP2 that is confined to the GABAergic interneurons of the NAc (Figure 6a,b,d). Intriguingly, co-injection of this D₂-class receptor agonist significantly reduces the extent of SKF81297-induced pMeCP2 in both the NAc ($p<0.001$) (Figure 6b), as well as in the hippocampus (Figure 6c). Furthermore, co-injection of SKF81297 and quinpirole restricts the induction of pMeCP2 in the NAc to the GABAergic interneurons (Figure 6d). These data are consistent with the known mechanism of action of AMPH on both D₁- and D₂-classes of receptors, and they suggest that combinatorial D₁- and D₂-class receptor signaling may restrict the pattern and extent of AMPH-induced pMeCP2 to a select population of neurons within the NAc.

In addition to examining induction of pMeCP2 following activation of DA

receptors, we also wanted to investigate the pattern of pMeCP2 produced by stimulation of 5-HT receptors. There are fourteen 5-HT receptor subtypes, which comprise seven different classes of receptors (Barnes and Sharp, 1999). Since 5-HT₂ and 5-HT₃ receptors are highly expressed in the NAc, we asked whether administration of quipazine (3 mg/kg or 4.5 mg/kg), a 5-HT receptor agonist that shows preferential activation of 5-HT₂ and 5-HT₃ receptors, can induce pMeCP2. ANOVA revealed a significant effect of treatment with quipazine [$F_{2,9}=7.898$, $p<0.01$]. Both 3 mg/kg and 4.5 mg/kg quipazine drove significant induction of pMeCP2 in the NAc, and these effects were restricted to the

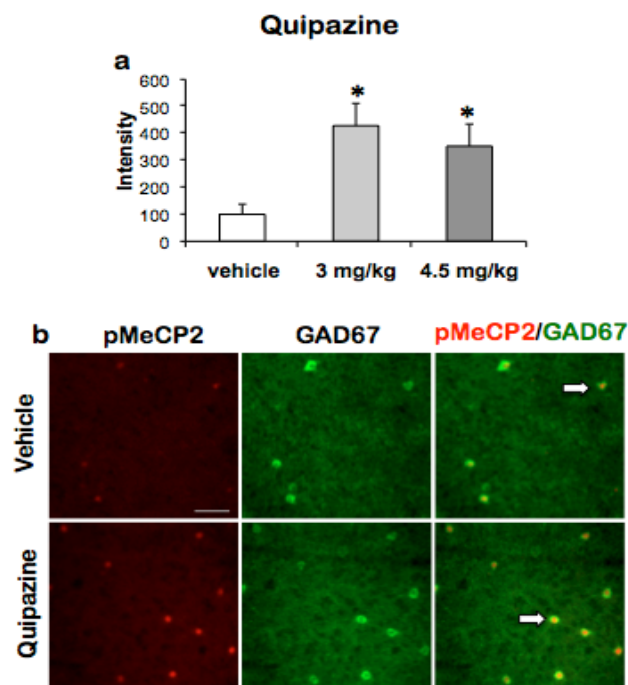


Figure 7: Activation of 5-HT receptors by quipazine induces pMeCP2 in the NAc. (a) Quantitation of pMeCP2 integrated intensity in the NAc 2 hrs after treatment with Veh or 3 or 4.5 mg/kg quipazine. (b) pMeCP2 (red), GAD67 (green), and overlay immunostaining in the NAc 2hrs after treatment with Veh or 3 mg/kg quipazine. White arrows indicate neurons coimmunolabeled with antibodies for pMeCP2 and GAD67. Values of quantitated immunofluorescence were normalized to Veh control. $n=4-6$ mice/group. * $p<0.05$ compared to Veh. Error bars indicated S.E.M. Scale bar = 20 μ m.

GABAergic interneurons ($p < 0.05$) (Figure 7a,b). We note that the cell-type specific induction of pMeCP2 in the NAc following quipazine is in contrast to the pattern of phosphorylation following administration of the indirect agonist citalopram, which can activate signaling at all fourteen 5-HT receptor subtypes and which leads to induction of pMeCP2 that is more widespread (Figure 5). Together, these data suggest that different classes of DA and 5-HT receptors may have distinct effects on the pattern of pMeCP2 induction in the NAc.

Among the pharmacological reagents tested here, we saw the most widespread induction of pMeCP2 following administration of a D₁-class DA receptor agonist. By contrast a D₂-class DA receptor agonist opposed the effects of D₁-class receptor induction of pMeCP2. Because D₁-class receptors are coupled through G_s to increases in intracellular cAMP whereas D₂ class receptors oppose the increase in cAMP through G_i, we considered the possibility that differential regulation of pMeCP2 by distinct DA and 5-HT receptors could be integrated at the level of cAMP signaling. To test whether elevation of cAMP is sufficient to induce pMeCP2 *in vivo*, we infused the adenylate cyclase activator forskolin directly into the striatum of C57BL/6J mice. All sections selected for staining had similar cannula placement (Figure 8a). Compared with saline infusion, forskolin robustly induced expression of the cAMP-regulated immediate early gene product Fos in neurons below the tip of the cannula, demonstrating the efficacy of the drug treatment ($p < 0.01$) (Figure 8b,c). Similarly, we found that forskolin infusion was sufficient to induce pMeCP2 ($p < 0.05$) (Figure 8b,d). Unlike the sparse pattern of pMeCP2 induced by systemic AMPH administration (Figure 3), intra-striatal forskolin induced pMeCP2 in most of the cells near the cannula tip. This forskolin-induced

pMeCP2 colocalized in cells with DARPP-32, a marker of MSNs (Figure 8e). Thus these data show that intra-striatal forskolin delivery is sufficient to induce pMeCP2 in MSNs.

Forskolin infusion into the striatum could drive pMeCP2 by activating postsynaptic signaling cascades that directly induce phosphorylation in MSNs. Alternatively, because forskolin can act on presynaptic terminals to enhance the probability of neurotransmitter release (Chen and Reger, 1997; Chavez-Noriega and Stevens, 1994) the induction of pMeCP2 in MSNs could be an indirect consequence of forskolin-induced release of neurotransmitter from the terminals of neurons that project to the striatum from other brain regions. To determine whether forskolin can act in MSNs to induce pMeCP2, we isolated the striatum from embryonic rat brains and treated dissociated cultures of striatal neurons with either forskolin or the D₁-class DA receptor agonist SKF38393. Although these treatments induced phosphorylation of the protein kinase A (PKA) target and transcription factor CREB at Ser133, elevation of cAMP in cultured striatal neurons was not sufficient to induce pMeCP2 (Figure 8f). By contrast, both membrane depolarization and NMDA application induced pMeCP2 in these neurons in a manner that was dependent on the activation of L-type voltage gated calcium channels and NMDA-type glutamate receptors respectively (Figure 8g). We cannot rule out that the inability of forskolin to activate pMeCP2 in cultured MSNs is not a consequence of the immaturity of these cells. Nonetheless taken all together our data suggest that the differential ability of specific DA and 5-HT receptor agonists to drive pMeCP2 in MSNs, 1) is integrated at the level of cAMP signaling and, 2) may depend, at least in part, on presynaptic cAMP-dependent effects.

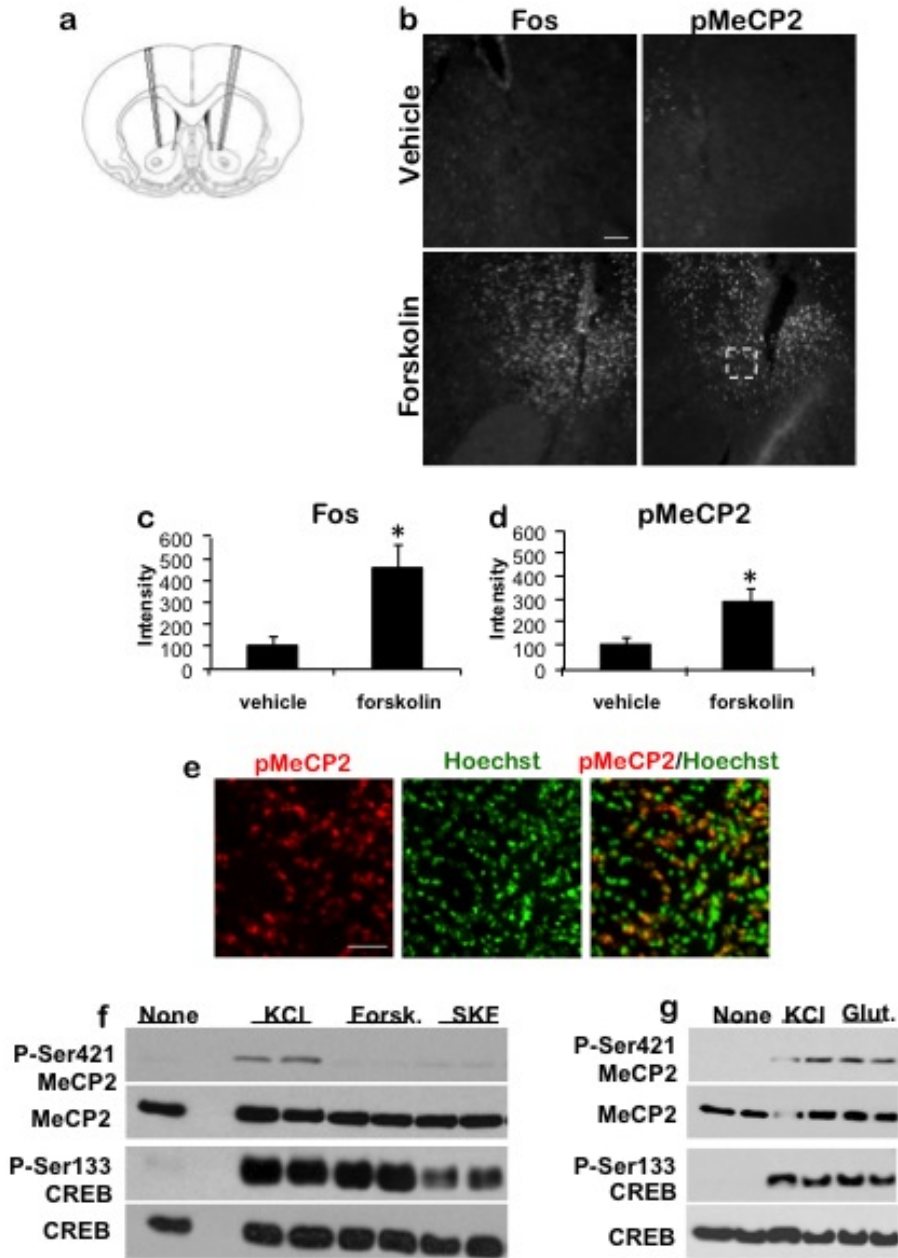


Figure 8: Forskolin is sufficient to induce pMeCP2 in the medium spiny neurons *in vivo* but not *in vitro*. (a) Anatomical location of microinjection sites in the striatum. (b) pMeCP2 and Fos immunostaining in the striatum 90 min after treatment with Veh or forskolin. (c,d) Quantitation of Fos and pMeCP2 integrated intensity in the striatum 90 min after treatment with Veh or forskolin. Values of quantitated immunofluorescence were normalized to Veh control. n=9 mice/group. *p<0.05 compared to Veh. Error bars indicated S.E.M. (e) Colocalization of pMeCP2 immunoreactivity with cell type markers in the region at the tip of the cannula in sections from forskolin-treated mice. pMeCP2

(red), the MSN marker DARPP-32 (green, top), the astrocyte marker GFAP (green, bottom). Scale bar= 20 μ m. **(f,g)** Cultured embryonic rat striatal neurons (5 days *in vitro*) were treated for 60 min with various pharmacological reagents, the cells were lysed directly in boiling SDS and separated by SDS-PAGE, western blotting was performed using the antibodies indicated, and the blots were visualized with chemiluminescence on film. **f)** Cultures were left either untreated (none), or treated with 55mM KCl in an isotonic solution, 10 μ M forskolin (Forsk.) to elevate intracellular cAMP, or 50 μ M of the D₁-class DA receptor agonist SKF38393 (SKF). Western blots were probed for pMeCP2 and total MeCP2, or pCREB (Ser133) and total CREB as a control for the activation of cAMP signaling pathways. No protein was loaded in lane 2. **g)** Cultures were left either untreated, or treated with 55mM KCl or 50 μ M NMDA as indicated. In the lanes indicated the L-type voltage gated calcium channel inhibitor Nimodipine (Nim.) or the NMDA-receptor antagonist APV were added 2 min before stimulation.

2.4.3 AMPH-induced pMeCP2 is reduced in SERT-KO mice

The data presented thus far have addressed the sufficiency of activating specific monoamine neurotransmitter systems for induction of pMeCP2. However to begin to understand whether regulation of specific monoamine neurotransmitter systems is required for the induction of pMeCP2 following AMPH administration, we assessed the ability of AMPH to induce pMeCP2 in the NAc in knockout strains of mice lacking expression of single monoamine transporters (Figure 9).

To determine whether AMPH can induce pMeCP2 in the NAc in the absence of the DAT, we administered either Veh or 3mg/kg AMPH to DAT-KO mice and their DAT-WT littermate controls, monitored their activity in the open field for 1 hr post-injection, and then quantified pMeCP2 in the NAc. A two-way ANOVA applied to locomotor activity 1 hr post-injection revealed an overall main effect of genotype [$F_{3,22}=74.516, p<0.001$], treatment [$F_{3,22}=8.911, p<0.008$], and a significant genotype by treatment interaction [$F_{3,22}=38.785, p<0.001$]. Consistent with previous reports (Gainetdinov *et al*, 1999; Giros *et al*, 1996), we found that DAT-KO mice had higher levels of baseline locomotor activity ($p<0.001$) compared to the DAT-WT Veh-controls

and that their locomotor activity decreased following AMPH exposure ($p < 0.001$) compared to DAT-KO mice given Veh (Figure 9a). When an ANOVA was applied to pMeCP2 immunoreactivity, a main effect of treatment [$F_{3,22}=17.709$, $p < 0.001$] was observed. However, there was no effect of genotype [$F_{3,22}=2.082$, $p < 0.166$], and the genotype by treatment interaction was not significant [$F_{3,22}=1.192$, $p < 0.289$]. Bonferroni corrected pair-wise comparisons noted that pMeCP2 levels were increased by AMPH in DAT-KO and DAT-WT mice compared to their Veh-treated controls ($p < 0.033$ and $p < 0.002$, respectively) (Figure 9b). However, the AMPH-induced levels of pMeCP2 did not differ between DAT-KO mice and their DAT-WT littermates ($p < 0.807$). Although the data did not reach significance, DAT-KO mice showed a trend toward increased basal levels of pMeCP2 compared with DAT-WT mice (Figure 9b), which may arise as a consequence of the increased basal levels of extracellular DA in DAT-KOs (Gainetdinov *et al*, 1999). Microdialysis studies have shown that psychostimulants can increase extracellular DA levels in the NAc of DAT-KO mice through mechanisms that may involve blockade of the SERT or NET, although the functional relevance of a further increase in extracellular DA in face of the chronic hyperdopaminergia found in this strain remains unclear (Gainetdinov *et al*, 2003; Carboni *et al*, 2001). Nonetheless, since AMPH can also bind the SERT and NET, we next asked whether these transporters are required for AMPH-induced pMeCP2.

To determine whether AMPH-induced pMeCP2 in the NAc is impaired in the absence of the SERT or NET, SERT-KO and NET-KO mice and their respective WT littermates were treated with Veh or AMPH, locomotor activity was monitored 1 hr post-injection, and subsequently pMeCP2 was quantified in the NAc. For the SERT mice, a

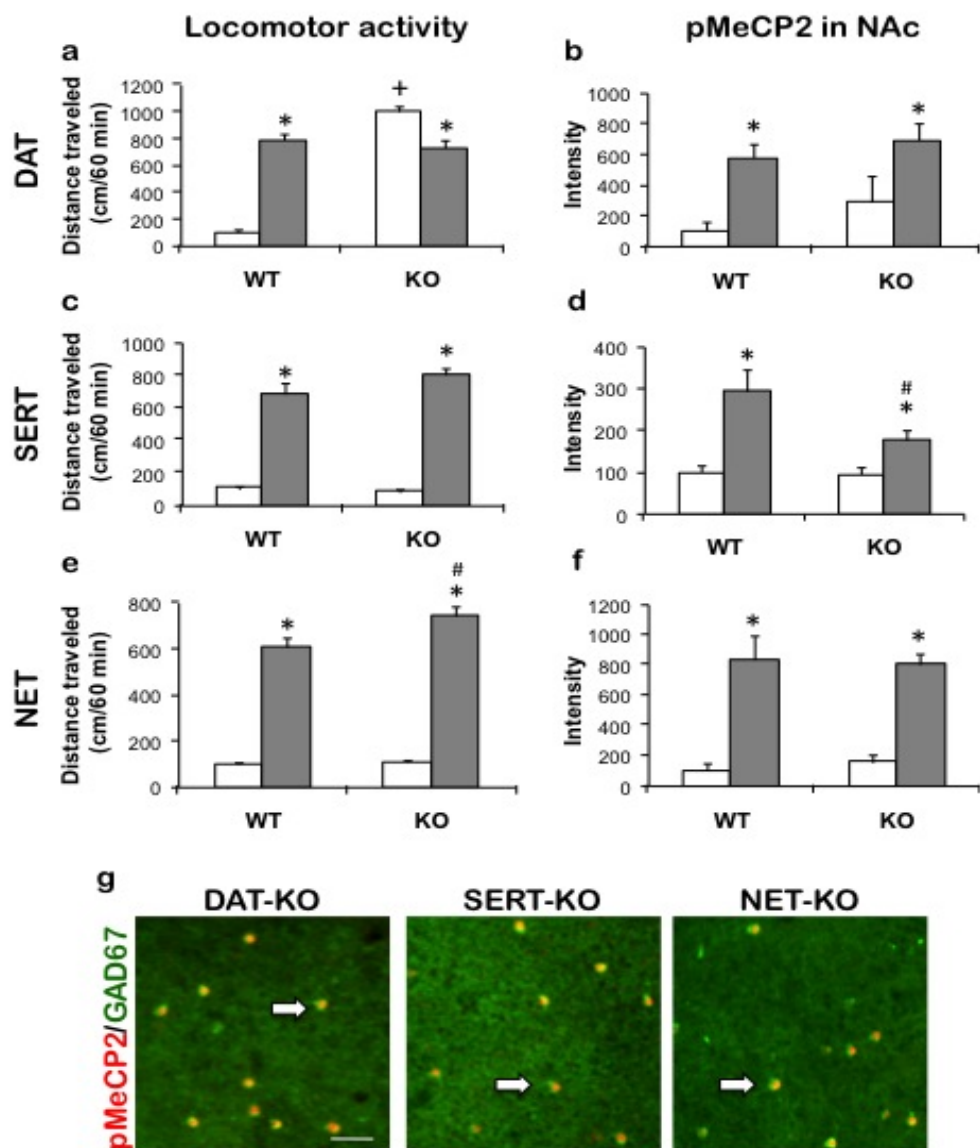


Figure 9: AMPH-induced pMeCP2 is reduced in the NAc of SERT-KO mice. (a,c,e) The effects of Veh or AMPH treatment on locomotor activity in DAT, SERT, and NET mice 1 hr post-injection. (b,d,f) pMeCP2 induction in the NAc following Veh or AMPH treatment in DAT, SERT and NET mice. All values of locomotor activity and quantitated immunofluorescence were normalized to the WT Veh control for each strain of mice. Veh treatment is indicated with a white bar, and AMPH treatment (3 mg/kg) is indicated with a dark gray bar. $n=6-8$ mice/group. $*p<0.05$ AMPH compared to Veh within the same genotype, $+p<0.05$ WT Veh compared to mutant Veh, $\#p<0.05$ WT AMPH compared to mutant AMPH. (g) pMeCP2 (red) and GAD67 (green overlay immunostaining in the NAc 2hrs after treatment with 3 mg/kg AMPH in the DAT, SERT, and NET knockout mice. White arrows indicate neurons coimmunolabeled with antibodies for pMeCP2 and GAD67. Error bars indicate S.E.M. Scale bar = 20 μ m.

two-way ANOVA for locomotor activity revealed only a significant effect of treatment [$F_{3,23}=38.262, p<0.001$]. Hence, locomotor activity was stimulated by AMPH to similar extents in both SERT-KO mice and their WT littermates (Figure 9c). When changes in pMeCP2 were considered, the ANOVA detected significant main effects of genotype [$F_{3,23}=5.542, p<0.029$] and treatment [$F_{3,23}=31.20, p<0.001$], and a significant genotype by treatment interaction [$F_{3,23}=5.467, p<0.03$]. Interestingly, Bonferroni comparisons demonstrated that AMPH-induced pMeCP2 was significantly reduced in SERT-KO mice compared with SERT-WTs ($p<0.003$), even though AMPH induced locomotor activity to the same extents in both genotypes (Figure 9d). Taken together with our pharmacological studies, the observation that AMPH-induced pMeCP2 in the NAc is significantly reduced in SERT-KO mice provides independent evidence of a role for 5-HT signaling in the regulation of pMeCP2 in the CNS.

With regards to NET-KO mice, a two-way ANOVA for locomotion revealed a significant effect of genotype [$F_{3,21}=22.008, p<0.001$], treatment [$F_{3,21}=641.144, p<0.001$], and significant treatment by genotype interaction [$F_{3,21}=20.578, p<0.001$]. As previously reported (Xu *et al*, 2000), NET-KO mice were hyperresponsive to the locomotor-stimulating effects of acute AMPH administration compared to their WT littermates ($p<0.001$) (Figure 9e). By contrast, an ANOVA for pMeCP2 immunoreactivity in the NAc found only a significant effect of treatment [$F_{3,21}=104.690, p<0.001$] (Figure 9f). Therefore, AMPH-induced pMeCP2 was not significantly altered in the absence of the NET.

Analysis of AMPH-stimulated pMeCP2 induction within the NAc revealed that in all genotypes tested pMeCP2 remained selective for GAD67-positive GABAergic

interneurons (Fig 9g). These data suggest that no single monoamine neurotransmitter system dictates the cell-type specificity of this pattern of pMeCP2 induction in the NAc. Furthermore, the evidence that genetic disruption of any single transporter failed to eliminate AMPH-induced pMeCP2 supports our pharmacological evidence that combinatorial signaling through multiple monoamine receptors drives the overall extent and pattern of pMeCP2 induced in the CNS.

2.4.4 pMeCP2 in the NAc following repeated AMPH does not predict behavioral sensitization

Beyond providing a means to study the mechanistic actions of pharmacological agents, monoamine transporter KO mice have proven to be useful for investigating the physiological functions of monoamine regulated signaling pathways (Gainetdinov and Caron, 2003). For example, these mice have been used to gain insight into the mechanisms that underlie behavioral sensitization (Rocha, 2003; Xu *et al.*, 2000), which is a progressive and persistent increase in behavioral responses to psychomotor stimulants that develops following their repeated administration (Pierce and Kalivas, 1997). Our previous data revealed a strong correlation between the magnitude of pMeCP2 induced in the NAc and the level of open field locomotor activity following repeated AMPH administration, which is one measure of behavioral sensitization (Deng *et al.*, 2010). To test the hypothesis that pMeCP2 levels in the NAc predict behavioral sensitization to AMPH, we next asked whether pMeCP2 would correlate with locomotor activity following repeated AMPH administration in the NET-KO mice, which fail to sensitize (Xu *et al.*, 2000).

NET-KO and their NET-WT littermates were injected with either Veh or AMPH once daily for 5 consecutive days in their home cages, then following a 7 day withdrawal they were administered an AMPH challenge in the open field to assess locomotor sensitization. The NET-KO mice were significantly more responsive to the locomotor stimulating effects of a single injection of AMPH in this paradigm than similarly treated WT littermates, as we have shown previously (Figure 9c). However, unlike their NET-WT littermates, the NET-KO mice failed to exhibit significantly enhanced locomotor activity following repeated AMPH administration ($p < 0.0033$ for WT and $p < 0.12$ for KO, VEH:AMPH compared to AMPH:AMPH) (Figure 10a,b). When changes in pMeCP2 were considered, ANOVA failed to detect significant effects of genotype [$F_{3,52} = 0.001$, $p < 0.98$] or treatment [$F_{3,52} = 0.063$, $p < 0.803$]. pMeCP2 in the NAc was induced to similar extents in the two treatment groups (Veh:AMPH or AMPH:AMPH) for each genotype (Figure 10c). These data confirm that the lack of NET expression has no effect on the magnitude of pMeCP2 induction following either acute or repeated AMPH exposure, thus allowing us to analyze the correlation between induced pMeCP2 and locomotor activity in these mice.

Surprisingly, when a correlational analysis was applied to locomotor activity and NAc pMeCP2 induction in individual mice a marked difference between the acute AMPH (VEH:AMPH) and repeated AMPH (AMPH:AMPH) treatment groups emerged for both NET genotypes (Figure 10d-g). No significant relationship between locomotor activity and pMeCP2 induction was observed in the VEH:AMPH group of either NET-WT ($r = 0.16$, $p = 0.578$) or NET-KO mice ($r = 0.25$, $p = 0.379$) (Figure 10d,f). By contrast, we observed a strong correlation of pMeCP2 immunoreactivity with locomotor activity in

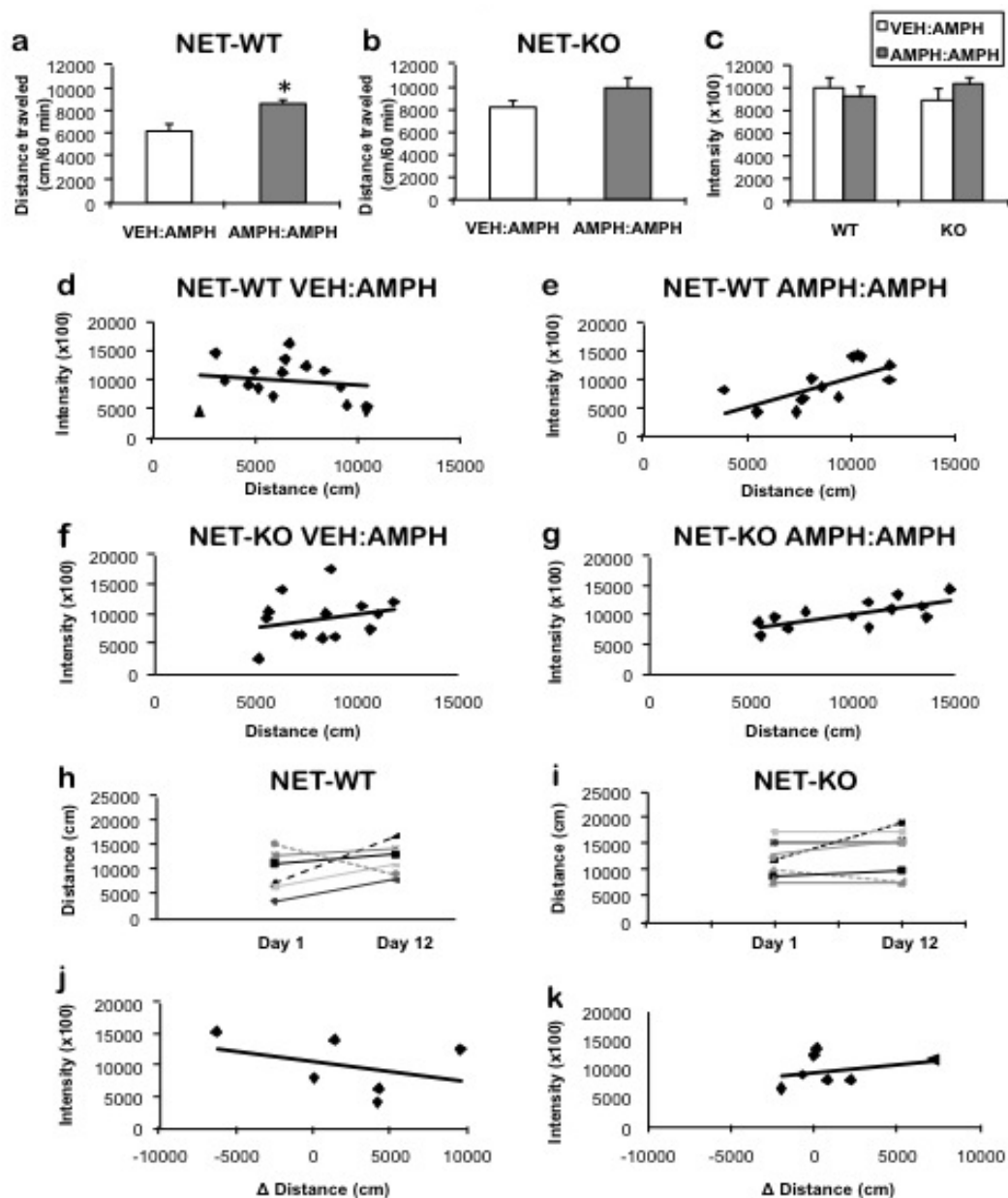


Figure 10: pMeCP2 in the NAc of NET-KO mice correlates with locomotor activity but not behavioral sensitization after repeated AMPH treatment. (a, b) The effects of acute (VEH:AMPH) or repeated (AMPH:AMPH) AMPH administration on locomotor activity in NET-WT and NET-KO mice 1 hr post-injection on the challenge day. (c) pMeCP2 integrated intensity in the NAc following AMPH treatment on the challenge day in NET-WT and NET-KO mice. (d-g) Pearson product correlations of pMeCP2 immunofluorescence intensity in the NAc and cumulative locomotor activity (1 hr following the challenge injection) from individual mice. (h, i) Comparison of locomotor activity 1 hr post-injection on Day 1 and the challenge day (Day 12) in NET-WT and NET-KO mice under the AMPH:AMPH condition. (j, k) Pearson product correlations of pMeCP2 immunofluorescence intensity in the NAc and the change in locomotor activity from Day 1 to Day 12 from individual mice in the NET-WT and NET-KO AMPH:AMPH groups. * $p < 0.05$ compared to VEH:AMPH. Error bars indicate S.E.M.

the AMPH:AMPH treatment group of both genotypes ($r=0.67$, $p=0.012$; NET-WT AMPH:AMPH and $r=0.71$, $p=0.007$ NET-KO AMPH:AMPH) (Figure 10e,g).

Although the level of locomotor activity after repeated AMPH can be used as an indication of behavioral sensitization, this metric does not reveal how the locomotor behavior of any single animal changed over the course of the repeated AMPH treatment. To obtain a more direct measure of locomotor sensitization in individual mice, we measured locomotor responses to AMPH in a different sensitization paradigm in which we monitored open field locomotor activity of each mouse on both the first day of AMPH treatment as well as on the challenge day. This experimental design allowed us to calculate a sensitization score for each mouse by subtracting the locomotor activity on the first day of AMPH treatment from the locomotor activity following AMPH exposure on the challenge day (Figure 10h,i). When a correlational analysis was applied to sensitization scores and NAc pMeCP2 levels in individual mice, no correlation was seen for either the NET-WT ($r=0.373$, $p=0.467$ AMPH:AMPH) or the NET-KO mice ($r=0.314$, $p=0.492$ AMPH:AMPH) (Figure 10j,k).

Taken together, these data replicate our previous observation that pMeCP2 levels correlate with open field locomotor activity only following repeated and not after acute AMPH. However the levels of pMeCP2 in the NAc after repeated AMPH administration do not predict the degree of behavioral sensitization in individual mice, at least as measured by open field locomotor activity. An alternate hypothesis suggested by our data is that levels of locomotor activity following repeated AMPH exposure and pMeCP2 levels in the NAc may instead reflect other functional consequences of repeated AMPH treatment that persist in the absence of NET expression.

2.5 DISCUSSION

The net effect of AMPH interactions with monoamine transporters in the CNS is the activation of multiple monoaminergic receptor-coupled signaling pathways, culminating in the induction of intracellular processes including gene expression (Moratalla *et al*, 1996). Previously we showed that AMPH administration induces Ser421 phosphorylation of MeCP2 in select populations of neurons within the NAc and PLC. Here we have characterized the specific monoaminergic neurotransmitter pathways that regulate this phosphorylation event. Our data demonstrate that activation of both DA and 5-HT signaling is sufficient to induce pMeCP2. By contrast we find no evidence for NE-dependent regulation of pMeCP2 even though three classes of NE receptors are expressed in the brain, several of which have been implicated in mediating certain aspects of behavioral responses to psychostimulants (Weinshenker and Schroeder, 2007; Xu *et al*, 2000; Laakso and Hietala, 2000). Although these data do not exclude roles for specific NE receptor-dependent regulation of pMeCP2 in other contexts, they do suggest that induction of pMeCP2 is selective for specific stimuli.

Interestingly, we find that the regional- and cell-type specific pattern of pMeCP2 induction depends on the particular combination of DA and 5-HT receptors activated. Consistent with the hypothesis that combinatorial signaling through multiple monoamine receptors sculpts the pattern of pMeCP2 *in vivo*, we find that genetic disruption of any single plasma membrane monoamine transporter in DAT-KO, SERT-KO, and NET-KO mice fails to completely block the ability of AMPH to induce pMeCP2 in the NAc and does not change the cell-type selectivity of the induced pattern. Parenthetically, VMAT2 is the other major target of AMPH in the CNS, and although VMAT2-KO mice are not

viable after birth, we find that AMPH induces a similar magnitude and pattern of pMeCP2 in the NAc of VMAT2-HETs compared with their VMAT2-WT littermates (data not shown). Analysis of the distribution of pMeCP2 in the CNS following the various pharmacological stimuli used in this study also suggests that no single transporter or receptor expression pattern is sufficient to fully explain the selectivity of pMeCP2 induction. For example, the DAT is highly concentrated in DA-rich brain regions including the neostriatum, NAc, and olfactory tubercle (Ciliax *et al*, 1995). By contrast, the SERT and NET have more widespread distributions in the brain; high levels of SERT are found in the dorsal striatum, cortex, hippocampus, amygdala, and brainstem (Sur *et al*, 1996), whereas NET expression is concentrated in the PLC, bed nucleus of stria terminalis, and ventral regions of the striatum, including the NAc (Schroeter *et al*, 2000). However, only selective inhibition of the DAT induces pMeCP2 in the PLC, even though the SERT and NET are also highly expressed in this brain region (Miner *et al*, 2003; Miner *et al*, 2000). Taken together with the failure of either AMPH or the selective DAT inhibitor GBR12909 to induce pMeCP2 in medium-spiny neurons of the NAc, which express high levels of DA receptors, these data suggest that either combinatorial patterns of transporter and receptor expression or additional mechanisms of specificity are important for the regulation of pMeCP2.

Our data suggest that one way different combinations of DA and 5-HT receptors influence the cell-type specific phosphorylation of MeCP2 is via the integration of receptor-induced signaling cascades at the level of cAMP. Both D₁- and D₂- class DA receptors as well as most types of 5-HT receptors are coupled by G-proteins to the regulation of adenylate cyclase and cAMP signaling (Barnes and Sharp, 1999; Missale *et*

al, 1998). D₁-class DA receptors elevate cAMP levels and we find that they drive widespread induction of pMeCP2 both in MSNs within the NAc and in other brain regions including the hippocampus. D₂-class DA receptors inhibit cAMP production and we see that they oppose the D₁-class DA receptor-dependent induction of pMeCP2 in MSNs and hippocampal neurons. Elevation of cAMP levels leads to the activation of intracellular signaling cascades that can directly regulate nuclear signaling events, such as the induction of PKA-dependent Ser133 phosphorylation on the transcription factor CREB (Yamamoto *et al*, 1988). However, MeCP2 Ser421 is not a direct target of phosphorylation by PKA (Zhou *et al*, 2006). Instead calcium-calmodulin activated kinases (CaMKII or CaMKIV) have been identified as the likely MeCP2 Ser421 kinases following the activation of NMDA-type glutamate receptors and the opening of L-type voltage-gated calcium channels (Tao *et al*, 2009; Zhou *et al*, 2006). It is possible that DA and 5-HT receptors could induce pMeCP2 via the regulation of intracellular calcium levels. G_{q/11} coupled DA and 5-HT receptors can release calcium from intracellular stores (Missale *et al*, 1998), and the 5-HT₃ receptor is unique in that it is a ligand-gated ion channel directly permeable to calcium (Derkach *et al*, 1989). Activation of D₁-class DA receptors in cultured striatal neurons can elevate intracellular calcium levels indirectly through a mechanism that may involve DA- and PKA-dependent phosphorylation of the NR1 subunit of the NMDA-type glutamate receptor (Dudman *et al*, 2003). Stimulation of D₁-class DA receptors also leads to PKA-dependent potentiation of L-type voltage gated calcium channels in striatal neurons (Surmeier *et al*, 1995), and the subsequent activation of CaMKII by this pathway has been shown to be required for the regulation of AMPA-type glutamate receptor trafficking in the NAc *in vivo* in a cocaine-seeking

paradigm (Anderson *et al*, 2008).

In addition to these postsynaptic sites of DA and 5-HT receptor action, our data raise the possibility that the induction of pMeCP2 in MSNs may be modulated by cAMP-regulated processes in presynaptic terminals of afferent neurons that project to the striatum. Forskolin has been widely shown to enhance presynaptic vesicle release probability (Robbe *et al*, 2001; Chen and Regher, 1997; Chavez-Noriega and Stevens, 1994). In striatal slice preparations, DA-dependent modulation of glutamate release from corticostriatal terminals allows for filtering of less active inputs and reinforcement of specific sets of corticostriatal synaptic connections (Bamford *et al*, 2004). Application of AMPH to this preparation inhibits presynaptic vesicle release from corticostriatal glutamatergic terminals in a manner that depends on D₂-class DA receptors (Bamford *et al*, 2004). Since NMDA-type glutamate receptors are robust activators of pMeCP2 in MSNs (Figure 6g), we propose that the inhibition of glutamate release by D₂-class receptors may underlie the ability of D₂-class receptor agonists to inhibit the D₁-class agonist induction of pMeCP2 in this population of neurons.

One commonality we observed among all of the DA and 5-HT reagents tested in this study is their ability to induce robust pMeCP2 in GAD67-positive GABAergic interneurons of the NAc. Although the signaling mechanisms that mediate this induction remain to be fully established, several lines of evidence suggest that this may reflect increases in firing of this cell population. In vivo recordings from presumed GAD67-positive striatal GABAergic interneurons in freely-moving rats demonstrate that AMPH administration induces a rapid increase in the firing rate of most of these neurons (Wiltschko *et al*, 2010). D₂-class receptors appear to play an important facilitative role in

this excitability because administration of the D₂-class receptor agonist eticlopride uniformly decreases the firing rate of these cells (Wiltchko *et al*, 2010). DA and 5-HT could act directly on GAD67-positive GABAergic interneurons to modulate their activity. Striatal GABAergic interneurons have been shown to express and be excited by D₁-class DA receptors; in slice preparations they are also activated indirectly through actions of presynaptic D₂-class receptors (Centonze *et al*, 2003; Bracci *et al*, 2002). Application of 5-HT to striatal slices also increases firing of GABAergic interneurons via activation of 5-HT_{2C} receptors (Blomeley and Bracci, 2009). Alternatively, DA and 5-HT could modulate properties of the afferent inputs to the striatum in a manner that changes the drive to GAD67-positive GABAergic interneurons. Excitatory input to GAD67-positive GABAergic interneurons in the NAc comes from the prefrontal cortex (Gruber *et al*, 2009), while the major source of GABAergic inhibitory feedback onto these neurons comes from the globus pallidus (Bevan *et al*, 1998). D₂-receptor antagonists enhance the expression of Fos in the globus pallidus (Billings and Marshall, 2003), suggesting that increased firing of globus pallidus neurons induced by D₂ blockade could contribute to the suppression in striatal GABAergic interneuron firing described above (Wiltchko *et al*, 2010). Increased firing of GABAergic interneurons would lead to the opening of voltage-gated calcium channels, thus activating the CaM kinases that phosphorylate MeCP2. Although GABAergic interneurons are not thought to express the α isoform of CaMKII (Liu *et al*, 1996), the β , γ , and δ isoforms are widely expressed throughout the brain although at much lower levels than CaMKII α (Sakagami *et al*, 1993; Tighilet *et al*, 1998). Interestingly a subset of hippocampal GABAergic interneurons have been shown to have an NMDA-receptor dependent form of long-term potentiation that is blocked by

CaM kinase inhibitors, suggesting the functional importance of non- α isoform mediated CaMKII activity in these neurons (Lamsa *et al*, 2007).

Finally, our behavioral data yield some insights into the functional implications of pMeCP2 induction. First, although the induction of pMeCP2 in the NAc is concurrent with the increase in locomotor activity following acute AMPH administration, pMeCP2 coincides with decreased locomotor activity following acute citalopram and with the paradoxical decrease in locomotor activity following AMPH administration in DAT-KO mice. Furthermore, following a single dose of AMPH there is no correlation between the level of pMeCP2 induced in the NAc and the locomotor activity of an individual animal (Deng *et al*, 2010). Thus pMeCP2 induction in the NAc reflects effects of these drugs on the brain that are not directly involved in determining or sensing the level of locomotor activity. Interestingly, pMeCP2 in the NAc does correlate with locomotor activity following repeated AMPH treatment. Locomotor activity after repeated AMPH exposure is one measure of behavioral sensitization, which presumably occurs as a result of psychostimulant-induced neural circuit adaptations, although these remain poorly defined (Kauer and Malenka, 2007). However, pMeCP2 still correlates with locomotor activity following repeated AMPH treatment in NET-KO mice, which do not sensitize. When we used a more direct measure of sensitization in individual mice by recording their locomotor activity on the first and last day of AMPH treatment, we found no correlation between pMeCP2 and sensitization in NET-WT or NET-KO mice. Importantly, although the NET-KO mice do not sensitize to repeated AMPH administration, they do show other behavioral adaptations to repeated psychostimulant administration. For example, the NET-KO mice show preference for the cocaine-paired chamber in a place-preference

assay (Xu *et al*, 2000), and they self-administer cocaine in a dose-dependent manner (Rocha, 2003). Thus we hypothesize that pMeCP2 induction may reflect the neural circuit activities that underlie these or other related behavioral adaptations to repeated AMPH. Because the phosphorylation of pMeCP2 is selective for GABAergic interneurons of the NAc following AMPH and many of the other drugs tested here, it is tempting to speculate that pMeCP2 may play a role in plasticity of this neuronal population. The functions of GAD67-positive GABAergic striatal interneurons in behavioral responses to AMPH are entirely unknown. However these cells exert robust feedforward inhibition over striatal output (Koos and Tepper, 1999), and changes in their firing patterns have been suggested to underlie the initiation of chosen actions while suppressing unwanted alternatives (Gage *et al*, 2010).

3. EXAMINATION OF THE BEHAVIORS THAT REQUIRE MECP2 PHOSPHORYLATION AT S421

3.1 SUMMARY

Systemic administration of citalopram and quipazine, two drugs that selectively activate serotonergic (5-HT) signaling induce MeCP2 phosphorylation at Ser421 (pMeCP2) in the nucleus accumbens (NAc), implicating a role for pMeCP2 in 5-HT-mediated behaviors, specifically anxiety-like and depression-like behavior. In order to assess the role of pMeCP2 in anxiety and depression, we examined behavior in mice bearing a knockin (KI) mutation that converts serine to alanine at 421 (S421A). We find that these mutant mice do not exhibit severe Rett syndrome (RTT)-like phenotypes but show altered behavioral flexibility in learning and memory tests that involve recognizing novel objects or mice. Furthermore, our data show that the KI mice do not display enhanced anxiety-like behaviors. However, the KI mice show increased immobility in the forced swim test relative to wild-type (WT) littermates. Together, these studies advance the understanding of the involvement of pMeCP2 in the behavioral features of RTT as well as uncover a novel role for pMeCP2 in depression-like behavior.

3.2 INTRODUCTION

Examination of the monoaminergic signaling pathways that regulate MeCP2 phosphorylation at S421 (pMeCP2) has revealed that both dopamine (DA) and serotonin (5-HT) induce pMeCP2 (Hutchinson *et al*, 2011). These data raise the possibility that serotonergic regulation of pMeCP2 could be important in a range of experimental paradigms and cell types. Drugs that target the serotonin transporter (SERT) and 5-HT receptors are widely used in treating neuropsychiatric disorders such as depression

(Krishnan and Nestler, 2008; Morilak and Frazer, 2004; Charney, 1998). In rodents, 5-HT regulation of affective behaviors has been shown in social-defeat stress and extended social isolation (Wallace *et al*, 2009; Tsankova *et al*, 2006), and drugs that alter 5-HT transmission modulate depressive-like behavior in these paradigms through mechanisms that are thought to involve changes in gene transcription (Vialou *et al*, 2010; Wallace *et al*, 2009; Tsankova *et al*, 2006; Nestler and Carlezon, 2006). Our evidence that a selective SERT inhibitor induces pMeCP2 in neural circuits that are functionally relevant to affective behaviors raises the possibility that this pathway could be involved in the mechanism of antidepressant action. From this perspective, investigating the regulation of pMeCP2 in anxiety- and depression-like behavior and in the response to antidepressant treatment may yield new insights into additional functional roles for MeCP2 in monoamine-regulated neural plasticity.

In order to examine the role of pMeCP2 in various behaviors and to assess the function of pMeCP2 *in vivo*, Cohen and colleagues generated a knockin (KI) mouse of MeCP2 in which Ser is converted to Ala at 421 (S421A) (Cohen *et al*, 2011). Prior to assessing anxiety- and depression-like behavior in the KI mice, it was first necessary to compare the phenotype of this mutant to other mouse models of Rett syndrome (RTT). Mice bearing mutations in MeCP2 exhibit motor deficits and cognitive impairments that make it difficult to put them through more complex behavioral assays (Moretti *et al*, 2006; Gemeli *et al*, 2005; Shahbazian *et al*, 2002). Furthermore, the contribution of activity-dependent pMeCP2 to the phenotype of RTT has not been determined. Therefore, we first assessed strength, agility, coordination, motor skills, learning and memory, and sociability in the KI mice. We find that the KI mice display no overt

defects and do not show major abnormalities in motor activity levels or function.

Although they do not show altered learning and memory in fear conditioning and the Morris water maze, the KI mice show abnormal behavioral responses to novel experience. After determining that the S421A mutant mice are suitable for more complex behavioral testing, we assessed anxiety- and depression-like behavior in these mice. We find that the KI mice do not display heightened anxiety, as confirmed by several different paradigms. However, the KI mice spend more time immobile in the forced swim test, supporting a novel role for pMeCP2 in depression-like behavior.

3.3 MATERIALS AND METHODS

3.3.1 Animals

Adult (8-10 week old) male KI mice (Cohen *et al*, 2011) were used in these studies. The wild-type (WT) and knockin littermates were generated from heterozygous (HET) breedings. Animals were weaned at 21-30 days of age, housed in groups of 3-5, except for during the assessment of spontaneous motor activity and sucrose preference. All animals were given free access to standard laboratory chow and water and were housed in a humidity- and temperature-controlled room on a 14 hr/10 hr light/dark cycle unless otherwise noted. All experiments were conducted with an approved protocol from the Duke University Institutional Animal Care and Use Committee in accordance with guidelines from the National Institutes of Health for the Care and Use of Laboratory Animals.

3.3.2 Neurophysiological screen

A neurophysiological screen was conducted to assess the general appearance of the mouse, coordination, grip strength, agility, balance, postural and righting reflexes, and orienting as previously described (Rodriguez and Wetsel, 2006).

3.3.3 Assessment of spontaneous motor activity

Adult mice between 20- and 24-weeks-old were singly housed in a 12 hour:12 hour light:dark cycle with free access to a running wheel, food and water. Locomotor activity was measured by automated monitoring of running wheel revolutions over a two-week period.

3.3.4 Rotarod assay

An accelerating rotarod designed for mice was used as previously described (Powell et al., 2004). On Day 1, after placing mice on the motionless rod, the rod was activated. The rod accelerated from 0 to 45 revolutions per minute (RPM) over a period of 5 minutes. The speed at which each mouse fell off the rod was recorded. The following day, the mice were placed on the rotarod once again. Instead of accelerating from 0 to 40 RPM, the rotarod immediately accelerated to a speed of 24 RPM once the rotarod was activated. During the 5 minute test, the time to fall off the rotarod was recorded for each mouse.

3.3.5 Light-dark box

The mice were placed in a mouse shuttle box, consisting of two chambers where the

chambers (20 X 16 X 21 cm/chamber) were separated by an automated sliding door (MedAssociates). One chamber was illuminated with a 170mA high-intensity light, and the other chamber was enclosed by a black cloth. Initially, the mice were placed in the lit chamber. 5 seconds later, the door to the other chamber was opened, and the mice were permitted access to both chambers for 5 minutes. MedAssociates software was used to determine the latency to enter the dark chamber, time spent in each chamber, head pokes into each side, and the number of crossings between chambers.

3.3.6 Elevated zero maze

The elevated zero maze consisted of a 5.5 cm-wide metal circular platform elevated 43 cm from the floor. Two opposite sides of the circle were enclosed by black metal walls 11 cm high; the open and closed sections of the maze were equal in area. The maze was illuminated at 50-60 lux, and behavior was recorded by a camera positioned above the maze. Mice that were not previously handled were placed in one of the closed sections of the maze and were permitted to explore the maze for 5 minutes. The behavior was scored using the Observer (version 5.0; Noldus Information Technology) by an individual blind to the genotypes of the mice. The scored behaviors included time spent in the open vs closed sections of the maze, latency to enter the open sections, number of transitions from the closed to open sections, stretch-attend postures, head-dips, grooming, rearing, and freezing behavior.

3.3.7 Assay of sociability and preference for social novelty

The protocol of these studies was adapted from Moy and colleagues (Moy *et al*,

2004). On each of the five days leading up to the test day, C57BL/6 male ‘stranger’ mice between 8 and 12 weeks-of-age were habituated to the small wire cages placed into the 3-chamber testing apparatus (custom made to specifications based on (Nadler *et al*, 2004), Noldus Information Technology) for 10 minutes/day. On testing days each stranger mouse was only used once. Stranger mice and test subjects had no contact prior to the behavioral assay. Before each test the apparatus was cleaned with water and dried with paper towels. At the end of each testing day the apparatus was cleaned with 70% ethanol and then rinsed with water and dried with paper towels.

Prior to testing, all mice were habituated to the testing room for at least 30 minutes. Each phase of the assay lasted for 10 minutes. Habituation phase: the test mouse was placed in the middle chamber of the apparatus with empty wire cages placed in side chambers, and the test subject was allowed to explore the entire apparatus for the duration of the habituation phase. After 10 minutes the doorways to the side chambers were closed off, and the test subject was contained in the middle chamber. Sociability test: with test mouse enclosed in center chamber, the first stranger mouse was placed in a wire cage in one of the side chambers (the location of stranger mouse 1 vs. 2 was randomized between test subjects). The doors to the side chambers were opened and the test subject was allowed to explore the full apparatus for ten minutes. After 10 minutes the test subject was again enclosed in the middle chamber. Preference for social novelty test: with test subject contained in middle chamber the second stranger mouse was placed in the wire cage in the opposite side chamber from the first stranger mouse. The doors to the side chambers were then re-opened and the test subject allowed to explore the entire apparatus for ten minutes. The amount of time the test subject spent in each

chamber during each phase of the behavioral assay was recorded.

3.3.8 Novel object recognition test

On day 1 (habituation), each mouse was habituated to an empty plexiglass arena.

Identical objects were placed at each end of the arena, and the mice were permitted to explore the arena and the objects for 10 minutes. On day 2 (short term memory), two trials were conducted, each 10 minutes long, with an inter-trial interval of 30 minutes.

During the first trial, the mice were placed in the arena with two identical objects, different from those presented on the habituation day, at each end of the arena (A1 and A2). In the second trial, one of the familiar objects (A1) was replaced with a novel object (N1). On day 3 (long term memory), 24 hours after the first trial on day 2, the mice were placed in the arena for 10 minutes with the same familiar object (A2) and a new novel object (N2) at opposite ends of the chamber. On days 2 and 3 the location of the novel object was randomized in order to minimize the effect of object and location preferences. For all trials, behavior was videotaped and scored with the Observer program (version 5.0; Noldus Information Technology) by a trained observer blind to the genotypes of the mice. Exploration of an object was defined as sniffing, touching, climbing, and sitting on the object.

3.3.9 Morris water maze

Water maze learning was conducted using methods previously described by the Duke University Mouse Behavioral and Neuroendocrine Core Facility. Mice were handled and acclimated to water for 5 days prior to the start of testing. The water maze was divided

into four quadrants (NE, NW, SE and SW) with a platform hidden 1 cm below the water surface in the NE quadrant. Water was made opaque with the addition of nontoxic white poster paint. Animals were trained daily to swim to the hidden platform over 6 days, with four 1-min test trials per day. Probe tests for the memory of the hidden platform location were given 1-hr following completion of the final test trial on days 2, 4, and 6. On day 7, the platform location was moved to the SW quadrant, and reversal training was conducted over 6 additional days. Probe tests for the new platform location were conducted on days 8, 10, and 12. Performance of the mice on all test trials was assessed by swim distance (cm), time (sec), and velocity (cm/sec) to the hidden platform using Noldus Ethovision (Noldus Information Technology). During probe tests the total time (sec) and distance (cm) mice spent swimming in each quadrant of the water maze was calculated for the 1-min trial. Swim velocities (cm/sec) were also scored.

3.3.10 Context-dependent fear conditioning

The mice were placed into a Med Associates fear conditioning chamber (26 x 22 x 12 cm) illuminated with a 100 mA house light. After 2 min, a 72 dB, 2900 Hz tone [conditioned stimulus (CS)] was presented for 30 s. The CS terminated simultaneously with a single 2 s, 0.4 mA scrambled foot shock [unconditioned stimulus (UCS)]. The mice remained in the chamber for 30 s after which they received a second and third CS-UCS pairing and were returned to the home cage 30 s following the third shock. Contextual fear conditioning was assessed 24 h later over 5 min in the absence of the CS or UCS. Freezing behavior was defined as the absence of all movement by the mouse other than that required for respiration. All behaviors were video recorded and scored

subsequently by trained observers using Noldus Observer 5 (Noldus Information Technology) by observers blind to genotype.

3.3.11 Forced Swim

In the forced swim test (Porsolt *et al*, 1977), mice were injected with vehicle or imipramine (10 mg/kg or 20 mg/kg) (i.p.) 30 minutes prior to testing. The mice were placed into a beaker (15 cm in diameter) of water held at 25 °C with a depth of 15 cm. The test was videotaped for 6 minutes from the side of the beaker and scored subsequently for struggling behavior. Immobility time refers to the time that mice spend floating or engaged in minimal activity to stay afloat. Subtle movements of the feet, tail, or head required to maintain the eyes, nose, and ears above the surface of the water were excluded as immobility. The videotapes were scored using Noldus Observer 5 (Noldus Information Technology) by observers blind to genotype and treatment condition.

3.3.12 Statistical analyses

Statistical analyses were performed using SPSS v11.0 statistical software (SPSS, Chicago, IL). The data are depicted as mean values and standard errors of the mean (SEM). Behavior of KI and WT mice in the running wheel, rotarod, context-dependent fear conditioning, novel object recognition, elevated zero maze, light-dark box assay, and forced swim test were assessed by student's unpaired *t*-tests. For the water maze, learning curves for acquisition and reversal training were analyzed with RMANOVA, using test trial as the within subject effect, and genotype as the between subject effect. Probe tests were analyzed with a nested RMANOVA, using arena quadrant and test day

as within subject effects, with test quadrant nested within test day, and genotype as the between subject effects. In all cases, Bonferroni corrected post-hoc comparisons were used to assess differences detected within main effects, or for decomposition of significant interactions. In all cases, $p < 0.05$ was considered statistically significant.

3.4 RESULTS

3.4.1 S421A mutant mice do not display major abnormalities in motor activity

Because the KI mice have defects in dendritic and synaptic development that are similar to other mouse models of RTT (Cohen *et al*, 2011), it was necessary to determine whether the S421A mutation contributes to behavioral abnormalities associated with RTT as well. Hallmark features of mouse models of RTT include tremors, irregular breathing, stereotypic forelimb claspings, decreased agility, changes in weight, and impairments in motor activity (Shahbazian *et al*, 2002; Chen *et al*, 2001; Guy *et al*, 2001). Therefore, we examined these behaviors prior to assessing anxiety- and depression-like behavior in the KI mice. Using a broad neurophysiological screen, we found that the KI mice exhibit no overt defects in agility, strength, coordination, righting reflexes, body weight, and respiration (data not shown). Unlike other mouse lines bearing mutations in MeCP2, the KI mice did not display stereotypic forelimb claspings. Furthermore, in contrast to *Mecp2-null* and *Mecp2³⁰⁸* mice, S421A mice do not show the development of RTT-like phenotypes as they age.

In order to further assess motor activity levels, KI mice and their WT littermates were singly-housed with free access to a running wheel, and the wheel running activity of the mice was monitored over a period of two weeks. The average number of revolutions

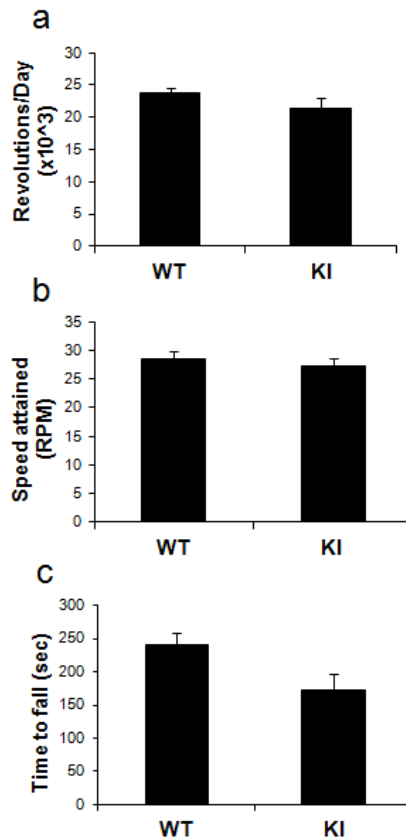


Figure 11: Loss of MeCP2 phosphorylation does not affect motor activity or coordination (a) WT and KI mice were allowed free access to a running wheel for two weeks, and the average number of revolutions per day was measured. (b) WT and KI mice were placed on a stationary rod, which was then gradually accelerated from 0 to 45 revolutions per minute (RPM) over a period of 5 minutes. The speed at which each mouse fell off the rod was recorded and averaged over 5 trials. (c) WT and KI mice were placed on a stationary rod, which was then accelerated to 24 RPM. The duration each mouse was able to remain on the rod for each of the 5 trials was recorded and averaged. n= 17-19 mice/group. Error bars indicate S.E.M.

per day was not significantly different between the KI mice and their WT littermates ($p < 0.19$) (Figure 11a). In addition, when we assessed motor coordination in an accelerating rotarod assay, there was no difference in the speed at which each genotype fell off the rod (Figure 11b). However, when the S421A mice and their WT littermates were placed on a stationary rod that was immediately accelerated to 24 RPM, the KI mice

appeared to fall off the rod more quickly than their WT littermates ($p < 0.05$) (Figure 11c). While the KI mice do not display overt motor phenotypes, performance on this challenging constant speed rotarod assay may indicate a subtle motor skills deficit or an endurance defect.

3.4.2 pMeCP2 at Ser421 is not required for learning and memory in the Morris water maze or context-dependent fear conditioning

In addition to coordination and motor deficits, mouse models of RTT also display abnormalities in learning and memory as assessed in the Morris water maze and context-dependent fear conditioning (Moretti *et al*, 2006). Furthermore, disruption in brain development such as those seen in the S421A mice can have profound impact on adaptive responses of the nervous system throughout life (Cohen *et al*, 2011), suggesting that the MeCP2 S421A mutation might result in abnormal behavior in adult S421A mice. Therefore, we assessed whether activity-dependent regulation of MeCP2 is required for learning and memory. In order to ask this question, we first tested the KI mice and their WT littermates in the Morris water maze. Mice were trained over a period of 7 days, and their latencies to locate a hidden platform in the NE quadrant were recorded. A RMANOVA revealed significant main effects for the within-subject effect of test day [$F_{(11,176)} = 51.503, p < 0.001$] but no significant interaction between test day and genotype [$F_{(11,176)} = 1.150, p < 0.326$], indicating that test performance was similar for KI mice and their WT littermates. During the first 6 days of acquisition training, all mice exhibited a reduction in swim time compared to test day 1 ($p < 0.001$), demonstrating that both genotypes learned the location of the platform hidden in the NE quadrant (Figure 12a).

Similarly, the distances the mice swam in order to locate the hidden platform were significantly reduced across acquisition training for both genotypes, and the average daily swim velocity did not differ between KI mice and WT littermates (data not shown). On test day 7, the hidden platform was moved to the SW quadrant. The time to locate the hidden platform increased on test day 7 compared to day 6 ($p < 0.001$), but rapidly decreased on test day 8 compared to test day 7 ($p < 0.004$) (Figure 12a). By test day 12, test performance during this reversal task was not different from the final day of acquisition learning (day 6) for either genotype, suggesting that the S421A mutation does not affect the ability to form a spatial memory of the platform location in the Morris water maze.

To test the ability of the mice to remember the spatial location of the hidden platform after training, probe tests were conducted 1 hr following training trials on days 2, 4, 6, 8, 10, and 12. RMANOVA found significant main effects for the within-subject effects of quadrant [$F_{(3,48)} = 50.708, p < 0.001$] but not for test day [$F_{(48,80)} = 1.803, p < 0.122$]. A significant interaction was found between quadrant and test day [$F_{(15,240)} = 42.696, p < 0.001$]. However, no significant quadrant by test day by genotype interaction was found [$F_{(15,240)} = 1.048, p < .407$]. Bonferroni corrected pair-wise comparisons showed that for test days 2, 6, and 8, all mice showed a marked preference for the NE quadrant where the hidden platform had been located during training; mice showed longer swim times in this quadrant compared to the NW, SE, and SW quadrants ($p < 0.006$) (Figure 12b). On test day 8, two days following the onset of reversal training, no significant differences were detected between the NE, NW, and SW quadrants for mice of either genotype, although time spent swimming in the SE quadrant ($p < 0.001$) was reduced

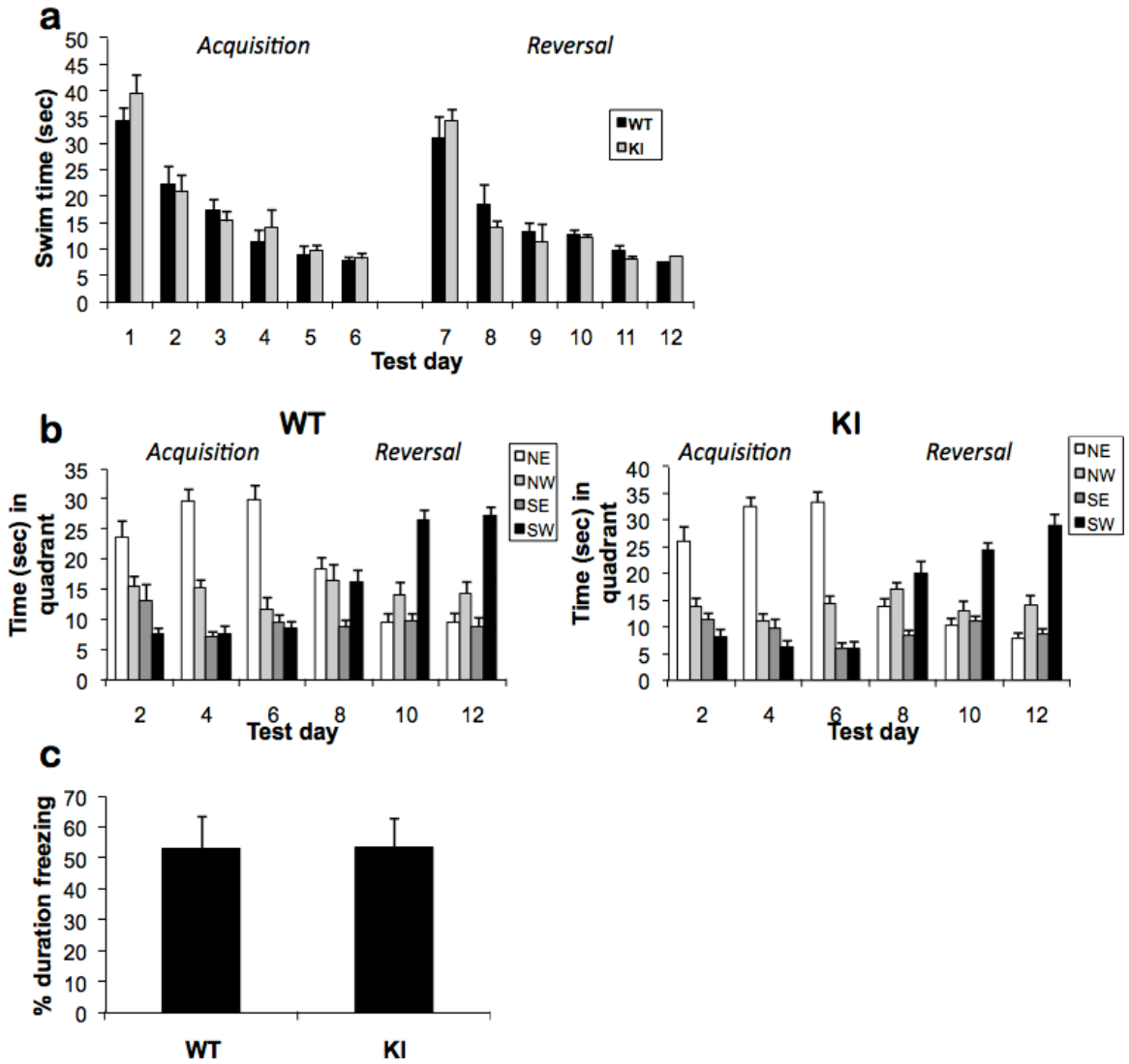


Figure 12: No abnormalities in spatial learning and memory in the MeCP2 S421A KI mice. (a) Mean swim time in order to locate a hidden platform during acquisition training and during the reversal task in the Morris water maze. (b) The amount of time WT and KI mice spent swimming during probe tests was measured in order to determine if the mice remembered the location of the hidden platform during training trials. (c) WT and KI mice were shocked in a novel context, and 24 h later, context-cued retention of the fear memory was assessed by returning the mice to the same context and measuring the percentage of time spent freezing. $n=10$ mice/group. Error bars indicate S.E.M.

compared to the other quadrants. By days 10 and 12, all mice showed increased time swimming in the SW quadrant ($p < 0.001$) relative to the other quadrants, demonstrating

that both genotypes could remember the new location of the hidden platform. These data show that the KI mice can learn the location of a hidden platform using spatial cues and can demonstrate learning plasticity when the platform is moved or reversed.

In order to further assess hippocampal-dependent learning and memory, we also tested the KI mice and their WT littermates in context-dependent fear conditioning (Fanselow and Pouls, 2005). All mice were conditioned on day 1 and tested in contextual fear conditioning on day 2, and the percentage of time spent freezing was used as an index of emotional memory. There was no difference between the percentages of time freezing between the two genotypes (Figure 12c). These data, in conjunction with the results from the Morris water maze, suggest that the KI mice are able to learn in several different contexts.

3.4.3 MeCP2 S421A mutation results in abnormal behavioral responses to novelty

In addition to the Morris water maze and context-dependent fear conditioning, we also assessed the ability of the KI mice to process and respond to novelty. Given the importance of MeCP2 in humans in the development of neural circuits that underlie social functions and adaptability, we analyzed the behavior of KI mice in an assay that was developed to assess sociability and the preferences for social novelty in mice (Moy *et al*, 2004). The KI mice and their WT littermates were placed in a three-chambered arena, and the behavior of the mice in this environment was monitored. A novel mouse that the test subject had never before encountered was placed within a small wire cage in one of the side-chambers of the arena. The test subject chose whether or not to enter the chamber containing the novel mouse, and the amount of time spent in each chamber of

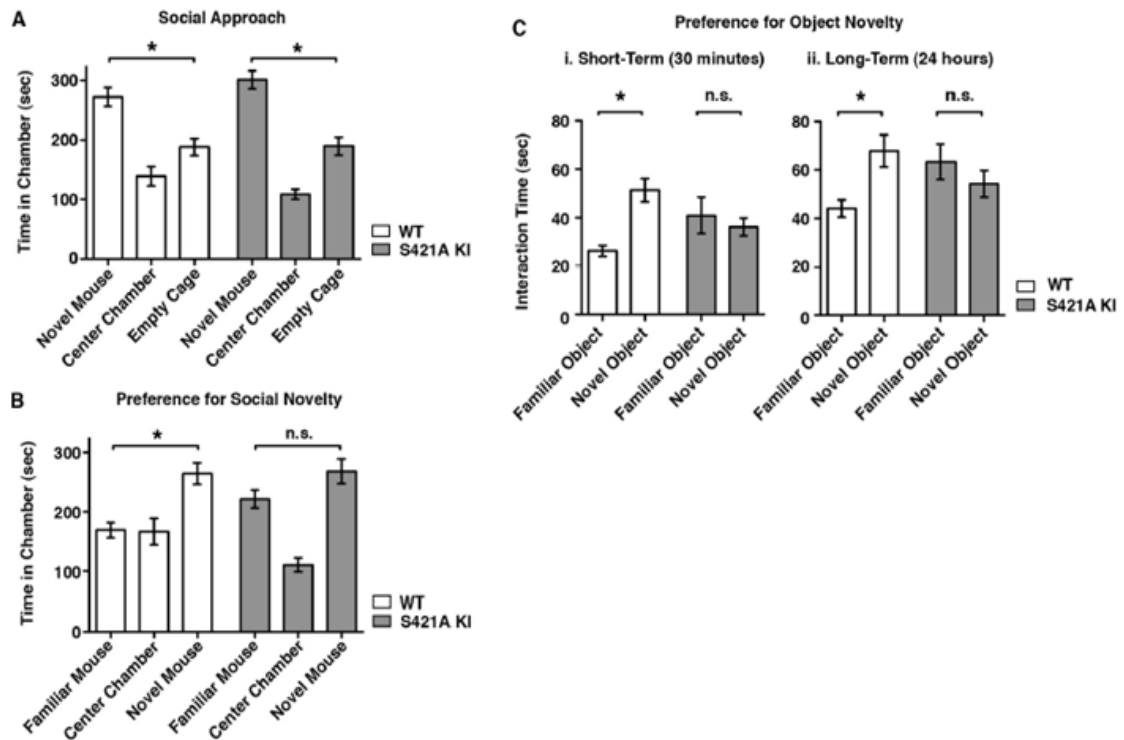


Figure 13: Defects in behavioral response to novel experience in MeCP2 S421A knock-in mice. (a) Behavior of WT and KI mice in a three-chamber apparatus with a single novel mouse placed in a small wire cage on one of the side chambers. Data shown are time spent in each chamber over the 10 minute trial period. (b) Behavior of WT and KI mice in a three-chamber apparatus with a familiar mouse placed in one of the side chambers and a novel mouse placed in the opposite side chamber. Time spent in each chamber over the 10 minute trial period is shown. (c) WT and KI mice were placed in an arena with a familiar inanimate object and a novel inanimate object placed at opposite ends. In the short-term assay (i), the familiar object was first introduced 30 minutes prior to the trial. In the long-term assay (ii), the familiar object was first introduced 24 hours prior to the trial. Total time spent exploring each object over a 10 minute trial period is shown for each assay. $n=21-24$ mice/group for (a,b) and 9 mice/group for (c). In all cases, $* p<0.05$. Error bars indicate S.E.M.

the arena was recorded. The WT mice were social and chose to spend more time in the chamber with another mouse ($p<0.001$) (Figure 13a). This social interaction behavior was unaffected in the KI mice ($p<0.01$), demonstrating their ability to recognize other mice and their appropriate interest in their physical and social environment.

Subsequently, a second mouse that the test subject had never before encountered was placed within a small wire cage in the side-chamber opposite the first, now familiar mouse. The WT mice spent the largest proportion of their time in the chamber containing the novel mouse that with the familiar mouse or alone ($p<0.01$) (Figure 13b). By contrast, the KI mice spent as much time with the familiar mouse as with the novel mouse.

Because the KI mice show appropriate interest in novel mice, it is unlikely that the increased time spent with familiar mice is due to a general deficit in social recognition upon loss of pMeCP2. Instead, the increased interest in the familiar mouse suggests that the KI mice cannot distinguish between familiar and novel mice. This lack of discrimination between novel and familiar stimuli was not limited to social behavior. When learning and memory was assessed in the novel object recognition test, the WT mice exhibited a preference for the novel object both 30 minutes and 24 hrs after the initial exposure to the familiar object ($p<0.01$ 30 min; $p<0.05$ 24 hrs) (Figure 13c). In contrast, the KI mice spent equal amounts of time investigating the familiar and the novel object in both the short-term and long-term memory tests. These findings support the conclusion that activity-dependent phosphorylation of MeCP2 at S421 is necessary to allow an animal to process novel experience and respond appropriately to previously encountered objects or animals. This defect cannot be attributed to an absence of all learning and memory in these mice, as the performance of the KI mice in the Morris water maze and fear conditioning is indistinguishable from WT mice. Together, these data suggest that activity-dependent pMeCP2 contributes to specific aspects of cognitive function underlying behavioral flexibility and that the disruption of this aspect of MeCP2

regulation in RTT may play a role in the cognitive impairments observed in affected individuals.

3.4.4 S421A knockin mice do not exhibit heightened anxiety

After assessing motor skills and cognitive function and determining that the KI mice do not exhibit severe RTT-like phenotypes, we then examined anxiety-like behavior in these mice. We have found that drugs that activate 5-HT signaling induce pMeCP2 (Hutchinson *et al*, 2011), and it has been previously shown that mutating MeCP2 in the amygdala (BLA) results in heightened anxiety-like behavior (Adachi *et al*, 2009); therefore, we hypothesized that the KI mice may exhibit abnormal anxious behavior. In order to ask this question, we tested the KI mice in the elevated zero maze. In this test, mice that display heightened anxiety tend to avoid the open regions of the maze. The WT and KI mice had similar latencies to enter the open arm of the maze, and did not significantly differ in the amount of time they spent in the open arm (Figure 14a,b). In order to further confirm that the KI mice do not display heightened anxiety, we also examined their behavior in the light-dark box test. In this test, mice that are anxious tend to avoid the brightly lit chamber (Crawley and Goodwin, 1998). No difference was observed between the KI mice and their WT littermates in the time spent in the lit chamber or the latency to enter the dark chamber (Figure 14c,d). The number of crossings between chambers, the number of head pokes into the dark chamber, and the time spent in the dark chamber were also not different between genotypes (data not shown). Furthermore, the KI mice and their WT littermates did not differ in the amount of time rearing or time spent in the perimeter, corners, or center of the open field (data

not shown). Therefore, our data show that activity-dependent pMeCP2 is not required for normal responses to anxiety-provoking situations.

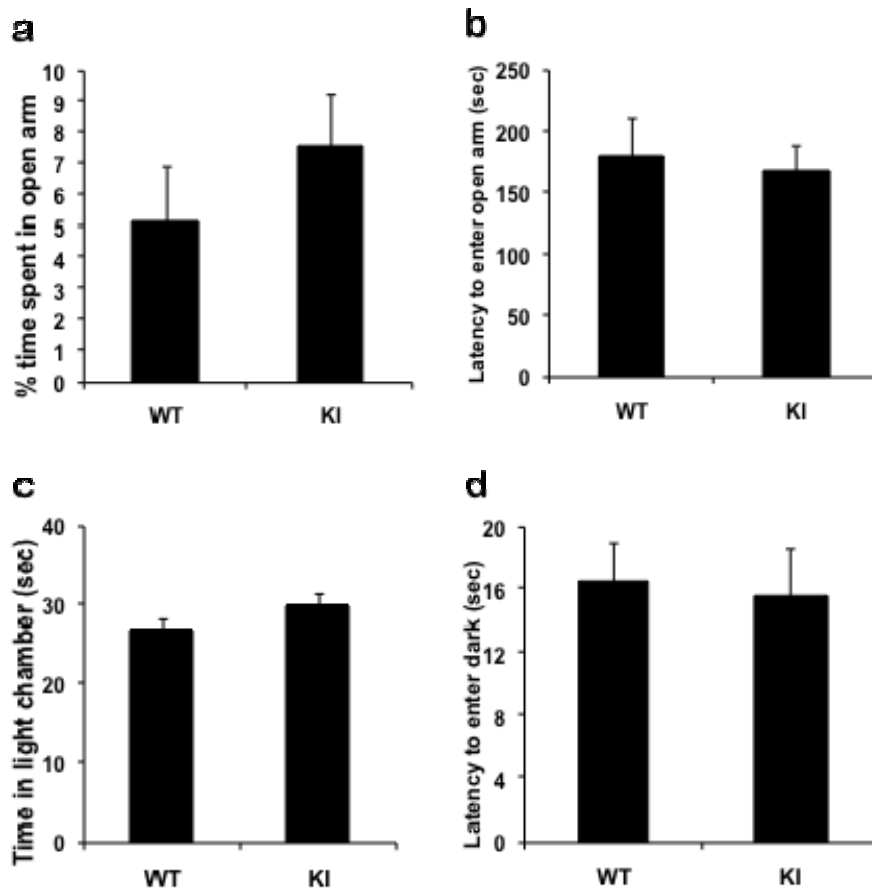


Figure 14: No evidence of abnormalities in anxious behavior in MeCP2 S421A mutant mice. (a,b) The percentage of time WT and KI mice spent in the open arm of the elevated zero maze (a), and the latency to enter the open arm. **(c,d)** The amount of time WT and KI mice spent in the lit chamber in the light-dark box assay (c), and the latency to enter the dark chamber (d). n=10 mice/group. Error bars indicate S.E.M.

3.4.5 S421A knockin mice display depression-like behavior

Although the KI mice do not show abnormal anxious behavior, it is possible that pMeCP2 plays a role in depression-like behavior. We tested the KI mice and their WT littermates in the forced swim, an assay used to assess the response to acute antidepressant treatment (Porsolt *et al*, 1977). Increased immobility and treading in this test could be indicative of a depression-like phenotype. We find that the KI mice spend more time immobile and treading than their WT littermates ($p < 0.006$) (Figure 15). Our data suggests that the KI mice may have a depression-like phenotype and implicates a role for pMeCP2 in behavioral responses to stressful stimuli.

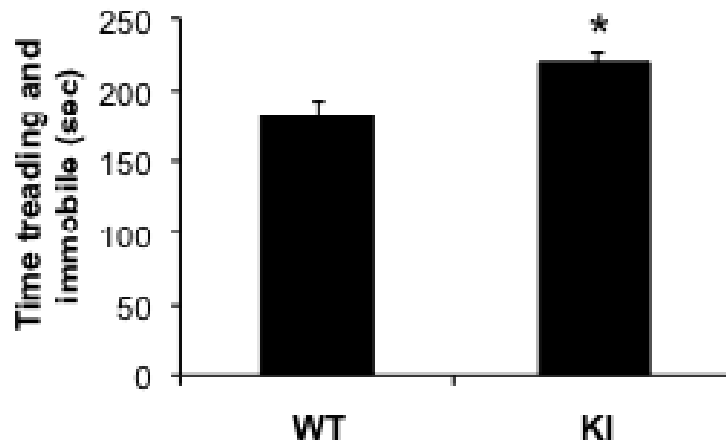


Figure 15: MeCP2 S421A mutant mice exhibit depression like behavior in the forced swim. The time spent treading and immobile in the forced swim assay over the six minutes of testing. $n = 18-20$ mice/group. $*p < 0.008$. Error bars indicate S.E.M.

3.5 DISCUSSION

The discovery that experience induces the phosphorylation of MeCP2 at S421 in the brain revealed a mechanism by which neuronal activity might modulate MeCP2 function and has provided a molecular handle to dissect the activity-dependent and – independent functions of MeCP2 (Zhou *et al*, 2006; Chen *et al*, 2003). In the present

study, we examined the behavior of mice in which the neuronal activity-dependent phosphorylation of MeCP2 at S421 is eliminated without otherwise affecting MeCP2 expression (Cohen *et al*, 2011). Compared to the effects of deleting *Mecp2*, mutating MeCP2 at Ser421 has a relatively mild effect on nervous system development. For example, the gross abnormalities, body weight dysregulation, seizures, impairments in motor skills, and certain learning and memory deficits observed in the MeCP2 knockout mice appear not to rely on activity-dependent pMeCP2.

Although the KI mice do not display many of the RTT-like phenotypes, they do show several behavioral abnormalities. Whereas *Mecp2*³⁰⁸ mice show deficits in hippocampus-dependent spatial memory and contextual fear memory (Moretti *et al*, 2006), the KI mice do not show deficits in the Morris water maze or context-dependent fear conditioning, suggesting that they are able to learn in several contexts. However, we find that loss of pMeCP2 results in defects in behavioral responses to novel versus familiar mice or objects, indicating that activity-dependent phosphorylation regulates aspects of cognitive function underlying behavioral flexibility. Importantly, because the KI mice show appropriate interest in mice versus inanimate objects, it is unlikely that the failure to spend more time with a novel mouse is due to a general deficit in social recognition upon loss of pMeCP2. Instead, the failure to show increased interest in novel mice and objects suggest that the KI mice cannot distinguish between novel and familiar.

Investigation of the signaling pathways that regulate pMeCP2 has shown that drugs that selectively activate 5-HT signaling are sufficient to induce pMeCP2 (Hutchinson *et al*, 2011). Here we examined the requirement of pMeCP2 for 5-HT-mediated behaviors, specifically anxiety- and depression-like behaviors. We find that the

KI mice do not exhibit heightened anxious behavior in several paradigms, supporting the notion that activity-dependent pMeCP2 is not involved in the behavioral responses to anxiety-evoking situations. Although anxiety disorders have considerable co-morbidity with depression (Zimmerman *et al*, 2002), mouse models of psychiatric disease can display a depressive-like phenotype that is devoid of anxiety-like behavior (Fukui *et al*, 2007). Similarly, the KI mice exhibit a depression-like phenotype in the absence of altered anxious behavior. The KI mice show increased immobility and treading in the forced swim compared to their WT littermates. Because the S421A mutation is constitutive, it is difficult to conclude whether it is the absence of activity-regulated pMeCP2 in the adult or the developing brain that is the cause of the phenotype we observe. Behavioral studies in inducible KI mice would be useful to differentiate between the roles of pMeCP2 in the developing mouse versus its function in the adult. However, our findings show that the KI mice may have a depression-like phenotype and suggest a role for pMeCP2 in the response to stressful stimuli.

4. ROLE OF PMeCP2 IN DEPRESSION-LIKE BEHAVIOR AND THE BEHAVIORAL RESPONSE TO CHRONIC ANTIDEPRESSANT TREATMENT

4.1 SUMMARY

Although classical antidepressants rapidly activate monoaminergic transmission, these drugs must be administered for an extended period of time to alleviate symptoms of depression, suggesting that molecular mechanisms downstream of receptor activation mediate changes in behavior. Here, we demonstrate a novel role for the chromatin-modifying protein MeCP2 in depression-like behavior and the response to chronic antidepressant treatment. We show that acute imipramine induces phosphorylation of MeCP2 at Ser 421 (pMeCP2) in the nucleus accumbens (NAc). Furthermore, in order to demonstrate the requirement of pMeCP2 for depression-like behavior, we utilize mice that bear a knockin (KI) mutation at Ser421 (S421A) and find that these mice display a depression-like phenotype in paradigms involving stress. Finally, we implicate pMeCP2 in the response to chronic antidepressant treatment, as the KI mice fail to show a behavioral response to chronic imipramine treatment following social defeat stress. These data reveal novel roles for pMeCP2 both in the behavioral response to stressful stimuli and the response to chronic imipramine treatment.

4.2 INTRODUCTION

Activation of monoamine receptors is essential to the mechanism by which antidepressants alleviate symptoms of depression (Morilak and Frazer, 2004; Manji, 2001). The majority of classical antidepressants increase monoaminergic transmission by selectively inhibiting one or more monoamine transporters or by inhibiting monoamine oxidase enzymes. Despite the fact that these drugs rapidly increase extracellular levels of

serotonin (5-HT) and norepinephrine (NE), antidepressants must be administered for several weeks or months in order to produce alterations in depression-like behavior (Krishnan and Nestler, 2008). This incongruity suggests that molecular mechanisms downstream of monoamine receptor activation are required for antidepressants to alleviate symptoms of depression.

Investigation of the molecular mechanisms induced by antidepressant treatment indicates that changes in gene expression contribute to the effects of these drugs on behavior (Berton *et al*, 2006; Tsankova *et al*, 2006; Nestler *et al*, 2002). A substantial body of evidence examining the molecular processes underlying antidepressant-induced changes in gene expression has revealed a role for epigenetic mechanisms of gene transcription, which are processes that mediate changes in gene expression by regulating chromatin structure (Vialou *et al*, 2010; Covington *et al*, 2009; Tsankova *et al*, 2006). Therefore, chromatin regulatory proteins that are targets of regulation by antidepressant treatment are strong candidates to mediate antidepressant treatment-induced changes in gene expression and behavior. Recently, we have shown that the methyl-CpG-binding protein-2 (MeCP2) is a strong candidate to mediate behavioral adaptations downstream of chronic monoaminergic signaling (Hutchinson *et al*, 2011; Deng *et al*, 2010). Furthermore, we find that psychostimulants, which also activate monoaminergic transmission, induce rapid and robust phosphorylation of MeCP2 at Ser421 (pMeCP2), a site that is thought to modulate MeCP2-dependent chromatin regulation (Cohen *et al*, 2011; Deng *et al*, 2010; Zhou *et al*, 2006; Chen *et al*, 2003). Investigation of the monoamines that contribute to the pattern of AMPH-induced pMeCP2 revealed that selective activation of dopaminergic (DA) and 5-HT transmission is sufficient to induce

pMeCP2 (Hutchinson *et al*, 2011). Due to the fact that drugs that selectively activate 5-HT transmission regulate pMeCP2, we considered the possibility that pMeCP2 may be implicated in 5-HT-mediated behaviors and the response to antidepressant treatment.

Here, we investigate the role of pMeCP2 in depression-like behavior as well as the behavioral response to chronic antidepressant treatment. We find that imipramine, a tricyclic antidepressant, is sufficient to induce pMeCP2 in the GABAergic interneurons of the nucleus accumbens (NAc). To determine the requirement of pMeCP2 for depression-like behavior, we conducted behavioral studies in mice bearing a knockin (KI) mutation that converts Ser to Ala at 421 (S421A), therefore rendering this site non-phosphorylatable (Cohen *et al*, 2011). The KI mice exhibit depression-like behavior in the forced swim and tail suspension, suggesting that pMeCP2 may be implicated in the behavioral responses to stressful stimuli. Finally, we find that whereas the wild-type (WT) littermates show a behavioral response to chronic antidepressant treatment following social defeat stress, the KI mice fail to respond to chronic treatment. Investigation of the brain regions in which pMeCP2 may be contributing to the behavioral response to chronic antidepressant treatment revealed that chronic and not acute imipramine treatment induces pMeCP2 in the lateral habenula (LHb), a brain region implicated in stress. Together, these findings support a novel role for pMeCP2 in the molecular mechanisms of antidepressant action.

4.3 MATERIALS AND METHODS

4.3.1 Animals

Adult (8-10 week old) male C57BL/6 mice (Jackson Laboratories, Bar Harbor, ME), retired CD1 breeders (Jackson Laboratories, Bar Harbor, ME), and MeCP2 S421A mice (Cohen *et al*, 2011) were used in these studies. The WT and KI littermates were generated from heterozygous (HET) breedings; HET females were crossed to C57BL/6 males. Animals were weaned at 21-30 days of age, housed in groups of 3-5 for imipramine and forced swim studies and were singly housed for sucrose preference and chronic social defeat stress. All animals were given free access to standard laboratory chow and water and were housed in a humidity- and temperature-controlled room on a 14 hr/10 hr light/dark cycle. All experiments were conducted with an approved protocol from the Duke University Institutional Animal Care and Use Committee in accordance with guidelines from the National Institutes of Health for the Care and Use of Laboratory Animals.

4.3.2 Immunofluorescent staining of brain sections

Two hrs after vehicle or drug injection, mice were perfused transcardially with 4% paraformaldehyde in 0.1M PBS. Brains were post-fixed in 4% paraformaldehyde/PBS overnight, then sunk into 20% (wt/vol) sucrose/PBS overnight. Coronal sections (40 μ m) were cut on a freezing microtome, and brain regions were identified by anatomical landmarks. One section from each brain region of interest was selected for each mouse, based upon anatomical structures to represent the closest approximation of identical sections between individual mice. To minimize technical variations in immunostaining

across genotypes, sections from different individual mice were first photographed for visual identification. The sections were then pooled and incubated with antibodies in a single chamber, and finally they were separated after processing for image analysis (see Deng *et al*, 2010). For immunostaining, tissue sections were permeabilized with either 1% (vol/vol) (for the pMeCP2 antibody) or 0.3% (vol/vol) (all other antibodies) Triton X-100 for 1 hr and then sections were blocked with 16% (vol/vol) goat serum in PBS. Sections were incubated with the following primary antibodies overnight at 4°C: rabbit anti-phospho-Ser421 MeCP2 1:15,000 (Deng *et al*, 2010), mouse anti-GAD67 1:500 (MAB5406; Chemicon/Millipore, Billerica, MA), and rabbit anti-c-Fos 1:15,000 (PC38; Calbiochem, San Diego, CA). Whenever possible, double immunostaining with primary antibodies raised in two different species was used for co-localization on single sections in order to determine the cell-type in which pMeCP2 was induced. After three washes in PBS, sections were incubated with the following species-specific fluorescent-conjugated secondary antibodies for 1 hr at room temperature: goat anti-mouse antibodies conjugated to Cy3 or Cy2 1:500 (Jackson ImmunoResearch, West Grove, PA) or Alexa Fluor 488 goat anti-rabbit antibodies at 1:500 (A11034; Molecular Probes/Invitrogen, Carlsbad, CA). Sections were washed in PBS, nuclei were labeled with Hoechst dye (Sigma) to facilitate anatomical localization of brain structures, sections were mounted and cover-slipped, and analyzed as described below.

4.3.3 Image Analyses

For quantitative immunofluorescence, images were captured on a Leica DMI4000 inverted fluorescence microscope using a Cascade 512B camera. Digital images were

quantified using MetaMorph 7 Image Analysis software (Molecular Devices, Sunnyvale, CA). To minimize variation between samples, images were captured with a uniform exposure time within a single experiment, and immunofluorescence was quantified across a constant-sized region from a single field of each section. We used the Count Nuclei module in MetaMorph 7.0 to first count the total number of cells per section that were positive for pMeCP2 or c-Fos immunoreactivity and then we determined the integrated immunofluorescence intensity of all the pMeCP2 or c-Fos positive nuclei in each image. We defined nuclei as objects of 3-8 μ m in diameter. For each experiment, an investigator blind to genotype and treatment condition chose a random section from which to set a single threshold value of fluorescence intensity above background to score objects of this size as positive for pMeCP2 or c-Fos expression. The threshold value was adjusted until the program's output of detected nuclei most closely matched the distribution of positive nuclei seen by eye. This threshold value was then held constant for every image within the experimental set. The first result of this analysis is a count of the number of cells that are pMeCP2 or c-Fos positive in each image. The Count Nuclei module then creates a mask that covers the area of all of the nuclei identified as positive on each section and quantifies the total immunofluorescence intensity under this area (the "integrated intensity") for each image. Thus our analysis allows us to tell how many cells have induced expression of pMeCP2 or c-Fos in each image as well as to evaluate the magnitude of pMeCP2 or c-Fos induction in these nuclei.

4.3.4 Forced swim

In the forced swim test (Porsolt *et al*, 1977), were injected with vehicle (Veh) or

imipramine (10 mg/kg or 20 mg/kg) (i.p.) 30 minutes prior to testing. The mice were placed into a beaker (15 cm in diameter) of water held at 25 °C with a depth of 15 cm. The test was videotaped for 6 minutes from the side of the beaker and scored subsequently for struggling behavior. Immobility time refers to the time that mice spent floating or engaged in minimal activity to stay afloat. Subtle movements of the feet, tail, or head required to maintain the eyes, nose, and ears above the surface of the water were excluded as immobility. The videotapes were scored using Noldus Observer 5 (Noldus Information Technology) by an observer blind to genotype and treatment condition. In this study, C57BL/6 mice were included in the WT group to increase numbers, as the behavior of these two strains is not significantly different in this assay (p s<0.20, 0.75, and 0.40 for Veh, 10 mg/kg imipramine, and 20 mg/kg imipramine, respectively).

4.3.5 Tail suspension

Thirty minutes prior to the start of the test, mutant mice and their WT littermates were injected with vehicle or imipramine (20 mg/kg). The tail suspension test was conducted in a MedAssociates apparatus in which mice were hung by their tails for six minutes. The body weight of the mouse was used as a control to determine the magnitude of its struggling activity, and the duration of immobility and struggling behavior was determined using MedAssociates software.

4.3.6 Sucrose preference test

Mice were housed individually for 7 days before and throughout the study. All studies were conducted in the home cage. Water bottles were removed 2.5 hours before the

beginning of the dark cycle. The mice were supplied with two bottles containing water 1.5 hours after the start of the dark cycle. The mice were allowed to drink for 1 hour, and then the original water bottle was returned. This protocol was performed for several days until stable water consumption was reached. Once consistent water drinking was achieved, the mice were tested in a two-bottle choice test over consecutive days. Water was paired with 0.1%, 0.25%, 0.5%, 1%, and 2% sucrose. The total volume of liquid consumed from each bottle was measured each day, and the preference for sucrose was determined by dividing the volume of sucrose consumed by total liquid consumption.

4.3.7 Chronic social defeat stress

Social defeat stress was carried out using a protocol similar to previously described methods (Krishnan *et al*, 2007; Tsankova *et al*, 2006; Berton *et al*, 2006). KI mice and WT littermates were exposed to a different CD1 aggressor mouse 10 minutes each day for 10 consecutive days in the aggressor's home cage. After the 10 minutes of physical contact, the test mice were returned to their home cage. Some of the bedding from the aggressor's cage was placed in the test mouse's cage to allow for sensory contact during the following 24 hours. Control mice were singly housed, but were not exposed to CD1 aggressors. Twenty-four hours after the last defeat session, defeated mice and controls were tested for social interaction. Mice were placed in a new arena with a small animal cage at one end, and their movement was tracked for 2.5 min in the absence of a CD1 aggressor, followed by 2.5 min in the presence of the caged aggressor. The five minute interaction test was filmed, and time spent in the interaction zone and corners was scored subsequently by a blind observer using Noldus Observer 5 (Noldus Information

Technology). For 4 weeks following the first interaction test, defeated mice in the chronic treatment group received daily (i.p.) injections of imipramine (20 mg/kg) in the home cage. Mice in the acute treatment group received vehicle (Veh) for 27 days and one dose of imipramine (20 mg/kg) on the last day of injections. All control mice received Veh injections for 28 days. The day after the last injection, the mice were retested for social interaction as previously described.

4.3.8 Statistical analyses

Statistical analyses were performed using SPSS v11.0 statistical software (SPSS, Chicago, IL). The data are depicted as means and standard errors of the mean (S.E.M). The pMeCP2 immunoreactivity over a time course was analyzed using univariate ANOVA for time. Time immobile and treading in the forced swim was analyzed using two-way ANOVA. Time immobile in the tail suspension and sucrose preference test were analyzed using RMANOVA. For social defeat stress, total time in the interaction zone and time spent in the corners were analyzed using two-way ANOVA for genotype and treatment. The pMeCP2 immunoreactivity in the LHb was analyzed using univariate ANOVA for treatment. Bonferroni corrected pair-wise comparisons were used as the *post hoc* tests. In all cases, $p < 0.05$ was considered statistically significant.

4.4 RESULTS

4.4.1 Imipramine is sufficient to induce pMeCP2 in the NAc

Pharmacological agents that selectively target 5-HT are sufficient to induce pMeCP2 in the NAc, suggesting that pMeCP2 might be involved in the behavioral response to antidepressant treatment (Hutchinson *et al*, 2011). Prior to assessing the functional role

of pMeCP2 in the response to antidepressant treatment, we first asked whether imipramine, an antidepressant that acts on the serotonin (SERT) and norepinephrine (NET) transporters, is sufficient to induce pMeCP2. C57BL/6 mice were administered either Veh or imipramine (20 mg/kg), and the mice were perfused at 0, 0.5, 2, 4, or 24 h post-injection to assess pMeCP2 immunoreactivity in the NAc. For pMeCP2 immunoreactivity in mice treated with imipramine, an ANOVA indicated a significant effect of time [$F_{4,22}=7.928$, $p<0.001$], and Bonferroni comparisons showed that pMeCP2

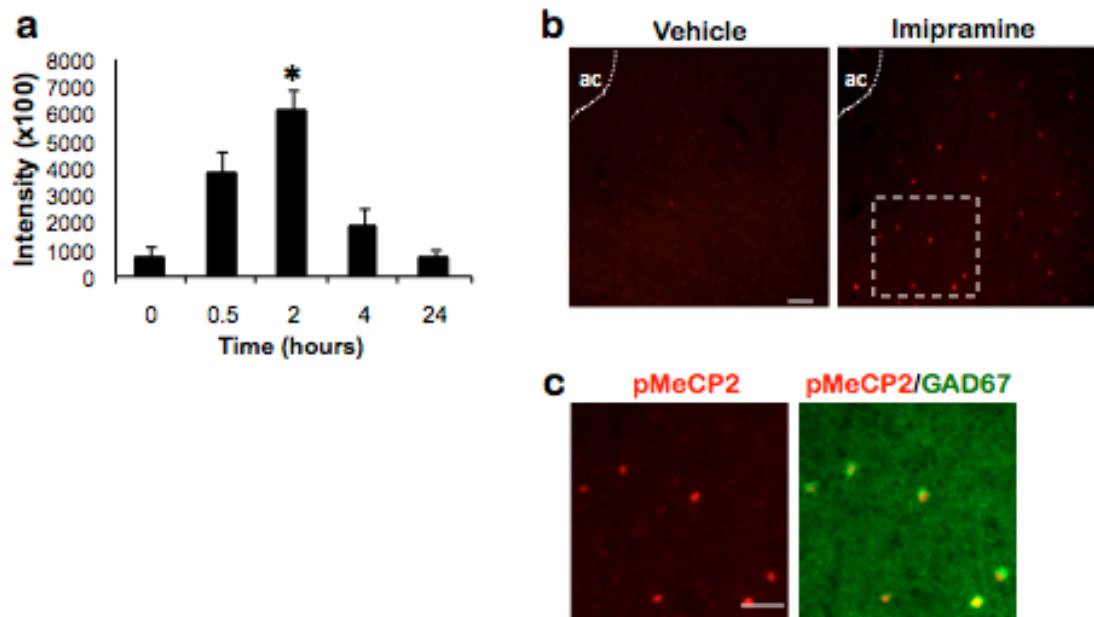


Figure 16: Imipramine induces pMeCP2 in the GABAergic interneurons of the NAc. (a) C57BL/6 mice were injected with imipramine (20 mg/kg i.p.) in the home cage and then perfused at 0, 0.5, 2, 4, and 24 h post-injection. pMeCP2 immunoreactivity in the NAc was quantified and averaged across mice at each time point. (b) pMeCP2 induction following vehicle or 20 mg/kg imipramine (2 h post-injection). Dashed white box was used as the inset image to examine pMeCP2 and GAD67 overlay in (c). ac, anterior commissure. (c) pMeCP2 (red), GAD67 (green), and overlay immunostaining in the NAc 2 h after treatment with 20 mg/kg imipramine. White arrows indicate neurons coimmunolabeled with antibodies for pMeCP2 and GAD67. Scale bar= 20 μ m. n= 4-5 mice/group. For (a), * $p<0.05$. Error bars indicate S.E.M.

intensity in the 2 h group was significantly higher than baseline levels ($p<0.003$) (Figure 16a). Imipramine stimulated a robust, but transient induction of pMeCP2 in a small population of neurons in the NAc (Figure 16b). We have previously shown that AMPH and drugs that target DA and 5-HT induce pMeCP2 in a specific population of GABAergic interneurons in the NAc (Hutchinson *et al*, 2011; Deng *et al*, 2010). In order to determine if imipramine induces pMeCP2 in this cell-type as well, we colabeled NAc sections from imipramine-treated mice with antibodies against both pMeCP2 and GAD67. Similar to AMPH, GBR12909, and quipazine, imipramine induced pMeCP2 only in GAD67-positive GABAergic interneurons of the NAc (Figure 16c). Taken together, these data indicate that imipramine is sufficient to induce pMeCP2 and suggest a role for pMeCP2 in the response to antidepressant treatment.

4.4.2 S421A mice show depression-like phenotype and respond to acute imipramine

In order to assess the role of pMeCP2 in the response to antidepressants, we first examined the behavior of the KI and their WT littermates in the forced swim, a test where increased immobility/treading time is used as an index of depressive-like behavior in rodents (Porsolt *et al*, 1977). In addition to screening for depression-like phenotypes, the forced swim test is also used to assess the response to acute antidepressant treatment. The KI and WT mice were injected with Veh or imipramine (10 mg/kg and 20 mg/kg) 30 min prior to the forced swim test. For the duration of time spent immobile and treading, a two-way ANOVA detected main effects of treatment [$F_{2,58}=17.312$, $p<0.001$] and a significant treatment by genotype interaction [$F_{2,58}=3.646$, $p<0.032$]. We observed that the KI mice treated with Veh display significant increases in time spent immobile and

treading compared with WT controls ($p < 0.025$) (Figure 17a). Furthermore, Bonferroni-corrected pairwise comparisons revealed that the time spent immobile and treading for the KI mice was significantly decreased by 10 mg/kg and 20 mg/kg imipramine ($p < 0.001$) and the time spent immobile and treading for the WT littermates was reduced for the 20 mg/kg dose ($p < 0.007$) (Figure 17a). Together, these results demonstrate that the KI mice spend more time immobile and treading in the forced swim test and this behavior is normalized with acute imipramine treatment.

The fact that the KI mice spend more time immobile and treading in the forced swim test suggests that these mice exhibit a depression-like phenotype. In order to further explore this possibility, we also examined the behavior of the KI mice and their WT littermates in the tail suspension, another assay in which struggling behavior is used to assess acute antidepressant responses and depression-like behavior (Steru *et al*, 1985). A RMANOVA for time spent below threshold 1 showed a significant within-subjects effect of time [$F_{5,55} = 13.424$, $p < 0.001$], indicating the amount of time immobile increased over the duration of the test. Furthermore, there was also a significant time by genotype interaction [$F_{5,55} = 2.788$, $p < 0.026$]. Although both genotypes spend similar amounts of time immobile during the first two minutes, the KI mice spend more time immobile during minutes 3 and 4 compared to their WT littermates ($p < 0.041$ and 0.010) (Figure 17b).

A core symptom of depression is anhedonia, which can be characterized as diminished interest or pleasure. In order to determine if the KI mice exhibit this feature of depression, we examined behavior in the sucrose preference test, which has been used to assess anhedonia in rodents (Monteggia *et al*, 2007; Barrot *et al*, 2002). The KI mice

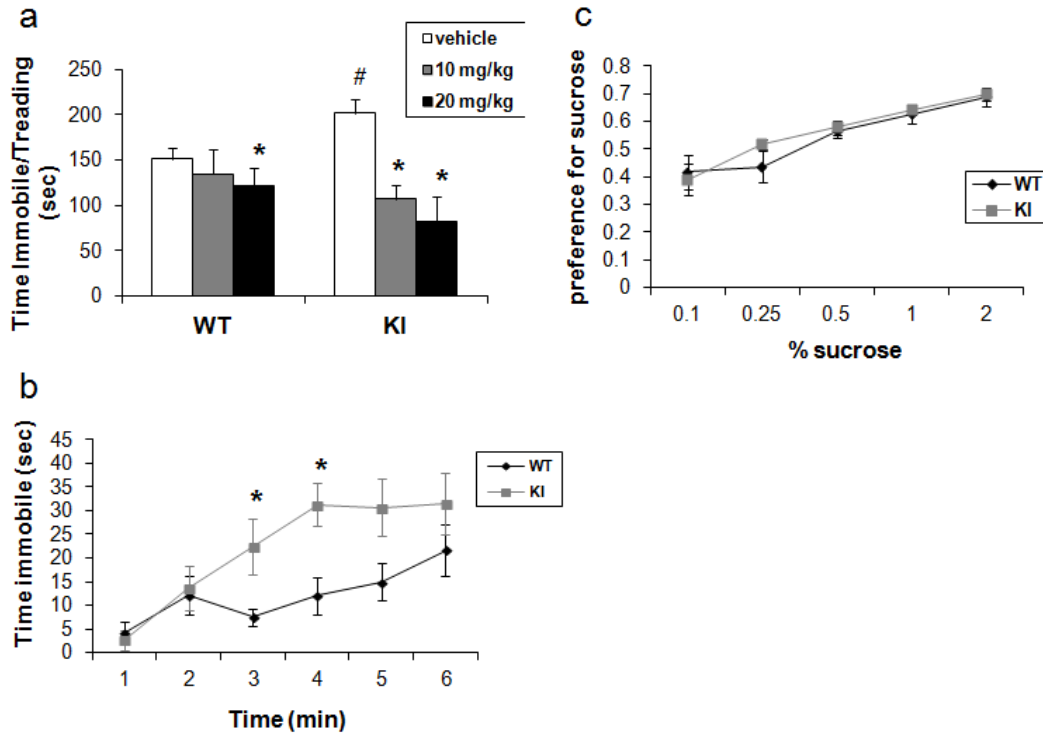


Figure 17: S421A KI mice exhibit a depression-like phenotype in assays involving stress. (a) KI mice and their WT littermates were injected with Veh or imipramine (10 or 20 mg/kg) 30 min prior to the forced swim. Total time immobile and treading over the six minute test was recorded. (b) KI mice and their WT littermates were injected with Veh 30 minutes prior to the tail suspension test, and the amount of time immobile each minute of the six minute test was recorded. (c) KI mice and WT littermates were tested for their preference for increasing concentrations of sucrose in a two-bottle choice test. n=4-14 mice/group for (a), n=6-7 mice/group for (b), and n=7-10 mice/group. For (a), * $p < 0.05$ compared to Veh within each genotype and # $p < 0.05$ WT Veh compared to KI Veh. For (b), * $p < 0.05$ compared to WT at each time point. Error bars indicate S.E.M.

and WT littermates were deprived of liquids and then tested for their preference for water or increasing percentages of sucrose (0.1, 0.25, 0.5, 1, or 2% sucrose). For sucrose, RMANOVA showed significant main effects of concentration but failed to show effects of genotype. Therefore, both genotypes showed a stronger preference for sucrose as the concentration of sucrose increased, and there was no difference between the genotypes in the preference for sucrose at any of the concentrations tested (Figure 17c). Although the KI mice show a depression-like phenotype in forced swim and tail suspension, they do

not appear to be anhedonic under the conditions tested. Therefore, activity-dependent pMeCP2 is not required for all emotional behavior. Rather, our data suggests that pMeCP2 may be specifically implicated in a subset of depression-like phenotypes.

4.4.3 S421A mice fail to respond to chronic imipramine treatment in social defeat stress

The depression-like phenotype of the KI mice in the forced swim and tail suspension but not the sucrose preference suggests that pMeCP2 may have a role in the behavioral response to stressful stimuli. Our previous findings suggest a role for pMeCP2 in the behavioral adaptations to chronic psychostimulant exposure (Deng *et al*, 2010). Therefore, we wanted to examine the behavior of the KI mice in social defeat stress, a paradigm involving a chronic stressor to induce depression-like symptoms that are alleviated by chronic but not acute antidepressant treatment (Golden *et al*, 2011; Berton *et al*, 2006; Kudryavtseva *et al*, 1991). Singly-housed mice were exposed to a different CD1 aggressor for 10 consecutive days and then tested for social interaction as previously described (Golden *et al*, 2011; Berton *et al*, 2006; Tsankova *et al*, 2006). The behavior of the defeated and control mice was monitored before and after a CD1 aggressor was placed in an enclosed, perforated chamber within an arena as shown in Figure 18a. Decreased time spent in the interaction zone as well as increased time spent in the corners of the arena was used to indicate defeat. In mice that are defeated, a percentage of the population fails to show decreased social avoidance and is therefore “non-susceptible” (Vialou *et al*, 2010; Krishnan *et al*, 2007). For our purposes, the 75th percentile of time in the interaction zone was determined for each genotype (58.23

seconds for WT and 59.49 for KI), and mice that spent more time in the interaction zone than these values were deemed “non-susceptible.” These mice were excluded from any subsequent data analyses.

A two-way ANOVA applied to total time in the interaction zone revealed an overall main effect of treatment [$F_{3,41}=101.119, p<0.0005$]. However, there was no effect of genotype [$F_{3,41}=0.029, p<0.866$], and the genotype by treatment interaction was not significant [$F_{3,41}=1.220, p<0.276$]. Bonferroni corrected pair-wise comparisons noted that the defeated mice spent more time in the interaction zone compared to non-defeated controls for each genotype ($p<0.0005$) (Figure 18b). Similarly, for total time spent in the corners, a two-way ANOVA showed an overall effect of treatment [$F_{3,41}=28.121, p<0.0005$] but failed to show an effect of genotype [$F_{3,41}=0.165, p<0.687$] and the genotype by treatment interaction [$F_{3,41}=0.355, p<0.555$] was not significant. *Post-hoc* analysis revealed that defeated mice of both KI and WT mice spent more time in the corners compared to non-defeated controls ($p<0.003$ and $p<0.0005$, respectively) (Figure 18c). Together, these results demonstrate that the KI mice and their WT littermates show comparable levels of social avoidance following 10 days of social defeat.

After defeating the mice and testing for social avoidance, we then treated the mice acutely (27 d of Veh injection with 1 injection of imipramine on day 28) or chronically (28 d of imipramine injections) with imipramine (20 mg/kg) in their home cages. In addition, the control following the last injection, the behavior of all mice was assessed in the social interaction test. For time in the interaction zone, a two-way ANOVA revealed a main effect of treatment [$F_{5,78}=21.171, p<0.0005$], genotype [$F_{5,78}=5.758, p<0.019$], and a significant treatment by genotype interaction [$F_{5,78}=4.931, p<0.010$]. For both

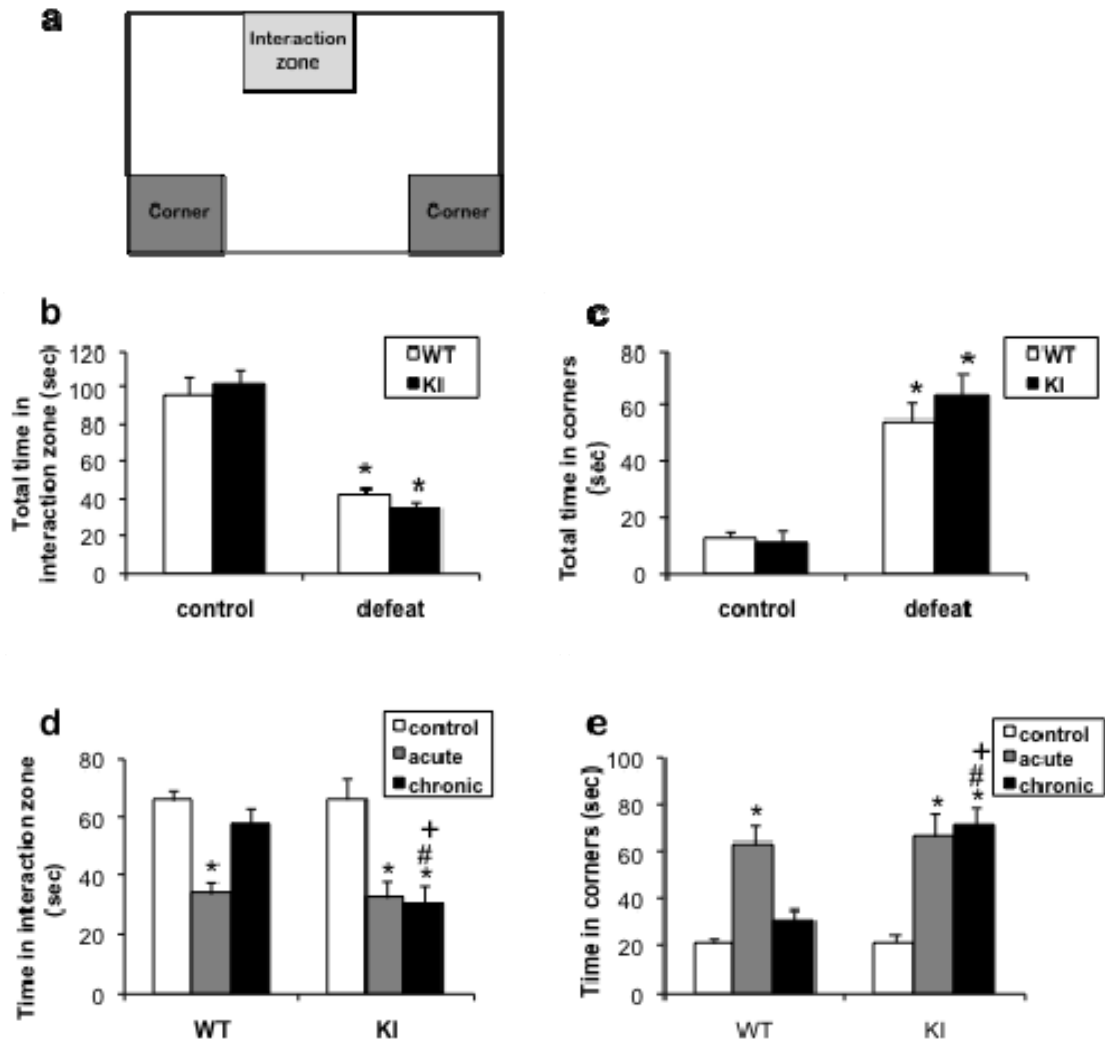


Figure 18: S421A mutant mice fail to show behavioral response to chronic imipramine treatment in social defeat stress. (a) Schematic representation of the chamber used for the social interaction test. The interaction zone is defined as the region directly surrounding the chamber that is either empty (first 2.5 min of test) or contains a CD1 mouse (last 2.5 min of test). (b,c) After 10 consecutive days of social defeat, KI and WT mice were tested for social interaction. The total time spent in the interaction zone (b) and the total time spent in the corners (c) in the presence of a CD1 aggressor. (d,e) Following 10 days of social defeat, KI and WT mice were treated acutely or chronically with imipramine for 28 days. On the day following the last injection, the mice were tested once again for social interaction. The total time in the interaction zone (d) and the total time in the corners (e) in the presence of a CD1 aggressor. $n = 6-19$ mice/group for (b,c), and $n = 6-13$ mice/group for (d,e). For (b,c), $*p < 0.001$ compared to control within each genotype. For (d,e), $*p < 0.001$ compared to control within each genotype and $\#p < 0.001$ WT chronic compared to KI chronic. Error bars indicate S.E.M.

genotypes, defeated mice that had been treated acutely with imipramine exhibited a significant reduction in time spent in the interaction zone compared to controls that had not been defeated ($p < 0.0005$ for WT control vs WT acute, $p < 0.0005$ for KI control vs KI acute) (Figure 18c). Therefore, both genotypes did not show a behavioral response to acute imipramine treatment. Defeated WT mice that had been treated chronically with imipramine exhibited a significant increase in the time spent in the interaction zone compared to the acute treatment group ($p < 0.001$), demonstrating that chronic imipramine treatment rescues social interaction after defeat. In contrast, defeated KI mice that had been treated chronically with imipramine failed to show increased time spent in the interaction zone compared to the acute treatment group ($p < 1.000$). The WT mice treated with chronic imipramine spent significantly more time in the interaction zone compared to the KI chronic treatment group ($p < 0.0005$).

Furthermore, for time spent in the corners, a two-way ANOVA revealed a main effect of treatment [$F_{5,76} = 25.660$, $p < 0.0005$], genotype [$F_{5,76} = 7.532$, $p < 0.008$], and a significant treatment by genotype interaction [$F_{5,76} = 6.223$, $p < 0.003$]. Defeated mice that had been treated acutely with imipramine spent significantly more time in the corners compared to controls that had not been defeated ($p < 0.0005$ for WT control vs WT acute, $p < 0.0005$ for KI control vs KI acute) (Figure 18d). Similar to the time spent in the interaction zone, these data demonstrate that a single dose of imipramine is insufficient to affect the behavior of defeated mice of either genotype. However, chronic imipramine treatment resulted in a significant decrease in time spent in the corners for WT mice compared to the acute treatment group ($p < 0.001$), whereas defeated KI mice treated with chronic imipramine did not show a difference in time spent in the corners compared to

the KI acute treatment group ($p < 1.000$). The amount of time the WT mice treated chronically with imipramine spent in the corners was significantly less than the KI chronic treatment group ($p < 0.0005$). Together, these results demonstrate that although the WT mice show a behavioral response to chronic imipramine treatment, the KI mice fail to respond, suggesting a role for pMeCP2 in the behavioral response to chronic imipramine treatment.

4.4.4 Acute and chronic imipramine treatment differentially regulate pMeCP2 following social defeat stress

Our finding that the KI mice respond to acute imipramine in the forced swim but fail to show a behavioral response to chronic imipramine in social defeat stress suggests that pMeCP2 may be involved in the downstream molecular and cellular processes that underlie antidepressant response. In order to investigate the brain regions in which pMeCP2 may contribute to the behavioral response to chronic imipramine treatment, we compared the pattern of pMeCP2 following Veh or acute or chronic imipramine treatment. C57BL/6 mice were defeated and treated acutely (27 d of Veh injection with 1 injection of imipramine on day 28) or chronically (28 d of imipramine injections) with imipramine (20 mg/kg) in their home cages. 2 h following the last injection, the mice were perfused, and brain sections from regions implicated in depression or antidepressant response were stained for pMeCP2. We found that acute and chronic imipramine treatment led to similar levels and patterns of pMeCP2 induction in the NAc compared to Veh treatment (Figure 19a). As previously reported for AMPH and drugs that activate DA and 5-HT transmission (Hutchinson *et al*, 2011; Deng *et al*, 2010), pMeCP2 is

induced basally in regions of the cortex, and there is no significant increase in pMeCP2 in the cingulate cortex or the PLC following acute or chronic imipramine treatment.

Furthermore, acute or chronic imipramine treatment was not sufficient to induce pMeCP2 in the, hippocampus, hypothalamus, amygdala (BLA), dorsal striatum, or the ventral tegmental area (VTA) (Figure 19a and data not shown).

In addition to the brain regions previously mentioned, we also examined pMeCP2 induction in the lateral habenula (LHb) as this structure has been implicated in the behavioral responses to pain, stress, anxiety, sleep, and reward (Hikosaka, 2010; Lecourtier and Kelly, 2007; Ullsperger and von Cramon, 2003; Morris, 1999). We find little to no induction of pMeCP2 in the LHb following Veh treatment and a small induction following acute imipramine treatment (Figure 19 a and b). In contrast, chronic imipramine treatment produces a significant induction of pMeCP2 in the LHb (Figure 19a and b). For pMeCP2 immunoreactivity in the LHb, an ANOVA indicated a significant effect of treatment [$F_{2,23}=4.699$, $p<0.021$], and Bonferroni comparisons showed that pMeCP2 levels were significantly higher in the chronic treatment group compared to Veh control ($p<0.022$) (Figure 19c). Therefore, chronic but not acute imipramine treatment is sufficient to induce pMeCP2 in the LHb. These findings suggest that pMeCP2 induction in the LHb may be implicated in the behavioral response to chronic imipramine treatment following social defeat..

Figure 17

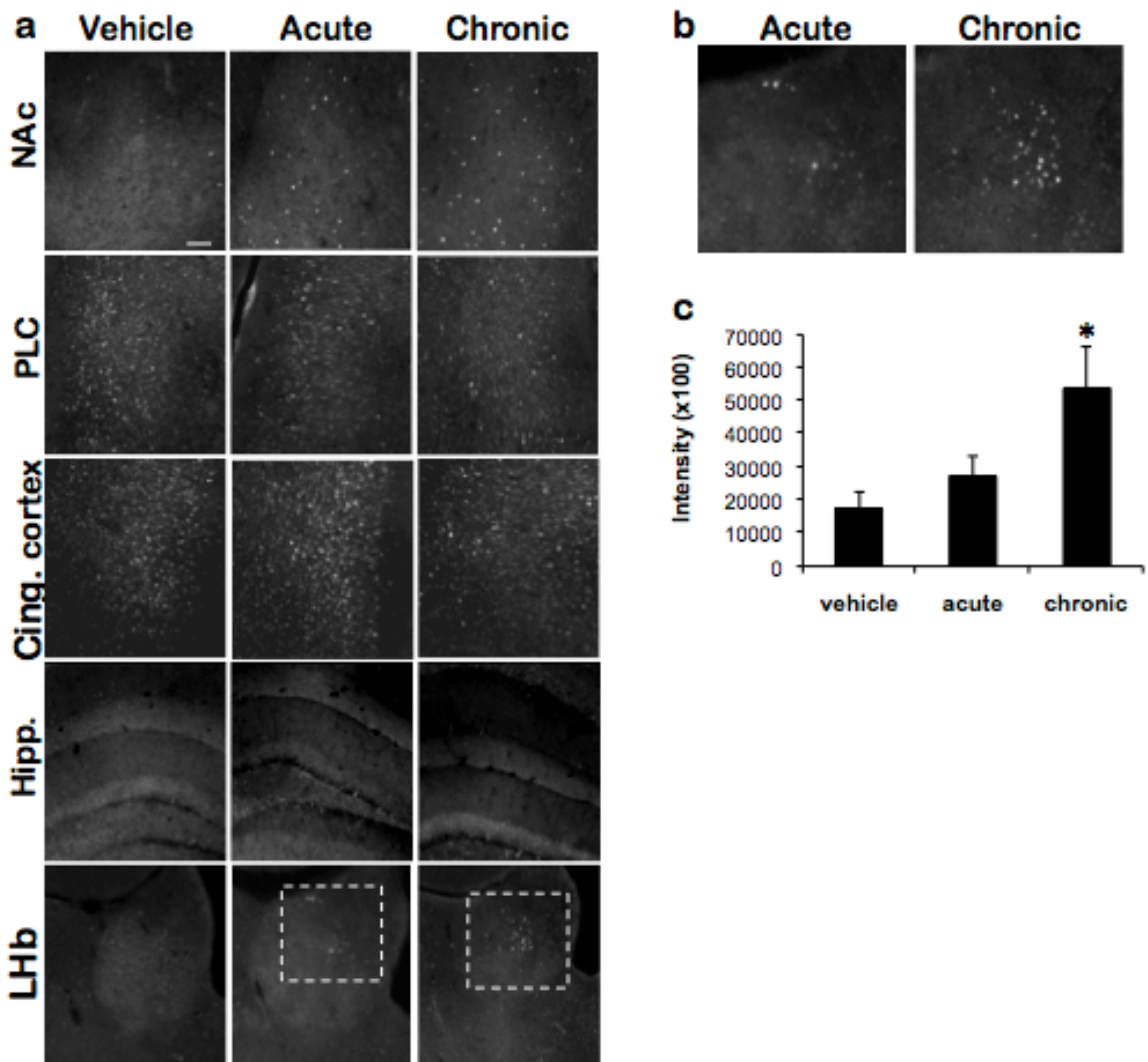


Figure 19: pMeCP2 in the lateral habenula is differentially induced by acute and chronic imipramine treatment following social defeat stress. (a) C57BL/6 mice were injected with Veh (28 d), acute imipramine (27 d of Veh injections followed by imipramine injection on day 28), or chronic imipramine (28 d) following 10 consecutive days of social defeat stress. pMeCP2 immunoreactivity was examined in the NAc, PLC, cingulate cortex, hippocampus, and LHb. (b) Inset image of the dashed white box in (a) of pMeCP2 immunoreactivity in the lateral habenula. (c) pMeCP2 immunoreactivity in the LHb following Veh or acute or chronic imipramine treatment. $n=8-9$ mice/group. For (c), $p<0.05$ compared to Veh. Error bars indicate S.E.M. Scale bars = $10\mu\text{m}$.

4.5 DISCUSSION

This study is the first to implicate MeCP2 in the behavioral response to stressful stimuli and chronic antidepressant treatment. A growing body of evidence indicates that transcriptional regulators contribute to the behavioral response to stressful stimuli and the long-lasting effects of chronic antidepressant treatment on behavior (Krishnan and Nestler, 2010). For example, Δ FosB, a Fos family transcription factor implicated in reward and stress, is induced following chronic social defeat stress in the NAc and is both sufficient and required for resilience to social defeat. (Vialou *et al*, 2010; Perrotti *et al*, 2004). Furthermore, Δ FosB induction in the NAc is also required for chronic fluoxetine treatment to reverse the social avoidance induced by social defeat. Chronic social defeat stress also increases the activity of cAMP response element binding protein (CREB) in the shell of the NAc (Barrot *et al*, 2002). Increases in CREB activity in the NAc have been shown to dampen the responsiveness to rewarding, aversive, and anxiogenic stimuli, as overexpression of CREB in the NAc produces depressive-like responses in the sucrose preference and forced swim tests (Barrot *et al*, 2002; Pliakas *et al*, 2001). Decreases in CREB function in the NAc cause antidepressant-like responses in the learned helplessness and forced swim tests (Newton *et al*, 2002; Pliakas *et al*, 2001). In contrast, antidepressants delivered systemically generally increase CREB protein levels and activity (Laifenfeld *et al*, 2005; Nibuya *et al*, 1996). These seemingly contradictory findings suggest that changes in CREB levels have different functions in different brain regions in response to stress and chronic antidepressant treatment. Therefore, further research in the brain region- and cell type-specific roles of transcriptional regulators is

required to fully elucidate the molecular mechanisms underlying the behavioral response to stressful stimuli and chronic antidepressant treatment.

Our data show that both acute and chronic imipramine is sufficient to induce pMeCP2 in the NAc. We have previously shown this for a number of drugs that selectively activate DA and 5-HT transmission (Hutchinson *et al*, 2011; Deng *et al*, 2010). Imipramine, a tricyclic compound, was first identified as an effective antidepressant more than 50 years ago and is now clinically used to treat depression (Kuhn, 1958; Richelson, 2003). Imipramine has multiple targets, but has the strongest affinity for the SERT (the inverse of the equilibrium dissociation constant (K_D) of imipramine for the human SERT is 70) and NET (K_D for the human NET is 2.7) (Richelson, 2003). Our previous findings indicate that the selective NET inhibitor reboxetine does not induce pMeCP2 in the NAc; therefore, it is unlikely that increases in NE transmission following imipramine treatment contribute to the pMeCP2 induction we observe (Hutchinson *et al*, 2011). In order to determine if pMeCP2 is induced selectively by antidepressants that activate monoaminergic transmission, it would be interesting to examine pMeCP2 induction following administration of antidepressants with different mechanisms of action. For example, ketamine is a non-competitive NMDA receptor antagonist that has been recently shown to have antidepressant effects in animal models of depression as well as clinical studies (Autry *et al*, 2011; Li *et al*, 2011; Berman *et al*, 2000). Unlike drugs that target SERT and NET, ketamine rapidly alleviates depression-like symptoms within hours of treatment (Sanacora *et al*, 2008; Zarate *et al*, 2006). Therefore, if pMeCP2 is selectively regulated by monoaminergic signaling, then we would not expect ketamine to induce pMeCP2, and we would not expect differences in

the response to ketamine treatment between the KI mice and their WT littermates following chronic social defeat stress. By examining the pattern of pMeCP2 induction following different antidepressant treatments and by investigating the behavioral response of the KI mice to these treatments, we can further elucidate the signaling pathways that regulate pMeCP2 and the mechanism by which the phosphorylation affects the behavioral response to antidepressant treatment.

In addition to demonstrating that imipramine induces pMeCP2, our data suggest that pMeCP2 plays a role in depression-like behavior, as mice bearing a knockin mutation at Ser421 exhibit increased immobility in both the forced swim and tail suspension tests compared to their WT littermates. In order to further examine the potential depression-like phenotype of the KI mice, we then assessed their behavior in the sucrose preference test, which can be used to measure anhedonia (Nestler and Hyman, 2010). The KI mice and their WT littermates have a similar preference for increasing concentrations of sucrose. The fact that the S421A mutation results in altered behavior in the forced swim and tail suspension tests but does not cause anhedonia as measured in the sucrose preference test suggests that pMeCP2 may be implicated specifically in the emotional response to stressful stimuli. The hypothalamic-pituitary-adrenal (HPA) axis controls an individual's ability to cope with stressful events, and dysregulation of this pathway has been implicated in depression (de Kloet *et al*, 2005; Barden, 2004). Therefore, if pMeCP2 contributes to the behavioral response to stressful stimuli, then we would expect to see alterations in components of the HPA axis. For example, the KI mice may have alterations in blood levels of glucocorticoids following an acute stressor or differences in the expression of glucocorticoid receptors compared to their WT

littermates. Identifying alterations in the HPA axis in conjunction with the behavioral findings would suggest a specific role for pMeCP2 in the behavioral response to stressful stimuli.

We find that the KI mice show decreased immobility and treading time in the forced swim following acute imipramine treatment compared to Veh, suggesting that the response to acute antidepressant treatments is not altered in these mice. In striking contrast, when we examined the behavior of the KI mice and their WT littermates following chronic antidepressant treatment in social defeat stress, we find that the KI mice fail to illicit a behavioral response to chronic imipramine treatment. These findings suggest that pMeCP2 is involved in the behavioral response to chronic imipramine treatment following social defeat stress. There are several plausible mechanisms by which pMeCP2 may mediate behavioral adaptations to chronic imipramine treatment. Results from *in vitro* studies suggested that MeCP2 binds to and represses specific genes, and pMeCP2 causes a conformational change in MeCP2 that relieves this repression (Zhou *et al*, 2006; Chen *et al*, 2003). Recently, evidence has shown that MeCP2 binding does not occur at specific genes but is rather distributed throughout the genome and is thought to regulate global changes in chromatin structure (Skene *et al*, 2010). Consistent with these findings, another study demonstrated that pMeCP2 does not regulate the expression of specific genes, as there are no significant changes in gene expression following membrane depolarization in cortical neuron cultures from KI mice compared to WT littermates (Cohen *et al*, 2011). Cohen and colleagues suggest that pMeCP2 may instead mediate global changes in chromatin structure in response to neuronal activity. Therefore, the altered response to chronic imipramine in the KI mice may be due to a loss

of chromatin restructuring that occurs in response to chronic imipramine treatment. Furthermore, it is possible that pMeCP2 does regulate the expression of subsets of genes but that these changes in gene expression are only detectable when a chronic stimulus is given. Our finding that the KI mice fail to respond to chronic imipramine treatment provides an excellent context in which the mechanism of pMeCP2 in can be examined.

In order to investigate the brain regions in which pMeCP2 might function in response to chronic imipramine treatment, we examined the pattern of pMeCP2 induction following Veh or acute or chronic imipramine treatment. Intriguingly, we find that chronic but not acute imipramine induces pMeCP2 in the LHb, a brain region shown to regulate stress and reward (Li *et al*, 2011; Bromberg-Martin and Hikosaka, 2011; Hikosaka, 2010). The LHb serves as a connection between the forebrain and midbrain structures that regulate emotional behaviors and has recently become a brain region of great interest because it influences the activity of both DA and 5-HT neurons (Hikosaka, 2010). In response to stress, aversive stimuli, or smaller-than-expected rewards, the LHb is activated and inhibits DA neurons in the VTA via the rostromedial tegmental nucleus (RMTg) (Hong *et al*, 2011; Hikosaka, 2010; Matsumoto and Hikosaka, 2009; Ji and Shepard, 2007). Dopaminergic hypoactivity following repeated exposure to aversive or stressful stimuli results in reduced motor activity and decreased motivation, two features of depression. In addition, repeated activation of the LHb can contribute to depression via its projections to the dorsal raphe nucleus (DRN) and the medial raphe nucleus (MRN). Activation of the LHb has been shown to both inhibit and facilitate 5-HT release (Kalen *et al*, 1989; Nishikawa and Scatton, 1985); therefore, activation of the LHb may also influence stress response via altering 5-HT transmission. Knowing that stressful

stimuli activate the LHb, it is interesting to observe increases in pMeCP2 following chronic antidepressant treatment. Comparing gene expression profiles in the LHb of KI and WT mice following chronic imipramine treatment could yield new insight into the function of pMeCP2 in the response to chronic antidepressant treatment.

5. DISCUSSION

Although the first antidepressants were discovered more than fifty years ago, little is known about their mechanisms of action. The fact that the majority of clinically available antidepressants increase 5-HT and NE transmission led to the notion that antidepressants exert their therapeutic effects via increasing levels of monoamines. However, although classical antidepressants rapidly increase monoaminergic transmission, these drugs must be taken for several weeks in order to alleviate symptoms of depression. Therefore, there has been a shift in the field from focusing on regulating levels of 5-HT and NE to examining the mechanisms downstream of monoamine receptors that are mediating the changes in behavior. In this work, I have shown that citalopram and imipramine induce phosphorylation of MeCP2 at Ser421, a site that is believed to modulate MeCP2's ability to affect chromatin structure (Cohen *et al*, 2011; Zhou *et al*, 2006; Chen *et al*, 2003). Furthermore, I have uncovered a novel role for pMeCP2 in the behavioral response to stressful stimuli and in the response to chronic imipramine treatment. These data broaden the current understanding of how antidepressants affect behavior and provide a new arena in which to examine the function of pMeCP2.

5.1 THE ROLE OF PMECP2 IN DEPRESSION-LIKE BEHAVIOR

Mice that bear a S421A knockin mutation in MeCP2 show increased immobility in forced swim and tail suspension, suggesting that these mice exhibit a depression-like phenotype. However, when the KI mice were examined for anhedonia, a core symptom of depression, in the sucrose preference test, they showed similar preferences for sucrose

compared to their WT littermates. These data suggest that pMeCP2 may be involved in a subset of depression-like behaviors. The forced swim and tail suspension involve stressful, aversive stimuli, whereas the sucrose preference assesses alterations in motivation and reward (Barrot *et al*, 2002; Steru *et al*, 1985; Porsolt *et al*, 1977). The KI mice are a key example of how it is necessary to conduct a wide range of behavioral tests to dissect a depression-like phenotype. Our data show that pMeCP2 plays a role in the response to stressful stimuli but is not implicated in the motivation for natural rewards or anxiety-like behavior (Cohen *et al*, 2011). Similarly, Wallace and colleagues found that CREB is involved in anxiety- but not anhedonia-like behavior following social isolation (Wallace *et al*, 2009). The involvement of proteins like MeCP2 and CREB in specific aspects of emotional behavior highlights the importance of continuing to develop elegant behavioral paradigms to tease out the function of these proteins.

In light of the forced swim and tail suspension results, it is surprising that there is not a significant difference in social avoidance between KI and WT mice following 10 days of social defeat stress. This may be due to the fact that social defeat is such an intense stressor that it is difficult to see differences in social avoidance; both genotypes respond to this stressor. Modifications of current protocols and more in-depth analyses of the results are necessary to further examine the role that pMeCP2 plays in the behavioral response to stressful stimuli. For example, in the traditional paradigm of social defeat stress, mice are exposed to a different aggressive mouse every day for 10 days, over which time they develop social avoidance (Golden *et al*, 2011; Berton *et al*, 2006; Tsankova *et al*, 2006). In order to see if pMeCP2 affects the threshold at which an individual can no longer cope with stressful stimuli, it would be interesting to compare

social avoidance in KI and WT mice following 1 or 5 days of social defeat. It is possible that WT mice need to be defeated for more days in order to induce social avoidance compared to KI mice. Another method to examine increased susceptibility to stress is to use a subthreshold microdefeat protocol in which mice are exposed to an aggressor 3 times in the same day (Krishan *et al*, 2007). Mice do not typically exhibit social avoidance in this protocol, but if the KI mice were more susceptible to stress, then they may show social avoidance to subthreshold defeat. In addition, recent examination of the degree of social avoidance across populations of defeated mice has shown that a percentage of mice show resilience to defeat (Vialou *et al*, 2010; Krishnan *et al*, 2007). Comparing the percentages of resilient KI and WT mice following 10 days of defeat could be a means to determine if pMeCP2 contributes to the mechanism of stress resilience. These in-depth analyses will further elucidate the role of pMeCP2 in the response to stress.

In our model, we propose that phosphorylation of MeCP2 at Ser421 is acting as an epigenetic mechanism, mediating long-lasting changes in chromatin structure and behavioral adaptations in response to repeated stimuli. However, the KI mice exhibit alterations in behavior in the forced swim and tail suspension, two paradigms that involve exposures to acute stimuli. The depression-like phenotype may be in part due to the absence of pMeCP2 in development rather than the loss of activity-dependent pMeCP2 in the adult. Supporting this possibility, Cohen and colleagues demonstrate that the KI mice have synaptic defects and alterations in the behavioral responses to novel experience (Cohen *et al*, 2011). Therefore, if pMeCP2 plays a role in the development of properly functioning synapses, then it is possible that the depression-like phenotype in the adult

mouse is due to developmental deficits. In order to isolate the role of activity-dependent pMeCP2 in the adult mouse, it would be necessary to generate a conditional KI in which the S421 could be mutated after development. Rescuing pMeCP2 function in the adult to see if the depression-like phenotype is eliminated in the adult would be another way to address this question.

Although there are many remaining questions as to how the lack of pMeCP2 alters the behavioral response to stressful stimuli, the work described here is the first to implicate a methyl-DNA binding protein in depression-like behavior and the response to antidepressant treatment. Initially, the majority of studies have focused on alterations in histone modifications in depression-like behavior and the behavioral response to antidepressant treatment (Covington *et al*, 2009; Tsankova *et al*, 2006). However, recent evidence has shown that chronic social defeat stress results in an increase in Dnmt3a, a DNA methyltransferase, in the NAc, and that overexpression of Dnmt3a is pro-depressive (LaPlant *et al*, 2010). Our findings along with those from LaPlant and colleagues suggest that DNA methylation and methyl DNA-binding proteins are emerging as promising new avenues for understanding the mechanisms underlying depression and stress, as well as the mechanisms of antidepressant action.

5.2 PMECP2 AS A MECHANISM OF ANTIDEPRESSANT ACTION

In addition to demonstrating that pMeCP2 is involved in the behavioral response to stressful stimuli, we also show that pMeCP2 is required for antidepressant effects of chronic imipramine after social defeat stress. The fact that the KI mice respond to acute but not chronic imipramine suggests that pMeCP2 is required for behavioral adaptations

to chronic monoaminergic signaling. In order to further explore this possibility, it would be interesting to defeat KI and WT mice and then treat them with ketamine, a non-competitive NMDA receptor antagonist that rapidly alleviates depression-like symptoms within a few hours of treatment (Sancora *et al*, 2008; Zarate *et al*, 2006). Therefore, if pMeCP2 is required for changes in gene expression or chromatin structure that happen over a longer time scale, one would predict that the behavioral response to ketamine would not be altered in the KI mice. In addition, future studies could also determine if pMeCP2 is required for the behavioral response to deep brain stimulation (DBS). Utilizing treatments with different time courses and mechanisms of action will deepen our understanding of the role pMeCP2 plays in antidepressant response.

In order to identify the brain regions in which pMeCP2 might be important for the response to imipramine treatment, we compared the brain regions in which pMeCP2 is induced following acute vs chronic imipramine treatment. We find that both acute and chronic imipramine induce pMeCP2 in the GABAergic interneurons of the NAc. Although most initial studies of antidepressant action focused on the hippocampus and the frontal cortex, recent studies have shown that the DA projections from the VTA to the NAc play a role in anhedonia and decreased motivation in depressed individuals (Berton and Nestler, 2006). Furthermore, changes in gene expression in the NAc have been associated with antidepressant response (Vialou *et al*, 2010; Wilkinson *et al*, 2009; Barrot *et al*, 2002). Our data suggest that pMeCP2 in the NAc may also be important for antidepressant action. Although pMeCP2 is induced in the NAc after both acute and chronic treatment, it is possible that repeated induction of pMeCP2 is necessary for the

plasticity in this region that underlies the behavioral adaptations to chronic imipramine treatment.

In addition to the NAc, we also show that imipramine treatment induces pMeCP2 in the LHb. Unlike the NAc, pMeCP2 is induced in the LHb following chronic but not acute antidepressant treatment. This is the only region in which we saw induction of pMeCP2 specifically following chronic treatment, suggesting that pMeCP2 in this region may be important for chronic antidepressant treatment. As mentioned earlier, the hippocampus and frontal cortex are no longer the only regions examined in depression, stress, and antidepressant response. A role for the LHb is emerging in the regulation of stress and reward (Li *et al*, 2011; Bromberg-Martin and Hikosaka, 2011; Hikosaka, 2010). In response to stress, aversive stimuli, or smaller-than-expected rewards, the LHb is activated and subsequently inhibits DA neurons in the VTA via the RMTg (Hong *et al*, 2011; Hikosaka, 2010; Matsumoto and Hikosaka, 2009; Ji and Shepard, 2007). Since activation of the LHb is associated with stress and depression, it is surprising that we observe pMeCP2 induction in this region following chronic antidepressant exposure, which alleviates symptoms of depression. In order to better understand the function of pMeCP2 induction in the LHb, it would be necessary to compare gene expression in KI and WT mice in this brain region following chronic treatment. Furthermore, manipulating pMeCP2 or MeCP2 in the LHb and examining social avoidance following chronic imipramine treatment would also be useful in determining if pMeCP2 induction in the LHb plays a functional role in antidepressant response. There are many remaining questions about the role of pMeCP2 induction in the LHb in antidepressant response;

however, our data contribute to the growing body of evidence that suggest that the LHB is involved in depression-like behavior.

5.3 UNDERSTANDING THE MECHANISM BY WHICH PMeCP2 MEDIATES BEHAVIORAL RESPONSES TO ANTIDEPRESSANT TREATMENT

Our data provide evidence that a single point mutation of MeCP2 at Ser421 affects the behavioral response to chronic imipramine treatment. These data suggest that activity-dependent pMeCP2 plays a role in mediating the behavioral adaptations to chronic stimuli. Currently, little is known about the mechanism by which MeCP2 and pMeCP2 specifically affects chromatin structure and ultimately behavior. Although MeCP2 was traditionally viewed as a gene-specific transcriptional repressor, recent studies have shown that MeCP2 is almost as abundant in neuronal nuclei as nucleosomes and that MeCP2 binding tracks the density of methylated DNA genome-wide (Skene *et al*, 2010). Skene and colleagues demonstrate that MeCP2 affects chromatin structure, as *Mecp2*-null mice have global increases in histone H3 acetylation and elevated transcription of repetitive elements. Further supporting a role for MeCP2 in regulating chromatin structure in a genome-wide fashion, there are no significant changes in gene expression in *Mecp2*-null mice compared to WT controls, suggesting that MeCP2 may not be acting as a gene-specific transcriptional regulator.

Consistent with the findings from Skene and colleagues, another study demonstrated that activity-dependent pMeCP2 does not occur on MeCP2 bound to specific sets of genes (Cohen *et al*, 2011). Rather, Cohen and colleagues find that pMeCP2 is induced uniformly across the genome, refuting the previous models that were

based on findings from *in vitro* studies. Furthermore, there are no significant differences in activity-dependent gene expression in the KI and WT mice, suggesting that pMeCP2 does not affect gene expression. Taken together, these data suggest that instead of regulating transcription of specific genes, pMeCP2 may play a more global role in mediating MeCP2-dependent changes in chromatin structure in response to neuronal activity.

Although these findings suggest that pMeCP2 does not modulate MeCP2's ability to regulate specific sets of genes, it is still possible that pMeCP2 does regulate gene expression in response to other stimuli than those examined. Cohen and colleagues compared gene expression profiles from KI and WT cortical neurons after a single stimulus. In our work, we administered chronic imipramine treatment *in vivo* and found a robust difference in behavior in adult KI and WT mice. These data suggest that pMeCP2 could influence gene expression after chronic stimuli. pMeCP2 could be mediating changes in chromatin structure that accumulate with repeated stimuli that subsequently alter gene expression. In addition to different stimuli differentially regulating pMeCP2, there are other possible mechanisms by which pMeCP2 may influence gene expression. For example, perhaps other post-translational modifications of MeCP2 (i.e. phosphorylation at additional sites) may be acting alongside pMeCP2 to affect gene expression. It is also possible that a genome-wide modification like pMeCP2 could have specificity by affecting the recruitment of gene-specific binding partners. The exact mechanism is unknown at this time; however, our finding that the KI mice fail to respond to chronic imipramine treatment provides an excellent context in which the mechanism of pMeCP2 can be examined.

Another reason that Cohen and colleagues did not detect differences in activity-regulated gene expression in KI and WT mice is that pMeCP2 regulates gene expression in specific cell-types. For example, we find that imipramine induces pMeCP2 selectively in the GABAergic interneurons of the NAc. Furthermore, chronic imipramine induces pMeCP2 in a subset of the neurons of the LHb. Therefore, in order to examine alterations in gene expression in the KI mice, it is necessary to isolate these populations in which pMeCP2 is normally induced. pMeCP2 is a prime example of the need to continue to develop cell-type specific knockouts and refine techniques to isolate neuron populations in the adult brain for gene expression analysis.

5.4 PMECP2, RTT, AND DEPRESSION

In addition to deepening the understanding of the function of pMeCP2, our findings also have implications for human disease and disorders. Here we have shown that loss of activity-dependent pMeCP2 contributes to some of the behavioral abnormalities of RTT (Cohen *et al*, 2011). The onset of RTT occurs around the time that sensory experience is driving the formation of functional circuits; therefore, the loss of activity-dependent pMeCP2 during this developmental window may contribute to RTT. Our findings suggest that focusing on specific sites of modification is important in understanding how loss of MeCP2 leads to RTT. Furthermore, restoring pMeCP2 function may be a potential avenue of treatment for this developmental disorder.

We also find that the loss of pMeCP2 may be implicated in depression-like behavior, specifically the behavioral response to stressful stimuli. Supporting this possibility, Ramocki and colleagues find that female *MECP2* duplication carriers display

heightened anxiety and depression-like symptoms (Ramocki *et al*, 2009). These findings suggest that there may be a link between alterations in *MECP2* and depression in adult humans. Also, the fact that the KI mice fail to respond to chronic imipramine treatment renders this strain as a possible model of treatment resistant depression. A great number of individuals do not respond to clinically available antidepressants; therefore, studies in the KI mice may provide insight into why this phenomenon occurs. Finally, our findings support the manipulation of chromatin-modifying proteins as novel therapeutic strategies in treating depression and stress disorders.

APPENDIX A: REDUCED CORTICAL BDNF EXPRESSION AND ABERRANT MEMORY IN CARF KNOCK-OUT MICE

A.1 SUMMARY

Transcription factors are a key point of convergence between the cell-intrinsic and extracellular signals that guide synaptic development and brain plasticity. Calcium-Response Factor (CaRF) is a unique transcription factor first identified as a binding protein for a calcium-response element in the gene encoding Brain-Derived Neurotrophic Factor (*Bdnf*). We have now generated *Carf* knockout (KO) mice to characterize the function of this factor *in vivo*. Intriguingly, *Carf* KO mice have selectively reduced expression of *Bdnf* exon IV-containing mRNA transcripts and BDNF protein in the cerebral cortex while BDNF levels in the hippocampus and striatum remain unchanged, implicating CaRF as a brain region-selective regulator of BDNF expression. At the cellular level, *Carf* KO mice show altered expression of GABAergic proteins at striatal synapses, raising the possibility that CaRF may contribute to aspects of inhibitory synapse development. *Carf* KO mice show normal spatial learning in the Morris water maze and normal context-dependent fear conditioning. However they have an enhanced ability to find a new platform location on the first day of reversal training in the water maze and they extinguish conditioned fear more slowly than their wild-type (WT) littermates. Finally, *Carf* KO mice show normal short-term and long-term memory in a novel object recognition task, but exhibit impairments during the remote memory phase of testing. Taken together these data reveal novel roles for CaRF in the organization and/or function of neural circuits that underlie essential aspects of learning and memory.

A.2 INTRODUCTION

Activity-dependent plasticity is an essential feature of the brain, allowing neuronal structure and function to adapt to changes in the environment. Changes in synaptic activity drive long-lasting alterations in neuronal function in part by regulating the expression of genes whose products affect cell morphology, synaptic function, and/or intrinsic excitability (Greer and Greenberg, 2008). Intracellular calcium signaling pathways are essential intermediates in this process, converging in the nucleus to regulate the expression and/or function of transcription factors (West et al., 2002).

In addition to receiving information from synapses, many activity-regulated transcription factors also contribute to experience-dependent synapse development and remodeling. For example, calcium-dependent activation of the transcription factor MEF2 induces the expression of gene products that subsequently drive the elimination of excitatory synapses (Flavell et al., 2006), while activity-dependent expression of the transcription factor NPAS4 controls the number of GABAergic synapses that form on excitatory neurons (Lin et al., 2008). Importantly, these transcriptional effects on synapses may have consequences for learned behaviors. For example, RNA interference-mediated knockdown of MEF2 in the striatum not only increases dendritic spine density but also attenuates persistent behavioral sensitization after chronic cocaine, suggesting a link between MEF2's effects on synapses and the behavioral consequences of psychostimulant exposure (Pulipparacharuvil et al., 2008). Hence study of transcriptional regulators that link environmental stimuli with synapses may yield new insights into cognition.

CaRF is a unique transcription factor that was first cloned and characterized as a binding protein for a calcium-response element (CaRE1) that is required for activity-

dependent transcription from promoter IV of the *Bdnf* gene (Tao et al., 2002). CaRF shares no homology with other transcription factors, however it is a nuclear, sequence-specific DNA binding domain protein, and it can act as a CaRE1-dependent transcriptional activator. Given that BDNF is a secreted neurotrophic factor that has numerous effects on synapses (Poo, 2001), the evidence that CaRF can regulate transcription of *Bdnf* raised the possibility that CaRF might contribute to neural development and/or plasticity. However the biological functions of CaRF have remained entirely unknown.

To study CaRF *in vivo*, we have generated a CaRF-specific antibody and *Carf* KO mice. Here we demonstrate a role for CaRF in the transcriptional regulation of *Bdnf*, and surprisingly we find that this requirement for CaRF is both brain region- and stimulus-selective. At the cellular level, we find that *Carf* KO mice have altered expression of GABAergic synaptic proteins in the striatum, raising the possibility that CaRF may contribute to aspects of inhibitory synapse development. Finally through a series of behavioral tasks, we demonstrate that *Carf* KO mice display alterations in discrete aspects of spatial, emotional, and recognition memory. Together these data demonstrate that CaRF is a biologically important transcription factor in the CNS, and suggest that CaRF-dependent programs of gene transcription may contribute to development and/or plasticity of the neural circuits that underlie learning and memory.

A.3 MATERIALS AND METHODS

A.3.1 Generation of *Carf* knockout mice and genotyping

All oligonucleotides used in this study were synthesized by Integrated DNA

Technologies (Coralville, IA) and are listed in **Suppl. Table S1**. To generate the genomic targeting vector, a 129S4 BAC library (Incyte Genomics, Palo Alto, CA) was screened using *Carf* primers against intron 7 and exon 8. BAC 27839 was selected as a template for the generation of a 5.3kB piece of *Carf* genomic DNA containing intron 7 through exon 9 (bp 37713501 to 37719853 of mouse chromosome 1, NT_039170.7, July 2007 build, www.genome.ucsc.edu) which was cloned in pBKS- from *EcoRI* to *NotI*. Using recombineering techniques (Angrand et al., 1999), an *FRT*-flanked pGK-*Neo* cassette and a single *loxP* site were placed 133 bp 5' to the beginning of exon 8, while a second *loxP* site was placed 425bp 3' to the end of exon 8. The *Carf* targeting vector was electroporated into 129S4/SvJae ES cells, clones were selected for integration with 150µg/mL G418, and genomic DNA from approximately 1200 individual neomycin-resistant clones was screened by southern blotting. Two properly targeted clones were identified. One clone (#112) showed a normal karyotype and was injected into C57BL/6J blastocysts, yielding three chimeric pups. Chimeras were mated to C57BL/6J wild-type mice (The Jackson Laboratory, Bar Harbor, ME) and germline transmission from two chimeras was confirmed by PCR genotyping of tail biopsies from the offspring. These mice were crossed to a 129S4/SVJae *Flp* deleter line (The Jackson Laboratory) (Farley et al., 2000) and germline recombination of the pGK-*Neo* cassette was confirmed by PCR. Finally, *Carf* ^{2lox},*Neo*^{-/+} mice were crossed to transgenic EIIa-*Cre* mice on a mixed C57BL/6-FVB background (The Jackson Laboratory) (Lakso et al., 1996) and germline recombination of *Carf* exon 8 was confirmed by PCR genotyping of tail biopsies. Mice were maintained on a mixed genetic background, and in all experiments *Carf* KOs were compared with their heterozygous (HET) and WT littermates. All experiments were

conducted with an approved protocol from the Duke University Institutional Animal Care and Use Committee.

A.3.2 Luciferase assays

293T cells were cultured and transfected as described (Tao et al., 2002). Luciferase assays were performed two days after transfection using the Dual Assay Luciferase kit (Promega; Madison, WI). Cotransfected TK-renilla luciferase was used to normalize samples for transfection efficiency and sample handling. All data presented are the average of at least three measurements from each of at least two independent experiments. To generate the CaRF cCaRE and mCaRE reporters, three 21bp repeats (**Suppl. Table S1**) were cloned into the firefly luciferase expression vector pOF-luc (a gift of J. Liu, Johns Hopkins University) at the *HindIII* and *XhoI* sites.

A.3.3 Preparation of recombinant mouse CaRF and antibody purification

Full length mouse *Carf* (NM_139150) was amplified by PCR and cloned in the baculoviral expression vector pAcGHLT-A (Pharmingen/BD Biosciences, San Jose, CA) to generate a N-terminal GST-CaRF fusion protein. Recombinant baculovirus was produced by Orbigen (San Diego, CA) then amplified in *Sf9* cells. For protein production, virus was incubated with *Sf21* cells grown in suspension in Hink's TNM-FH medium (JRH Biosciences), 10% insect tested FBS (Sigma, St. Louis, MO), 1X Pluronic F-68 (Sigma) and Pen/Strep (Sigma). 72 hours later cells were spun down and lysed in 50mM Tris pH 8.0, 150mM NaCl₂, 0.7% CHAPS, 1% Tx-100, and 5mM DTT. GST-CaRF was purified from the lysate by incubation with glutathione-agarose beads, and eluted with

20mM reduced glutathione (Sigma). Purified GST-CaRF protein was injected into 3 rabbits (Covance, Berkeley, CA) and screened by western blotting for detection of recombinant CaRF. Antiserum from one rabbit (#4510) was purified by ammonium sulfate precipitation of IgG, then it was passed over an Affigel 15 column (BioRad) on which we had mounted purified GST-CaRF. The flowthrough was discarded and the antibody was eluted with glycine, dialyzed, and stored in PBS with glycerol.

A.3.4 Nuclear extracts

Nuclear extracts were prepared following a high-salt extraction procedure (Tao et al., 1998). Protein concentration was determined by protein assay (BioRad).

A.3.5 Western blotting

10µg nuclear extract or 20µg striatal lysate was loaded on 8-10% SDS-PAGE gels for separation transferred to PVDF membrane. Following blocking, primary antibodies were incubated for 60 min at room temperature, and secondary antibodies conjugated to HRP (Jackson ImmunoResearch, West Grove, PA) were used at 1:10,000. Bands were visualized by reacting blots with ECL (Pierce, Rockford, IL) and exposing to film. For quantitation, multiple exposures were taken to establish the linear range, and films were scanned for densitometry using ImageJ (<http://rsbweb.nih.gov/ij/>). All bands were normalized to actin in the same sample as a loading control. Primary antibodies used in this study include rabbit anti-CaRF 1:500 (#4510, this study), rabbit anti-Histone H3 1:5,000 (Millipore, Billerica, MA, cat. #070-690), mouse anti-MEF2D 1:1000 (BD Biosciences, Sparks, MD, cat. #610774), rabbit anti-CREB 1:1000 (Upstate/Millipore

cat. #06-863), rabbit anti-synaptophysin 1:10,000 (Zymed/Invitrogen cat. #18-0130), rabbit anti-DARPP-32 1:1000 (Chemicon/Millipore cat. #AB1656), mouse anti-GAD-67 1:5000 (Chemicon cat. #MAB5406), mouse anti-GABA-A β 2/3 (Chemicon cat. #MAB341), rabbit anti-GABA-A γ 2 1:500 (Chemicon cat. #AB5954), mouse anti-GAD-65 1:500 (Millipore cat. #MAB351), mouse anti-NR1 1:1000 (Affinity Bioreagents, Rockford, IL cat. #OMA1-04010), rabbit anti-SAPAP3 1:1000 (a gift of Dr. G. Feng, Duke University Medical Center), mouse anti-PSD-95 1:1000 (Chemicon cat. #MAB1596), mouse anti-Actin 1:1000 (Chemicon cat. #MAB1501).

A.3.6 Electrophoretic mobility shift assay

2-5 μ g nuclear extracts were incubated with 50 fmol 32 P end-labeled oligonucleotide probes for 20 min at room temperature prior to separation on a 6% non-denaturing acrylamide gel in Tris-borate buffer (pH=7.5). In competition assays, unlabeled probes were added to nuclear extracts in 100-fold molar excess to the radiolabeled probe for 30 min prior to addition of the labeled probe. Gels were dried and visualized by phosphorimager and shifts were quantitated relative to probe intensity in the same lane using the ImageQuant image analysis program (GE Healthcare; Piscataway, NJ).

A.3.7 Mouse embryonic fibroblasts

Mouse embryonic fibroblasts were generated as described (Xu, 2005) from individual E13.5 embryos of a *Carf*^{HET} x HET cross. For luciferase assays, 1 x 10⁶ cells were transfected using AMAXA (Lonza, Walkersville, MD, cat. #VCA-1003) following the manufacturer's instructions and using program A-23.

A.3.8 RNA harvesting and RT-PCR

Brain tissue was rapidly dissected on ice, snap frozen in liquid nitrogen, and stored at -80°C. RNA was harvested using the Absolutely RNA kit (Stratagene; La Jolla, CA). 500ng of RNA was used for reverse transcription with oligo dT primers and Superscript II (Invitrogen, Gaithersburg, MD). cDNA was used for quantitative PCR of gene transcripts (Power SYBR green, ABI 7300 real time PCR machine; Applied Biosystems, Foster City, CA) with the intron-spanning primers listed in **Suppl. Table S1**. Each sample was measured in triplicate, and expression of the housekeeping gene *Gapdh* was used as a normalizing control for RNA quantity and sample processing. All data shown are derived from at least three samples from each of at least two independent experiments.

A.3.9 Neuronal and glial cell cultures

Neuron-enriched cultures were generated from E16 CD1 mouse embryos (Charles River Labs, Raleigh, NC). Briefly the cortex was dissected, cells were dissociated with papain (Worthington Biochemicals, Lakewood, NJ), and the cell suspension was plated on poly-D-lysine coated dishes or glass coverslips in Neurobasal medium with B27 supplements (Invitrogen) and Pen/Strep. For analysis of CaRF expression cultures were treated on DIV5 with 1µM tetrodotoxin (TTX; Sigma) or 55mM KCl in an isotonic solution (Tao et al., 2002). Glial cultures were generated by dissociating P0/P1 cortices and plating the cells on tissue culture dishes in DMEM with 5% FBS and Pen/Strep. Cells were fed and passaged over a period of 3 weeks prior to RNA harvesting. For immunocytochemistry of mixed neural/glial cultures, dissociated cortical cells from P0 embryos were plated on

PDL-coated glass coverslips in Neurobasal medium with B27 supplements, AraC was added to 10 μ M beginning on DIV2. At DIV10 the cells were fixed for 10 min in 4% paraformaldehyde, blocked with 16% goat serum and permeabilized with 0.2% TritonX-100. Primary antibodies were incubated overnight at 4°C and, after washing, fluorescent secondary antibodies were applied for 60 min at room temperature at 1:500. Hoechst dye was included in the final washes to label DNA. Antibodies used are purified rabbit anti-CarF (#4510, this study) 1:100, and chicken anti-MAP2 1:400 (Chemicon, cat. # AB5543).

A.3.10 BDNF protein measurements

Brain extracts from frontal cortex, hippocampus, or striatum of *Carf* WT and KO mice were prepared as described (Hong et al., 2008). BDNF protein was measured using a two-site enzyme-linked immunoabsorbant assay (ELISA) using the BDNF E_{max} ImmunoAssay System (Promega). All samples were measured in triplicate and compared against a standard curve on the same plate.

A.3.11 Synapse immunohistochemistry

Six month old adult *Carf* KO mice or their WT littermates were anesthetized and 10transcardially perfused with 4% paraformaldehyde in 0.1M PBS. Brains were postfixed in 4% paraformaldehyde/PBS overnight, then sunk in 30% sucrose/PBS overnight. 40 μ m coronal sections were cut on a freezing microtome and brain regions were identified by reference to anatomical landmarks. To minimize variation in immunostaining across treatment groups, sections from individual mice were first placed and spread into a Petri

dish filled with PBS and photographed with a high-resolution digital camera (Sony DSC-H1). All sections were then mixed for immunolabeling and processed within a single chamber. Sections were incubated with primary antibodies overnight at 4°C and with fluorescent-conjugated secondary antibodies for 1 hr at room temperature. Nuclei were labeled with Hoechst dye (Sigma) to facilitate anatomical localization of structures, sections were mounted and coverslipped, then fluorescent images were captured on a Leica DMI4000 inverted fluorescence microscope using a Cascade 512B camera. Digital images were quantified using MetaMorph 7.0 Image Analysis software (Molecular Devices, Sunnyvale, CA). All images within one experiment were taken with a constant exposure time and aperture, and quantified using a single threshold value. To reduce variation between mice, we measured expression of synaptic markers from a constant-sized region across the shell of the nucleus accumbens (NAc). Four separate images from each brain were captured with a 63x oil lens. Images were captured in a z-stack in MetaMorph and subjected to 3-D deconvolution processing using AutoQuant X2.1.1 software (Media Cybernetics, Inc., Bethesda, MD). After 3D-deconvolution, a four consecutive image stack (equivalent to 2µm thickness) was merged using the Average Stack Arithmetic module in MetaMorph. The merged images were then quantitated using the Count Nuclei module in MetaMorph to evaluate both numbers of synaptic punctae as well as the integrated intensities of these punctate spots of immunoreactivity. Punctae were defined in MetaMorph as local regions 2-4 pixels in size with intensity a set threshold above the local background. Primary antibodies used in this study include mouse anti-GAD65 1:1000 (Millipore) and rabbit anti-synaptophysin 1:1000 (Zymed).

A.3.12 SHIRPA phenotypic screen

Naïve male *CaRF* WT (n = 10), HET (n = 20), and KO (n = 12) littermates were subjected to a standard observational SHIRPA test for purposes of comprehensive behavioral and functional profiling (Rogers et al., 1997). All parameters were scored by two investigators blind to the genotype of the mice. Briefly, each mouse was first assessed by observing undisturbed behavior in a viewing jar for the features listed in **Suppl. Table S2**. Next each mouse was transferred to an arena to examine transfer arousal and open field behavior, as well as response to a sequence of manipulations using tail suspension and a grid laid across the width of the arena. Finally, each mouse was restrained in a supine position to record autonomic behaviors prior to measurement of the righting reflex. Throughout this procedure vocalization, urination and general fear, and irritability and aggression were recorded.

A.3.13 Morris water maze

Following the SHIRPA screen, male *CaRF* WT (n = 10), HET (n = 20), and KO (n = 12) littermates 2.5 to 4 months of age received 7 days of water maze training during the light phase of their light-dark cycle. The maze consisted of a circular pool approximately 1.2 m in diameter and filled with room temperature water. A circular platform 10 cm in diameter was submerged 2 cm below the surface of the water, and the water was clouded by non-toxic powdered tempera paint to ensure that the mice could not see the platform. The pool was located in a well-lit room (approximately 5.8 m × 2.6 m in dimension) with salient extramaze cues, such as a table with a computer, shelving that contained large objects, pictures of large black shapes adhered to a curtain and room walls, a large metal

trash bin, and the experimenter who sat in a chair near the computer. The water maze was divided into 4 quadrants (north, south, east, and west) with the hidden platform located in the center of one target quadrant. For all training trials, mice were placed in a random start location in the pool (north, south, east, west) facing the wall of the pool and given 60 sec to locate the hidden platform. If a mouse did not find the platform by the end of 60 sec, it was gently guided to the platform. Mice were allowed to sit on the platform for 15 sec after climbing on to it. Following each training trial, mice were removed from the water maze, dried with a towel, allowed to rest for 60 sec, and then immediately began the next trial.

On days 1-4, mice received 4 training trials per day on a place learning water maze task where the hidden platform remained in the same spatial location for each trial. On day 4, mice received a single immediate probe trial in between trials 2 and 3. During probe trials, the platform was removed and mice were allowed to swim for 60 sec. After the probe trial, each mouse completed trials 3 and 4 with the platform present to prevent extinction of prior learning. Twenty-four hrs later on day 5, mice received a single 24 hr-probe trial, followed by 3 additional training trials, and then a single curtain trial. During the curtain trial, a large curtain was drawn around the maze to eliminate all extramaze cues from view. This allowed us to determine whether mice were using extramaze spatial cues to find the hidden platform. On day 6, mice received 4 training trials on a reversal learning task where the platform location was moved to a new location in a different quadrant in the pool. Finally, on day 7, each mouse received 4 training trials on a visible platform task where the platform was raised above the water line and labeled with white tape. On each trial, the location of the platform changed.

For all trials, performance on the task was recorded using a computerized tracking system (HVS Image, Hampton, UK). For training trials, latency (sec) to locate the platform was recorded as a measure of spatial learning. For probe trials, the percentage of time spent searching in each quadrant was a measure of spatial memory. To determine the search strategy of each mouse when initially challenged with learning a new platform location during reversal learning, we also recorded percentage of time spent in each quadrant during the first trial of reversal learning.

A.3.14 Fear Conditioning

Mice were tested for context fear conditioning and extinction using methods previously described for the mouse (Schmalzigaug et al., 2009). Mice (8 WT and 11 KO) were examined at the same time each day, between 1000 and 1300 hrs. On day 0 (conditioning), the mice were placed into a Med-Associates (St. Albans, VT) fear conditioning chamber (26 x 22 x 12 cm) illuminated with a 100 mA house light. After 2 min, a 72 dB 2900 Hz tone (CS) was presented for 30 sec. The CS terminated simultaneously with a single 2 sec 0.4 mA scrambled foot-shock (UCS). Animals remained in the conditioning chamber for 30 sec, after which they received a second CS-UCS pairing, and were returned to the home cage after 30 sec. Contextual fear conditioning was assessed 24 hrs later (day 1) over 5 min in the absence of the CS or UCS. Cued fear conditioning was evaluated 48 hrs after initial conditioning (i.e., day 2). Mice were placed into a neutral environment for 2 min and the CS was presented continually over the next 3 min. Extinction of contextual fear conditioning began on day 3. It included the same procedures as described for day 1 of testing and was continued for

13 consecutive days, by which time freezing behavior had reached the level of pre-conditioning on day 0 and did not change over three consecutive days. Freezing behavior was defined the absence of all movement by the animal other than that required for respiration. All behaviors were video-recorded. The recordings were scored subsequently by trained observers using Noldus Observer 5 (Noldus Information Technology, Leesburg, VA). All observers were blind to genotype. The results are presented as the percent time spent freezing at conditioning, testing, and extinction.

A.3.15 Novel object recognition

Novel object recognition was examined using methods previously described for the mouse (Rodríguez et al., 2007). (Rodríguez et al., 2007). Before commencing testing, each mouse was habituated to an empty plexiglas arena (48 x 22 x 18 cm) for 3 consecutive days. On the first day of testing mice were exposed to two identical objects (T1 and T2, 4 x 4 x 2 cm) placed at opposite ends of the arena. The animals were permitted to explore the arena and the objects for 10 min before being returned to the home cage. After 20 min mice were returned to the arena for a short-term memory test where they were presented for 10 min with one of the familiar objects (T1) and a novel object (N1) of similar dimensions. Twenty-four hrs later mice were familiar for long-term memory. Each animal was returned to the arena for 10 min with the familiar object (T1) and a second novel object (N2). Ten days later mice were tested for remote memory. Each animal was returned to the arena for 10 min and was presented with the familiar object (T1) and another novel object (N3). For each test, objects were always placed in the same two locations; however, the location of the novel object relative to the familiar object was

randomized for each test across mice. All tests were conducted under indirect 80-100 lux illumination between 1000 and 1400 hrs, behaviors were videotaped and scored subsequently with Noldus Ethovision XT 7.0 (Noldus Information Technology). The automated Ethovision XT software program used multiple-point tracking to identify the main body axis of the animal and it tracked the location of the nose relative to each object. Contact with a given object was defined as the mouse approaching the object nose-first with the nose being within 1 cm of the object boarder. Duration and frequency of nose contacts with each object was scored. Preference for the novel object was calculated by subtracting the time spent with the familiar object (T1) from the time spent with the novel object (N1, N2 or N3) and dividing this amount by the total time spent with both objects. Positive scores signified preference for the novel object, negative values indicated preference for the familiar object, and scores of “0” denoted no preference for either object. To confirm that the Ethovision XT program was scoring videos accurately, several test videos were randomly selected and analyzed by trained observers using Noldus Observer 5.0 (Noldus Information Technology, Leesburg, VA). Kappa scores between automated scoring and live coder scoring for duration and contacts with objects exceeded 0.92.

A.3.16 Statistical analyses

The results are presented as means and standard errors of the mean (SEM). The mRNA and protein expression data were analyzed by unpaired two-tailed t-test using GraphPad Software (GraphPad Software Inc., La Jolla, CA). The statistical analyses of behavioral data were performed using SPSS 11 (SPSS Inc., Chicago, IL). For object testing,

RMANOVA were conducted within each test day (STM, LTM and remote memory) for duration spent with objects, frequency of contacts with objects, and preference scores for the within subject effects of object (familiar and novel) and the between subject effect of genotype with the interaction between these two main effects. For fear conditioning and extinction, the percent time freezing was assessed using RMANOVA with within subject effects of test day, between subject effects of genotype, and the interactions. In all cases, *Aposteriori* analyses were conducted using Bonferroni corrected pair-wise comparisons, $p < 0.05$ was considered statistically significant.

A.4 RESULTS

A.4.1 Generation of *Carf* knockout mice and validation of a CaRF-specific antibody

To investigate the physiological functions of CaRF *in vivo* we generated a *Carf* KO mouse. The *Carf* gene is comprised of 16 exons spanning 52.7kB of mouse chromosome 1 (**Fig. 20A**; *Mus musculus* Chr. 1, 60155125-60207878, July 2007 assembly, www.genome.ucsc.org). The locus also encodes a shorter *Carf* variant that utilizes an alternative polyadenylation site in the intron following exon 8 (orthologous to the short variant of human *ALS2CR8*, Genbank Acc. #AB053310). We chose to target exon 8 for deletion because this exon encodes an evolutionarily conserved domain in CaRF that is required for DNA binding (Tao et al., 2002). *loxP* sites were placed around exon 8, and an *FRT*-flanked pGK-*Neo* cassette was inserted just 5' to the *loxP* site in intron 7 (**Fig. 20A**). The targeting vector was introduced into ES cells, and homologous recombination at the *Carf* locus was validated by Southern blotting (**Fig. 20B**). Germline transmission was confirmed by PCR (**Fig. 20C**), the *Neo* cassette was excised by crossing

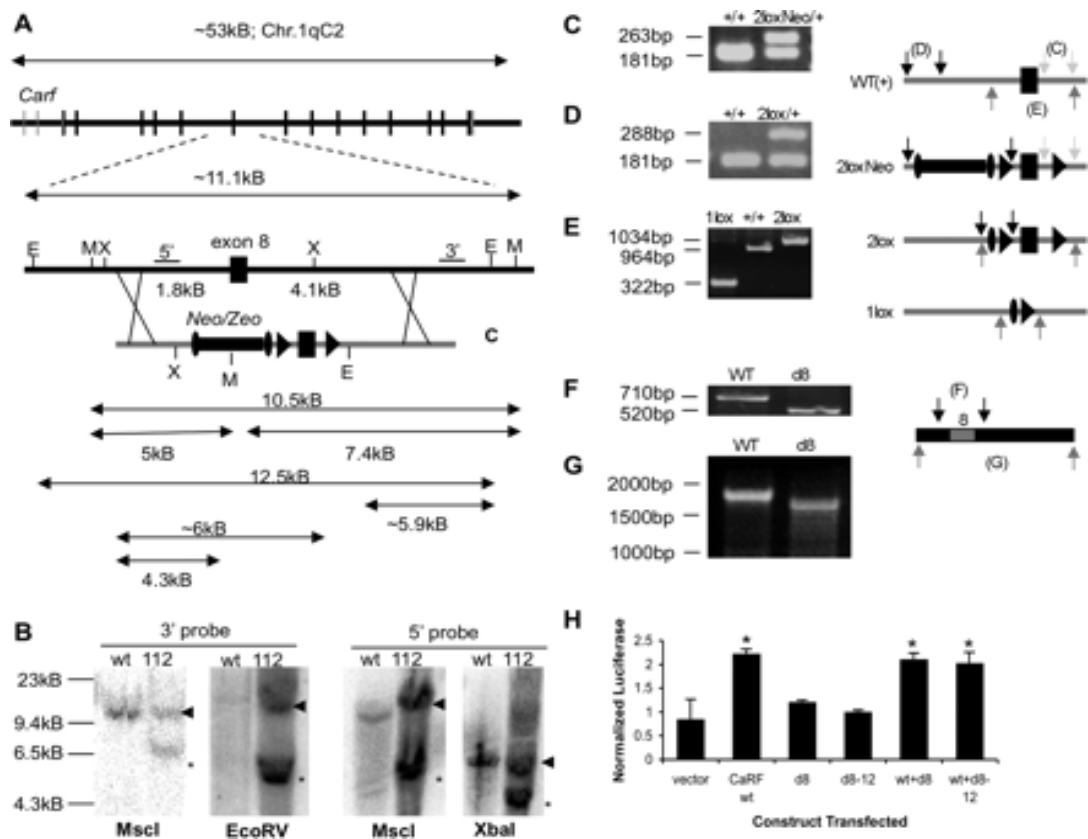


Figure 20: Generation of a *Carf* exon 8 KO mouse. (a) Genomic organization of the *Mus musculus Carf* gene which spans 53kB on chromosome 1. Boxes represent exons. E: *EcoRV*, M: *MscI*, X: *XbaI*. Ovals show *FRT* sites, triangles show *loxP* sites. The box under *Neo/Zeo* represents the position of the *neomycin* resistance gene in the targeting vector. The numbers and arrows indicate the size of genomic fragments generated on Southern blotting by cleavage with the indicated enzymes. (b) Southern blot analysis of ES cell line 112. Positions of the 5' and 3' probes are indicated in part A. WT, wild-type, 112, ES clone 112 with targeted mutation of *Carf* gene. Arrowhead indicates WT allele, asterisk shows targeted allele. c-e) PCR analysis of targeted clone 112. (c) Primers across the 3' *loxP* site show the 40bp insertion. Position of primers is indicated by the light gray arrows (d) Recombination of the Neomycin resistance cassette. Position of primers is indicated by the black arrows. (e) Deletion of exon 8 with primers that cross the deletion. Position of primers is indicated by the medium gray arrows. (f-g) PCR analysis of cDNA made from neurons of nonrecombined (WT) or *Cre* recombined (d8) targeted mice. (f) Primers spanning from exons 7-9 (black arrows). (g) Primers spanning the full coding region (gray arrows) show a single band approximately 190bp shorter than full length *Carf*. (h) *Bdnf* promoter IV enhanced luciferase reporter gene expression in transfected 293T cells with cotransfected CaRF deletion constructs. d8: deletion of exon 8; d8-12: deletion of exons 8-12. Bars represent the mean and error bars show S.E.M. All data are the result of at least three independent replicates. * $p < 0.05$.

Carf *2lox-Neo/+* mice to a *Flp* deleter strain (**Fig. 20D**) (Farley et al., 2000), then *Carf* *2lox/+* mice were crossed to a *Cre* deleter strain (Lakso et al., 1996) to obtain germline recombination at the *Carf* locus (**Fig. 20E**). Heterozygous *Carf* *+/-* mice (HET) were maintained on a mixed 129/C57BL6 background and in all subsequent experiments, *Carf* *-/-* (KO) mice were compared to wild-type *Carf* *+/+* (WT) littermates as control.

Carf mRNA is still detected in KO mice, however this mRNA is shorter than WT *Carf* by an amount consistent with the deletion of exon 8 (**Fig. 20F,G**). Extensive sequencing across the deletion revealed no evidence of alternative exons or splicing that would generate novel in-frame transcripts (data not shown). We tested the consequences of potential residual protein expression from the *Carf* locus, but found no evidence that CaRF variants lacking exon 8 were capable of driving CaRE1-dependent transcription or acting in a dominant negative fashion to suppress CaRF-dependent transcription (**Fig. 20H**). Although we cannot exclude that putative functions of CaRF mediated solely by the N-terminal domain may not be disrupted in the *Carf* exon 8 deleted mice, we anticipate that these mice are null for the nuclear and transcriptional functions of CaRF.

To validate that *Carf*- KO mice lack functional nuclear CaRF protein, we first isolated nuclear extracts from the brains of *Carf* WT or KO mice and assayed for CaRF expression by Western blotting with a polyclonal antiserum raised against purified recombinant full-length mouse CaRF. Four immunoreactive bands ranging in size from 85-100kD are seen in nuclear extracts from WT mice and these are selectively lost in extracts from the KO mice, suggesting that all four protein species are encoded by the *Carf* locus (**Fig. 21A**). Although the specific molecular nature of these multiple CaRF variants is not known, they may represent products of alternatively spliced *Carf*

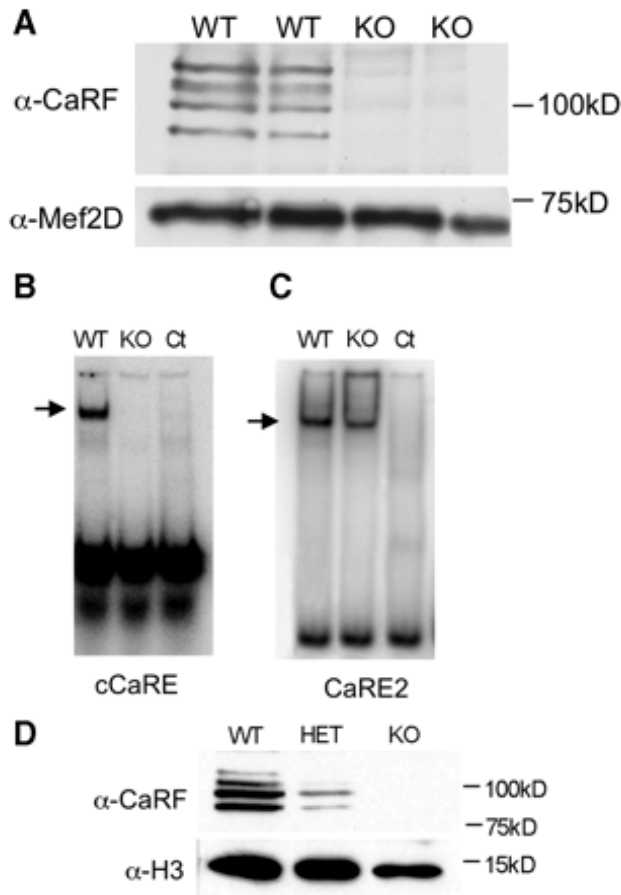


Figure 21: *Carf* exon 8 KO mice lack nuclear CaRF protein and CaRF-dependent transcription. (a) Western blot of nuclear extracts from brains of *Carf* WT and *Carf* KO mice. 10 μ g nuclear extract was separated by SDS-PAGE and transferred to PVDF membrane for probing with antibodies against CaRF and the neuronal transcription factor MEF2D. Four immunoreactive bands spanning from 85-100kD are seen in the WT lanes and absent in the KO lanes. MEF2D is shown as a loading control. (b-c) EMSA with nuclear extracts from neurons of *Carf* WT and KO mice. 1 μ g nuclear extract was incubated with 50fmol ³²P labeled DNA probes containing either (b) a high-affinity consensus CaRF-binding element (cCaRE) or (c) a USF1/2 binding element from the *Bdnf* gene (CaRE2) (Chen et al., 2003). The specificity of slowly migrating bands was determined by competition of the complex with a 100-fold molar excess of unlabeled probe (Ct). Specific retarded bands are marked with an arrow. (d) Western blot of CaRF expression in cultured embryonic fibroblasts from *Carf* WT, HET, and KO mice. 10 μ g nuclear extract was separated by SDS-PAGE and transferred to PVDF for probing with antibodies against CaRF. Histone H3 is shown as a loading control.

transcripts or differentially post-translationally modified CaRF proteins. Because CaRF is a sequence-specific DNA binding protein, we next asked whether *Carf* KO mice retain any binding activity for a DNA probe containing a high-affinity CaRF binding sequence (**Suppl. Table S1**, A.E. West, unpublished data). When a radiolabeled DNA probe containing the consensus CaRF binding site is incubated with nuclear extracts from *Carf* WT mice and separated on a nondenaturing gel in an electrophoretic mobility shift assay (EMSA), a slowly migrating band is visible, indicating the association with a binding protein (**Fig. 21B**). By contrast, no slowly migrating bands are observed when the probe is incubated with nuclear extracts from *Carf* KO brains, demonstrating that these mutants lack all CaRF-like binding activity. As a control for preparation of the nuclear extracts, we show that both WT and *Carf* KO nuclear extracts display similar amounts of binding activity for a DNA probe with binding sites for the USF family of transcription factors (Chen et al., 2003) (**Fig. 21C**).

Finally, to quantify the effects of *Carf* exon 8 deletion on CaRF-dependent transcription, we transfected primary embryonic fibroblasts from CaRF WT, HET or KO mice with a CaRF-dependent firefly luciferase reporter plasmid. *Carf* HET cells express $42\pm 7\%$ as much *Carf* mRNA as WT cells and show a corresponding reduction in CaRF protein (**Fig. 21D**). When normalized to a cotransfected control TK-renilla luciferase plasmid in order to scale CaRF-dependent expression in each cell line, HET cells show only $33.6\pm 12\%$ of the CaRF-dependent gene expression seen in WT cells, indicating that the loss of CaRF protein we detect is accompanied by a corresponding decrease in CaRF-dependent gene expression. These data demonstrate that our *Carf* KO mouse lacks both nuclear CaRF protein and CaRF-binding site dependent transcription, suggesting that

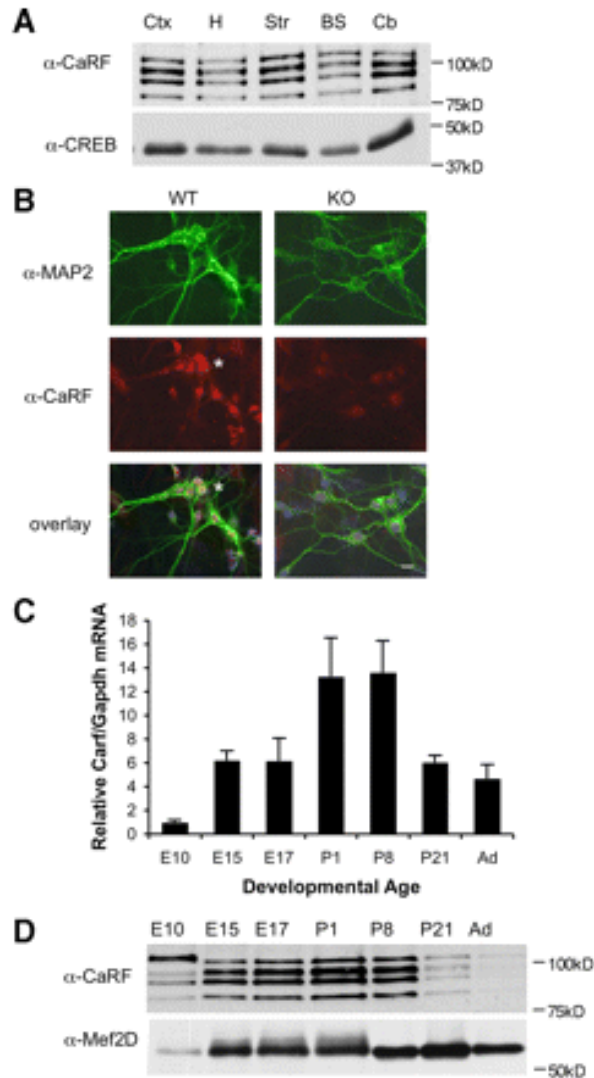


Figure 22: Distribution and developmental regulation of CaRF in the CNS. (a) Western blot of CaRF expression in nuclear extracts from adult brain regions. 10 μ g nuclear extract was loaded for each region. Ctx, cortex; H, hippocampus; Str, striatum; BS, brainstem; Cb, cerebellum. CREB is shown as a control for comparison. (b) Double immunostaining of cortical neuron cultures for CaRF and the neuronal marker MAP2. P0+10DIV *Carf* WT or KO neurons on PDL-coated coverslips were incubated with antibodies against CaRF (red) and MAP2 (green). Nuclei were labeled with Hoeschst in blue. Bright CaRF immunoreactivity is visible in the nuclei of MAP2 positive cells (example marked with white asterisks) in WT cultures, but is not present in KO cultures. (c) *Carf* mRNA expression from brain at different developmental ages. E10, E15, E17, embryonic days; P1, P8, P21, postnatal days; Ad, adult. Expression was normalized to the housekeeping gene *Gapdh* and is depicted as fold change relative to expression at E10. (d) Western blot of CaRF protein expression in whole brain nuclear extracts harvested at different developmental ages. 10 μ g nuclear extract was loaded into each lane. MEF2D is shown for comparison.

these mutants will be useful for investigating the biological functions of CaRF-dependent transcription.

A.4.2 CaRF expression in the CNS

We were able to use the *Carf* KO mice to validate our CaRF-specific antibody (**Fig. 21A**), therefore we first sought to establish the distribution of CaRF protein expression in the CNS. In the adult brain, CaRF immunoreactivity is present at similar levels in nuclear extracts from all regions surveyed including cortex, hippocampus, striatum, brainstem and cerebellum (**Fig. 22A**). Because these extracts do not allow us to distinguish whether CaRF is expressed in neurons, glia, or both, we dissociated embryonic mouse brains and cultured the cells under conditions that yield highly enriched populations of either neurons or glial cells. Although *Carf* mRNA and CaRF protein (data not shown) are detectable under both culture conditions, *Carf* mRNA is expressed at significantly higher levels in neuronally-enriched cultures compared with glia (neurons = $100 \pm 15\%$, glia = $26 \pm 5\%$, $p=0.003$). To confirm that CaRF protein is expressed in neurons, we made cortical cultures from P0 brains of *Carf* WT or KO mice and performed double immunostaining for CaRF and the neuronal marker protein MAP2 (**Fig. 22B**). MAP2-expressing cells show intense nuclear CaRF immunoreactivity that is absent from MAP2-positive cells in the *Carf* KO cultures, further validating the nuclear localization and expression of CaRF in neurons.

Finally, to determine whether expression of CaRF changes during development, we harvested both RNA and nuclear extracts from mouse cortex at a series of time-points across embryonic and postnatal development. Intriguingly, we found that CaRF expression changes significantly across developmental time, reaching its highest levels in

the first two weeks after birth. Expression of CaRF then declines, although it persists at levels well above detection threshold into adulthood (**Fig. 22C,D**). Overall these expression data support a role for CaRF in CNS neurons, and they suggest that CaRF may be of particular importance during early postnatal development.

A.4.3 Brain-region selective role for CaRF in regulation of *Bdnf* expression

CaRF was first identified as a transcription factor based on its affinity for a neuronal- and calcium-selective response element (CaRE1) in promoter IV of the *Bdnf* gene (Tao et al., 2002). Consistent with the *in vitro* evidence that CaRF can act as a CaRE1-dependent transcriptional activator of *Bdnf* promoter IV, we found that *Bdnf* exon IV levels were significantly reduced in the cortex of postnatal KO mice compared with their WT littermates (WT $100 \pm 8\%$, KO $68 \pm 9\%$; **Fig. 23A**) confirming a requirement for CaRF in the regulation of *Bdnf* expression *in vivo*. To determine whether CaRF contributes to changes in transcription driven by the activation of intracellular calcium signaling pathways, we measured *Bdnf* exon IV mRNA expression in P0 cortical cultures either in the presence of tetrodotoxin (TTX), which blocks action potential firing and evoked synaptic activity, or following membrane depolarization induced by the elevation of extracellular potassium (KCl), which opens L-type voltage-gated calcium channels. In the presence of TTX, *Bdnf* exon IV levels were significantly reduced in KO compared with WT cultures (WT $100 \pm 18\%$, KO $68 \pm 10\%$, **Fig. 23A**). Because the CaRE1 element is required for the induction of neuronal activity-dependent transcription from *Bdnf* promoter IV following KCl-induced membrane depolarization (Tao et al., 2002), we anticipated that CaRF might be required for *Bdnf* transcription induced by this stimulus.

However we were surprised to find that in response to acute membrane depolarization, *Bdnf* exon IV expression was strongly induced in both *Carf* WT and KO neurons with a similar magnitude and timecourse (**Fig. 23B**). Overall, these data further support a role for CaRF in transcriptional regulation of *Bdnf* promoter IV. However they suggest that the requirement is stimulus-specific and demonstrate that CaRF is dispensable for induction of *Bdnf* exon IV expression following acute membrane depolarization of cultured neurons.

Transcription of the *Bdnf* gene is complex; this locus contains at least eight promoters that are differentially regulated by distinct complexes of transcription factors (Aid et al., 2007; West, 2008). To determine whether *Carf* KO mice show a selective disruption of *Bdnf* transcripts arising from transcription initiated at promoter IV, where CaRF is hypothesized to be bound, we examined the expression of the four most highly expressed *Bdnf* splice variants (Exon I, II, IV, and VI-containing *Bdnf* mRNAs) (Timmusk et al., 1993; Aid et al., 2007) in samples from the cerebral cortex of adult *Carf* WT and KO mice. *Bdnf* exon IV expression was significantly reduced in samples from the cerebral cortex of adult KO mice compared with WT mice (WT $100 \pm 5\%$, KO $76.6 \pm 4\%$; **Fig. 23C**) indicating that CaRF continues to contribute to *Bdnf* regulation in these neurons under conditions of ongoing synaptic activity *in vivo*. By contrast, we found no differences in expression of exon I-, II-, or VI-containing *Bdnf* transcripts between *Carf* WT and KO mice, indicating that the effects of the *Carf* KO on *Bdnf* mRNA expression are exon IV specific (**Fig. 23C**). These data are consistent with the hypothesis that CaRF is a direct activator of *Bdnf* promoter IV-dependent transcription in cortical neurons. Interestingly, when we measured *Bdnf* exon IV expression in the hippocampus, we found

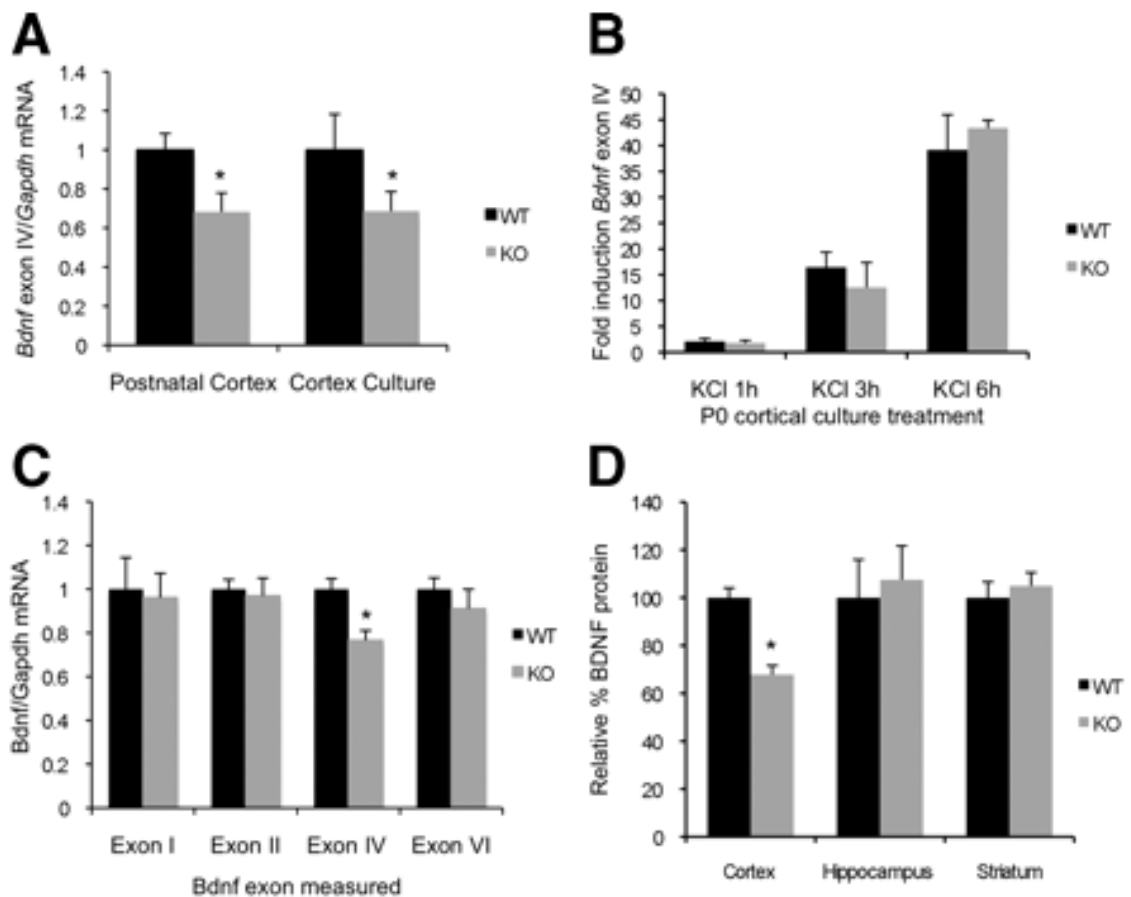


Figure 23: Expression of *Bdnf* exon IV and BDNF protein is reduced in *Carf* KO cortex. (a) *Bdnf* exon IV mRNA expression in cortex dissected from *Carf* WT and KO mice during the first 2 weeks of postnatal life or from P0 cortex cultures that were made from individual WT or KO siblings of HET x HET crosses. Cultured neurons were treated with 1 μ M TTX overnight before mRNA harvesting. Gene expression is normalized to *Gapdh* to control for sample handling and results are scaled to the average value of the WT sample (WT average = 1). Postnatal cortex, $n=7$ WT and 6KO, P0 cortex culture $n=3$ WT and 4KO. (b) KCl-dependent induction of *Bdnf* exon IV expression in *Carf* WT and KO neurons cultured as in (a). Membrane depolarization was induced by addition of 55mM extracellular KCl for 1, 3, or 6 hours prior to mRNA harvesting. $n=2$ WT and 3KO at each time point. c) Expression of *Bdnf* exon I, II, IV, or VI-containing mRNA transcripts in cerebral cortex dissected from adult *Carf* WT and KO mice 2-6 months of age. $n=8$ WT and 10KO. D) BDNF protein expression in frontal cortex, hippocampus, or striatum dissected from adult *Carf* WT or KO mice. Results are scaled relative to the average WT level in each tissue (WT average = 100%). Frontal cortex, $n=8$ WT and 9KO; hippocampus $n=3$ WT and 3KO; striatum $n=7$ WT and 8KO. Bars show the mean and error bars show SEM. * $p<0.05$.

no significant difference between WT and KO mice (WT $100 \pm 6\%$, KO $113 \pm 11\%$; $n=3$ WT and 3 KO, $p=0.366$). Hence these data suggest that CaRF differentially contributes to expression of *Bdnf* in different brain regions.

Finally to determine if these changes in *Bdnf* exon IV mRNA levels result in reduced BDNF protein expression, we measured BDNF by ELISA in brain lysates taken from the frontal cortex, hippocampus, or striatum of adult *Carf* mice. Consistent with our mRNA results, we found that BDNF protein levels were significantly reduced in samples of frontal cortex from *Carf* KO mice compared with their WT siblings (WT $100 \pm 4\%$, KO $68 \pm 4\%$; **Fig. 23D**). However we found no differences in BDNF levels in samples from the hippocampus or striatum. In total these data demonstrate that CaRF contributes to region-, stimulus-, and exon-selective expression of *Bdnf* mRNA transcripts *in vivo*, and that CaRF is required for maintenance of normal BDNF protein levels in the frontal cortex of adult mice.

A.4.4 Altered GABAergic synaptic protein expression in *Carf* KO mice

Many activity regulated transcription factors contribute to the development and/or plasticity of synapses (Ramanan et al., 2005; Flavell et al., 2006; Lin et al., 2008). To determine whether mutation of *Carf* affects synapses, we first quantified expression of a panel of GABAergic and glutamatergic synaptic marker proteins by Western blotting in lysates from different regions of *Carf* WT and KO brains. No significant differences were found between WT and KO mice in the frontal cortex or hippocampus (data not shown). However Western blotting of striatal lysates revealed significantly increased expression in KO mice of three proteins that are concentrated at GABAergic synapses (**Fig. 24A,B**):

the presynaptic GABA synthesizing enzyme GAD-65 (1.8 fold increase in KO versus WT, $p=0.001$), and the postsynaptic GABA-A receptor $\beta 2/3$ (6.4 fold increase in KO versus WT, $p=0.0003$) and $\gamma 2$ subunits (2.8 fold increase in KO versus WT, $p=0.006$). By contrast we found no significant differences between genotypes in the expression of three proteins enriched at glutamatergic synapses: NR1 ($p=0.610$), SAPAP3 ($p=0.463$), and PSD-95 ($p=0.882$). Similarly there were no changes in expression of DARPP-32 ($p=0.290$), a signaling protein highly enriched in striatal medium spiny neurons; GAD-67 ($p=0.601$), a marker of GABAergic interneurons; or synaptophysin ($p=0.913$), an integral synaptic vesicle protein common to all synapses.

To determine whether this increase in the expression of GABAergic synaptic proteins is associated with an increase in the expression of these proteins at synapses, we performed immunohistochemistry on coronal brain sections through the ventral striatum of *Carf* WT and KO mice and quantified the intensities of immunolabeling at synaptic punctae (**Fig. 24C,D**). Consistent with our observations in cell lysates, the intensity of GAD-65 immunoreactivity was significantly increased at synaptic punctae in KO mice (WT = $1.51 \pm 0.23 \times 10^6$, KO = $2.45 \pm 0.36 \times 10^6$, $p=0.034$) while the intensity of synaptophysin immunoreactivity was unchanged between genotypes (WT = $15.33 \pm 1.589 \times 10^6$, KO = $14.59 \pm 1.026 \times 10^6$, $p=0.697$). We also observed an increase in the total number of GAD-65 expressing synaptic punctae in KO compared with WT mice (WT = 427 ± 50 , KO = 640 ± 79 , $p=0.031$). This result could indicate that *Carf* KO mice have an increased number of GABAergic synapses, or it could arise as a secondary consequence of the overall increased intensity of GAD-65 immunoreactivity, which may allow us to detect smaller punctae. Supporting this latter interpretation, no difference was observed

between genotypes in the total number of synapses as measured by counting punctae of synaptophysin immunoreactivity (WT = 2923 ± 171, KO = 2947 ± 111, $p=0.905$). Taken together these data reveal that expression of both pre- and post-synaptic components of GABAergic synapses are significantly upregulated in the striatum of *Carf* KO mice compared with their WT littermates.

A.4.5 Behavioral analyses of *Carf* KO mice

Although CaRF is expressed during embryogenesis and in multiple tissues (Tao et al., 2002), *Carf* WT, HET, and KO mice are born at the expected Mendelian frequencies (data not shown) indicating that this protein is not essential for early development. *Carf* KO mice are both viable and fertile, and brains of adult *Carf* KO mice appear grossly anatomically normal compared to their WT siblings (data not shown). To quantitatively assess a broad range of neurobehavioral phenotypes, two investigators blind to the genotypes of the mice evaluated *Carf* WT, HET, and KO mice using the SHIRPA phenotypic screen. This analysis can suggest the presence of neurological abnormalities by screening for defects in gait or posture, motor control and coordination in excitability and aggression, and changes in salivation, gross changes in sensory function, alterations lacrimation, piloerection, defecation, muscle tone and temperature. It also provides a gross measure of analgesia (Rogers et al., 1997). No notable differences were found on any measure in this screen across *Carf* genotypes (**Suppl. Table S2**). These data indicate that *Carf* KO mice have no gross physical, sensory, or motor deficits that would impact interpretation of their performance on more complex behavioral tasks.

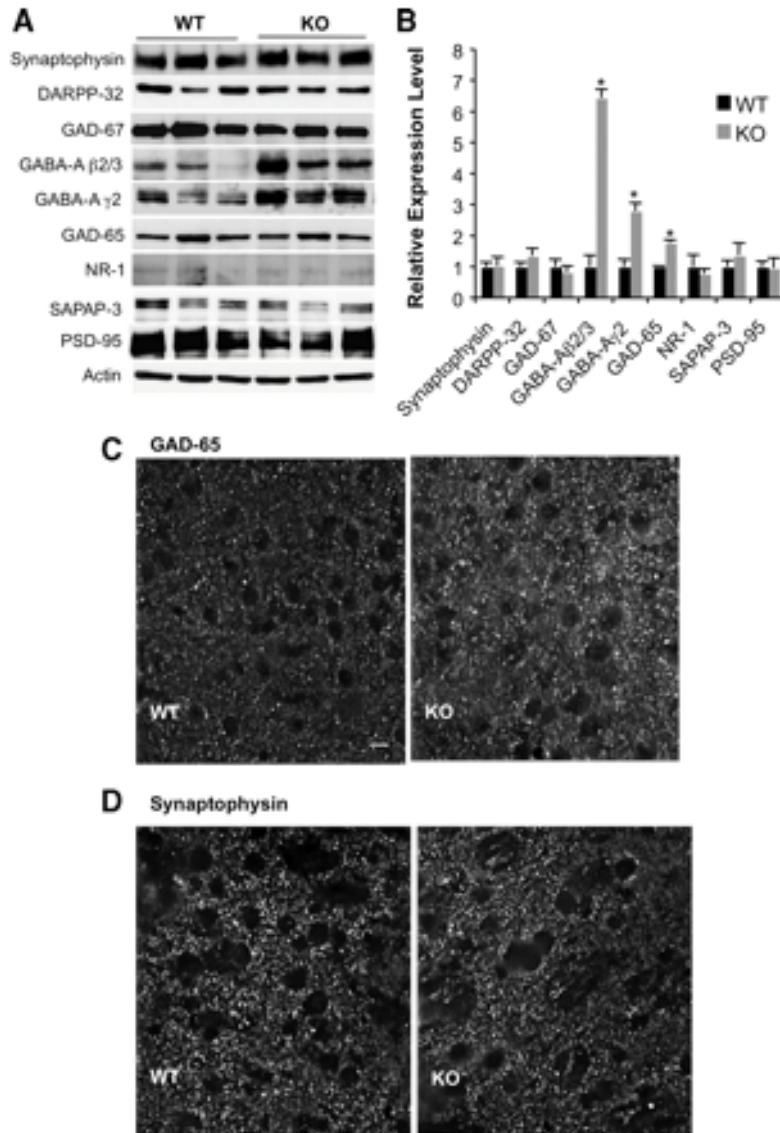


Figure 24: Increased expression of GABAergic synaptic proteins in the striatum of *Carf* KO mice. (a) Striata were freshly dissociated from coronal sections of 3 *Carf* WT (left three lanes) and 3 KO (right three lanes) adult mouse brains, then the samples were weighed and homogenized in Laemli SDS sample buffer. 20 μ g total lysate was used for immunoblotting with the indicated antibodies and immunoreactivities were visualized with ECL. (b) Quantification of the data shown in (a). WT samples are shown in black, KO in gray. Multiple film exposures were taken for each immunoblot and scanned, then band density in each lane was quantified using ImageJ. Expression was normalized to actin for each sample. (c) Representative images of GAD-65 immunostaining in coronal sections through the NAc of *Carf* WT or KO brains. Images were chosen that had integrated intensity values closest to the mean for each genotype. The bar shows 10 μ m. (d) Representative images of synaptophysin staining in coronal sections as in (c). Bars show the mean and error bars show SEM. * p <0.05 compared with WT.

Spatial learning and memory

Considerable evidence suggests that several aspects of learning and memory rely on the regulation of new gene transcription (Nguyen et al., 1994; Korzus et al., 2004; Ramanan et al., 2005). To test multiple distinct aspects of memory acquisition and retention, we trained *Carf* WT and KO mice on several cognitive tasks. First, to assess spatial learning and memory, we measured the performance of *Carf* WT, HET, and KO mice in the Morris water maze. Mice were trained over a period of 7 days, and their latencies to locate a hidden platform were recorded. During days 1-4 of training, all three genotypes learned to locate the hidden platform with similar reductions in mean escape latencies (**Fig. 25A**). This was confirmed by RMANOVA with a significant main effect of day ($F(3,117) = 21.55, p < 0.001$), while no significant day by genotype interaction was evident ($F < 1$). On day 5, mice were first given 3 training trials with extramaze cues, followed by one curtain trial that occluded all extramaze cues. A mean latency was recorded for the extramaze cue trials for each mouse. Only a single curtain trial was administered to discourage mice from changing to an alternate search strategy. A 2(trial type) by 3(genotype) mixed ANOVA revealed a significant main effect of trial type ($F(1, 39) = 58.38, p < 0.001$), confirming that when spatial cues were removed from the task arena on day 5, all three genotypes similarly increased their swim latencies to the platform (**Fig. 25B**). Thus, all mice were using spatial cues when navigating the maze.

To test the ability of the mice to remember the spatial location of the hidden platform after training, mice were administered an immediate and a 24-hour probe trial with the platform removed. Mice were allowed to swim freely for 60 sec and the amount of time spent searching each quadrant was assessed. For both the immediate and 24-hour

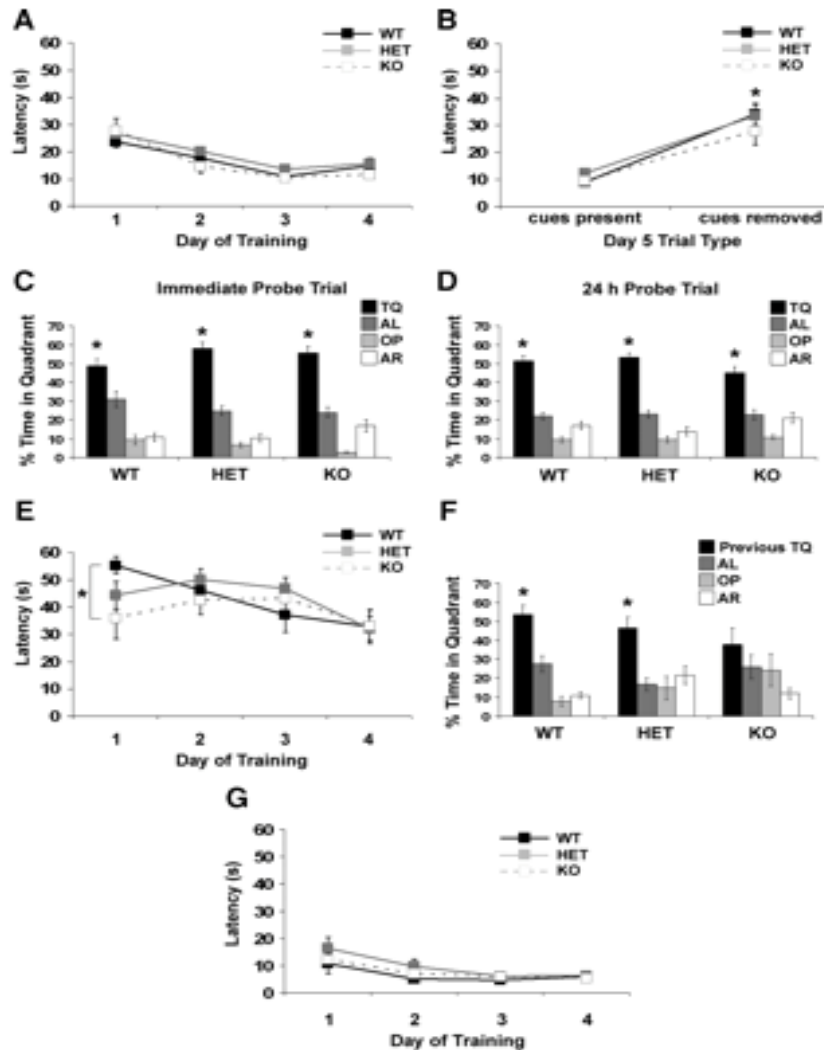


Figure 25: *Carf* KO mice show normal acquisition of hippocampal-dependent spatial learning and memory, and enhanced performance on a reversal learning task. (a) Mean latency to escape to a hidden platform is shown for *Carf* WT, HET, or KO mice over the first 4 consecutive training days. (b) Mean latency to escape to a hidden platform on day 5 of training is shown for *Carf* WT, HET and KO mice when spatial cues are visible (cues present) or when curtain has been pulled around the pool (cues removed). (c) Percent of total swimming time (60 seconds) spent in each quadrant of the pool when the platform was removed and mice were tested immediately after training. TQ, target quadrant (black); AL, adjacent right quadrant (dark gray); OP, opposite quadrant (light gray); AR, adjacent right quadrant (white). (d) Percent of total swimming time (60 seconds) spent in each quadrant of the pool when the platform was removed and mice were tested after a 24 hr retention interval. (e) Latency to escape to hidden platform during 4 daily trials of reversal learning over 4 days. (f) Percent time spent swimming in each quadrant of the pool on the first day of reversal learning with a new hidden platform location. Quadrants are labeled with respect to the position of the previous target quadrant (previous TQ, black). (g) Latency to escape to a visible platform over 4 days of training following reversal learning.

probe trials, separate RMANOVAs for each genotype revealed a main effect of quadrant for each genotype for each probe (WT: immediate, $F(3,27) = 25.08, p < 0.001$, 24-hr, $F(3,27) = 23.57, p < 0.001$; HET: immediate, $F(3,57) = 55.90, p < 0.001$, 24-hr, $F(3,57) = 74.88, p < 0.001$; KO: immediate, $F(3,33) = 68.68, p < 0.001$, 24-hr, $F(3,33) = 54.78, p < 0.001$). *Post-hoc* tests revealed that all three genotypes spent a significantly greater amount of time in the target quadrant compared to the other pool quadrants for both probe trials (all p s < 0.05 ; **Fig. 25C,D**), confirming that all mice had formed a spatial memory of the platform location.

To test the ability to learn a new spatial location, mice were given 4 trials of reversal learning in the water maze on Day 6. A 2-way mixed ANOVA revealed a main effect of trial where there was an overall decrease in latencies across trials 1-4 ($F(3, 117) = 5.05, p < 0.01$). However, inspection of the means revealed that KO mice did not progressively change latency over repeated trials, as was demonstrated by both WT and HET mice (**Fig. 25E**). Indeed, separate RMANOVAs revealed a significant effect of trial for WT mice ($F(3,27) = 5.37, p < 0.01$), and HET mice ($F(3,57) = 4.12, p < 0.01$), but not for KO mice ($F < 1$). Interestingly, KO mice also had significantly shorter latencies on the first trial than WT mice ($p < 0.05$) with WT mice taking, on average, nearly the entire 60 sec to locate the new platform for the first time. We therefore investigated the performance of mice on the first trial of reversal learning and examined how much time each mouse spent searching for the platform in each quadrant. Separate RMANOVAs for each genotype revealed a main effect of quadrant for WT mice ($F(3, 27) = 18.97, p < 0.001$), and HET mice ($F(3,57) = 7.10, p < 0.001$), whereas WT and HET mice spent significantly more time searching in the quadrant that held the previous platform location

(**Fig. 25F**). In contrast, there was no effect of quadrant for KO mice, suggesting that unlike WT and HET mice, KO mice did not persevere on the previously learned platform location while searching for the new platform location for the first time.

Finally, on Day 7 mice were tested on a visible platform version of the water maze task to ensure that all mice were capable of locating the platform and were motivated to escape the pool. All mice located the visible platform with comparable latencies to those of the spatial learning water maze task and all mice showed decreased latencies across trials 1-4 with the platform in a different locations on each trial (main effect of trial, $F(3,117) = 8.15, p < 0.001$; **Fig. 25G**).

These data indicate that the *Carf* KO and HET mice can learn and remember for at least 24 hrs the spatial location of a hidden platform in the water maze; they rely on extramaze spatial cues to guide their navigation; and they are as motivated to escape onto a platform in the water maze as are their WT littermates. *Carf* KO mice do, however, show a different pattern of searching behavior at the beginning of learning a new platform location, since compared to WT and HET mice, they do not initially persevere on the previously learned platform location.

Contextual fear conditioning and extinction

Similar to the use of the Morris water maze to test spatial learning and memory, contextual fear conditioning can be used to test distinct phases of acquiring, remembering and relearning emotional memories (Fanselow and Poulos, 2005). *Carf* WT and KO mice were conditioned on day 1, tested in contextual fear conditioning on day 2, tested in cued fear conditioning on day 3, and subjected to extinction on days 4-16. Percent time freezing (**Fig. 26**) was used as an index of emotional memory in the mice. Following the

CS-UCS pairing at conditioning, WT and KO mice exhibited similar levels of freezing on day 0, indicating that the genotypes had similar sensitivities to the foot-shock. In contextual testing, no genotype differences were discerned. Similarly, in cued testing, no differences were observed between WT and KO mice (data not shown), however, prior to presentation of the CS levels of freezing were significantly elevated above baseline, suggesting that the mice generalized the shock memory beyond the paired context. In contextual fear extinction, *Carf* KO mice did not as readily extinguish this response when compared to WT controls. RMANOVA for time spent freezing during the 14 days of context testing showed a marked within subjects effect for time, $F(13,221) = 31.033, p < 0.001$, indicating that freezing responses slowly attenuated over time. However, while the within subjects effects for the test day by genotype interaction was not significant, the non-linear quadratic trend for within subject contrasts for the test day by genotype interaction was significant ($F(1,17) = 7.656, p < 0.013$). In addition, the between subjects effects for genotype were also significant, $F(1,17) = 7.679, p < 0.019$. Bonferroni corrected pair-wise comparisons revealed that the KO animals showed higher levels of freezing on test days 4, 6, 7, 8, and 9 ($ps < 0.039$) compared to WT controls. To examine the pattern of extinction within each genotype, the level of freezing across days was analyzed relative to that observed on the first day of testing. Interestingly, both WT and *Carf* KO mice showed significant reductions on context test days 4 through 14 ($ps < 0.032$) relative to test day 1. Taken together these findings show that like their WT littermates, *Carf* KO mice can both learn and extinguish a conditioned fear response; however, the KOs show a significant delay in extinction learning.

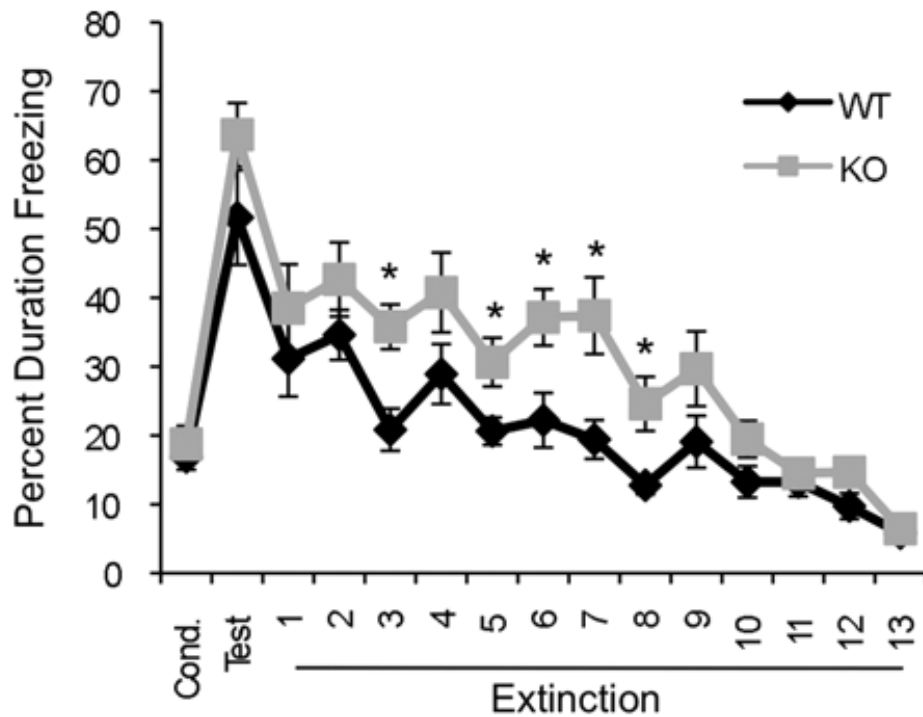


Figure 26: Impaired extinction of contextual fear conditioning in *Carf* KO mice. On day 0, 11 KO and 7 WT mice were shocked in a novel context (Cond.), and 24 hrs later context-cued retention of the fear memory was measured by returning the animals to the same context (Test). Extinction of fear conditioning was run over 13 consecutive days. The average percent of total time spent freezing over the 5 min test period is graphed for each day. Points indicate mean, and errors show S.E.M. * $p < 0.05$ for KO compared with WT on a given test day.

Novel object recognition

Finally we examined the *Carf* WT and KO mice for recognition memory in a novel object recognition task (Clark and Martin, 2005). In this test, mice are habituated in a single trial to a chamber with two identical objects. One of the familiar objects is then replaced with a novel object 30 min following training and preference for the novel object is assessed as an indicator of short-term memory. The animals are later examined at 24 hrs and 10 days for long-term and remote memory, respectively.

During adaptation to the arena, WT and KO mice demonstrated similar levels of exploration and locomotion (data not shown) and during object training on day 1, both WT and *Carf* KO similarly explored the two training objects (WT: 197.5 ± 17.5 interactions; 142.6 ± 22.1 sec; KO: 194.5 ± 19.8 interactions, 129.5 ± 17.8 sec). When examined for short-term memory, WT mice (**Fig. 27A**) showed a strong preference for the novel object during the first 3 min of testing, and this preference rapidly decreased over the final 6 min of testing. By comparison, the *Carf* KO mice showed little preference for the novel object during the first 6 min of testing, but in the final 3 min, exhibited a pronounced preference for the novel object. RMANOVA for the short term memory test did not reveal a significant within subjects effect for time, but did show a significant within subjects effect for the time by genotype interaction, $F(2,28) = 15.896$, $p < 0.001$. Bonferroni corrected pair-wise comparisons showed that in the WT mice had a greater preference for the novel object during the first 3 min of testing compared to KOs ($p < 0.007$) but that in the final 3 min of testing, it was the KO mice that had a stronger preference for the novel object relative to WT controls ($p < 0.001$). It is important to note that the 0-3 min preference score for WT and the 6-9 min preference score for KO mice did not differ from one another ($p = 0.844$), indicating there was no difference in the short-term recognition of the novel object by the *Carf* mutants relative to controls. Moreover, total time spent with the objects (**Suppl. Table S3**) and the frequency of interactions with the novel and familiar objects (**Suppl. Table S4**) did not reveal any differences as a function of genotype or time. These data provide further evidence that short-term memory is intact in the *Carf* mutants. During long term memory testing, WT and *Carf* KO mice (**Fig. 27B**) patterns of retention were similar during the first 6 min of testing,

with WT and KO mice showing low preference scores during the first 3 min of testing, and stronger preference scores during the 3-6 min interval. RMANOVA revealed a within subjects effect for time, $F(2,28) = 3.395$, $p < 0.050$, but no significant time by genotype interaction. The between- subject test for genotype also did not reveal any significant effects for long-term preference scores. With regards to total time spent with the two test objects during long term memory (**Suppl. Table S1**), no genotype differences were observed. These analyses indicate that long-term recall between the *Carf* WT and KO mice is similar.

Examination of remote memory in the mice was conducted after 10 days, at which time it is generally considered to be a test of cortical function (Frankland and Bontempi, 2005). During remote memory testing, KO mice showed a significant reduction in preference for the novel object relative to WT controls (**Fig. 27C**). Although a RMANOVA found no significant within subjects effect for time, the time by genotype interaction was statistically significant, $F(2,28) = 3.614$, $p < 0.040$. *Carf* WT and KO mice markedly differed in their preference for the novel object during the first 3 min of testing ($p < 0.048$), and KO mice also showed a marginal reduction in preference at the 4-6 min interval ($p < 0.064$). During the first 3 min of remote memory testing, no differences were found between WT and KO mice for the time spent with the objects (**Suppl. Table S1**). However, at the 4-6 and 7-9 min intervals, KOs spent more time with the objects compared to WT controls. Moreover, whereas WT mice reduced the time spent with objects during the final two intervals of testing compared to the first 3 min, this reduction was not observed among the *Carf* KO animals. Interactions with novel and familiar objects (**Suppl. Table S2**) also differed during this test for WT and mutants; controls had

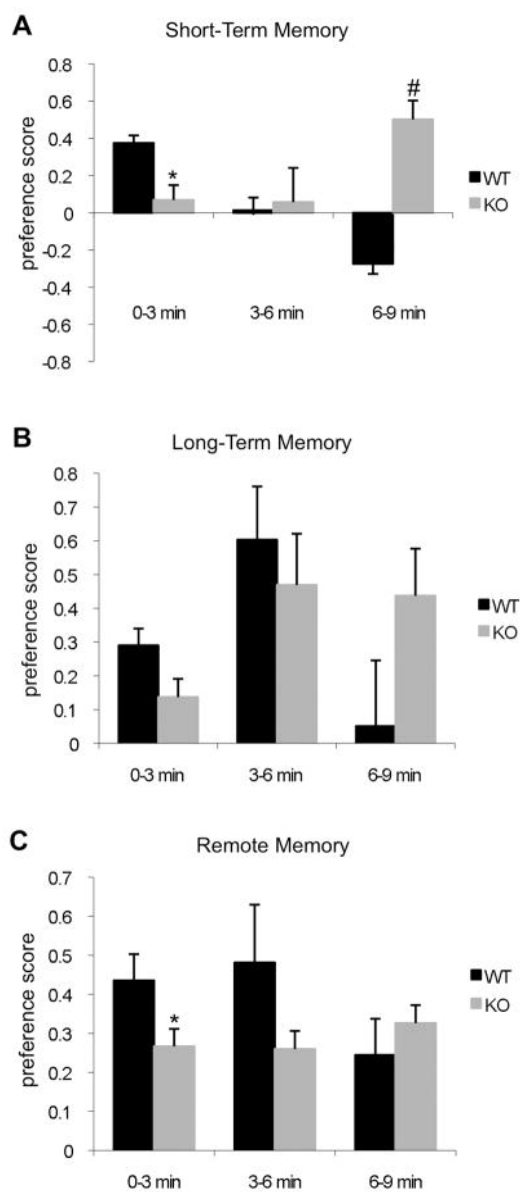


Figure 27: Impaired remote memory for novel object recognition in *Carf* KO mice. **a)** Preference for novel object when returned to the test arena 20 min after initial object exposure. **b)** Preference for novel object when returned to the test arena 24 hrs after initial object exposure. **c)** Preference for novel object when returned to the test arena 10 days after initial object exposure. Times of interaction and number of interactions are shown in **Suppl. Tables S3-S4**. Bars indicate mean, and errors show S.E.M. $n=11$ KO and 7 WT mice. * $p<0.05$ compared with WT at 0-3 min # $p<0.05$ compared with WT at 6-9 min.

more interactions with the novel compared to familiar object during each of the 3 test intervals, whereas KOs had the same rate of interaction for novel and familiar objects during the course of testing. Moreover, KO mice had more interactions with the familiar object than WT controls. These data indicate that *Carf* KO mice show impairment in remote object recognition relative to their WT littermate controls. Taken together, the results of the object recognition testing show that compared to WT controls, *Carf* KO mice have intact short-term and long-term memory, but are deficient in cortical-regulated remote memory.

A.5 DISCUSSION

CaRF-dependent regulation of BDNF expression

The identification of CaRF as a binding protein for the CaRE1 element in *Bdnf* promoter IV suggested that CaRF might be a physiologically relevant activator of *Bdnf* transcription (Tao et al., 2002). Consistent with this hypothesis, we now find that levels of *Bdnf* exon IV mRNA are significantly reduced in the cerebral cortex of *Carf* KO mice *in vivo* (**Fig. 23**). This disruption is selective for exon IV-containing *Bdnf* transcripts, supporting the hypothesis that association of CaRF with the CaRE1 element in promoter IV of the *Bdnf* gene directly enhances transcription from the exon IV start site. However we find that this requirement for CaRF is brain region selective, as *Carf* KO mice show normal levels of *Bdnf* mRNA in the hippocampus. This regional selectivity is not due to differential expression of CaRF, because we find CaRF protein expressed at similar levels in all of the brain regions we have tested. Our data also indicate that the requirement for CaRF is stimulus-selective. *Bdnf* exon IV mRNA levels are reduced in

Carf KOs under conditions of normal ongoing synaptic activity *in vivo* and following TTX-mediated blockade of evoked neurotransmission in cultured neurons. However CaRF is dispensable for activity-dependent upregulation of *Bdnf* exon IV in response to membrane depolarization in cultured neurons. These data were somewhat surprising because the CaRE1 element, which CaRF binds, is required for activity-dependent expression of *Bdnf* exon IV in response to membrane depolarization (Tao et al., 2002).

One possible explanation for the region- and stimulus-selective requirements for CaRF may be that additional CaRE1-binding proteins can serve as effectors of this element. Functional redundancy among transcription factors is common (Blendy et al., 1996; Chen et al., 2003) and distinct binding proteins may contribute to the function of CaRE1 in different cellular contexts. Importantly our data do not exclude the possibility that CaRF may contribute to stimulus-dependent *Bdnf* exon IV transcription under conditions other than those tested here. Membrane depolarization selectively activates gene expression through signaling pathways that are coupled to the opening of L-type voltage-gated calcium channels (Bading et al., 1993). By contrast, *Bdnf* exon IV transcription is activated by distinct intracellular signaling cascades following other kinds of stimuli such as synaptic NMDA-receptor activation (Zhang et al., 2007), BDNF-TrkB signaling (Xiong et al., 2002), and cocaine treatment (Liu et al., 2006) and these signaling cascades could converge on distinct sets of CaRE1-binding proteins. Understanding the basis for the selective requirement for CaRF in region- and stimulus-specific *Bdnf* expression will open new windows into the intricate regulation of this important neural gene.

Importantly, although BDNF is an attractive candidate to underlie the synaptic and

behavioral phenotypes of *Carf* KO mice, as a transcription factor, CaRF is likely to contribute to the expression of hundreds of gene products in addition to *Bdnf*. Using the anti-CaRF antibody developed here, we have recently performed chromatin immunoprecipitation followed by sequencing of coimmunoprecipitated genomic DNA (ChIP-Seq) to identify 176 sites of CaRF binding across the genome (West A.E., unpublished observations). Characterization of this CaRF regulon will be an essential step toward a fuller understanding of the molecular mechanisms underlying the phenotypes in *Carf* KO mice.

Roles for CaRF in GABAergic synapse development

GABA is the major inhibitory neurotransmitter in the adult CNS, and by regulating the temporal patterns of pyramidal neuron firing, GABAergic neurotransmission contributes to complex aspects of network computation and neural circuit function (Sohal et al., 2009). Expression of several GABA receptor subunits is subject to modulation by environmental stimuli, and interestingly, changes in GABAergic synaptic composition have been suggested to contribute to stimulus-induced behavioral plasticity. For example, expression of the GABA-A receptor $\beta 2$ and $\gamma 2$ subunits is increased in the amygdala coincident with extinction of fear conditioning (Heldt and Ressler, 2007), and neonatal maternal separation leads to persistent alterations in hippocampal GABA receptor subunit expression that are correlated with altered behavioral stress responses in adulthood (Hsu et al., 2003). We find that *Carf* KO mice have increased expression of three GABAergic synaptic proteins (GAD-65, GABA- $A\beta 2/3$ and GABA- $A\gamma 2$) in the striatum while the number of synapses and the expression of several glutamatergic synaptic proteins remain

unchanged (**Fig. 24**). GABA-A receptors are pentamers, and most are composed of combinations of two α subunits, two β subunits, and one γ or δ subunit (Jacob et al., 2008). Differential subunit composition confers distinct pharmacology and physiology upon GABA-A receptors, as well as regulating their subcellular distribution (Jacob et al., 2008). Thus it is possible that these changes in synaptic protein expression we detect could alter GABAergic neurotransmission in the striatum of *Carf* KO mice. Future studies that address when these synaptic changes first arise during development and what functional consequences these alterations have for neuronal physiology will significantly inform our understanding of how CaRF-dependent transcription may modulate neural circuit function.

Learning and memory changes in Carf KO mice

The Morris water maze is a robust spatial learning task commonly used to identify deficits in learning and memory in genetically altered mice (Vorhees and Williams, 2006). *Carf* KOs performed as well as their WT and HET littermates in both the acquisition and the memory phases of this task. However, on the first day of reversal training the KO mice were able to find the new location significantly faster than WT or HET mice. Reversal learning in the Morris water maze can suggest procedural and cognitive flexibility (Crawley, 2007). Alternately, it may suggest that *Carf* KO mice have a weaker memory trace than WT mice, because they did not persevere on the previously learned platform location. To begin to differentiate among these possibilities, we further assessed cognitive function in the *Carf* KOs using additional memory tests.

In the fear conditioning experiments, *Carf* KOs and WTs showed similar levels of

immobility on the first day they were returned to the shock-paired context, suggesting that the KOs can learn this association. However upon repeated exposure to the context, *Carf* KOs extinguished their freezing responses more slowly than their WT littermates. Fear extinction is not simply forgetting of the fear memory, rather it is an active relearning process that appears to require function of several brain regions (Myers and Davis, 2007). Although the increased freezing during extinction by the *Carf* KO mice could suggest amygdala dysfunction, preliminary data on a small set of *Carf* WT and KO mice indicate that fear potentiated startle, a test of amygdala function, does not differ (data not shown). This suggests that delayed extinction in the *Carf* KOs may be more attributable to deficits in the plasticity of this learned response, rather than over-activation of the amygdala during the experiencing of an emotional event.

Extinction of fear conditioning is induced when the CS (in this case the context) is repeatedly presented in the absence of the UCS (the shock) (Myers and Davis, 2007). For the new lack of association between the CS and the UCS to be learned during extinction training, it is necessary that the animal accurately remember the previous expected relationship between these two stimuli. Thus impaired extinction of fear conditioning could arise as a result of a weakened memory trace of the CS-UCS association that leads to generalization of fear responses. Consistent with the possibility that memory traces are less persistent in the *Carf* KO mice, we found that they had significantly impaired recognition of a novel object 10 days after training, even though their short- and long-term memory of the investigated object was not significantly different from that of WT mice. Interestingly, novel object recognition after 10 days in this test is thought to depend on transfer of the memory trace from the hippocampus to the cortex, as hippocampal

lesions 10 days after training fail to disrupt remote memory (Frankland and Bontempi, 2005). Furthermore, BDNF is among the molecular mediators that are thought to play an essential role in fear extinction, as several different genetic manipulations that reduce expression of BDNF have all been associated with delayed fear extinction (Gorski et al., 2003; Heldt et al., 2007; Soliman et al., 2010). Taken together, these data raise the possibility that disruption of cortical function in the *Carf* KO mice, perhaps due in part to reduced cortical BDNF expression, may contribute to abnormal memory retention in these animals.

A.6 REFERENCES

- Aid T, Kazantseva A, Piirsoo M, Palm K, Timmusk T (2007) Mouse and rat BDNF gene structure and expression revisited. *J Neurosci Res* 85:525-535.
- Angrand PO, Daigle N, van der Hoeven F, Scholer HR, Stewart AF (1999) Simplified generation of targeting constructs using ET recombination. *Nucleic Acids Res* 27:e16.
- Bading H, Ginty DD, Greenberg ME (1993) Regulation of gene expression in hippocampal neurons by distinct calcium signaling pathways. *Science* 260:181-186.
- Blendy JA, Kaestner KH, Schmid W, Gass P, Schutz G (1996) Targeting of the CREB gene leads to up-regulation of a novel CREB mRNA isoform. *EMBO J* 15:1098-1106.
- Chahrour M, Zoghbi HY (2007) The story of Rett syndrome: from clinic to neurobiology. *Neuron* 56:422-437.
- Chen WG, West AE, Tao X, Corfas G, Szentirmay M, Sawadogo M, Vinson C, Greenberg ME (2003) Upstream stimulatory factors are mediators of calcium-responsive transcription in neurons. *J Neurosci* 23:2572-2581.
- Crawley JN (2007) Mouse behavioral assays relevant to the symptoms of autism. *Brain Pathol* 17:448-459.
- Fanselow MS, Poulos AM (2005) The neuroscience of mammalian associative learning. *Annu Rev Psychol* 56:207-234.

- Farley FW, Soriano P, Steffen LS, Dymecki SM (2000) Widespread recombinase expression using FLPeR (flipper) mice. *Genesis* 28:106-110.
- Flavell SW, Cowan CW, Kim TK, Greer PL, Lin Y, Paradis S, Griffith EC, Hu LS, Chen C, Greenberg ME (2006) Activity-dependent regulation of MEF2 transcription factors suppresses excitatory synapse number. *Science* 311:1008-1012.
- Frankland PW, Bontempi B (2005) The organization of recent and remote memories. *Nat Rev Neurosci* 6:119-130.
- Gorski JA, Balogh SA, Wehner JM, Jones KR (2003) Learning deficits in forebrain-restricted brain-derived neurotrophic factor mutant mice. *Neuroscience* 121:341-354.
- Greer PL, Greenberg ME (2008) From synapse to nucleus: calcium-dependent gene transcription in the control of synapse development and function. *Neuron* 59:846-860.
- Heldt SA, Ressler KJ (2007) Training-induced changes in the expression of GABAA-associated genes in the amygdala after the acquisition and extinction of Pavlovian fear. *Eur J Neurosci* 26:3631-3644.
- Heldt SA, Stanek L, Chhatwal JP, Ressler KJ (2007) Hippocampus-specific deletion of BDNF in adult mice impairs spatial memory and extinction of aversive memories. *Mol Psychiatry* 12:656-670.
- Hong EJ, McCord AE, Greenberg ME (2008) A biological function for the neuronal activity-dependent component of *Bdnf* transcription in the development of cortical inhibition. *Neuron* 60:610-624.
- Hsu FC, Zhang GJ, Raol YS, Valentino RJ, Coulter DA, Brooks-Kayal AR (2003) Repeated neonatal handling with maternal separation permanently alters hippocampal GABAA receptors and behavioral stress responses. *Proc Natl Acad Sci U S A* 100:12213-12218.
- Jacob TC, Moss SJ, Jurd R (2008) GABA(A) receptor trafficking and its role in the dynamic modulation of neuronal inhibition. *Nat Rev Neurosci* 9:331-343.
- Korzus E, Rosenfeld MG, Mayford M (2004) CBP histone acetyltransferase activity is a critical component of memory consolidation. *Neuron* 42:961-972.
- Lakso M, Pichel JG, Gorman JR, Sauer B, Okamoto Y, Lee E, Alt FW, Westphal H (1996) Efficient in vivo manipulation of mouse genomic sequences at the zygote stage. *Proc Natl Acad Sci U S A* 93:5860-5865.
- Lin Y, Bloodgood BL, Hauser JL, Lapan AD, Koon AC, Kim TK, Hu LS, Malik AN, Greenberg ME (2008) Activity-dependent regulation of inhibitory synapse development by *Npas4*. *Nature* 455:1198-1204.

- Liu QR, Lu L, Zhu XG, Gong JP, Shaham Y, Uhl GR (2006) Rodent BDNF genes, novel promoters, novel splice variants, and regulation by cocaine. *Brain Res* 1067:1-12.
- Myers KM, Davis M (2007) Mechanisms of fear extinction. *Mol Psychiatry* 12:120-150.
- Nelson ED, Kavalali ET, Monteggia LM (2006) MeCP2-dependent transcriptional repression regulates excitatory neurotransmission. *Curr Biol* 16:710-716.
- Nguyen PV, Abel T, Kandel ER (1994) Requirement of a critical period of transcription for induction of a late phase of LTP. *Science* 265:1104-1107.
- Poo M-m (2001) Neurotrophins as synaptic modulators. *Nat Rev Neurosci* 2:1-9.
- Pulipparacharuvil S, Renthal W, Hale CF, Taniguchi M, Xiao G, Kumar A, Russo SJ, Sikder D, Dewey CM, Davis MM, Greengard P, Nairn AC, Nestler EJ, Cowan CW (2008) Cocaine regulates MEF2 to control synaptic and behavioral plasticity. *Neuron* 59:621-633.
- Ramanan N, Shen Y, Sarsfield S, Lemberger T, Schutz G, Linden DJ, Ginty DD (2005) SRF mediates activity-induced gene expression and synaptic plasticity but not neuronal viability. *Nat Neurosci* 8:759-767.
- Rodriguiz RM, Gadnidge K, Ragnauth A, Dorr N, Yanagisawa M, Wetsel WC, Devi LA (2007) Animals lacking endothelin-converting enzyme-2 are deficient in learning and memory. *Genes Brain Behav*
- Rogers DC, Fisher EM, Brown SD, Peters J, Hunter AJ, Martin JE (1997) Behavioral and functional analysis of mouse phenotype: SHIRPA, a proposed protocol for comprehensive phenotype assessment. *Mamm Genome* 8:711-713.
- Schmalzigaug R, Rodriguiz RM, Bonner PE, Davidson CE, Wetsel WC, Premont RT (2009) Impaired fear response in mice lacking GIT1. *Neurosci Lett* 458:79-83.
- Sohal VS, Zhang F, Yizhar O, Deisseroth K (2009) Parvalbumin neurons and gamma rhythms enhance cortical circuit performance. *Nature* 459:698-702.
- Soliman F, Glatt CE, Bath KG, Levita L, Jones RM, Pattwell SS, Jing D, Tottenham N, Amso D, Somerville L, Voss HU, Glover G, Ballon DJ, Liston C, Teslovich T, Van Kempen T, Lee FS, Casey BJ (2010) A Genetic Variant BDNF Polymorphism Alters Extinction Learning in Both Mouse and Human. *Science*
- Tao X, Finkbeiner S, Arnold DB, Shaywitz AJ, Greenberg ME (1998) Ca²⁺ influx regulates BDNF transcription by a CREB family transcription factor-dependent mechanism. *Neuron* 20:709-726.
- Tao X, West AE, Chen WG, Corfas G, Greenberg ME (2002) A calcium-responsive transcription factor, CaRF, that regulates neuronal activity-dependent expression of BDNF. *Neuron* 33:383-395.

- Timmusk T, Palm K, Metsis M, Reintam T, Paalme V, Saarma M, Persson H (1993) Multiple promoters direct tissue-specific expression of the rat BDNF gene. *Neuron* 10:475-489.
- Tropea D, Giacometti E, Wilson NR, Beard C, McCurry C, Fu DD, Flannery R, Jaenisch R, Sur M (2009) Partial reversal of Rett Syndrome-like symptoms in MeCP2 mutant mice. *Proc Natl Acad Sci U S A* 106:2029-2034.
- Vorhees CV, Williams MT (2006) Morris water maze: procedures for assessing spatial and related forms of learning and memory. *Nat Protoc* 1:848-858.
- West AE (2008) Activity-Dependent Regulation of Brain-derived neurotrophic factor Transcription. In: *Transcriptional Regulation by Neuronal Activity* (Dukek S, ed), pp 155-174. New York, NY: Springer.
- West AE, Griffith EC, Greenberg ME (2002) Regulation of transcription factors by neuronal activity. *Nat Rev Neurosci* 3:921-931.
- Xiong H, Futamura T, Jourdi H, Zhou H, Takei N, Diverse-Pierluissi M, Plevy S, Nawa H (2002) Neurotrophins induce BDNF expression through the glutamate receptor pathway in neocortical neurons. *Neuropharmacology* 42:903-912.
- Xu J (2005) Preparation, culture, and immortalization of mouse embryonic fibroblasts. *Current protocols in Molecular Biology*:28.21.21-28.21.28.
- Zhang SJ, Steijaert MN, Lau D, Schutz G, Delucinge-Vivier C, Descombes P, Bading H (2007) Decoding NMDA receptor signaling: identification of genomic programs specifying neuronal survival and death. *Neuron* 53:549-562.
- Zhou Z, Hong EJ, Cohen S, Zhao WN, Ho HY, Schmidt L, Chen WG, Lin Y, Savner E, Griffith EC, Hu L, Steen JA, Weitz CJ, Greenberg ME (2006) Brain-specific phosphorylation of MeCP2 regulates activity-dependent Bdnf transcription, dendritic growth, and spine maturation. *Neuron* 52:255-269.

APPENDIX B: TRANSCRIPTIONAL REGULATORS THAT MEDIATE NEURAL AND BEHAVIORAL ADAPTATIONS TO PSYCHOSTIMULANTS

B.1 SUMMARY

Repeated exposure to drugs of abuse drives persistent changes in behavior that can lead to the devastating personal and social consequences of drug addiction. Considerable evidence suggests that drug-induced changes in gene expression are essential for the long-lasting alterations in striatal neuron function that underlie many of these behavioral adaptations. A growing number of transcriptional regulators have been implicated in the cellular response to drugs of abuse, including both sequence-specific DNA binding transcription factors as well as chromatin regulatory proteins that impact gene transcription by altering chromatin structure. Here we review the evidence for the set of transcriptional regulators that are targets of regulation by psychostimulants *in vivo*, and we discuss the importance of developing a framework for understanding how the functions of multiple transcriptional pathways are integrated to generate the net response to drugs of abuse.

B.2 INTRODUCTION

Activation of monoaminergic receptors is essential to the mechanism by which drugs of abuse exert long-lasting changes in behavior (Capper-Loup et al., 2002; Laakso et al., 2002; Xu et al., 1994). Psychostimulants (i.e. amphetamine and cocaine) bind directly to the dopamine (DA), serotonin (5-HT), and norepinephrine (NE) transporters and increase extracellular levels of these monoamines. However despite the fact that these drugs rapidly increase monoaminergic transmission, repeated exposure over long periods of time is necessary to produce persistent alterations in behavior (Hyman et al.,

2006). Therefore, it is likely that molecular mechanisms downstream of chronic monoaminergic transmission mediate the observed behavioral adaptations.

Regulation of gene transcription offers a compelling mechanism to mediate stable changes in cell function (Nestler, 2001). The first evidence that new gene transcription might be part of the cellular response to psychostimulants was the observation that expression of the immediate early gene (IEG) *Fos* was rapidly induced in striatal neurons following cocaine or amphetamine treatment (Graybiel et al., 1990; Young et al., 1991). More recently, gene expression profiling studies have revealed that both acute and chronic exposure to psychostimulants differentially regulate expression of a large set of gene products (Heiman et al., 2008; Maze et al., 2010; McClung and Nestler, 2003; Yuferov et al., 2003). Importantly in addition to the traditional transcription factor IEGs, these studies have identified psychostimulant-dependent genes whose products function at synapses, in signaling pathways, and in the control of neuronal excitability, suggesting new ideas about how regulation of gene transcription might modulate striatal function.

To determine how psychostimulant-induced DA receptor signaling leads to changes in gene expression, investigators have searched for the transcriptional regulators that are targets of modulation by DA. As discussed in the first section below, the majority of these studies have addressed roles for sequence-specific DNA binding transcription factors in both cellular and behavioral adaptations to drug exposure. However as recent data have implicated chromatin regulatory mechanisms in the long-lasting changes of gene expression induced by environmental stimuli, in the second section we review the evidence for psychostimulant-dependent regulation of histone modifying enzymes and effectors of DNA methylation. Throughout this review our focus will be on acute and

chronic psychostimulant-mediated regulation of transcription in the striatum, as this reflects the most commonly used experimental paradigm and thus will allow us to compare studies of different transcriptional regulators. The similarities and differences in the activation and importance of the transcriptional pathways discussed here in other brain regions (ventral tegmental area, prefrontal cortex, locus coeruleus), by alternative drug exposure paradigms (binge, self-administration), and by other drugs of abuse (nicotine, opiates, alcohol) is an important topic for discussion elsewhere.

B.3 SEQUENCE-SPECIFIC DNA-BINDING TRANSCRIPTION FACTORS

Environmental stimuli regulate transcription factor function by two primary mechanisms. For transcription factors that are constitutively expressed, activity is modulated by stimulus-induced posttranslational modifications that change protein-protein interactions or nuclear localization. Alternatively, transcription factor function can be regulated by stimuli that alter the expression of the factor. Very rapid changes in transcription factor function by necessity use the first mechanism, whereas slower secondary responses to stimuli primarily utilize the second. Importantly, alterations in transcription factor expression are often mediated by the action of constitutively expressed stimulus-regulated factors, defining an important point of interaction between these two distinct modes of regulated transcription.

B.3.1 Cyclic-AMP Response Element Binding Protein (CREB)

CREB is a member of the bZIP domain family of transcription factors (Lonze and Ginty, 2002). CREB is a nuclear protein that binds DNA either as a homodimer or as a

heterodimer with the closely related bZIP factors CREM and ATF1. As its name implies, CREB was first studied for its role in mediating cAMP-dependent changes in gene expression following hormone stimulation of neuroendocrine cells via its association with the cAMP response element (CRE) (Montminy and Bilezikjian, 1987). cAMP signaling induces activation of CREB via PKA-dependent phosphorylation of CREB serine 133 (Ser133)(Gonzalez and Montminy, 1989) (**Fig. 28**). To date, all stimuli that activate CREB-dependent transcription (e.g. receptor tyrosine kinases, calcium signaling pathways, etc) require induced phosphorylation at this residue, although distinct Ser133 kinases including CaMKIV, MAPK, and Akt mediate phosphorylation in response to different stimuli (Mayr and Montminy, 2001). Phosphorylation of CREB at Ser133 induces its association with the transcriptional coactivator CREB Binding Protein (CBP) (Chrivia et al., 1993). CBP promotes transcription both by physically connecting sequence specific DNA binding proteins such as CREB to components of the basal transcription machinery, as well as by acting as a histone acetyltransferase, as described in the *Chromatin* section below (Goodman and Smolik, 2000).

Amphetamine treatment drives rapid induction of CREB Ser133 phosphorylation in neurons of the Nucleus Accumbens (NAc) in a DA D1 receptor-dependent manner, which suggested that psychostimulants could modulate CREB-dependent programs of transcription (Konradi et al., 1994). Consistent with this possibility, amphetamine induces β -gal expression in the NAc of a CRE-LacZ reporter mouse following both acute and chronic treatment with this drug (Shaw-Lutchman et al., 2003). Although the endogenous gene targets of psychostimulant-activated CREB in striatal neurons are not fully known, long-term transgenic overexpression of CREB in adult mice was shown to be sufficient to

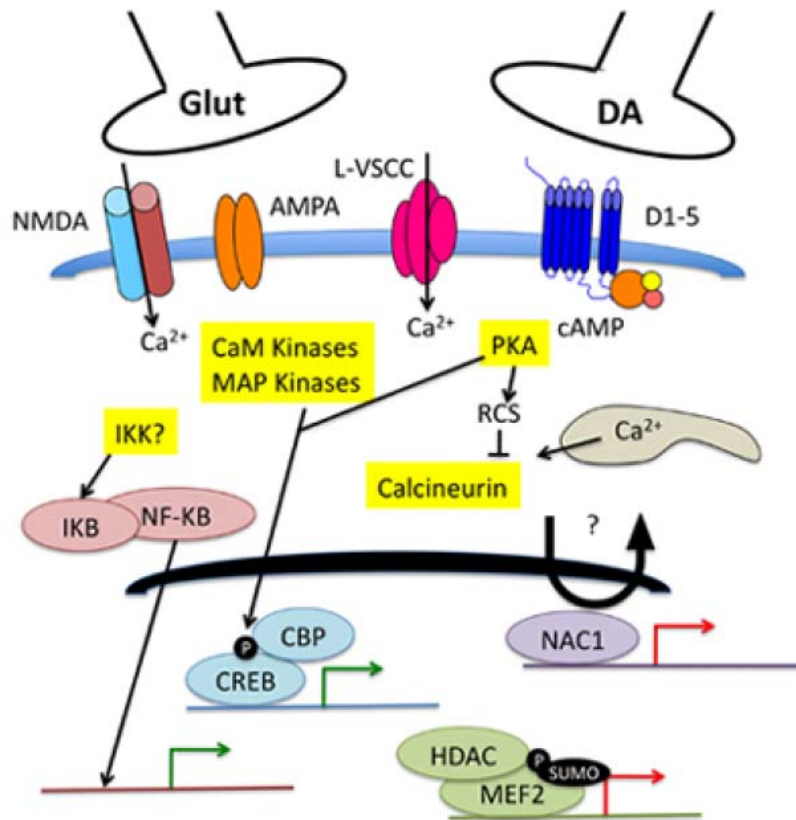


Figure 28: Modulation of transcriptional regulatory pathways by psychostimulant-induced intracellular signaling cascades. Psychostimulants block and/or reverse the dopamine (DA) transporter, leading to an elevation of extracellular DA in the synaptic cleft that activates DA receptors (D1-5). NAc neurons also receive glutamatergic synaptic inputs (Glut) from the prefrontal cortex that activate the AMPA and NMDA-type glutamate receptors. Subsequent membrane depolarization leads the opening of voltage-sensitive calcium channels (L-VSCCs). Calcium (Ca^{2+}) levels may also be elevated by the release of calcium from intracellular stores. The activation of G-protein coupled and calcium-dependent signaling cascades leads to the activation or repression of the kinases and phosphatases shown in yellow. These enzymes regulate phosphorylation of transcription factors or transcription factor associated proteins to modulate the activation of transcriptional pathways. Some transcription factors are regulated by nuclear localization (NF- κ B, NAC1) while others are regulated by posttranslational modifications that alter their association with transcriptional co-regulators (CREB, MEF2). These changes lead to psychostimulant dependent activation (green arrow) or repression (red arrow) of target gene expression.

drive the expression of over 100 genes, most of which were repressed when a similar strategy was used to overexpress mCREB (McClung and Nestler, 2003). In addition to well-known CREB targets such as *Bdnf*, *Fos*, and *Sst* (somatostatin), CREB has also been shown to regulate the striatal expression of the behaviorally relevant neuropeptides *Penk* (proenkephalin) and *Pdyn* (prodynorphin) (Carlezon et al., 1998; Cole et al., 1995), as well as a number of genes whose expression is regulated by psychostimulants (Bilbao et al., 2008; McClung and Nestler, 2003).

Because CREB is a target of regulation by cAMP signaling, which had been extensively linked with the cellular and behavioral consequences of psychostimulants (Missale et al., 1998; Self et al., 1998), this transcription factor was among the first to be genetically evaluated for its role in psychostimulant-regulated behaviors. Carlezon and colleagues addressed this question by using stereotactic injection of recombinant herpes simplex virus (HSV) to overexpress a mutant form of CREB (mCREB) in the NAc of rats (Carlezon et al., 1998). mCREB contains a single point mutation of CREB (Ser133Ala) that prevents phosphorylation at this site without altering the ability of CREB to bind to CRE sites in gene promoters. Hence mCREB acts in a dominant negative fashion to block CRE-dependent transcription. As a behavioral measure for the rewarding effects of cocaine, the authors studied cocaine-induced conditioned place preference (CPP), an associative conditioning task in which mice learn over the course of several days to associate one side of three chambered place conditioning apparatus with injection of cocaine or amphetamine. Following conditioning, wild type mice show a dose-dependent preference for the drug-paired side of the chamber. This dose-response curve was shifted to the left in mCREB-expressing mice, suggesting that the rewarding properties of

cocaine were *enhanced* when CREB-dependent transcription was impaired. Walters and colleagues reached a similar conclusion using a very different genetic approach, by studying cocaine-induced behaviors in mice bearing a hypomorphic mutation in the *Creb* gene (Walters and Blendy, 2001). Although these mice lack expression of two of the major isoforms of CREB, they retain expression of a shorter but active CREB isoform and have functionally compensatory upregulation of the CREB-family protein CREM (Blendy et al., 1996). The net result of this mutation is a significant reduction but not elimination of CRE binding activity in neurons. Similar to the effects of mCREB overexpression, the *Creb* hypomorph mice also showed a reduction in the dose of cocaine required to induce CPP. As a second measure of neural adaptations induced by psychostimulants the authors tested behavioral sensitization, in which repeated administration of psychostimulant drugs induces progressively enhanced locomotor activity that persists following drug withdrawal (Kalivas and Stewart, 1991). Consistent with the enhancement of CPP, the *Creb* hypomorphs showed enhanced sensitization of locomotor activity following repeated cocaine (Walters and Blendy, 2001). Taken together these data suggest that CREB activation functions in a homeostatic fashion to limit the behavioral response to psychostimulants. An analogous homeostatic role for CREB in the control of cAMP signaling in the locus coeruleus has been described during the development of opiate dependence (Lane-Ladd et al., 1997).

However a recent report of cocaine-induced behaviors in *Creb* null mice complicates this picture (Bilbao et al., 2008). Like the *Creb* hypomorphs, the null mutation in *Creb* does not eliminate CRE binding activity or CRE-dependent transcription because of functional redundancy with the closely related factor CREM. By

contrast genetic elimination of both *Crem* and *Creb* leads to neuronal degeneration over a period of weeks, suggesting that loss of both of these CREB family members is required to reduce CRE-dependent transcription to levels that can reveal biological requirements for the CREB family (Mantamadiotis et al., 2002). Surprisingly, in light of the results described above, *Camk2a-Cre* mediated deletion of *Creb* in the forebrain of a *Crem* null mouse had no effect on either CPP or locomotor sensitization to cocaine, even though mice bearing this mutation had severely reduced cocaine-dependent gene transcription in the striatum (Bilbao et al., 2008). One possibility is that the different outcomes of these studies may have arisen as a result of procedural differences, such as the age of the animals used when the studies were performed or the methods used for CPP. However genetic considerations limit the interpretations of each of these studies. Dominant negative overexpression of mCREB not only blocks CREB-dependent transcription, but it may also sequester transcriptional coregulatory complexes that are required for the function of CREB-independent pathways. The constitutive nature of the hypomorphic *Creb* mutation may alter brain development, and the upregulation of CREM in these animals could fundamentally alter the properties of CRE-dependent transcription. Finally although the *Camk2a-Cre* transgenic line used to recombine the floxed *Creb* allele significantly reduced overall CREB expression in striatum (Mantamadiotis et al., 2002), use of this promoter to drive Cre may leave CREB expression intact in some cell types, especially interneurons which express little CaMKIIalpha (Sik et al., 1998). More detailed analyses of the *Creb* hypomorphic and null strains may help to resolve some of the apparent conflicts. Alternatively new genetic models such as a recently reported

conditional *Creb* Ser133Ala knockin mouse strain (Wingate et al., 2009), may provide additional insights into the essential biological functions of CREB.

For CREB to play a role in drug-induced behaviors, activation or inhibition of CREB-dependent transcription might be expected to have an impact on the physiology of striatal neurons. To investigate this possibility, Dong and colleagues used viral vectors to overexpress either dominant negative (dnCREB, mCREB) or constitutively active (caCREB, CREB-VP16) versions of CREB in slice cultures of the NAc (Dong et al., 2006). These manipulations of CREB had no effect on passive membrane properties of striatal medium spiny neurons (MSNs) but they significantly altered intrinsic excitability, with caCREB increasing evoked action potential firing while dnCREB had the opposite effect. Current clamp recordings in the presence of a panel of ion channel blockers suggested that the effects of CREB are mediated by changes in both Na⁺ and K⁺ channel conductances that combine to produce the net effects on excitability. These results were somewhat unexpected, however, as previous studies of cocaine-regulated ionic conductances had predicted that cocaine, which induces CREB activity, would reduce MSN excitability (Zhang et al., 1998). Dong confirmed this prediction by demonstrating significantly reduced intrinsic excitability of MSNs in slice preparations made from animals that had received 3 days of cocaine exposure *in vivo* (Dong et al., 2006). However they also found that *in vivo* viral overexpression of caCREB not only prevented the cocaine-induced depression of excitability but further increased excitability above control levels. By contrast expression of dnCREB decreased excitability below that seen in cocaine-treated rats. These findings are consistent with the model suggested by the behavioral genetics in which CREB works to counteract the effects of cocaine. More

importantly these data also raised the possibility that changes in MSN excitability might underlie the behavioral responses to drugs of abuse. To directly test whether changes in MSN excitability are sufficient to alter cocaine-induced behaviors, Dong virally overexpressed the inwardly rectifying potassium channel Kir2.1 in NAc, as expression of this channel reliably depresses evoked action potential firing in MSNs in slice preparations *in vitro*. Although the rewarding properties of cocaine were not assessed following this manipulation, mice overexpressing Kir2.1 showed enhanced sensitivity to the locomotor stimulating effects of a single injection of cocaine, thus demonstrating that alterations in MSN excitability are sufficient to modulate at least some aspects of cocaine-induced behaviors.

As the most widely studied stimulus-regulated transcription factor in the central nervous system, CREB is too often used as a proxy for all regulated transcription pathways. However perhaps the most important contribution of the CREB studies reviewed here is the demonstration that regulation of any single transcriptional pathway cannot explain all of the cellular and behavioral adaptations to psychostimulants. In the simplest model, cocaine-dependent activation of CREB would sit atop of a cascade of events that eventually results in the adaptations measured by assays like behavioral sensitization and CPP. By contrast the evidence shows that activation of CREB limits cellular adaptations to cocaine and that persistent changes in behavior occur even in the absence of signaling through this transcriptional pathway. In the sections that follow we will begin to fill in the picture by reviewing the evidence for some of the other transcriptional players that work together with CREB to orchestrate the cellular response to psychostimulants.

B.3.2 Fos, FosB and ΔFosB

The Fos family of transcription factors is comprised of four members - *Fos*, *Fosb*, *Fosl1* (Fra1), and *Fosl2* (Fra2). Fos transcription factors dimerize with members of the Jun family to form activator protein 1 (AP-1) complexes that bind AP-1 elements in the regulatory regions of many genes (Herdegen and Leah, 1998). AP-1 activity is primarily regulated by inducible expression of the Fos and Jun family transcription factors. Induction of these genes is a cardinal feature of the Immediate-Early Gene (IEG) response to a wide variety of stimuli in many cell types (Morgan and Curran, 1991). Inducible transcription of Fos/Jun family proteins is mediated by the activation of stimulus-regulated transcription factors including CREB and the Serum Response Factor (SRF) (Herdegen and Leah, 1998). Expression of the AP-1 complex then regulates transcription of secondary response genes in a cell type and stimulus-specific manner depending on the differential recruitment of AP-1 complexes to distinct sets of gene promoters (Hill and Treisman, 1999).

Acute exposure to a single dose of cocaine or amphetamine leads to robust induction in the striatum of many of the Fos/Jun family members including *Fos*, *Fosb*, *Fosl2*, and *Junb* (Zhang et al., 2002). This induction is dependent on DA D1 receptor activation and occurs preferentially in both the D1 receptor- and Prodynorphin-expressing medium spiny neurons of the dorsal and ventral striatum as well as local GABAergic interneurons (Moratalla et al., 1996a; Moratalla et al., 1996b; Trevitt et al., 2005). In response to repeated cocaine exposure expression of these genes show time varying changes that are generally associated with desensitization of inducibility despite continued stimulus-dependent activation of the upstream signaling pathways (Hope et al.,

1992; Moratalla et al., 1996a). Recently the intriguing hypothesis has been raised that epigenetic mechanisms of chromatin regulation (as discussed in the *Chromatin* section below) may play a role in promoter desensitization of these IEGs (Renthal et al., 2008).

However a particularly interesting temporal pattern of regulation by chronic cocaine is observed for the short variant isoform of *Fosb*, known as Δ FosB. Alternative splicing of the *Fosb* gene leads to expression an mRNA that encodes the first 237 amino acids of FosB, including the full DNA binding domain, but then contains a premature stop coding thus preventing expression of the C-terminal domain of full-length FosB (Mumberg et al., 1991; Nakabeppu and Nathans, 1991). As a result of this deletion Δ FosB has a much longer half-life than other Fos family members (Hope et al., 1994). Whereas expression of other Fos/Jun family proteins is eliminated within 24 hours of their induction, Δ FosB expression persists. In response to repeated activation of the *Fosb* promoter by chronic cocaine treatment, Δ FosB protein progressively accumulates and eventually becomes the dominant Fos-like protein in striatal neurons (Hope et al., 1994).

Loss-of-function genetics present special challenges for the Fos family given the functional redundancy among family members and the widespread use of Fos upregulation as a general mechanism for stimulus-dependent transcriptional coupling. However across a range of different mouse models, multiple studies support the hypothesis that Fos family expression contributes to aspects of psychostimulant-regulated behaviors. For example, constitutive *Fosb* knockout mice show enhanced sensitivity to the locomotor stimulating effects of cocaine and a leftward dose-response shift for the induction of CPP (Hiroi et al., 1997). Recombination of a floxed *Fos* allele in DA D1 receptor expressing neurons has no effect on locomotor sensitivity to acute cocaine or on

the acquisition of CPP, however these mice show attenuated sensitization to repeated cocaine treatment and an impaired ability to extinguish CPP (Zhang et al., 2006). Finally, a third model used overexpression of an inducible dominant negative version of cJun (Δ cJun) in the striatum, which can dimerize with and inhibit the action of all Fos family members. These mice showed decreased development of cocaine-induced CPP but displayed normal locomotor sensitivity to acute cocaine treatment, and normal development of sensitization to repeated cocaine (Peakman et al., 2003). Interpreting what these results say about the distinct biological functions of Fos family members is beyond the scope of the current review, but these data are presented here to suggest that further understanding of Fos family function is relevant for dissecting the transcriptional contributions to psychostimulant-induced behaviors.

By contrast, a more approachable genetic strategy is to mimic the accumulation of Δ FosB expression that occurs with chronic cocaine. Kelz and colleagues generated bitransgenic mice in which Δ FosB could be selectively and inducibly overexpressed in D1-receptor expressing neurons (Kelz et al., 1999). A strain with expression of the tetracycline transactivator protein (tTA) under control of the neuron specific enolase (NSE) promoter was crossed to mice with a Δ FosB transgene under control of a tetracycline responsive promoter. An NSE-tTA line was chosen in which expression was restricted to the striatum, and 11 weeks after dox withdrawal, high levels of Δ FosB expression was observed in D1-receptor expressing neurons of the dorsal and ventral striatum. Mice overexpressing Δ FosB demonstrated enhanced sensitivity to the locomotor stimulating effects of cocaine but normal development of locomotor sensitization. They also showed a left shift in the dose-response sensitivity to the rewarding effects of

cocaine as measured by CPP (Kelz et al., 1999). Because this increased sensitivity to cocaine mimics some aspects of the behavioral responses to psychostimulants seen following chronic drug treatment, these data raise the possibility that Δ FosB expression could directly mediate the expression of these behaviors.

What cellular process might underlie the increase in cocaine sensitivity promoted by Δ FosB overexpression? One way to change behavioral responses to cocaine is modulate connectivity of the mesolimbocortical circuit. Overexpression of Δ FosB is associated with increased expression of the AMPA-type glutamate receptor GluR2 in striatal neurons, suggesting a mechanism to alter synaptic properties in these cells (Kelz et al., 1999). Furthermore, chronic cocaine has been shown to increase the density of dendritic spines on MSNs in the striatum, and this increase correlates with sensitized locomotor responses to cocaine and cocaine reward as measured by CPP (Robinson and Kolb, 1997). Dendritic spines are the primary sites of excitatory synapses on MSNs, thus these structural changes may represent changes in synaptic input. AAV-mediated overexpression of Δ FosB increased spine density independent of cocaine treatment (Maze et al., 2010), consistent with the possibility that this genetic manipulation could affect synapses. One Δ FosB target gene that may contribute to changes in spine density is the kinase Cdk5 (Norrholm et al., 2003). Like Δ FosB, Cdk5 levels rise following chronic cocaine and Cdk5 expression can be induced by Δ FosB overexpression (Bibb et al., 2001). How and whether altered spine density affects the function of MSNs and what impact this alteration may have on behavioral responses to drugs of abuse remains an active area of investigation.

B.3.3 Myocyte Enhancer Factor (MEF2)

The MEF2 family is defined by a conserved DNA binding and dimerization domain (the MADS box) that targets these factors to an A/T rich element in gene regulatory regions (McKinsey et al., 2002). These transcription factors were first identified for their role in muscle differentiation (Molkentin et al., 1995), however the four members of the MEF2 family (MEF2A-D) are expressed in many tissues and are found in distinct but overlapping patterns in neurons throughout the developing and adult CNS (Leifer et al., 1993; Lyons et al., 1995). Intriguingly, in neurons MEF2 family members have been found to regulate excitatory synapse number (Flavell et al., 2006; Shalizi et al., 2006), thus they are well-poised to be directly involved in changing the function of neural networks.

Although the expression of some MEF2 family members is subject to regulation by stimuli including psychostimulants (Renthal et al., 2009), in most neurons these transcription factors are constitutively expressed nuclear proteins. However the transcriptional activity of MEF2 is highly sensitive to regulation by a complex array of stimulus-dependent posttranslational modifications that modulate MEF2s interactions with multiple transcriptional cofactors (McKinsey et al., 2002; Shalizi et al., 2006). Depending on its protein-protein interactions, MEF2 can be either an activator or a repressor of transcription, and stimulus-induced signaling pathways converge on MEF2 to switch between these states. In its repressor state, class IIa histone deacetylases (HDACs, described in the *Chromatin* section below) bind to the N-terminal domain of the MEF2s and contribute to repression of MEF2's activity by promoting deacetylation and SUMOylation of Lys403 in MEF2's transactivation domain. Calcium signaling

pathways activate MEF2-dependent transcription by at least two mechanisms. First CaMK-dependent phosphorylation of the HDACs leads to their export from the nucleus. Second, calcium dependent activation of the phosphatase calcineurin leads to dephosphorylation of multiple Ser and Thr residues on MEF2. Dephosphorylation of Ser408 promotes a switch from SUMOylation to acetylation at Lys403 that promotes MEF2 activation and its association with coactivator proteins.

Given these mechanisms of MEF2 regulation, two lines of evidence raised the possibility that MEF2 activity might be actively repressed by psychostimulants. First one important MEF2 Ser408 kinases is Cdk5 (Gong et al., 2003), and as described above, Cdk5 is a target of Δ FosB whose expression is upregulated by chronic cocaine (Bibb et al., 2001). Second, DA D1-receptor has been shown to repress calcineurin activation via its effects on the Regulator of Calmodulin Signaling (RCS) (Rakhilin et al., 2004). PKA-dependent phosphorylation of RCS at Ser55 induces a direct interaction of pRCS with Ca^{2+} -calmodulin, leading to a competitive inhibition of calmodulin-regulated processes including the activation of calcineurin. Consistent with the importance of these pathways in MEF2 regulation, chronic but not acute exposure to cocaine induces MEF2 phosphorylation at Ser408 in neurons of the NAc that persists for at least 24 hours (Pulipparacharuvil et al., 2008). Thus these data raised the possibility that MEF2 could be a target of regulation by chronic cocaine.

To test the cellular and behavioral effects of modulating MEF2 activity *in vivo*, Pulipparacharuvil and colleagues used adeno-associated viruses (AAV) to express either shRNAs targeting MEF2A and D or a constitutively active form of MEF2 (MEF2-VP16) in the NAc (Pulipparacharuvil et al., 2008). Consistent with previous reports that

implicate transcriptional activity of MEF2 in excitatory synapse elimination, RNAi of MEF2 enhanced basal dendritic spine density of MSNs while expression of MEF2-VP16 blocked the ability of chronic cocaine to increase spine density. Because spine density rises with chronic cocaine, this structural plasticity had been suggested to be a positive mediator of the alterations in behavior that accompany chronic cocaine exposure (i.e. behavioral sensitization and CPP). However behavioral analysis of mice treated with the MEF2 shRNA virus showed reduced locomotor sensitization upon repeated cocaine treatment and reduced persistence of sensitization upon withdrawal. By contrast, MEF2-VP16 expressing mice showed very rapid induction of sensitization and enhanced CPP. Thus the effects of MEF2 activity on spine density are in direct opposition to their effects on behavior.

There are two important conclusions to be drawn from these results. First, these data suggest that cocaine-dependent regulation of MEF2 acts to limit behavioral responses to cocaine. However, whereas cocaine activates CREB it inactivates MEF2 to achieve the same overall effect on behavior (**Fig. 29**). Second these data show that changes in spine density can be dissociated from behavioral sensitivity to cocaine. There are many possible explanations for this outcome, which are too numerous to review here. However what is most important about these data is that they highlight the fact that the molecular and cellular bases of behavioral responses to cocaine remain surprisingly unknown. Studies like this one that discover new correlations between cellular processes and behavior while identifying coincident programs of gene expression have the potential to open new windows of understanding into this complex phenomenon.

B.3.4 Nuclear Factor κ B (NF- κ B)

NF- κ B refers to the activity of a set of five mammalian Rel-domain DNA binding subunits – RelA (p65), NF- κ B2 (p52/p100), NF- κ B1 (p50/p105), RelB, and c-Rel (Liou and Baltimore, 1993). In some cell types, most notably activated immune cells, NF- κ B activity is constitutive. However in other cell types NF- κ B is held in the cytosol in an

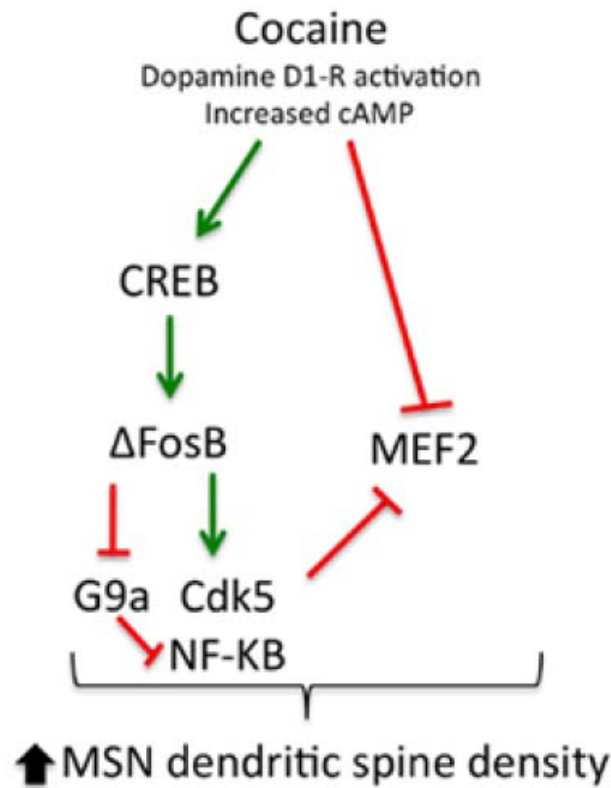


Figure 29: Transcriptional regulatory pathways that converge on enhancement of dendritic spine density. Activation is indicated by green arrows, inhibition by red bars. Dopamine D1 receptor dependent increases in cAMP activate CREB and inactivate MEF2. CREB drives transcription of Δ FosB, which represses transcription of the histone methyltransferase G9a. Because G9a represses NF- κ B, the net outcome is to increase NF- κ B transcription. Δ FosB also activates transcription of Cdk5, which further inhibits MEF2. The net result of simultaneous activating CREB, Δ FosB, NF- κ B and Cdk5 while inactivating MEF2 and G9a is to drive an increase in MSN dendritic spine density.

inactive form through its association with one of the inhibitory I κ B subunits. Nuclear translocation of NF- κ B is induced by stimuli that lead to phosphorylation and degradation of I κ B (Mercurio et al., 1997). NF- κ B is best known for its role in inflammation and immune responses, however this transcription factor is also expressed in neurons where it can be activated by stimuli including kainate, glutamate, and nitric oxide (Meffert and Baltimore, 2005).

Whether psychostimulant treatment induces acute nuclear translocation of NF- κ B subunits is unknown, however chronic treatment with cocaine has been reported to drive expression of the NF- κ B subunits RelA and NF- κ B1 in the NAc (Ang et al., 2001). This increased expression appears to be associated with increased NF- κ B transcriptional activity, as repeated cocaine treatment increases β gal expression in an NF- κ B-LacZ reporter mouse in both the NAc and the caudate-putamen (Bhakar et al., 2002; Russo et al., 2009). β gal expression is also transiently upregulated 4-6 hours following a single dose of cocaine independent of changes in NF- κ B subunit expression, raising the possibility that additional uncharacterized psychostimulant-regulated signaling mechanisms may contribute to the transcriptional activity of this pathway.

To address potential biological functions of NF- κ B pathway activity in the NAc, Russo and colleagues used HSV to overexpress constitutively active and dominant negative variants of the I κ B kinase IKK (caIKK and dnIKK). In the NAc, overexpression of caIKK enhanced β gal expression above basal levels in the NF- κ B-LacZ reporter mouse, while dnIKK reduced the basal constitutive expression of β gal in these mice demonstrating the actions of these modulators on NF- κ B activity. Similar to the MEF2 analysis described above, the authors examined the effects of their manipulations on both

MSN dendritic spine density and cocaine-induced behaviors. At the cellular level, activation of NF- κ B by caIKK was associated with a basal increase in dendritic spine density, whereas inactivation of NF- κ B by dnIKK caused a basal reduction in spine density and prevented the ability of cocaine to induce an increase in spine density. Behaviorally, expressing dnIKK reduced sensitivity to the rewarding effects of cocaine as measured by CPP, while caIKK had no effect on either standard or reward-sensitized CPP paradigms at the doses tested. One explanation of the failure to see opposite effects of the two IKK manipulations may have to do with their differential ability to block different modes of NF- κ B transcription. caIKK can enhance only inducible NF- κ B function, whereas dnIKK has the ability to block the activity of both constitutive and inducible NF- κ B. However regardless of the implications of these data for mechanisms of NF- κ B action, these data are notably different from the MEF2 study described in the previous section, and once again raise the question of the relationship between MSN spine density and behavioral responses to psychostimulants.

It is possible that the different correlations between spine density and cocaine induced behaviors in mice with manipulations of MEF2 or IKK signaling could arise as a consequence of procedural differences between the experiments, such as the cocaine injection schedule used to induce spine density changes or the extent of cell infection in NAc upon HSV versus AAV delivery. However these data also raise the possibility that changes in dendritic spine density (or any other cellular property) are not necessarily sufficient to cause specific cocaine-induced behaviors independent of the cellular context in which they occur. So for example if the net excitability of MSNs is what underlies cocaine sensitivity, then the sum total of changes in both dendritic spine density

(representing the strength of excitatory input) as well as alterations in intrinsic excitability would together determine the behavioral effects of any genetic manipulation. Future studies that examine the functional consequences of spine density changes for MSN firing and that determine whether additional changes in cell excitability or synapse composition accompany these changes in spine density will be important for resolving these apparent contradictions.

B.3.5 Nuclear Factor of Activated T Cells (NFAT)

Although evolutionarily related to the Rel/NF- κ B family, the NFAT transcription factors (NFAT1-4) are distinguished by their sensitivity to intracellular Ca^{2+} and their regulation by the Ca^{2+} -dependent serine/threonine phosphatase calcineurin (Hogan et al., 2003). A fifth NFAT family member (NFAT5/TonEBP) shares homology to the NFAT DNA binding domain but lacks calcium sensitivity and instead plays important roles in cellular responses to changes in extracellular tonicity (Miyakawa et al., 1999). NFAT family members have been most highly studied for their role in regulation of cytokine gene expression in T cells, however these proteins are widely expressed in numerous tissues including the nervous system (Vihma et al., 2008). Genetic studies have revealed that NFAT is required for neurotrophin- and netrin-dependent axon outgrowth during embryonic development (Graef et al., 2003) and for serum and activity-dependent survival of cerebellar granule neurons (Benedito et al., 2005). However the substantial redundancy in function among the four calcium-regulated members of this family and the requirement for these factors in development of other organ systems have limited genetic analysis of adult brain functions in knockout mice.

Like NF- κ B, the activity of NFAT is regulated by nucleocytoplasmic shuttling. In response to stimuli that elevate intracellular calcium and induce the release of calcium from intracellular stores, the phosphatase calcineurin dephosphorylates multiple Ser and Thr residues in NFAT, which facilitates nuclear translocation (Okamura et al., 2000). Although NFAT can bind DNA as a dimer at regulatory elements that resemble NF- κ B binding sites, NFAT also binds and cooperates with a number of other nuclear transcription factors including Fos/Jun family members and MEF2 (collectively known as “NFATn”) to synergistically promote gene transcription (Hogan et al., 2003). NFAT-dependent transcription is terminated by nuclear export following rephosphorylation of the protein by a number of constitutively active kinases including GSK3 (Graef et al., 1999).

To determine whether psychostimulants may regulate the transcriptional activity of NFAT, Groth and colleagues used antibodies against NFAT3 to study the nuclear localization of this protein in neurons of the NAc before and after cocaine (Groth et al., 2008). Repeated exposure to cocaine (15mg/kg for 5 days) in rats led to enhanced nuclear localization of NFAT3 in striatal lysates. Consistent with the possibility that this nuclear localization represents increased NFAT activity, cocaine was also found to increase expression of *Itpr1* (IP3R) and *Gria2* (GluR2), two putative NFAT target genes (Graef et al., 1999; Groth et al., 2008). In dissociated striatal cultures, activation of DA D1-receptors enhanced transcription of an NFAT reporter plasmid, and this effect was blocked either by application of a D1-receptor agonist or the L-type voltage-sensitive calcium channel (L-VSCC) blocker nifedipine. These data suggest that DA signaling activates NFAT via cAMP-induced activation of L-VSCCs. However it remains difficult

to reconcile these data with other studies in the literature. As described in the MEF2 section above, both DA D1-receptor activation in striatal slices (Rakhilin et al., 2004) and chronic cocaine exposure *in vivo* (Pulipparacharuvil et al., 2008) induce phosphorylation of the calmodulin binding protein RCS, which via its competitive inhibition of calcineurin activation would be predicted to repress NFAT. In addition a previous study reported that forskolin mediated elevation of cAMP inhibited L-VSCC induced nuclear import of NFAT3 in cultured hippocampal neurons (Belfield et al., 2006). It is possible that the differences between these studies could be explained by cell type differences in the relative importance of these signaling pathways for modulation of NFAT or differential sensitivity of MEF2 and NFAT to the actions of RCS on calcineurin activity, and further investigation of NFAT regulation will likely resolve these uncertainties. Most importantly, future studies that utilize genetics to determine the requirements of NFAT in behavioral responses to drugs of abuse will significantly enhance understanding of the importance of this transcriptional regulatory pathway.

B.3.6 Nucleus Accumbens 1 (NAC1)

The early studies of psychostimulant-regulated transcription factor expression focused on Fos/Jun IEGs because the expression of these factors is dramatically and rapidly induced following drug treatment. However given that neural adaptations develop slowly over weeks following drug exposure, interest quickly turned to identifying transcription factors whose expression is altered on a slower time scale. Cha and colleagues identified Nucleus Accumbens 1 (NAC1), POZ/BTB domain transcription factor, as a factor whose expression was selectively enhanced in the NAc 3 weeks after

cessation of a 3 week period of cocaine self-administration (Cha et al., 1997). NAC1 is a nuclear protein that is widely expressed in different tissues and brain regions (Mackler et al., 2000). NAC1 associates with coREST and HDACs and appears to act as a transcriptional repressor (Korutla et al., 2007; Korutla et al., 2005b; Mackler et al., 2000). Follow-up studies showed that psychostimulant-regulated expression of NAC1 is biphasic – similar to the IEGs it is induced within 1 hour of a single dose of cocaine, then falls back to basal levels within hours. However unlike most IEG transcription factors, NAC1 expression is induced again within 1 week of cocaine withdrawal (Cha et al., 1997). These temporal data raised the possibility that NAC1 could play multiple roles at different times during the process of drug-induced neural adaptations.

Three different genetic strategies were taken to address the biological functions of NAC1 in behavioral responses to psychostimulants. To acutely reduce NAC1 expression in the NAc of adult animals, antisense oligonucleotides were stereotactically injected directly into the NAc. Antisense reduced NAC1 expression by 26% and significantly enhanced locomotor sensitivity to a single injection of cocaine without affecting the cocaine-dependent elevation of DA in the NAc (Kalivas et al., 1999). Next to address potential functions of the chronic upregulation of NAC1, Mackler and colleagues overexpressed this protein in the NAc using AAV (Mackler et al., 2000). Overexpression had no effect on baseline locomotor activity or the ability of a single dose of cocaine to stimulate locomotion, however with repeated cocaine treatment the NAC1 overexpressing mice failed to develop locomotor sensitization. Taken together with the antisense experiments these data suggested a model in which the upregulation of NAC1 by cocaine may act via one or more mechanisms in a compensatory fashion to limit

behavioral responses to cocaine. However, to more generally address the requirement for NAC1 in psychostimulant behaviors, Mackler and colleagues generated a *Nac1* knockout mouse (Mackler et al., 2008). Surprisingly, given their previous studies, these mice showed reduced sensitivity to the acute locomotor stimulating effects of cocaine, and with repeated cocaine treatment they were able to develop locomotor sensitization and CPP that was indistinguishable from wild-type responses. The reduced sensitivity to drug treatment may be explained by alterations in the development or function of other parts of the mesolimbocortical circuit, because unlike the data reported following local antisense knockdown of NAC1, the knockout mice have blunted cocaine-stimulated elevation of DA in the NAc. Further understanding of these developmental changes will enhance understanding of NAC1 function in different regions of the brain, and more refined genetic manipulations (local knockdown, conditional deletion) may help to resolve the specific functions of NAC1 in psychostimulant-mediated behaviors.

Interestingly, in addition to being regulated at the level of expression, recent data show that NAC1 is also subject to activity-dependent nucleocytoplasmic shuttling. Unlike the nuclear distribution of NAC1 in the NAc, under basal conditions NAC1 was found to have a diffuse cytoplasmic distribution in cultured cortical neurons (Korutla et al., 2005a). The localization of NAC1 in these neurons is subject to activity-dependent regulation, as blockade of synaptic activity with TTX induced nuclear accumulation of NAC1 in cortical neurons whereas membrane depolarization induced a cytoplasmic redistribution of NAC1 in undifferentiated PC12 cells. What might be the function of this redistribution of NAC1? An intriguing study raises the possibility that NAC1 may mediate a novel nucleus to synapse signaling pathway that recruits components of the

ubiquitin pathway to dendritic spines. BTB/POZ domain proteins are known to be substrates for ubiquitination, and Shen and colleagues demonstrated an association between NAC1 and the cullin Cul3, which is a component of E3 ubiquitin ligase complexes (Shen et al., 2007). Interestingly, treatment with stimuli that induce nuclear export of NAC1 lead to co-translocation of Cul3 to the cytoplasm. Following 12 hours of activity induced by treatment with bicuculline, both NAC1 and the 20S proteasome localize in dendritic spines juxtaposed to punctae of synaptophysin suggesting these are functional synapses. Activity-dependent regulation of protein ubiquitination at synapses has been suggested to be an important means of altering synaptic function (Yi and Ehlers, 2005) thus this NAC1 associated relocation of proteasome subunits raises the possibility that NAC1 could interact with this process. The relevance synaptic protein degradation for behavioral responses to psychostimulants remains unknown, however these data raise an intriguing and unexpected mechanism by which NAC1 might influence synapses and the function of neural networks.

B.3.7 Summary

The six transcription factors families reviewed here represent those for which the most substantial data has accrued to support their role in cellular and behavioral adaptations to psychostimulants. However there will almost certainly be additional transcriptional pathways that coordinate cellular responses to psychostimulants, such as the zinc finger transcription factor NZF-2b (*Myt1*) (Chandrasekar and Dreyer, 2010) and the SRF/TCF factor Elk-1 (Valjent et al., 2000). Identifying the set of transcription factors that are subject to cocaine-dependent regulation is an essential first step. In the future, it will be

important to understand how these pathways work together to produce the net cellular and behavioral effects of psychostimulants.

B.4 CHROMATIN REGULATION

With the advent of genome-level methods to map transcription factor binding sites, it has quickly become apparent that only a small fraction of consensus binding elements in the genome are actually occupied by their cognate transcription factors (Farnham, 2009; Zhang et al., 2005). The accessibility of binding sites is controlled in part by the secondary structure of nuclear chromatin, which is comprised of genomic DNA and its associated histone proteins. The basic repeating unit of chromatin is the nucleosome, which contains 147bp of DNA wrapped around a protein octamer containing two copies of each of the core histones (H2A, H2B, H3, and H4) (Peterson and Laniel, 2004). Epigenetic mechanisms of gene transcription are those which modify this structure in ways that make it either more or less permissive for transcription. There are three primary mechanisms of chromatin regulation (Jaenisch and Bird, 2003): (1) Chemical modification of the DNA itself, which occurs primarily by the methylation of cytosine in the sequence 5-methyl-CpG, (2) ATP-dependent enzymatic sliding of the nucleosomes and (3) Posttranslational modification of specific amino acid residues near the flexible N-terminal tails of the histone proteins. Histones H3 and H4 are subject to site-specific modification at a number of residues by acetylation, methylation, phosphorylation, ubiquitination, and ADP-ribosylation, and the observed consequences of specific modifications for activation or repression of transcription has been termed the histone code (Strahl and Allis, 2000). In addition to affecting nucleosome dynamics, these

modifications of chromatin also influence the probability of transcription by providing docking sites for the recruitment of transcriptional coactivators and corepressors onto gene regulatory regions (Fuks et al., 2003; Shi et al., 2006).

A growing body of evidence suggests that the regulation of histone modifications and DNA methylation may contribute to persistent stimulus-dependent changes in gene expression and long-lasting plasticity in the brain. In 2005, Kumar and colleagues (Kumar et al., 2005) first reported that cocaine exposure induces long lasting changes in the acetylation and phosphoacetylation of histones associated with drug-responsive genes in the striatum. Furthermore, inhibition of histone deacetylases was shown to enhance not only drug-induced gene expression but also both the locomotor stimulating and rewarding properties of cocaine, suggesting that these modifications were an essential component of the molecular processes underlying behavioral adaptations to drugs of abuse.

A recent genome-level study of histone modifications induced in the striatum by cocaine exposure extended the range of cocaine-regulated modifications to include histone methylation, and offered the first insights into the significance of this processes across the genome as a whole (Renthal et al., 2009). In order to study genome-wide chromatin modifications following chronic cocaine, Renthal and colleagues utilized a technique called ChIP-chip. Chromatin immunoprecipitation (ChIP) is a method used to determine the location of DNA binding sites for a protein of interest. An antibody is used to immunoprecipitate the protein and co-immunoprecipitated DNA is identified by one of a number of methods. In ChIP-chip the association of the proteins with promoter regions is quantified by hybridizing the co-immunoprecipitated DNA with a promoter microarray

(a chip). One of the most interesting findings of this study was the observation that histones were only modified at a select set of genes and that different kind of histone modifications were induced by cocaine at different gene promoters. These observations point to the importance of identifying the chromatin regulatory proteins that are targets of modulation by psychostimulant-induced signaling pathways. Here we review the evidence for psychostimulant-dependent regulation of four such enzymes that catalyze histone modifications, and we preview the possibility that other chromatin regulatory processes may be targets of drug-dependent modulation as well.

B.4.1 CREB Binding Protein (CBP).

As described in the section on *CREB* above, recruitment of the transcriptional coactivator CBP is thought to be the major mechanism by which Ser133 phosphorylation induces CREB-dependent transcription. CBP is a large multi-domain protein that has enzymatic activity as a histone acetyltransferase (HAT) (Goodman and Smolik, 2000). The CREB target gene *Fos* is among those that have been shown to show enhanced acetylation of promoter-associated histones following cocaine exposure (Kumar et al., 2005), raising the possibility that CBP might mediate this process. To investigate the role of CBP in cocaine-induced histone acetylation, Levine and colleagues (Levine et al., 2005) examined regulation of the *Fosb* gene, another known CREB target. Using the ChIP assay, they found increases in CBP binding to the *Fosb* promoter after acute cocaine treatment that was coincident with increased acetylation of *Fosb* promoter associated histone H4. To determine the requirement for CBP in acetylation at *Fosb*, the authors utilized CBP haploinsufficient mice, which carry only one functional allele at the

Crebbp locus and are functionally hypomorphic for many CBP-dependent cellular processes (Tanaka et al., 1997). The authors found that these mice have wild-type levels of *Fosb* expression under basal conditions, but reduced induction of *Fosb* following a single injection of cocaine and reduced accumulation of Δ FosB protein following repeated cocaine exposure. These changes in *Fosb* gene expression were accompanied by a reduction in cocaine-mediated recruitment of both CBP and AcH4 to the *Fosb* promoter. Finally as further evidence that histone acetylation plays a role in cocaine-induced gene expression, the authors demonstrated that pharmacological treatment of wild-type mice with the histone deacetylase inhibitor SAHA increased cocaine-dependent induction of *Fosb* expression while having no effect on basal transcriptional levels. Taken together these data support the model that cocaine-induced transcription of CREB-dependent genes involves local recruitment of CBP and histone acetylation.

Since mutation of the CBP binding site on CREB (phospho-Serine 133) is associated with increased sensitivity to the rewarding effects of cocaine, loss of CBP function might be expected to phenocopy this mutation. Instead the CBP haploinsufficient mice show reduced sensitivity to the locomotor stimulating effects of cocaine and reduced sensitization to repeated cocaine exposure compared with their wild-type littermates (Levine et al., 2005). There are a number of potential explanations for these data including the important possibility that constitutive haploinsufficiency of CBP might alter brain development. In addition, it is also important to keep in mind that beyond CREB, CBP also binds to a number of other transcription factors implicated in the neuronal response to psychostimulants including MEF2 and Jun family members (Goodman and Smolik, 2000). Given the distinct roles of different transcription factors in

behavioral adaptations to psychostimulants, it remains possible that the behaviors seen in the CBP haploinsufficient mice represent the summation of altered regulation through multiple parallel transcription factor pathways.

B.4.2 Histone Deacetylases (HDACs)

Histone acetylation is a dynamic posttranslational modification that is regulated by the balance between histone acetyltransferases like CBP and the histone deacetylase activity of HDACs. The eleven “classical” HDAC proteins remove acetyl groups via hydrolysis and are characterized into three families (class I, class IIa/b, and class IV) based on their structure, enzymatic function, and pattern of expression (Butler and Bates, 2006). HDAC 1, 2, 3, and 8 comprise the class I family and are ubiquitously expressed and predominantly localize to the nucleus. HDAC 4, 5, 7, and 9 belong to the class IIa family, while HDACs 6 and 10 form class IIb. Class II HDACs can associate with transcription factors, but unlike class I, they shuttle between the nucleus and the cytoplasm in a stimulus-dependent fashion, regulating the function of their transcription factor partners. Finally, HDAC11 is the only member of the class IV family and is localized to the nucleus. This HDAC is expressed in brain but little is known about its function. Despite their nomenclature, members of the HAT and HDAC family can also regulate acetylation of other proteins in addition to histones, and the non-nuclear HDACs have several biological functions that are unrelated to transcriptional regulation (Pandey et al., 2007).

In addition to the evidence that acute and chronic cocaine increase histone acetylation at the promoters of genes known to be regulated by cocaine, nonspecific

HDAC inhibitors increase cocaine sensitivity as measured both by gene induction and by behavior (Kumar et al., 2005). These data suggest that the actions of HDACs on chromatin structure are functionally relevant for behavior downstream of activation of monoaminergic signaling, but the specific HDACs involved in cocaine reward and sensitivity were unknown. Of the class I and II HDACs, all but HDAC2 are expressed in the striatum, and none show cocaine-dependent changes in expression (Renthal et al., 2007). However since the class II HDACs are subject to stimulus-dependent phosphorylation and nuclear export, Renthal and colleagues asked whether this process could be induced by cocaine treatment (Renthal et al., 2007). Interestingly, chronic, but not acute, cocaine exposure induced rapid phosphorylation and nuclear export of HDAC5, raising the possibility that this enzyme might be particularly important for the regulation of cellular responses and behavioral adaptations to repeated cocaine exposure.

To address the behavioral significance of HDAC5 regulation by chronic cocaine, Renthal utilized HSV vectors to overexpress HDAC5 in the NAc *in vivo* (Renthal et al., 2007). HDAC5 overexpression decreased the rewarding effects of cocaine as measured by CPP. Overexpression of the related class IIa member HDAC4 had a similar effect, but there was no effect of overexpressing HDAC9, suggesting specificity of action within this subfamily. The actions of HDAC5 on CPP require the histone deacetylase domain, and treating HDAC5 overexpressing mice with the HDAC inhibitor TSA blocks the effects of overexpression. Conversely loss of HDAC5 expression in an *Hdac5* knockout mouse was associated with increased expression of CPP. This effect was detected only in mice that had been previously sensitized with previous cocaine exposure prior to CPP, not cocaine naïve mice – a requirement for previous cocaine that mirrors the regulation of

phosphorylation. Restoring HDAC5 in the NAc of the knockout mice normalized the reward hypersensitivity, confirming that HDAC5 is acting in the NAc to regulate the behavioral adaptations to chronic cocaine. HDAC4 knockout mice die before adulthood and thus could not be tested, however HDAC9 knockout mice showed normal CPP compared with wild-type controls, consistent with the viral experiments. Taken together these data suggest that HDAC5 and possibly HDAC4 are important for behaviorally relevant changes in protein acetylation in response to cocaine.

Given the known importance of HDACs in regulation of gene transcription, it is reasonable to assume that the alterations in cocaine-induced behavior in the HDAC5 knockouts might be caused by changes in gene expression programs. Using a series of comparisons of microarray data between wild-type and HDAC5 knockout mice treated repeatedly with either saline or cocaine, Renthal identified 172 genes that were significantly differentially expressed in HDAC5 knockouts (Renthal et al., 2007). Despite the fact that HDAC5 is a transcriptional repressor, this HDAC5 knockout gene set contained a substantial number of downregulated genes. One possibility is that this may arise as a secondary consequence of interrelated pathways of gene regulation (i.e. HDAC5 knockout increases expression of a repressor that subsequently decreases expression of another gene). These data raise the importance of identifying the direct targets of HDAC5 and understanding the mechanisms of specificity in gene regulation by these kinds of co-regulatory proteins. Interestingly previous studies have shown that HDAC5 binds to MEF2 (Belfield et al., 2006), however the MEF2 binding domain of HDAC5 is not required for its effects on CPP (Renthal et al., 2007), suggesting that other sequence-specific binding proteins may be involved.

In addition to the 11 “classical” HDACs, there are also 7 “nonclassical” HDACs known as the sirtuins. Unlike the other HDACs, the sirtuins employ a unique NAD⁺-dependent mechanism to remove acetyl groups from histones (Blander and Guarente, 2004). In addition to deacetylating histones, the sirtuins also deacetylate other cellular proteins including the transcription factors p53, NFκB, and FOXO3 (Brunet et al., 2004), as well as non-transcription related proteins such as tubulin. In the course of a genome-level ChIP-chip study of histone modifications induced by acute and chronic cocaine in striatal neurons, Renthal and colleagues (Renthal et al., 2009) detected an increase in acetylated H3 on both the *Sirt1* and *Sirt2* promoters following chronic cocaine. The enrichment of these activation-associated chromatin modifications at the promoters was associated with increases in *Sirt1* and *Sirt2* mRNA expression. In order to determine if cocaine alters the catalytic activity of SIRT1 and SIRT2, cocaine-treated NAc lysates were incubated with fluorescent substrates of SIRT1 and SIRT2, which revealed that chronic, but not acute, cocaine exposure increased SIRT1 and SIRT2 catalytic activity. Thus in addition to the phosphorylation-dependent regulation of class IIa HDAC function, cocaine may also alter histone acetylation via increased expression of the sirtuins.

Although the sirtuins have been shown to play intriguing roles in energy metabolism, longevity, and healthspan (Michan and Sinclair, 2007), little is known about the function of this class of proteins that would suggest how they might contribute to drug-induced neuronal plasticity in the striatum. Given the relevance of this class of proteins for human disease, potent inhibitors (sirtinol) and activators (resveratrol) of the sirtuins have been developed, and Renthal employed these drugs to assess the cellular and

behavioral consequences of sirtuin activation and inhibition (Renthal et al., 2009). In whole-cell current clamp recordings from medium spiny neurons in striatal slice preparations, incubation with sirtinol was found to decrease the excitability of MSN neurons, whereas resveratrol had the opposite effect. When delivered *in vivo* (resveratrol was delivered systemically while sirtinol was delivered directly to the NAc), treatment with resveratrol was shown to enhance CPP conditioning, while sirtinol attenuated it. Taken together with the evidence for regulation of sirtuin expression, the authors suggest that sirtuins may function in a positive feedback loop to enhance the rewarding properties of cocaine and promote additional drug taking. Much still needs to be understood about this process, in particular whether or not it is transcriptional since sirtuins have many targets. However, the most interesting implication of this model is the idea that inhibitors of sirtuins might be useful as drugs to treat the compulsive drug-taking of addiction.

B.4.3 Histone Methyltransferases (HMTs)

Histone methylation is a particularly information-rich modification of chromatin that is strongly correlated with regulation of gene expression. Histones H3 and H4 can be mono, di, or tri-methylated (me1, me2, or me3) at several lysine (K) and arginine (R) residues (Lachner and Jenuwein, 2002). Depending on the positions modified, histone methylation has been associated both with activation (H3K4, H3K36, H3K79) as well as repression (H3K9, H3K27, H4K20) of transcription. Histone methylation is thought to regulate transcription through the local site-specific recruitment of transcriptional coregulatory complexes (Ringrose et al., 2004; Shi et al., 2006). Histones are methylated on lysine by a large family of SET-domain containing enzymes (Dillon et al., 2005).

Assessed at the level of the entire cell, methylation was known to be a very long-lasting modification of histone proteins, and for many years was thought to be irreversible (Honda et al., 1975; Trojer and Reinberg, 2006). However when a large family of enzymes with site-specific histone demethylase activity was characterized, these data raised the possibility that histone methylation was far more dynamic than previously assumed (Klose et al., 2006; Shi, 2007). Subsequent studies have demonstrated that both histone methyltransferases and histone demethylases act locally at specific sets of target genes, thus explaining how they can regulate gene transcription without affecting global levels of histone methylation (Lan et al., 2007; Metzger et al., 2005; Peng et al., 2009).

In the course of their genome-wide promoter analysis of chromatin modifications following chronic cocaine, in addition to the alterations of histone acetylation discussed above, Renthal also found that there were alterations in dimethylation of H3 lysine 9 (H3K9me2) and trimethylation of H3 lysine 27 (H3K27me3) at a subset of gene promoters. However nothing was known about how activation of monoamine receptors might influence the function of histone methyltransferases or histone demethylases. In order to address this question, Maze and colleagues (Maze et al., 2010) investigated if levels of enzymes controlling lysine methylation were altered following chronic cocaine. Only two histone methyltransferases, G9a and G9a-like protein (GLP), showed persistent downregulation 24 hours after chronic cocaine. These enzymes specifically catalyze the methylation of H3K9me2. To investigate the significance of G9a repression after chronic cocaine, HSV vectors expressing either GFP or G9a were delivered directly into the NAc. Overexpression of G9a induces H3K9me2 and reduces CPP in a manner that depends on the HMT domain. By contrast local viral Cre-mediated excision of G9a in the NAc of a

G9a floxed mouse reduced H3K9me2 and enhanced CPP. A similar result was seen in mice treated with the G9a inhibitor BIX01294 providing pharmacological confirmation of the role of this pathway as playing a role limiting the response to cocaine. Furthermore overexpression of G9a blocks cocaine-induced spine formation whereas recombination of floxed G9a increases spine density in the absence of cocaine treatment. Together, these suggest that G9a would be expected to promote cocaine reward acting in a positive fashion after chronic cocaine.

B.4.4 DNA methylation

Among the biochemical mechanisms that mediate epigenetic regulation of gene transcription, DNA methylation is perhaps the most intriguing and yet the most poorly understood. In differentiated mammalian cells DNA is methylated predominantly on cytosines that occur in the dinucleotide sequence CpG by the enzymatic action of a small family of DNA methyltransferases (DNMT1, DNMT3a, and DNMT3b) (Jaenisch and Bird, 2003). DNA methylation is found throughout both expressed and non-expressed regions of the genome, though the density of methylation varies in different regions (Lister et al., 2009). Despite the general functional association of DNA methylation with gene repression, methylation within gene bodies is positively correlated with gene expression, and overall levels of DNA methylation are higher on the active than the inactive X chromosome (Hellman and Chess, 2007; Suzuki and Bird, 2008). However methylation levels are specifically lower in regulatory regions of highly expressed genes, and transcription factor binding sites are particularly methylation poor (Hellman and Chess, 2007; Lister et al., 2009). Differential DNA methylation within these regulatory

regions is associated with cell type specific repression of gene transcription during development and with pathological dysregulation of gene transcription in cancer (Lister et al., 2009; Ting et al., 2006). These data raise the possibility that stimulus-dependent changes in promoter DNA methylation could contribute to transcriptional regulation.

One of the reasons why DNA methylation is such an interesting molecular mechanism is because of its persistence. This molecular property is important for a memory mechanism with the idea that methylation induced at one point in time could influence gene expression much later. For example, in a fascinating example of how stimulus-dependent alterations in DNA methylation during development might couple to the expression of behaviors, Weaver and colleagues demonstrated that the level of maternal care delivered to rat pups during the perinatal period strongly correlated with methylation of a specific CpG sequence in the promoter of a glucocorticoid receptor gene in the hippocampus of the rat pups (Weaver et al., 2004). Methylation at this site was shown to be associated both with persistent changes in expression of the glucocorticoid receptor and with alterations in the way the pups responded to stress several months later in life.

However for DNA methylation to be important for stimulus-dependent changes in gene expression, there must be mechanisms to acutely regulate this mark. A growing body of evidence strongly suggests that DNA methylation is dynamically regulated by environmental stimuli in postmitotic cells (Kangaspeska et al., 2008; Ma et al., 2009; Martinowich et al., 2003; Metivier et al., 2008; Miller and Sweatt, 2007; Nelson et al., 2008; Weaver et al., 2005). However the mechanisms of stimulus-dependent changes in

methylation remain unknown as the specific nature of the DNA demethylating enzymes in mammalian cells is a subject of debate (Zhu, 2009).

A more tractable way to approach the function of DNA methylation is to focus on the effectors of this modification (Klose and Bird, 2006). DNA methylation acts on transcription by two primary mechanisms: either methylation blocks the association of a transcription activator with a required regulatory element (Weaver et al., 2004) or methylation provides a docking site for a methyl-DNA binding domain (MBD) containing protein that subsequently recruits complexes of DNA and histone-modifying enzymes locally to this region of chromatin that change the likelihood of transcription (Klose and Bird, 2006). The mammalian genome contains 5 well-characterized MBD family members with unique biological functions (Klose and Bird, 2006). Thus studying the binding sites, gene targets, and functions of these methyl-DNA binding proteins represents one practical way to advance understanding of the impact of epigenetic transcriptional regulatory pathways on brain development, behavior, and psychiatric illness.

Whether DNA methylation is subject to modulation by psychostimulant exposure remains unknown. However one study has reported that 10 days of either cocaine or fluoxetine injections in rats was associated with increased expression of the methyl-DNA binding proteins MeCP2 and MBD1 in the caudate putamen, the frontal cortex, and the dentate gyrus subregion of the hippocampus (Cassel et al., 2006). In a second study the same group found that self-administration of cocaine increased MeCP2 expression in cingulate cortex, NAc, and caudate putamen (Host et al., 2009). Whether increased expression of MeCP2 and MBD1 alters either DNA methylation or methylation-

dependent programs of transcription is unknown, but increased MeCP2 expression is associated with neurological disorders (Chahrour and Zoghbi, 2007), suggesting that levels of these proteins could have functional significance. Addressing the genetic requirements for these proteins in the cellular and behavioral responses to drugs of abuse as well as understanding the mechanisms that link these proteins to monoaminergic stimuli will be interesting studies to pursue.

B.4.5 Summary

The observation that chromatin modifications are subject to regulation by psychostimulants adds a new dimension to our understanding of drug-modulated gene regulatory pathways in the striatum. The studies described here represent the first insights into the regulation of histone modifying enzymes and methyl-DNA binding proteins by drugs of abuse. In the future, elucidating the distinct roles of different epigenetic marks and investigating the mechanisms that confer gene specificity on chromatin regulatory factors will substantially enhance our understanding of this intriguing process.

B.5 CONCLUSIONS

In the 20 years since Fos expression was first shown to be induced in the NAc by psychostimulant treatment, a massive quantity of data has affirmed the importance of transcriptional regulatory pathways in cellular and behavioral adaptations to these drugs (**Fig. 30**). Substantial progress has been made in the identification of transcriptional regulators whose activity is subject to psychostimulant-dependent modulation. Molecular genetic alterations in these pathways have revealed new insights into the kinds of cellular

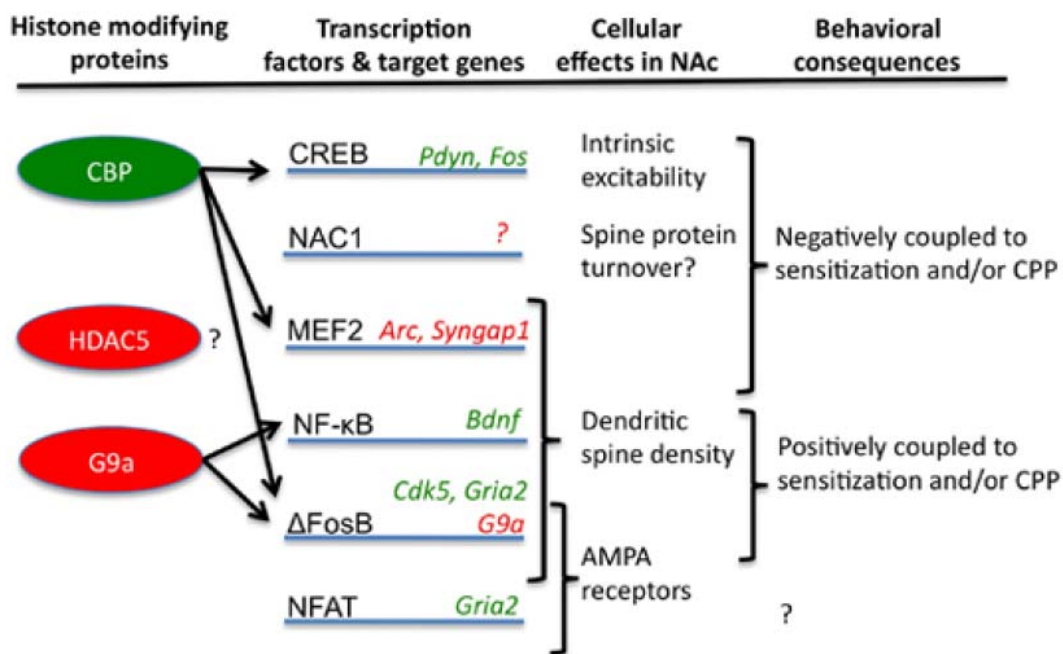


Figure 30: Summary of transcriptional regulatory pathways that contribute to the behavioral response to psychostimulants. Red indicates repressors and repression of gene expression, green indicates transcriptional activators and activation of transcription.

processes and forms of synaptic plasticity that may underlie the behavioral changes seen with chronic drug exposure. Future studies will need to integrate the effects of these multiple parallel and interconnected transcriptional pathways to produce a more complete picture of the cellular response to drugs of abuse.

B.6 REFERENCES

Ang, E., Chen, J., Zagouras, P., Magna, H., Holland, J., Schaeffer, E., and Nestler, E.J. (2001). Induction of nuclear factor-kappaB in nucleus accumbens by chronic cocaine administration. *J Neurochem* 79, 221-224.

Belfield, J.L., Whittaker, C., Cader, M.Z., and Chawla, S. (2006). Differential effects of Ca²⁺ and cAMP on transcription mediated by MEF2D and cAMP-response element-binding protein in hippocampal neurons. *J Biol Chem* 281, 27724-27732.

- Benedito, A.B., Lehtinen, M., Massol, R., Lopes, U.G., Kirchhausen, T., Rao, A., and Bonni, A. (2005). The transcription factor NFAT3 mediates neuronal survival. *J Biol Chem* 280, 2818-2825.
- Bhakar, A.L., Tannis, L.L., Zeindler, C., Russo, M.P., Jobin, C., Park, D.S., MacPherson, S., and Barker, P.A. (2002). Constitutive nuclear factor-kappa B activity is required for central neuron survival. *J Neurosci* 22, 8466-8475.
- Bibb, J.A., Chen, J., Taylor, J.R., Svenningsson, P., Nishi, A., Snyder, G.L., Yan, Z., Sagawa, Z.K., Ouimet, C.C., Nairn, A.C., *et al.* (2001). Effects of chronic exposure to cocaine are regulated by the neuronal protein Cdk5. *Nature* 410, 376-380.
- Bilbao, A., Parkitna, J.R., Engblom, D., Perreau-Lenz, S., Sanchis-Segura, C., Schneider, M., Konopka, W., Westphal, M., Breen, G., Desrivieres, S., *et al.* (2008). Loss of the Ca²⁺/calmodulin-dependent protein kinase type IV in dopaminergic neurons enhances behavioral effects of cocaine. *Proc Natl Acad Sci U S A* 105, 17549-17554.
- Blander, G., and Guarente, L. (2004). The Sir2 family of protein deacetylases. *Ann Rev Biochem* 73, 417-435.
- Blendy, J.A., Kaestner, K.H., Schmid, W., Gass, P., and Schutz, G. (1996). Targeting of the CREB gene leads to up-regulation of a novel CREB mRNA isoform. *EMBO J* 15, 1098-1106.
- Brunet, A., Sweeney, L.B., Sturgill, J.F., Chua, K.F., Greer, P.L., Lin, Y., Tran, H., Ross, S.E., Mostoslavsky, R., Cohen, H.Y., *et al.* (2004). Stress-dependent regulation of FOXO transcription factors by the SIRT1 deacetylase. *Science* 303, 2011-2015.
- Butler, R., and Bates, G.P. (2006). Histone deacetylase inhibitors as therapeutics for polyglutamine disorders. *Nat Rev Neurosci* 7, 784-796.
- Capper-Loup, C., Canales, J.J., Kadaba, N., and Graybiel, A.M. (2002). Concurrent activation of dopamine D1 and D2 receptors is required to evoke neural and behavioral phenotypes of cocaine sensitization. *J Neurosci* 22, 6218-6227.
- Carlezon, W.A., Jr., Thome, J., Olson, V.G., Lane-Ladd, S.B., Brodtkin, E.S., Hiroi, N., Duman, R.S., Neve, R.L., and Nestler, E.J. (1998). Regulation of cocaine reward by CREB. *Science* 282, 2272-2275.
- Cassel, S., Carouge, D., Gensburger, C., Anglard, P., Burgun, C., Dietrich, J.B., Aunis, D., and Zwiller, J. (2006). Fluoxetine and cocaine induce the epigenetic factors MeCP2 and MBD1 in adult rat brain. *Mol Pharmacol* 70, 487-492.
- Cha, X.Y., Pierce, R.C., Kalivas, P.W., and Mackler, S.A. (1997). NAC-1, a rat brain mRNA, is increased in the nucleus accumbens three weeks after chronic cocaine self-administration. *J Neurosci* 17, 6864-6871.

- Chahrouh, M., and Zoghbi, H.Y. (2007). The story of Rett syndrome: from clinic to neurobiology. *Neuron* 56, 422-437.
- Chandrasekar, V., and Dreyer, J.L. (2010). The brain-specific Neural Zinc Finger transcription factor 2b (NZF-2b/7ZFMyl1) causes suppression of cocaine-induced locomotor activity. *Neurobiol Dis* 37, 86-98.
- Chrivia, J.C., Kwok, R.P., Lamb, N., Hagiwara, M., Montminy, M.R., and Goodman, R.H. (1993). Phosphorylated CREB binds specifically to the nuclear protein CBP. *Nature* 365, 855-859.
- Cole, R.L., Konradi, C., Douglass, J., and Hyman, S.E. (1995). Neuronal adaptation to amphetamine and dopamine: molecular mechanisms of prodynorphin gene regulation in rat striatum. *Neuron* 14, 813-823.
- Dillon, S.C., Zhang, X., Trievel, R.C., and Cheng, X. (2005). The SET-domain protein superfamily: protein lysine methyltransferases. *Genome Biol* 6, 227.
- Dong, Y., Green, T., Saal, D., Marie, H., Neve, R., Nestler, E.J., and Malenka, R.C. (2006). CREB modulates excitability of nucleus accumbens neurons. *Nat Neurosci* 9, 475-477.
- Farnham, P.J. (2009). Insights from genomic profiling of transcription factors. *Nat Rev Genet* 10, 605-616.
- Flavell, S.W., Cowan, C.W., Kim, T.K., Greer, P.L., Lin, Y., Paradis, S., Griffith, E.C., Hu, L.S., Chen, C., and Greenberg, M.E. (2006). Activity-dependent regulation of MEF2 transcription factors suppresses excitatory synapse number. *Science* 311, 1008-1012.
- Fuks, F., Hurd, P.J., Wolf, D., Nan, X., Bird, A.P., and Kourzarides, T. (2003). The Methyl-CpG-binding protein MeCP2 links DNA methylation to histone methylation. *J Biol Chem* 278, 4035-4040.
- Gong, X., Tang, X., Wiedmann, M., Wang, X., Peng, J., Zheng, D., Blair, L.A., Marshall, J., and Mao, Z. (2003). Cdk5-mediated inhibition of the protective effects of transcription factor MEF2 in neurotoxicity-induced apoptosis. *Neuron* 38, 33-46.
- Gonzalez, G.A., and Montminy, M.R. (1989). Cyclic AMP stimulates somatostatin gene transcription by phosphorylation of CREB at serine 133. *Cell* 59, 675-680.
- Goodman, R.H., and Smolik, S. (2000). CBP/p300 in cell growth, transformation, and development. *Genes Dev* 14, 1553-1577.

Graef, I.A., Mermelstein, P.G., Stankunas, K., Neilson, J.R., Deisseroth, K., Tsien, R.W., and Crabtree, G.R. (1999). L-type calcium channels and GSK-3 regulate the activity of NF-ATc4 in hippocampal neurons. *Nature* *401*, 703-708.

Graef, I.A., Wang, F., Charron, F., Chen, L., Neilson, J., Tessier-Lavigne, M., and Crabtree, G.R. (2003). Neurotrophins and netrins require calcineurin/NFAT signaling to stimulate outgrowth of embryonic axons. *Cell* *113*, 657-670.

Graybiel, A.M., Moratalla, R., and Robertson, H.A. (1990). Amphetamine and cocaine induce drug-specific activation of the c-fos gene in striosome-matrix compartments and limbic subdivisions of the striatum. *Proc Natl Acad Sci U S A* *87*, 6912-6916.

Groth, R.D., Weick, J.P., Bradley, K.C., Luoma, J.I., Aravamudan, B., Klug, J.R., Thomas, M.J., and Mermelstein, P.G. (2008). D1 dopamine receptor activation of NFAT-mediated striatal gene expression. *Eur J Neurosci* *27*, 31-42.

Heiman, M., Schaefer, A., Gong, S., Peterson, J.D., Day, M., Ramsey, K.E., Suarez-Farinas, M., Schwarz, C., Stephan, D.A., Surmeier, D.J., *et al.* (2008). A translational profiling approach for the molecular characterization of CNS cell types. *Cell* *135*, 738-748.

Hellman, A., and Chess, A. (2007). Gene body-specific methylation on the active X chromosome. *Science* *315*, 1141-1143.

Herdegen, T., and Leah, J.D. (1998). Inducible and constitutive transcription factors in the mammalian nervous system: control of gene expression by Jun, Fos, and Krox, and CREB/ATF proteins. *Brain Res Rev* *28*, 370-490.

Hill, C.S., and Treisman, R. (1999). Growth factors and gene expression: fresh insights from arrays. *Sci STKE* *1999*, PE1.

Hiroi, N., Brown, J.R., Haile, C.N., Ye, H., Greenberg, M.E., and Nestler, E.J. (1997). FosB mutant mice: loss of chronic cocaine induction of Fos-related proteins and heightened sensitivity to cocaine's psychomotor and rewarding effects. *Proc. Natl. Acad. Sci. U. S. A.* *94*, 10397-10402.

Hogan, P.G., Chen, L., Nardone, J., and Rao, A. (2003). Transcriptional regulation by calcium, calcineurin, and NFAT. *Genes Dev* *17*, 2205-2232.

Honda, B.M., Candido, P.M., and Dixon, G.H. (1975). Histone methylation. Its occurrence in different cell types and relation to histone H4 metabolism in developing trout testis. *J Biol Chem* *250*, 8686-8689.

Hope, B., Kosofsky, B., Hyman, S.E., and Nestler, E.J. (1992). Regulation of immediate early gene expression and AP-1 binding in the rat nucleus accumbens by chronic cocaine. *Proc Natl Acad Sci U S A* *89*, 5764-5768.

- Hope, B.T., Nye, H.E., Kelz, M.B., Self, D.W., Iadarola, M.J., Nakabeppu, Y., Duman, R.S., and Nestler, E.J. (1994). Induction of a long-lasting AP-1 complex composed of altered Fos-like proteins in brain by chronic cocaine and other chronic treatments. *Neuron* *13*, 1235-1244.
- Host, L., Dietrich, J.B., Carouge, D., Aunis, D., and Zwiller, J. (2009). Cocaine self-administration alters the expression of chromatin-remodelling proteins; modulation by histone deacetylase inhibition. *J Psychopharmacol Epub ahead of print*.
- Hyman, S.E., Malenka, R.C., and Nestler, E.J. (2006). Neural Mechanisms of Addiction: The Role of Reward-Related Learning and Memory. *Annu Rev Neurosci*.
- Jaenisch, R., and Bird, A. (2003). Epigenetic regulation of gene expression: how the genome integrates intrinsic and environmental signals. *Nat Genet* *33 Suppl*, 245-254.
- Kalivas, P.W., Duffy, P., and Mackler, S.A. (1999). Interrupted expression of NAC-1 augments the behavioral responses to cocaine. *Synapse* *33*, 153-159.
- Kalivas, P.W., and Stewart, J. (1991). Dopamine transmission in the initiation and expression of drug- and stress-induced sensitization of motor activity. *Brain Res Brain Res Rev* *16*, 223-244.
- Kangaspeska, S., Stride, B., Metivier, R., Polycarpou-Schwarz, M., Ibberson, D., Carmouche, R.P., Benes, V., Gannon, F., and Reid, G. (2008). Transient cyclical methylation of promoter DNA. *Nature* *452*, 112-115.
- Kelz, M.B., Chen, J., Carlezon, W.A., Jr., Whisler, K., Gilden, L., Beckmann, A.M., Steffen, C., Zhang, Y.J., Marotti, L., Self, D.W., *et al.* (1999). Expression of the transcription factor deltaFosB in the brain controls sensitivity to cocaine. *Nature* *401*, 272-276.
- Klose, R.J., and Bird, A.P. (2006). Genomic DNA methylation: the mark and its mediators. *Trends Biochem Sci* *31*, 89-97.
- Klose, R.J., Kallin, E.M., and Zhang, Y. (2006). JmjC-domain-containing proteins and histone demethylation. *Nat Rev Genet* *7*, 715-727.
- Konradi, C., Cole, R.L., Heckers, S., and Hyman, S.E. (1994). Amphetamine regulates gene expression in rat striatum via transcription factor CREB. *J Neurosci* *14*, 5623-5634.
- Korutla, L., Champtiaux, N., Shen, H.W., Klugmann, M., Kalivas, P.W., and Mackler, S.A. (2005a). Activity-dependent subcellular localization of NAC1. *Eur J Neurosci* *22*, 397-403.
- Korutla, L., Degnan, R., Wang, P., and Mackler, S.A. (2007). NAC1, a cocaine-regulated POZ/BTB protein interacts with CoREST. *J Neurochem* *101*, 611-618.

- Korutla, L., Wang, P.J., and Mackler, S.A. (2005b). The POZ/BTB protein NAC1 interacts with two different histone deacetylases in neuronal-like cultures. *J Neurochem* *94*, 786-793.
- Kumar, A., Choi, K.H., Renthal, W., Tsankova, N.M., Theobald, D.E., Truong, H.T., Russo, S.J., Laplant, Q., Sasaki, T.S., Whistler, K.N., *et al.* (2005). Chromatin remodeling is a key mechanism underlying cocaine-induced plasticity in striatum. *Neuron* *48*, 303-314.
- Laakso, A., Mohn, A.R., Gainetdinov, R.R., and Caron, M.G. (2002). Experimental genetic approaches to addiction. *Neuron* *36*, 213-228.
- Lachner, M., and Jenuwein, T. (2002). The many faces of histone lysine methylation. *Curr Opin Cell Biol* *14*, 286-298.
- Lan, F., Zaratiegui, M., Villen, J., Vaughn, M.W., Verdel, A., Huarte, M., Shi, Y., Gygi, S.P., Moazed, D., and Martienssen, R.A. (2007). *S. pombe* LSD1 homologs regulate heterochromatin propagation and euchromatic gene transcription. *Mol Cell* *26*, 89-101.
- Lane-Ladd, S.B., Pineda, J., Boundy, V.A., Pfeuffer, T., Krupinski, J., Aghajanian, G.K., and Nestler, E.J. (1997). CREB (cAMP response element-binding protein) in the locus coeruleus: biochemical, physiological, and behavioral evidence for a role in opiate dependence. *J Neurosci* *17*, 7890-7901.
- Leifer, D., Krainc, D., Yu, Y.T., McDermott, J., Breitbart, R.E., Heng, J., Neve, R.L., Kosofsky, B., Nadal-Ginard, B., and Lipton, S.A. (1993). MEF2C, a MADS/MEF2-family transcription factor expressed in a laminar distribution in cerebral cortex. *Proc Natl Acad Sci U S A* *90*, 1546-1550.
- Levine, A.A., Guan, Z., Barco, A., ZXu, S., Kandel, E.R., and Schwartz, J.H. (2005). CREB-binding protein controls response to cocaine by acetylating histones at the fosB promoter in the mouse striatum. *Proc Natl Acad Sci U S A* *102*, 19186-19191.
- Liou, H.C., and Baltimore, D. (1993). Regulation of the NF-kappa B/rel transcription factor and I kappa B inhibitor system. *Curr Opin Cell Biol* *5*, 477-487.
- Lister, R., Pelizzola, M., Dowen, R.H., Hawkins, R.D., Hon, G., Tonti-Filippini, J., Nery, J.R., Lee, L., Ye, Z., Ngo, Q.M., *et al.* (2009). Human DNA methylomes at base resolution show widespread epigenomic differences. *Nature* *462*, 315-322.
- Lonze, B.E., and Ginty, D.D. (2002). Function and regulation of CREB family transcription factors in the nervous system. *Neuron* *35*, 605-623.
- Lyons, G.E., Micales, B.K., Schwarz, J., Martin, J.F., and Olson, E.N. (1995). Expression of mef2 genes in the mouse central nervous system suggests a role in neuronal maturation. *J Neurosci* *15*, 5727-5738.

- Ma, D.K., Jang, M.H., Guo, J.U., Kitabatake, Y., Chang, M.L., Pow-Anpongkul, N., Flavell, R.A., Lu, B., Ming, G.L., and Song, H. (2009). Neuronal Activity-Induced Gadd45b Promotes Epigenetic DNA Demethylation and Adult Neurogenesis. *Science* 323, 1074-1077.
- Mackler, S., Pacchioni, A., Degnan, R., Homan, Y., Conti, A.C., Kalivas, P., and Blendy, J.A. (2008). Requirement for the POZ/BTB protein NAC1 in acute but not chronic psychomotor stimulant response. *Behav Brain Res.* 187, 48-55.
- Mackler, S.A., Korutla, L., Cha, X.Y., Koebbe, M.J., Fournier, K.M., Bowers, M.S., and Kalivas, P.W. (2000). NAC-1 is a brain POZ/BTB protein that can prevent cocaine-induced sensitization in the rat. *J Neurosci* 20, 6210-6217.
- Mantamadiotis, T., Lemberger, T., Bleckmann, S.C., Kern, H., Kretz, O., Villalba, A.M., Tronche, F., Kellendonk, C., Gau, D., Kapfhammer, J., *et al.* (2002). Disruption of CREB function in brain leads to neurodegeneration. *Nat Gen* 31, 47-54.
- Martinowich, K., Hattori, D., Wu, H., Fouse, S., He, F., Hu, Y., Fan, G., and Sun, Y.E. (2003). DNA methylation-related chromatin remodeling in activity-dependent BDNF gene regulation. *Science* 302, 890-893.
- Mayr, B., and Montminy, M. (2001). Transcriptional regulation by the phosphorylation-dependent factor CREB. *Nat Rev Mol Cell Biol* 2, 599-609.
- Maze, I., Covington, H.E., 3rd, Dietz, D.M., LaPlant, Q., Renthal, W., Russo, S.J., Mechanic, M., Mouzon, E., Neve, R.L., Haggarty, S.J., *et al.* (2010). Essential role of the histone methyltransferase G9a in cocaine-induced plasticity. *Science* 327, 213-216.
- McClung, C.A., and Nestler, E.J. (2003). Regulation of gene expression and cocaine reward by CREB and DeltaFosB. *Nat Neurosci* 6, 1208-1215.
- McKinsey, T.A., Zhang, C.L., and Olson, E.N. (2002). MEF2: a calcium-dependent regulator of cell division, differentiation and death. *Trends Biochem Sci.* 27, 40-47.
- Meffert, M.K., and Baltimore, D. (2005). Physiological functions for brain NF-kappaB. *Trends Neurosci* 28, 37-43.
- Mercurio, F., Zhu, H., Murray, B.W., Shevchenko, A., Bennett, B.L., Li, J., Young, D.B., Barbosa, M., Mann, M., Manning, A., and Rao, A. (1997). IKK-1 and IKK-2: cytokine-activated IkappaB kinases essential for NF-kappaB activation. *Science* 278, 860-866.
- Metivier, R., Gallais, R., Tiffoche, C., Le Peron, C., Jurkowska, R.Z., Carmouche, R.P., Ibberson, D., Barath, P., Demay, F., Reid, G., *et al.* (2008). Cyclical DNA methylation of a transcriptionally active promoter. *Nature* 452, 45-50.

Metzger, E., Wissmann, M., Yin, N., Muller, J.M., Schneider, R., Peters, A.H., Gunther, T., Buettner, R., and Schule, R. (2005). LSD1 demethylates repressive histone marks to promote androgen-receptor-dependent transcription. *Nature* 437, 436-439.

Michan, S., and Sinclair, D. (2007). Sirtuins in mammals: insights into their biological function. *Biochem J.* 404, 1-13.

Miller, C.A., and Sweatt, J.D. (2007). Covalent modification of DNA regulates memory formation. *Neuron* 53, 857-869.

Missale, C., Nash, S.R., Robinson, S.W., Jaber, M., and Caron, M.G. (1998). Dopamine receptors: from structure to function. *Physiol Rev* 78, 189-225.

Miyakawa, H., Woo, S.K., Dahl, S.C., Handler, J.S., and Kwon, H.M. (1999). Tonicity-responsive enhancer binding protein, a rel-like protein that stimulates transcription in response to hypertonicity. *Proc Natl Acad Sci U S A* 96, 2538-2542.

Molkentin, J.D., Black, B.L., Martin, J.F., and Olsen, E.N. (1995). Cooperative activation of muscle gene expression by MEF2 and myogenic bHLH proteins. *Cell* 83, 1125-1136.

Montminy, M.R., and Bilezikjian, L.M. (1987). Binding of a nuclear protein to the cyclic-AMP response element of the somatostatin gene. *Nature* 328, 175-178.

Moratalla, R., Elibol, B., Vallejo, M., and Graybiel, A.M. (1996a). Network-level changes in expression of inducible Fos-Jun proteins in the striatum during chronic cocaine treatment and withdrawal. *Neuron* 17, 147-156.

Moratalla, R., Xu, M., Tonegawa, S., and Graybiel, A.M. (1996b). Cellular responses to psychomotor stimulant and neuroleptic drugs are abnormal in mice lacking the D1 dopamine receptor. *Proc Natl Acad Sci U S A* 93, 14928-14933.

Morgan, J.I., and Curran, T. (1991). Stimulus-transcription coupling in the nervous system: involvement of the inducible proto-oncogenes fos and jun. *Annu Rev Neurosci* 14, 421-451.

Mumberg, D., Lucibello, F.C., Schuermann, M., and Muller, R. (1991). Alternative splicing of fosB transcripts results in differentially expressed mRNAs encoding functionally antagonistic proteins. *Genes Dev* 5, 1212-1223.

Nakabeppu, Y., and Nathans, D. (1991). A naturally occurring truncated form of FosB that inhibits Fos/Jun transcriptional activity. *Cell* 64, 751-759.

Nelson, E.D., Kavalali, E.T., and Monteggia, L.M. (2008). Activity-dependent suppression of miniature neurotransmission through the regulation of DNA methylation. *J Neurosci* 28, 395-406.

- Nestler, E.J. (2001). Molecular basis of long-term plasticity underlying addiction. *Nat Rev Neurosci* 2, 119-128.
- Norrholm, S.D., Bibb, J.A., Nestler, E.J., Ouimet, C.C., Taylor, J.R., and Greengard, P. (2003). Cocaine-induced proliferation of dendritic spines in nucleus accumbens is dependent on the activity of cyclin-dependent kinase-5. *Neuroscience* 116, 19-22.
- Okamura, H., Aramburu, J., Garcia-Rodriguez, C., Viola, J.P., Raghavan, A., Tahiliani, M., Zhang, X., Qui, J., Hogan, P.G., and Rao, A. (2000). Concerted dephosphorylation of the transcription factor NFAT1 induces a conformational switch that regulates transcriptional activity. *Mol Cell* 6, 539-550.
- Pandey, U.B., Nie, Z., Batlevi, Y., McCray, B.A., Ritson, G.P., Nedelsky, N.B., Schwartz, S.L., DiProspero, N.A., Knight, M.A., Schuldiner, O., *et al.* (2007). HDAC6 rescues neurodegeneration and provides an essential link between autophagy and the UPS. *Nature* 447, 859-863.
- Peakman, M.C., Colby, C., Perrotti, L.I., Tekumalla, P., Carle, T., Ulery, P., Chao, J., Duman, C., Steffen, C., Monteggia, L., *et al.* (2003). Inducible, brain region-specific expression of a dominant negative mutant of c-Jun in transgenic mice decreases sensitivity to cocaine. *Brain Res* 970, 73-86.
- Peng, J.C., Valouev, A., Swigut, T., Zhang, J., Zhao, Y., Sidow, A., and Wysocka, J. (2009). Jarid2/Jumonji coordinates control of PRC2 enzymatic activity and target gene occupancy in pluripotent cells. *Cell* 139, 1290-1302.
- Peterson, C.L., and Laniel, M.A. (2004). Histones and histone modifications. *Curr Biol* 14, R546-551.
- Pulipparacharuvil, S., Renthal, W., Hale, C.F., Taniguchi, M., Xiao, G., Kumar, A., Russo, S.J., Sikder, D., Dewey, C.M., Davis, M.M., *et al.* (2008). Cocaine regulates MEF2 to control synaptic and behavioral plasticity. *Neuron* 59, 621-633.
- Rakhilin, S.V., Olson, P.A., Nishi, A., Starkova, N.N., Fienberg, A.A., Nairn, A.C., Surmeier, D.J., and Greengard, P. (2004). A network of control mediated by regulator of calcium/calmodulin-dependent signaling. *Science* 306, 698-701.
- Renthal, W., Carle, T.L., Maze, I., Covington, H.E., 3rd, Truong, H.T., Alibhai, I., Kumar, A., Montgomery, R.L., Olson, E.N., and Nestler, E.J. (2008). Delta FosB mediates epigenetic desensitization of the c-fos gene after chronic amphetamine exposure. *J Neurosci* 28, 7344-7349.
- Renthal, W., Kumar, A., Xiao, G., Wilkinson, M., Covington, H.E., 3rd, Maze, I., Sikder, D., Robison, A.J., LaPlant, Q., Dietz, D.M., *et al.* (2009). Genome-wide analysis of chromatin regulation by cocaine reveals a role for sirtuins. *Neuron* 62, 335-348.

- Renthal, W., Maze, I., Krishnan, V., Covington, H.E., 3rd, Xiao, G., Kumar, A., Russo, S.J., Graham, A., Tsankova, N., Kippin, T.E., *et al.* (2007). Histone deacetylase 5 epigenetically controls behavioral adaptations to chronic emotional stimuli. *Neuron* *56*, 517-529.
- Ringrose, L., Ehret, H., and Paro, R. (2004). Distinct contributions of histone H3 lysine 9 and 27 methylation to locus-specific stability of polycomb complexes. *Mol Cell* *16*, 641-653.
- Robinson, T.E., and Kolb, B. (1997). Persistent structural modifications in nucleus accumbens and prefrontal cortex neurons produced by previous experience with amphetamine. *J Neurosci* *17*, 8491-8497.
- Russo, S.J., Wilkinson, M.B., Mazei-Robison, M.S., Dietz, D.M., Maze, I., Krishnan, V., Renthal, W., Graham, A., Birnbaum, S.G., Green, T.A., *et al.* (2009). Nuclear factor kappa B signaling regulates neuronal morphology and cocaine reward. *J Neurosci* *29*, 3529-3537.
- Self, D.W., Genova, L.M., Hope, B.T., Barnhart, W.J., Spencer, J.J., and Nestler, E.J. (1998). Involvement of cAMP-dependent protein kinase in the nucleus accumbens in cocaine self-administration and relapse of cocaine-seeking behavior. *J Neurosci* *18*, 1848-1859.
- Shalizi, A., Gaudilliere, B., Yuan, Z., Stegmuller, J., Shirogane, T., Ge, Q., Tan, Y., Schulman, B., Harper, J.W., and Bonni, A. (2006). A calcium-regulated MEF2 sumoylation switch controls postsynaptic differentiation. *Science* *311*, 1012-1017.
- Shaw-Lutchman, T.Z., Impey, S., Storm, D., and Nestler, E.J. (2003). Regulation of CRE-mediated transcription in mouse brain by amphetamine. *Synapse* *48*, 10-17.
- Shen, H., Korutla, L., Champtiaux, N., Toda, S., LaLumiere, R., Vallone, J., Klugmann, M., Blendy, J.A., Mackler, S.A., and Kalivas, P.W. (2007). NAC1 regulates the recruitment of the proteasome complex into dendritic spines. *J Neurosci* *27*, 8903-8913.
- Shi, X., Hong, T., Walter, K.L., Ewalt, M., Michishita, E., Hung, T., Carney, D., Pena, P., Lan, F., Kaadige, M.R., *et al.* (2006). ING2 PHD domain links histone H3 lysine 4 methylation to active gene repression. *Nature* *442*, 96-99.
- Shi, Y. (2007). Histone lysine demethylases: emerging roles in development, physiology and disease. *Nat Rev Genet* *8*, 829-833.
- Sik, A., Hajos, N., Gulacsi, A., Mody, I., and Freund, T.F. (1998). The absence of a major Ca²⁺ signaling pathway in GABAergic neurons of the hippocampus. *Proc Natl Acad Sci U S A* *95*, 3245-3250.

- Strahl, B.D., and Allis, C.D. (2000). The language of covalent histone modifications. *Nature* 403, 41-45.
- Suzuki, M.M., and Bird, A. (2008). DNA methylation landscapes: provocative insights from epigenomics. *Nat Rev Genet* 9, 465-476.
- Tanaka, Y., Naruse, I., Maekawa, T., Masuya, H., Shiroishi, T., and Ishii, S. (1997). Abnormal skeletal patterning in embryos lacking a single Cbp allele: a partial similarity with Rubinstein-Taybi syndrome. *Proc Natl Acad Sci U S A* 94, 10215-10220.
- Ting, A.H., McGarvey, K.M., and Baylin, S.B. (2006). The cancer epigenome--components and functional correlates. *Genes Dev* 20, 3215-3231.
- Trevitt, J.T., Morrow, J., and Marshall, J.F. (2005). Dopamine manipulation alters immediate-early gene response of striatal parvalbumin interneurons to cortical stimulation. *Brain Res* 1035, 41-50.
- Trojer, P., and Reinberg, D. (2006). Histone lysine demethylases and their impact on epigenetics. *Cell* 125, 213-217.
- Valjent, E., Corvol, J.C., Pages, C., Besson, M.J., Maldonado, R., and Caboche, J. (2000). Involvement of the extracellular signal-regulated kinase cascade for cocaine-rewarding properties. *J Neurosci* 20, 8701-8709.
- Vihma, H., Pruunsild, P., and Timmusk, T. (2008). Alternative splicing and expression of human and mouse NFAT genes. *Genomics* 92, 279-291.
- Walters, C.L., and Blendy, J.A. (2001). Different requirements for cAMP response element binding protein in positive and negative reinforcing properties of drugs of abuse. *J Neurosci* 21, 9438-9444.
- Weaver, I.C., Cervoni, N., Champagne, F.A., D'Alessio, A.C., Sharma, S., Seckl, J.R., Dymov, S., Szyf, M., and Meaney, M.J. (2004). Epigenetic programming by maternal behavior. *Nat Neurosci* 7, 847-854.
- Weaver, I.C., Champagne, F.A., Brown, S.E., Dymov, S., Sharma, S., Meaney, M.J., and Szyf, M. (2005). Reversal of maternal programming of stress responses in adult offspring through methyl supplementation: altering epigenetic marking later in life. *J Neurosci* 25, 11045-11054.
- Wingate, A.D., Martin, K.J., Hunter, C., Carr, J.M., Clacher, C., and Arthur, J.S. (2009). Generation of a conditional CREB Ser133Ala knockin mouse. *Genesis* 47, 688-696.
- Xu, M., Hu, X.T., Cooper, D.C., Moratalla, R., Graybiel, A.M., White, F.J., and Tonegawa, S. (1994). Elimination of cocaine-induced hyperactivity and dopamine-

mediated neurophysiological effects in dopamine D1 receptor mutant mice. *Cell* 79, 945-955.

Yi, J.J., and Ehlers, M.D. (2005). Ubiquitin and protein turnover in synapse function. *Neuron* 47, 629-632.

Young, S.T., Porrino, L.J., and Iadarola, M.J. (1991). Cocaine induces striatal c-fos-immunoreactive proteins via dopaminergic D1 receptors. *Proc Natl Acad Sci U S A* 88, 1291-1295.

Yuferov, V., Krosiak, T., Laforge, K.S., Zhou, Y., Ho, A., and Kreek, M.J. (2003). Differential gene expression in the rat caudate putamen after "binge" cocaine administration: advantage of triplicate microarray analysis. *Synapse* 48, 157-169.

Zhang, D., Zhang, L., Lou, D.W., Nakabeppu, Y., Zhang, J., and Xu, M. (2002). The dopamine D1 receptor is a critical mediator for cocaine-induced gene expression. *J Neurochem* 82, 1453-1464.

Zhang, J., Zhang, L., Jiao, H., Zhang, Q., Zhang, D., Lou, D., Katz, J.L., and Xu, M. (2006). c-Fos facilitates the acquisition and extinction of cocaine-induced persistent changes. *J Neurosci* 26, 13287-13296.

Zhang, X., Odom, D.T., Koo, S.H., Conkright, M.D., Canettieri, G., Best, J., Chen, H., Jenner, R., Herbolsheimer, E., Jacobsen, E., *et al.* (2005). Genome-wide analysis of cAMP-response element binding protein occupancy, phosphorylation, and target gene activation in human tissues. *Proc Natl Acad Sci U S A* 102, 4459-4464.

Zhang, X.F., Hu, X.T., and White, F.J. (1998). Whole-cell plasticity in cocaine withdrawal: reduced sodium currents in nucleus accumbens neurons. *J Neurosci* 18, 488-498.

Zhu, J.K. (2009). Active DNA demethylation mediated by DNA glycosylases. *Annu Rev Genet* 43, 143-166.

REFERENCES

- Adachi M, Autry AE, Covington HE 3rd, Monteggia LM (2009). MeCP2-mediated transcription repression in the basolateral amygdale may underlie heightened anxiety in a mouse model of Rett syndrome. *J Neurosci* **29**(13): 4218-4227.
- Amir RE, Van den Veyver IB, Wan M, Tran CQ, Francke U, Zoghbi HY (1999). Rett syndrome is caused by mutations in X-linked MECP2, encoding methyl-CpG-binding protein 2. *Nat Genet* **23**(2): 185-188.
- Autry AE, Adachi M, Nosyreva E, Na ES, Los MF, Cheng P, *et al* (2011). NMDA receptor blockade at rest triggers rapid behavioural antidepressant responses. *Nature* **475**(7354): 91-95.
- Balmer D, Goldstine J, Rao YM, LaSalle JM (2003). Elevated methyl-CpG-binding protein 2 expression is acquired during postnatal human brain development and is correlated with alternative polyadenylation. *J Mol Med* **81**(1): 61-68.
- Barden N (2004). Implication of the hypothalamic-pituitary-adrenal axis in the pathophysiology of depression. *Psychiatry Neurosci* **29**(3): 185-193.
- Barrot M, Olivier JD, Perrotti LI, DiLeone RJ, Berton O, Eisch AJ, *et al* (2002). CREB activity in the nucleus accumbens shell controls gating of behavioral responses to emotional stimuli. *Proc Natl Acad Sci* **99**(17): 11543-11440.
- Berman RM, Cappiello A, Anand A, Oren DA, Heninger GR, Charney DS, *et al* (2000). Antidepressant effects of ketamine in depressed patients. *Biol Psychiatry* **47**(4): 351-354.
- Berton O, McClung CA, Dileone RJ, Krishnan V, Renthal W, Russo SJ, *et al* (2006). Essential role of BDNF in the mesolimbic dopamine pathway in social defeat stress. *Science* **311**(5762): 864-868.
- Berton O, Nestler EJ (2006). New approaches to antidepressant drug discovery: beyond monoamines. *Nat Rev Neurosci* **7**(2): 137-151.
- Bibb JA, Chen J, Taylor SR, Svenningsson P, Nishi A, Snyder GL, *et al* (2001). Effects of chronic exposure to cocaine are regulated by the neuronal protein Cdk5. *Nature* **410**(6826a): 376-380.
- Bienvenu T, Carrie A, de Roux N, Vinet MC, Jonveaux P, Couvert P, *et al* (2000). MeCP2 mutations account for most cases of typical forms of Rett syndrome. *Hum Mol Genet* **9**(9): 1377-1384.
- Borrelli E, Nestler EJ, Allis CD, Sassone-Corsi P (2008). Decoding the epigenetic language of neuronal plasticity. *Neuron* **60**(6): 961-974.

- Brenes JC, Fornaguera J (2009). The effect of chronic fluoxetine on social isolation-induced changes on sucrose consumption, immobility behavior, and on serotonin and dopamine function in hippocampus and ventral striatum. *Behavioural Brain Research* **198**(1): 199-205.
- Bromberg-Martin ES, Hikosaka O (2011). Lateral habenula neurons signal errors in the prediction of reward information. *Nat Neurosci* **14**(9): 1209-1216.
- Cassel S, Carouge D, Gensburger C, Anglard P, Burgun C, Dietrich JB, *et al* (2006). Fluoxetine and cocaine induce the epigenetic factors MeCP2 and MBD1 in adult rat brain. *Mol Pharmacol* **70**(2): 487-492.
- Chahrour M, Jung SY, Shaw C, Zhou X, Wong STC, Qin J, *et al* (2008). MeCP2, a key contributor to neurological disease, activates and represses transcription. *Science* **320**(5880): 1224-1229.
- Chahrour M, Zoghbi (2007). The story of Rett syndrome: from clinic to neurobiology. *Neuron* **56**(3): 422-437.
- Chao HT, Zoghbi HY, Rosenmund C (2007). MeCP2 controls excitatory synaptic strength by regulating glutamatergic synapse number. *Neuron* **56**(1): 58-65.
- Chen RZ, Akbarian S, Tudor M, Jaenisch R (2001). Deficiency of methyl-CpG binding protein-2 in the CNS results in a Rett-like phenotype in mice. *Nat Genet* **27**(3): 327-331.
- Chen WG, Chang Q, Lin Y, Meissner A, West AE, Griffith EC, *et al* (2003). Derepression of BDNF transcription involves calcium-dependent phosphorylation of MeCP2. *Science* **302**(5646): 885-889.
- Cohen S, Gabel HW, Hemberg M, Hutchinson AN, Sadacca LA, Ebert DH, *et al* (2011). Genome-wide activity-dependent MeCP2 phosphorylation regulates nervous system development and function. *Neuron* **72**(1): 72-85.
- Collins AL, Levenson JM, Vilaythong AP, Richman R, Armstrong DL, Noebels JL, *et al* (2004). Mild overexpression of MeCP2 causes a progressive neurological disorder in mice. *Hum Mol Genet* **13**(21): 2679-2689.
- Covington HE 3rd, Maze I, LaPlant QC, Vialou VF, Ohnishi YN, Berton O, *et al* (2009). Antidepressant actions of histone deacetylase inhibitors. *J Neurosci* **29**(37): 11451-11460.
- Crawley J, Goodwin FK (1980). Preliminary report of a simple animal behavior model for the anxiolytic effects of benzodiazepines. *Pharmacol Biochem Behav* **13**(2): 167-170.

- Dani VS, Chang Q, Maffei A, Turrigiano GG, Jaenisch R, Nelson SB (2005). Reduced cortical activity due to a shift in the balance between excitation and inhibition in a mouse model of Rett syndrome. *Proc Natl Acad Sci* **102**(35): 12560-12565.
- De Kloet ER, Joels M, Holsboer F (2005). Stress and the brain: from adaptation to disease. *Nat Rev Neurosci* **6**(6): 463-475.
- Deng JV, Rodriguiz RM, Hutchinson AN, Kim IH, Wetsel WC, West AE (2010). MeCP2 in the nucleus accumbens contributes to neural and behavioral responses to psychostimulants. *Nat Neurosci* **13**(9): 1128-1136.
- Fanselow MS, Poulos AM (2005). The neuroscience of mammalian associative learning. *Annu Rev Psychocol* **56**: 207-234.
- Fukui M, Rodriguiz RM, Zhou J, Jiang SX, Phillips LE, Caron MG, *et al* (2007). Vmat2 heterozygous mutant mice display a depressive-like phenotype. *J Neurosci* **27**(39): 10520-10529.
- Gainetdinov RR, Caron MG (2003). Monoamine transporters: from genes to behavior. *Annu Rev Pharmacol Toxicol* **43**: 261-284.
- Gemelli T, Berton O, Nelson ED, Perrotti LI, Jaenisch R, Monteggia LM (2005). Postnatal loss of Methyl-CpG binding protein 2 in the forebrain is sufficient to mediate behavioral aspects of Rett syndrome in mice. *Biol Psychiatry* **59**(5): 468-476.
- Georgel PT, Horowitz-Scherer RA, Adkins N, Woodcock CL, Wade PA, Hansen JC (2003). Chromatin compaction by human MeCP2. Assembly of novel secondary chromatin structures in the absence of DNA methylation. *J Biol Chem* **278**(34): 32181-32188.
- Giacometti E, Luikenhuis S, Beard C, Jaenisch R (2007). Partial rescue of MeCP2 deficiency by postnatal activation of MeCP2. *Proc Natl Acad Sci* **104**(6): 1931-1936.
- Golden SA, Covington HE 3rd, Berton O, Russo SJ (2011). A standardized protocol for repeated social defeat stress in mice. *Nat Protoc* **6**(8): 1183-1191.
- Goodman RH, Smolik S (2000). CBP/p300 in cell growth, transformation, and development. *Genes Dev* **14**(13): 1553-1577.
- Grimm JW, Lu L, Hayashi T, Hope BT, Su TP, Shaham Y (2003). Time-dependent increases in brain-derived neurotrophic factor protein levels within the mesolimbic dopamine system after withdrawal from cocaine: implications for incubation of cocaine craving. *J Neurosci* **23**(3): 742-747.
- Guy J, Gan J, Selfridge J, Cobb S, Bird A (2007). Reversal of neurological defects in a mouse model of Rett syndrome. *Science* **315**(5815): 1143-1147.

- Guy J, Hendrich B, Holmes M, Martin JE, Bird A (2001). A mouse Mecp2-null mutation causes neurological symptoms that mimic Rett syndrome. *Nat Genet* **27**(3): 322-326.
- Hagberg B, Aicardi J, Dias K, Ramos O (1983). A progressive syndrome of autism, dementia, ataxia, and loss of purposeful hand use in girls: Rett's syndrome: report of 35 cases. *Ann Neurol* **14**(4): 471-479.
- Hikosaka, O (2010). The habenula: from stress evasion to value-based decision-making. *Nat Rev Neurosci* **11**(7): 503-513.
- Hong S, Zhou TC, Smith M, Saleem KS, Hikosaka O (2011). Negative reward signals from the lateral habenula to dopamine neurons are mediated by rostromedial tegmental nucleus in primates. *J Neurosci* **31**(32): 11457-11471.
- Horike S, Cai S, Miyano M, Cheng J, Kohwi-Shigematsu T (2004). Loss of silent-chromatin looping and impaired imprinting of *DLX5* in Rett syndrome. *Nat Genet* **37**(1): 31-40.
- Host L, Dietrich JB, Carouge D, Aunis D, Zwiller J (2009). Cocaine self-administration alters the expression of chromatin-remodeling proteins; modulation by histone deacetylase inhibition. *J Psychopharmacol* **25**(2): 222-229.
- Huang YH, Lin Y, Mu P, Lee BR, Brown TE, Wayman G, *et al* (2009). In vivo cocaine experience generates silent synapses. *Neuron* **63**(1): 40-47.
- Hutchinson AN, Deng JV, Aryal DK, Wetsel WC, West AE (2011). Differential regulation of MeCP2 phosphorylation in the CNS by dopamine and serotonin. *Neuropsychopharmacol* Epub ahead of print.
- Hyman SE, Malenka RC, Nestler EJ (2006). Neural mechanisms of addiction: the role of reward-related learning and memory. *Annu Rev Neurosci* **29**: 565-598.
- Im HI, Hollander JA, Bali P, Kenny PJ (2010). MeCP2 controls BDNF expression and cocaine intake through homeostatic interactions with microRNA-212. *Nat Neurosci* **13**(9): 1120-1127.
- Jiang Y, Langley B, Lubin FD, Renthal W, Wood MA, Yasui DH, *et al* (2008). Epigenetics in the nervous system. *J Neurosci* **28**(46): 11753-11759.
- Ji H, Shepard PD (2007). Lateral habenula stimulation inhibits rat midbrain dopamine neurons through a GABA(A) receptor-mediated mechanism. *J Neurosci* **27**(26): 6923-6930.
- Jaenisch R, Bird A (2003). Epigenetic regulation of gene expression: how the genome integrates intrinsic and environmental signals. *Nat Genet* **33** Suppl: 245-254.

- Kalen P, Karlson M, Wiklund L (1985). Possible excitatory amino acid afferents to nucleus raphe dorsalis of the rat investigated with retrograde wheat germ agglutinin and D-[³H]aspartate tracing. *Brain Res* **360**(1-2): 285-297.
- Kawaguchi Y, Wilson CJ, Augood SJ, Emson PC (1995). Striatal interneurons; chemical, physiological and morphological characterization. *Trends Neurosci* **18**(12): 527-535.
- Kishi N, Macklis JD (2004). MeCP2 is progressively expressed in post-migratory neurons and is involved in neuronal maturation rather than cell fate decisions. *Mol Cell Neurosci* **27**(3): 306-321.
- Kriaucionis S, Bird A (2003). DNA methylation and Rett syndrome. *Hum Mol Genet* **12 Spec No 2**: R221-227.
- Krishnan V, Nestler EJ (2010). Linking molecules to mood: new insights into the biology of depression. *Am J Psychiatry* **167**(11): 1305-1320.
- Krishnan V, Nestler EJ (2008). The molecular neurobiology of depression. *Nature* **455**(7215): 894-902.
- Krishnan V, Han MH, Graham DL, Berton O, Renthal W, Russo SJ, *et al* (2007). Molecular adaptations underlying susceptibility and resistance to social defeat in brain reward regions. *Cell* **131**(2): 391-404.
- Kudryavtseva NN, Bakshtanovskaya IV, Koryakina LA (1991). Social model of depression in mice of C57BL/6J strain. *Pharmacol Biochem Behav* **38**(2): 315-320.
- Kuhn R (1958). The treatment of depressive states with G 22355 (imipramine hydrochloride). *Am J Psychiatry* **115**(5): 459-464.
- Kumar A, Choi KH, Renthal W, Tsankova NM, Theobald DE, Truong HT, *et al* (2005). Chromatin remodeling is a key mechanism underlying cocaine-induced plasticity in striatum. *Neuron* **48**(2): 303-314.
- Laifenfeld D, Karry R, Grauer E, Klein E, Ben-Shachar D (2005). Antidepressants and prolonged stress in rats modulate CAM-L1, laminin, and pCREB, implicated in neuronal plasticity. *Neurobiol Dis* **20**(2): 432-441.
- LaPlant Q, Vialou V, Covington HE 3rd, Dumitriu D, Feng J, Warren BL, *et al* (2010). Dnmt3a regulates emotional behavior and spine plasticity in the nucleus accumbens. *Nat Neurosci* **13**(9): 1137-1143.
- Lecourtier L, Kelly PH (2007). A conductor hidden in the orchestra? Role of the habenular complex in monoamine transmission and cognition. *Neurosci Biobehav Rev* **31**(5): 659-672.

- Levine AA, Guan Z, Barco A, Xu S, Kandel ER, Schwartz JH (2005). CREB-binding protein controls response to cocaine by acetylating histones at the fosB promoter in the mouse striatum. *Proc Natl Acad Sci* **102**(52): 19186-19191.
- Li B, Piriz J, Mirrione M, Chung C, Proulx CD, Schulz D, *et al* (2011). Synaptic potentiation onto habenula neurons in the learned helplessness model of depression. *Nature* **470**(7335): 535-539.
- Li H, Zhong X, Chau KF, Williams EC, Chang Q (2011). Loss of activity-induced phosphorylation of MeCP2 enhances synaptogenesis, LTP and spatial memory. *Nat Neurosci* **14**(8): 1001-1008.
- Li N, Liu RJ, Dwyer JM, Banasr M, Lee B, Son H, *et al* (2011). Glutamate N-methyl-D-aspartate receptor antagonists rapidly reverse behavioral and synaptic deficits caused by chronic stress exposure. *Biol Psychiatry* **69**(8): 754-761.
- Manji HK, Drevets WC, Charney DS (2001). The cellular neurobiology of depression. *Nat Med* **7**(5): 541-547.
- Matsumoto M, Hikosaka (2009). Representation of negative motivational value in the primate lateral habenula. *Nat Neurosci* **12**(1): 77-84.
- Mayr B, Montminy M (2001). Transcriptional regulation by the phosphorylation-dependent factor CREB. *Nat Rev Mol Cell Biol* **2**(8): 599-609.
- Maze I, Covington HE 3rd, Dietz DM, LaPlant Q, Renthal W, Russo SJ, *et al* (2010). Essential role of the histone methyltransferase G9a in cocaine-induced plasticity. *Science* **327**(5962): 213-216.
- Missale C, Nash SR, Robinson SW, Jaber M, Caron MG (1998). Dopamine receptors: from structure to function. *Physiol Rev* **78**(1): 189-225.
- Monteggia LM, Kavalai ET (2009). Rett syndrome and the impact of MeCP2 associated transcriptional mechanisms of neurotransmission. *Biol Psychiatry* **65**(3): 204-210.
- Monteggia LM, Luikart B, Barrot M, Theobald D, Malkovska I, Nef S, *et al* (2007). Brain-derived neurotrophic factor conditional knockouts show gender differences in depression-related behaviors. *Biol Psychiatry* **61**(2): 187-197.
- Moratalla R, Elibol B, Vallejo M, Graybiel AM (1996). Network-level changes in expression of inducible Fos-Jun proteins in the striatum during chronic cocaine treatment and withdrawal. *Neuron* **17**(1): 147-156.
- Moretti P, Levenson JM, Battaglia F, Atkinson R, Teague R, Antalffy B (2006). Learning and memory and synaptic plasticity are impaired in a mouse model of Rett syndrome. *J Neurosci* **26**(1): 319-327.

- Morgan JI, Cohen DR, Hempstead JL, Curran T (1987). Mapping patterns of c-fos expression in the central nervous system after seizure. *Science* **237**(4811): 192-197.
- Morilak DA, Frazer A (2004). Antidepressants and brain monoaminergic systems: a dimensional approach to understanding their behavioural effects in depression and anxiety disorders. *Int J Neuropsychopharmacol* **7**(2): 193-218.
- Morris JS, Smith KA, Cowen PJ, Friston KJ, Dolan RJ (1999). Covariation of activity in habenula and dorsal raphe nuclei following tryptophan depletion. *Neuroimage* **10**
- Moy SS, Nader JJ, Perez A, Barbaro RP, Johns JM, Magnuson TR, *et al* (2004). Sociability and preference for social novelty in five inbred strains: an approach to assess autistic behavior in mice. *Genes Brain Behav* **3**(5): 287-302.
- Nadler JJ, Moy SS, Dold G, Trang D, Simmons N, Perez A, *et al* (2004). Automated apparatus for quantitation of social approach behaviors in mice. *Genes Brain Behav* **3**(5): 303-314.
- Nan X, Ng HH, Johnson CA, Laherty CD, Turner BM, Eisenman RN, *et al* (1998). Transcriptional repression by the methyl-CpG-binding protein MeCP2 involves a histone deacetylase complex. *Nature* **393**(6683): 386-389.
- Nan X, Campoy FJ, Bird A (1997). MeCP2 is a transcriptional repressor with abundant binding sites in genomic chromatin. *Cell* **88**(4): 471-481.
- Nelson ED, Kavalali ET, Monteggia LM (2006). MeCP2-dependent transcription repression regulates excitatory neurotransmission. *Curr Biol* **16**(7): 710-716.
- Nestler EJ (2001). Molecular basis of long-term plasticity underlying addiction. *Nat Rev Neurosci* **2**(2): 119-128.
- Nestler EJ, Barrot M, DiLeone RJ, Eisch AJ, Gold SJ, Monteggia LM (2002). Neurobiology of depression. *Neuron* **34**(1): 13-25.
- Newton SS, Thome J, Wallace TL, Shirayama Y, Schlesinger L, Sakai N, *et al* (2002). Inhibition of cAMP response element-binding protein or dynorphin in the nucleus accumbens produces an antidepressant-like effect. *J Neurosci* **22**(24): 10883-10890.
- Nibuya M, Nestler EJ, Duman RS (1996). Chronic antidepressant administration increases the expression of cAMP response element binding protein (CREB) in rat hippocampus. *J Neurosci* **16**(7): 2365-2372.
- Nibuya M, Morinobu S, Duman RS (1995). Regulation of BDNF and trkB mRNA in rat brain by chronic electroconvulsive seizure and antidepressant drug treatments. *J Neurosci* **15**(11): 7539-7547.

- Nishikawa T, Scatton B (1985). Inhibitory influence of GABA on central serotonergic transmission. Involvement of the habenulo-raphé pathways in the GABAergic inhibition of ascending cerebral serotonergic neurons. *Brain Res* **331**(1): 81-90.
- Nuber UA, Kriaucionis S, Roloff TC, Guy J, Selfridge J, Steinhoff C, *et al* (2005). Up-regulation of glucocorticoid-regulated genes in a mouse model of Rett syndrome. *Hum Mol Genet* **14**(15): 2247-2256.
- Perrotti LI, Hadeishi Y, Ulery PG, Barrot M, Monteggia L, Duman RS, *et al* (2004). Induction of deltaFosB in reward-related brain structures after chronic stress. *J Neurosci* **24**(47): 10594-10602.
- Pliakas AM, Carlson RR, Neve RL, Konradi C, Nestler EJ, Carlezon WA Jr. (2001). Altered responsiveness to cocaine and increased immobility in the forced swim test associated with elevated cAMP response element-binding protein expression in the nucleus accumbens. *J Neurosci* **21**(18): 7397-7403.
- Pulipparacharuvil S, Renthal W, Hale CF, Taniguchi M, Xiao G, Kumar A, *et al* (2008). Cocaine regulates MEF2 to control synaptic and behavioral plasticity. *Neuron* **59**(4): 621-633.
- Porsolt RD, Le Pichon M, Jalfre M (1977). Depression: a new animal model sensitive to antidepressant treatments. *Nature* **266**(5604): 730-732.
- Ramocki MB, Peters SU, Tavyev YJ, Zhang F, Carvalho CM, Schaaf CP, *et al* (2009). Autism and other neuropsychiatric symptoms are prevalent in individuals with MeCP2 duplication syndrome. *Ann Neurol* **66**(6): 771-782.
- Renthal W, Kumar A, Xiao G, Wilkinson M, Covington HE 3rd, Maze I, *et al* (2009). Genome-wide analysis of chromatin regulation by cocaine reveals a role for sirtunins. *Neuron* **62**(3): 335-348.
- Renthal W, Nestler EJ (2009). Chromatin regulation in drug addiction and depression. *Dialogues Clin Neurosci* **11**(3): 257-268.
- Renthal W, Maze I, Krishnan V, Covington HE 3rd, Xiao G, Kumar A, *et al* (2007). Histone deacetylase 5 epigenetically controls behavioral adaptations to chronic stimuli. *Neuron* **56**(3): 517-529.
- Robinson TE, Kolb B (1997). Persistent structural modifications in nucleus accumbens and prefrontal cortex neurons produced by previous experience with amphetamine. *J Neurosci* **17**(21): 8491-8497.
- Rodriguez RM, Wetsel WC (2006). Assessments of cognitive deficits in mutant mice. In Levine, E. & Buccafusco, J.J. (eds), *Animal Models of Cognitive Impairment*. CRC Press, Boca Raton, 223-284.

- Russo SJ, Wilkinson SB, Mazei-Robison MS, Dietz DM, Maze I, Krishnan V, *et al* (2009). Nuclear factor kappa B signaling regulates neuronal morphology and cocaine reward. *J Neurosci* **29**(11): 3529-3537.
- Sanacora G, Zarate CA, Krystal JH, Manji HK (2008). Targeting the glutamatergic system to develop novel, improved therapeutics for mood disorders. *Nat Rev Drug Discov* **7**(5): 426-437.
- Shahbazian M, Young J, Yuva-Paylor L, Spencer C, Antalffy B, Noebels J, *et al* (2002). Mice with truncated MeCP2 recapitulate many Rett syndrome features and display hyperacetylation of histone H3. *Neuron* **35**(2): 243-254.
- Shuen JA, Chen M, Gloss B, Calakos N (2008). Drd1a-tdTomato BAC transgenic mice for simultaneous visualization of medium spiny neurons in the direct and indirect pathways of the basal ganglia. *J Neurosci* **28**(11): 2681-2685.
- Skene PJ, Illingworth RS, Webb S, Kerr AR, James KD, Turner DJ, *et al* (2010). Neuronal MeCP2 is expressed at near histone-octamer levels and globally alters the chromatin state. *Mol Cell* **37**(4): 457-468.
- Steru L, Chermat R, Thierry B, Simon P (1985). The tail suspension test: a new method for screening antidepressants in mice. *Psychopharmacol* **85**(3): 367-370.
- Tao J, Hu K, Chang Q, Wu H, Sherman NE, Martinowich K, *et al* (2009). Phosphorylation of MeCP2 at Serine 80 regulates its chromatin association and neurological function. *Proc Natl Acad Sci* **106**(12): 4882-4887.
- Thomas MJ, Beurrier C, Bonci A, Malenka RC (2001). Long-term depression in the nucleus accumbens: a neural correlate of behavioral sensitization to cocaine. *Nat Neurosci* **4**(12): 1217-1223.
- Tsankova NM, Renthal W, Kumar A, Nestler EJ (2007). Epigenetic regulation in psychiatric disorders. *Nat Rev Neurosci* **8**(5): 355-367.
- Tsankova NM, Berton O, Renthal W, Kumar A, Neve RL, Nestler EJ (2006). Sustained hippocampal chromatin regulation in a mouse model of depression and antidepressant action. *Nat Neurosci* **9**(4): 519-525.
- Tsankova NM, Kumar A, Nestler EJ (2004). Histone modifications at gene promoter regions in rat hippocampus after acute and chronic electroconvulsive seizures. *J Neurosci* **24**(24): 5603-5610.
- Tudor M, Akbarian S, Chen RZ, Jaenisch R (2002). Transcriptional profiling of a mouse model for Rett syndrome reveals subtle transcriptional changes in the brain. *Proc Natl Acad Sci* **99**(24): 15536-15541.

- Ullsperger M, von Cramon DY (2003). Error monitoring using external feedback: specific roles of the habenular complex, the reward system, and the cingulate motor area revealed by functional magnetic resonance imaging. *J Neurosci* **23**(10): 4308-4314.
- Vialou V, Robison AJ, LaPlant QC, Covington HE 3rd, Dietz DM, Ohnishi YN, *et al* (2010). DeltaFosB in brain reward circuits mediates resilience to stress and antidepressant response. *Nat Neurosci* **13**(6): 745-742.
- Wallace DL, Han MH, Graham DL, Green TA, Vialou V, Iniguez SD, *et al* (2009). CREB regulation of nucleus accumbens excitability mediates social isolation-induced behavioral deficits. *Nat Neurosci* **12**(2): 200-209.
- Weaver IC, Cervoni N, Champagne FA, D'Alessio AC, Sharma S, Seckl JR, *et al* (2004). Epigenetic programming by maternal behavior. *Nat Neurosci* **7**(8): 847-854.
- Wilkinson MB, Xiao G, Kumar A, LaPlant Q, Renthal RW, Sikder D, *et al* (2009). Imipramine treatment and resiliency exhibit similar chromatin regulation in the mouse nucleus accumbens in depression models. *J Neurosci* **29**(24): 7820-7832.
- Xu M, Koeltzow TE, Santiago GT, Moratalla R, Cooper DC, Hu XT, *et al* (1997). Dopamine D3 receptor mutant mice exhibit increased behavioral sensitivity to concurrent stimulation of D1 and D2 receptors. *Neuron* **19**(4): 837-848.
- Zarate CA Jr, Singh JB, Carlson PJ, Brutsche NE, Ameli R, Luckenbaugh DA, *et al* (2006). A randomized trial of an N-methyl-D aspartate antagonist in treatment-resistant major depression. *Arch Gen Psychiatry* **63**(8): 856-864.
- Zhou Z, Hong EJ, Cohen S, Zhao WN, Ho HY, Schmidt L, *et al* (2006). Brain-specific phosphorylation of MeCP2 regulates activity-dependent Bdnf transcription, dendritic growth, and spine maturation. *Neuron* **52**(2): 255-269.
- Zimmerman M, Chelminski I, McDermut W (2002). Major depressive disorder and axis diagnostic comorbidity. *J Clin Psychiatry* **63**(3): 187-193.

BIOGRAPHY

Ashley Nicole Hutchinson was born on August 26, 1984 in Colorado Springs, Colorado. She attended Regis University in Denver, CO from August 2003 until May 2007 and received her B.S. in Biology. In addition, she attended Duke University in Durham, NC from August 2007 until December 2011 and received her PhD in Pharmacology. During her time at Duke, she was awarded a Duke Endowment Fellowship from 2007-2011, the Department of Pharmacology Fitzgerald Poster Award in 2009, a Ruth L. Kirschstein National Research Service Award (NRSA) in 2010-2011, and the Department of Pharmacology Robert Fitzgerald Scholar Award in 2011.

Publications:

Cohen, S., Gabel, H.W., **Hutchinson, A.N.**, Sadacca, L.W., Ebert, D.H., Harmin, D.A., Greenberg, R.S., Verdine, V.K., Zhou, Z., Wetsel, W.C., West, A.E. and Greenberg, M.E. (2011) Genome-wide activity-dependent MeCP2 phosphorylation regulates nervous system development and function. *Neuron* **72**(1): 72-85.

Hutchinson, A.N., Deng, J.V., Aryal, D.K., Wetsel, W.C., West, A.E. (2011) Differential regulation of MeCP2 phosphorylation in the CNS by dopamine and serotonin. *Neuropsychopharmacol* Epub ahead of print.

Deng, J.V., Rodriguez, R.M., **Hutchinson, A.N.**, Kim, I-H, Wetsel, W.C. and West, A.E. (2010) MeCP2 in the nucleus accumbens contributes to neural and behavioral responses to psychostimulants. *Nat Neurosci* **13**(9): 1128-1136.

McDowell, K.A. *, **Hutchinson, A.N.***, Wong-Goodrich, S.J.E., Presby, M.M., Su, D., Law, K.C., Williams, C.L., Wetsel, W.C. and West, A.E. (2010) Knockout of *Carf* impairs locomotor sensitivity to psychostimulants and enhances striatal GABAergic synaptic protein expression. *J Neurosci* **30**(22): 7453-7465. (* Authors contributed equally to work)

Hutchinson, A.N. and West, A.E. (2010) Transcriptional regulators that mediate neural and behavioral adaptations to psychostimulants. *Cell Science* **6**: 140-177.